

34501



National Library of Canada

Bibliothèque nationale du Canada

CANADIAN THESES ON MICROFICHE

THÈSES CANADIENNES SUR MICROFICHE

V

NAME OF AUTHOR/NOM DE L'AUTEUR TAYLOR, GRAHAM WALTER

TITLE OF THESIS/TITRE DE LA THÈSE ANALYTICAL MODELLING OF PRESTRESSED CONCRETE BOX GIRDERS SUBJECT TO COMBINED LOADING

UNIVERSITY/UNIVERSITÉ UNIVERSITY OF ALBERTA EDMONTON ALBERTA

DEGREE FOR WHICH THESIS WAS PRESENTED/ GRADE POUR LEQUEL CETTE THÈSE FUT PRÉSENTÉE PH. D. IN CIVIL ENGINEERING

YEAR THIS DEGREE CONFERRED/ANNÉE D'OBTENTION DE CE GRADE 1977

NAME OF SUPERVISOR/NOM DU DIRECTEUR DE THÈSE DR. J. WAWARUK

Permission is hereby granted to the NATIONAL LIBRARY OF CANADA to microfilm this thesis and to lend or sell copies of the film.

L'autorisation est, par la présente, accordée à la BIBLIOTHÈQUE NATIONALE DU CANADA de microfilmer cette thèse et de prêter ou de vendre des exemplaires du film.

The author reserves other publication rights, and neither the thesis nor extensive extracts from it may be printed or otherwise reproduced without the author's written permission.

L'auteur se réserve les autres droits de publication; ni la thèse ni de longs extraits de celle-ci ne doivent être imprimés ou autrement reproduits sans l'autorisation écrite de l'auteur.

DATED/DATÉ OCTOBER 19, 1977 SIGNED/SIGNÉ J. W. Taylor

PERMANENT ADDRESS/RÉSIDENCE FIXE KEP, PRIESTMAN AND ASSOCIATES LTD. #400, 380 DOUGLAS STREET, VICTORIA, B.C. V8W 2B8



National Library of Canada

Cataloguing Branch  
Canadian Theses Division

Ottawa, Canada  
K1A 0N4

Bibliothèque nationale du Canada

Direction du catalogage  
Division des thèses canadiennes

## NOTICE

The quality of this microfiche is heavily dependent upon the quality of the original thesis submitted for microfilming. Every effort has been made to ensure the highest quality of reproduction possible.

If pages are missing, contact the university which granted the degree.

Some pages may have indistinct print especially if the original pages were typed with a poor typewriter ribbon or if the university sent us a poor photocopy.

Previously copyrighted materials (journal articles, published tests, etc.) are not filmed.

Reproduction in full or in part of this film is governed by the Canadian Copyright Act, R.S.C. 1970, c. C-30. Please read the authorization forms which accompany this thesis.

**THIS DISSERTATION  
HAS BEEN MICROFILMED  
EXACTLY AS RECEIVED**

## AVIS

La qualité de cette microfiche dépend grandement de la qualité de la thèse soumise au microfilmage. Nous avons tout fait pour assurer une qualité supérieure de reproduction.

S'il manque des pages, veuillez communiquer avec l'université qui a conféré le grade.

La qualité d'impression de certaines pages peut laisser à désirer, surtout si les pages originales ont été dactylographiées à l'aide d'un ruban usé ou si l'université nous a fait parvenir une photocopie de mauvaise qualité.

Les documents qui font déjà l'objet d'un droit d'auteur (articles de revue, examens publiés, etc.) ne sont pas microfilmés.

La reproduction, même partielle, de ce microfilm est soumise à la Loi canadienne sur le droit d'auteur, SRC 1970, c. C-30. Veuillez prendre connaissance des formules d'autorisation qui accompagnent cette thèse.

**LA THÈSE A ÉTÉ  
MICROFILMÉE TELLE QUE  
NOUS L'AVONS REÇUE**

THE UNIVERSITY OF ALBERTA

ANALYTICAL MODELLING OF  
PRESTRESSED CONCRETE BOX GIRDERS  
SUBJECTED TO COMBINED LOADING

by



GRAHAM TAYLOR

A THESIS

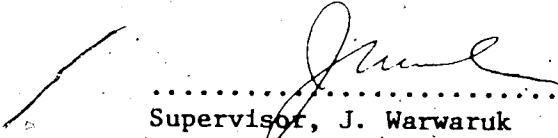
SUBMITTED TO THE FACULTY OF GRADUATE STUDIES AND RESEARCH  
IN PARTIAL FULFILMENT OF THE REQUIREMENTS FOR THE DEGREE  
OF DOCTOR OF PHILOSOPHY  
IN CIVIL ENGINEERING

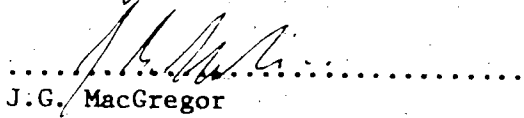
EDMONTON, ALBERTA

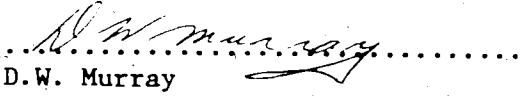
FALL 1977

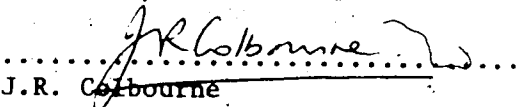
THE UNIVERSITY OF ALBERTA  
FACULTY OF GRADUATE STUDIES AND RESEARCH

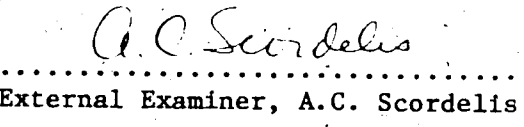
The undersigned certify that they have read, and recommend to the Faculty of Graduate Studies and Research, for acceptance, a thesis entitled ANALYTICAL MODELLING OF PRESTRESSED CONCRETE BOX GIRDERS SUBJECTED TO COMBINED LOADING submitted by GRAHAM TAYLOR in partial fulfilment of the requirements for the degree of Doctor of Philosophy in Civil Engineering.

  
.....  
Supervisor, J. Warwaruk

  
.....  
J.G. MacGregor

  
.....  
D.W. Murray

  
.....  
J.R. Colbourne

  
.....  
External Examiner, A.C. Scordelis

Date .. October 11, 1977 ..

## ABSTRACT

An analytical computer model has been developed for the analysis of reinforced or prestressed concrete multi-celled box girders acted upon by loading combinations comprised of torque, bending moment, and shear. Any cross-sectional geometry defined by linear segments can be accommodated, and generality of loading or boundary conditions is ensured by the inherent characteristics of finite element modelling. The analytical model features the incorporation of non-linear material behaviour, aggregate interlock, dowel action, and the warping restraint and cross-sectional distortional stiffness of diaphragms.

To assist in the evaluation of the analytical model performance, seven double-celled prestressed concrete box girders were cast and tested, five beams having a rectangular cross-section and the remaining two a trapezoidal cross-section. All seven beams were subjected to various torque, bending moment, and shear load combinations.

Performance of the computer model was assessed through comparison with experimental and current theoretical results. The satisfactory outcome of the assessment verified the value of the analytical model as a flexible, sophisticated method of analysis.

## ACKNOWLEDGEMENTS

This research was conducted within the Civil Engineering Department at the University of Alberta. The testing facilities of the I.F. Morrison Structural Engineering Laboratory were used in the experimental phase of this thesis, and the programming phase was accomplished through the services of the University of Alberta Computing Centre.

The author wishes to convey sincere gratitude to his supervisor, Dr. J. Warwaruk, for his guidance and unqualified support throughout this program. In associated technical aspects, Dr. D.W. Murray offered valuable advice that greatly expedited programming progress. Whenever a literature survey was undertaken, Dr. J.G. MacGregor was most helpful and resourceful in locating or providing relevant publications. To both Dr. Murray and Dr. MacGregor I am most grateful.

Messrs. L. Burden, R. Helfrich, and A. Dunbar were instrumental in the successful completion of the experimental program, and my thanks are extended to them. Preparation of the final manuscript was achieved through the excellent assistance of Mrs. L. Haswell in drafting and Mrs. D. Wyman in typing.

Concluding acknowledgement is given to the National Research Council of Canada, the Province of Alberta, and the Department of Civil Engineering at the University of Alberta for their financial assistance in the course of this doctoral program.

## TABLE OF CONTENTS

	Page
Abstract .....	iv
Acknowledgements .....	v
Table of Contents .....	vi
List of Tables .....	x
List of Figures .....	xi
List of Plates .....	xvi
List of Symbols .....	xvii
CHAPTER I - INTRODUCTION .....	1
1.1 Need for Research .....	1
1.2 Thesis Objective and Scope .....	2
CHAPTER II - RESEARCH EVOLUTION .....	4
2.1 Introduction .....	4
2.2 Review of Developments to Current State of Art .....	4
2.2.1 Experimental Approach .....	4
2.2.2 Development of Theoretical Analyses .....	7
2.2.3 Analytical Computer Solutions .....	11
2.3 Definition of Thesis Approach .....	14
2.3.1 Analytical Model Aspect .....	14
2.3.2 Experimental Aspect .....	15
CHAPTER III - ANALYTICAL COMPUTER MODEL .....	17
3.1 Introduction .....	17
3.2 Finite Element Types Employed .....	18
3.2.1 Concrete Wall Element .....	18

	Page
3.2.2 Reinforcement Element .....	22
3.2.3 Diaphragm Elements .....	23
3.3 Choice of Plane Stress Concrete Wall Element .....	25
3.4 Computer Program Description .....	28
3.4.1 General Characteristics .....	28
3.4.2 Simulation of Material Behaviour .....	31
3.4.2.1 Concrete Stiffness Under Biaxial Stresses .....	31
3.4.2.2 Concrete Crack Width .....	35
3.4.2.3 Aggregate Interlock .....	35
3.4.2.4 Dowel Effect .....	37
3.4.2.5 Cracked Concrete Stiffness .....	38
3.4.2.6 Warping Resistance of Thin Concrete Diaphragms .....	39
3.4.2.7 Warping Resistance of Thick Concrete Diaphragms .....	40
3.4.2.8 Shear Rigidity of Equivalent Diaphragms .....	42
3.4.2.9 Concrete - Reinforcement Bond .....	42
3.4.2.10 Reinforcement Stiffness .....	43
3.4.3 Failure Criteria .....	44
3.4.4 Numerical Methods .....	45
3.4.5 Flow Chart for Main Program .....	46
3.4.6 Derivation of Subroutine Logic .....	49
3.5 Program Usage .....	49
3.5.1 Capabilities and Restrictions .....	49
3.5.2 Structure Discretization .....	51
3.5.3 Input Specifications .....	52
3.5.4 Output Description and Interpretation .....	52
<b>CHAPTER IV - EXPERIMENTAL PROGRAM .....</b>	<b>65</b>
4.1 Introduction .....	65



	Page
4.2 Definition of Basic Experimental Parameters .....	65
4.3 Design of Test Specimens .....	67
4.4 Specimen Fabrication .....	69
4.5 Loading Apparatus Design .....	70
4.5.1 Beam Supports .....	70
4.5.2 Application of Bending Moment and Shear .....	71
4.5.3 Application of Torque .....	71
4.6 Instrumentation .....	72
4.7 Testing Procedure .....	73
 CHAPTER V - EXPERIMENTAL RESULTS .....	 85
5.1 Format of Presentation of Results .....	85
5.2 Test Measurements .....	86
5.3 Observed Behaviour .....	87
5.4 Potential Sources of Anomalies .....	88
 CHAPTER VI - EVALUATION OF COMPUTER MODEL RESULTS .....	 107
6.1 Introduction .....	107
6.2 Extraordinary Influences on Computer Model Response .....	108
6.2.1 Material Behaviour Aspects .....	108
6.2.2 Structural Aspects .....	109
6.3 Comparison of Computer Model and Experimental Results .....	113
6.4 Comparison of Computer Model Results with Current Theory .....	115
6.4.1 Ultimate Strength .....	116
6.4.2 Torsion - Bending Interaction .....	119
6.4.3 Torsion - Bending - Shear Interaction .....	120

	Page
6.5 Assessment of Computer Model Results .....	122
6.5.1 Computer Model Assessment in Light of Experimentation .....	122
6.5.1.1 Prominent Aspects of Model Performance .....	122
6.5.1.2 Review of Individual Beam Results .....	127
6.5.1.3 Summary .....	131
6.5.2 Computer Model Assessment in Light of Current Theory .....	131
6.5.2.1 Ultimate Strength .....	131
6.5.2.2 Combined Loading Interaction .....	134
6.5.2.3 Limitations in Application of Theory .....	135
6.5.2.4 Summary .....	137

## CHAPTER VII - CONCLUSION AND SUMMARY

7.1 Principal Implications of Comparison .....	165
7.2 Application of Analytical Model .....	166
7.3 Summary .....	168
7.4 Conclusion .....	170
REFERENCES .....	171
APPENDIX A - SIGN CONVENTIONS AND SYSTEMS .....	177
APPENDIX B - SYMBOLIC NAMES .....	181
APPENDIX C - MAIN PROGRAM LISTING .....	185
APPENDIX D - SUBROUTINES LISTING .....	189
APPENDIX E - SUBROUTINE LOGIC NOTES .....	220
APPENDIX F - INPUT DATA FILE EXAMPLE .....	224
APPENDIX G - OUTPUT EXAMPLE .....	229
APPENDIX H - INPUT PREPARATION NOTES .....	250
APPENDIX I - EXPERIMENTAL PROGRAM TEST RESULTS .....	265

LIST OF TABLES

Table		Page
3.1	Deformations Considered in Concrete Finite Element Selection .....	54
3.2(a)	$[A]^{-1}$ For Element Type 1 .....	54
3.2(b)	$[A]^{-1}$ For Element Type 2 .....	55
4.1	Concrete Mix Proportions .....	74
4.2	Concrete Strength .....	74
4.3	Beam Design Tabulation .....	75
5.1	Beam Strength .....	91
5.2	Pre-cracked Beam Stiffness .....	91
5.3	Nomenclature For Conventional Reinforcement Stress-Load Curves .....	92
6.1	Experimental and Computer Model Cracking and Ultimate Loading .....	138
6.2	Model and Theoretical Ultimate Strengths .....	139
6.3	Computer Model Results .....	140
I-1	Shrinkage Stresses .....	267
I-2	Beam T1 Test Results .....	268
I-3	Beam T2 Test Results .....	269
I-4	Beam R3 Test Results .....	270
I-5	Beam R4 Test Results .....	271
I-6	Beam R5 Test Results .....	272
I-7	Beams T1 and T2 Test Results .....	273

## LIST OF FIGURES

Figure		Page
2.1	Skew Bending Model .....	16
2.2	Space Truss Model .....	16
3.1	Simplified Representative Finite Element Mesh .....	56
3.2	Notation for Derivation of St. Venant Shear Stress Distribution .....	56
3.3	Bi-linear Isoparametric Serendipity Finite Element .....	56
3.4	Three Finite Element Meshes Used in Concrete Element Selection Process .....	57
3.5(a)	Direct Bending Stresses for Three Concrete Finite Elements .....	58
3.5(b)	St. Venant Torsion Shear Stresses for Three Concrete Finite Elements .....	58
3.6(a)	Element Type 1 .....	59
3.6(b)	Element Type 2 .....	59
3.6(c)	Two-Dimensional Beam Assemblage of McCleod Finite Elements .....	59
3.7	Theoretical and Experimental Concrete Compression Stress-Strain Curves .....	59
3.8	Box Beam Models with Thick Diaphragms .....	60
3.9	Diaphragm Warping Restraint Curves .....	60
3.10(a)	Conventional Reinforcement Stress- Strain Curve .....	61
3.10(b)	Prestress Reinforcement Stress- Strain Curve .....	61
3.11	Kupfer, Hilsdorf, Rüschi Biaxial Stress Envelope .....	62

Figure		Page
3.12	Simplified Analytical Model Biaxial Stress Envelope .....	62
3.13(a)	Runge-Kutta Method .....	63
3.13(b)	Modified Newton-Rapson Method .....	63
3.14	Finite Element Mesh Discretization .....	64
4.1	Load-Elongation Curve for Prestress Strand .....	76
4.2	Stress Strain Curve for #3 Deformed Bar Reinforcement .....	77
4.3(a)	Rectangular Beam Cross-Section .....	78
4.3(b)	Trapezoidal Beam Cross-Section .....	78
4.4(a)	Reinforcement for Beams R1, R2 .....	79
4.4(b)	Reinforcement for Beams R3, R4, R5 .....	79
4.4(c)	Reinforcement for Beams T1, T2 .....	79
4.5	Interaction Equations for Test Beams Under Combined Bending and Torsion .....	80
4.6	Formwork Section .....	81
4.7	Test Beam Supports .....	81
4.8	Point Load Apparatus With Roller Housing Bracing .....	82
4.9	Torsion Load Arm .....	82
5.1	Torque-Rotation Curves for Beams R1, R2 .....	93
5.2	Torque-Rotation Curves for Beams R3, R5 .....	94
5.3	Torque-Rotation Curves for Beams T1, T2 .....	95
5.4	Moment-Deflection Curves for Beams R1, R2, R3, R4, R5 .....	96
5.5	Moment-Deflection Curves for Beams T1, T2 .....	97
5.6	Stress-Load Curves for Beam R1 Reinforcement .....	98

Figure		Page
5.7	Stress-Load Curves for Beam R2 Reinforcement .....	99
5.8	Stress-Load Curves for Beam R3 Reinforcement .....	100
5.9	Stress-Load Curves for Beam R4 Reinforcement .....	101
5.10	Stress-Load Curves for Beam R5 Reinforcement .....	102
5.11	Stress-Load Curves for Beam T1 Reinforcement .....	103
5.12	Stress-Load Curves for Beam T2 Reinforcement .....	104
5.13	Cracking Patterns for Beams R4, R5 .....	105
6.1(a)	Method of Modelling Web Reinforcement .....	140
6.1(b)	Translation Procedure .....	140
6.2	Model and Test Bending Moment - Deflection Curves for Beam R1 .....	141
6.3	Model and Test Torque - Rotation Curves for Beam R1 .....	142
6.4(a)	Test and Model Longitudinal Conventional Reinforcement Stresses for Beam R1 .....	143
6.4(b)	Test and Model Hoop Reinforcement Stresses for Beam R1 .....	143
6.5	Model and Test Bending Moment - Deflection Curves for Beam R2 .....	144
6.6	Model and Test Torque - Rotation Curves for Beam R2 .....	145
6.7(a)	Test and Model Longitudinal Conventional Reinforcement Stresses for Beam R2 .....	146
6.7(b)	Test and Model Hoop Reinforcement Stresses for Beam R2 .....	146
6.8	Model and Test Bending Moment - Deflection Curves for Beam R3 .....	147

Figure		Page
6.9	Model and Test Torque - Rotation Curves for Beam R3 .....	148
6.10(a)	Test and Model Longitudinal Conventional Reinforcement Stresses for Beam R3 .....	149
6.10(b)	Test and Model Hoop Reinforcement Stresses for Beam R3 .....	149
6.11	Model and Test Bending Moment - Deflection Curves for Beam R4 .....	150
6.12(a)	Test and Model Longitudinal Conventional Reinforcement Stresses for Beam R4 .....	151
6.12(b)	Test and Model Hoop Reinforcement Stresses for Beam R4 .....	151
6.13	Model and Test Bending Moment - Deflection Curves for Beam R5 .....	152
6.14	Model and Test Torque - Rotation Curves for Beam R5 .....	153
6.15(a)	Test and Model Longitudinal Conventional Reinforcement Stresses for Beam R5 .....	154
6.15(b)	Test and Model Hoop Reinforcement Stresses for Beam R5 .....	154
6.16	Model and Test Bending Moment - Deflection Curves for Beam T1 .....	155
6.17	Model and Test Torque - Rotation Curves for Beam T1 .....	156
6.18(a)	Test and Model Longitudinal Conventional Reinforcement Stresses for Beam T1 .....	157
6.18(b)	Test and Model Hoop Reinforcement Stresses for Beam T1 .....	157
6.19	Model and Test Bending Moment - Deflection Curves for Beam T2 .....	158
6.20	Model and Test Torque - Rotation Curves for Beam T2 .....	159
6.21	Test and Model Longitudinal Conventional Reinforcement Stresses for Beam T2 .....	160

Figure		Page
6.22	Central Load Variation for Beam R4 .....	161
6.23	Torque - Bending Moment Interaction Diagram for Model Evaluation .....	162
6.24	Interaction Diagram for Bending Moment and Shear .....	163
6.25	Adjusted Torque - Bending Moment - Shear Interaction Diagram for Beams R3 and R4 .....	164
A-1	Node Numbering Sequence for Rectangular Concrete Elements .....	180
F-1	Beam Mesh for Input Data File Example .....	228
I-1	Loading Systems .....	274



LIST OF PLATES

		Page
4.1	Formwork Before Casting .....	83
4.2	Linear Displacement Transducers .....	83
4.3	Complete Experimental Testing Setup .....	84
5.1	Failure Mode of Beam R4 .....	106
5.2	Local Failure of Beam T1 .....	106

## LIST OF SYMBOLS

In all equations presented in the text, the introduced symbols are defined immediately following the respective equations. The most commonly occurring symbols are listed below for reference purposes. Computer program symbolic names are provided in Appendix B.

- A = aggregate interlock shear modulus
- $A_1, A_2$  = coefficients
- $A', A_0$  = area enclosed by corner longitudinal reinforcement
- $A_c$  = cross-sectional area
- B = matrix relating finite element strains to nodal displacement
- b = beam width defined by corner stringers
- $b_n$  = net beam width
- c = crack width
- D = concrete constitutive matrix
- $D_b$  = bar diameter
- $D_f$  = dowel force at failure
- d = beam depth defined by top and bottom flange stringers
- E = initial elastic modulus for concrete
- $E_s$  = secant modulus for concrete
- $E_{st}$  = steel elastic modulus
- $F_{yl}$  = yield force of longitudinal stringers in bottom flange.
- $f_c'$  = ultimate concrete compressive strength
- $f_s$  = steel stress
- G = concrete shear modulus
- h = ultimate bending moment lever arm
- $K'$  = stiffness term

- $K_s$  = St. Venant torsion constant for closed cell
- $K_{s1}$  = St. Venant torsion constant for equivalent open cell
- $K_{s2}$  = St. Venant torsion constant proportional to additional torque arising from closing the equivalent open cell
- $k$  = finite element stiffness matrix
- $L_{av}$  = average crack width
- $M$  = bending moment
- $M_o$  = ultimate bending moment capacity
- $q$  = uniform shear flow
- $R_i$  = force at node  $i$
- $r_i$  = displacement at node  $i$
- $r$  = ratio of yield strength of top flange longitudinal reinforcement to bottom flange longitudinal reinforcement
- $S_y$  = yield force of hoop reinforcement
- $s$  = perimeter coordinate
- $T$  = St. Venant torque
- $T_o$  = ultimate torque capacity
- $T_{s1}$  = St. Venant torque resultant for an open cell
- $t$  = wall thickness
- $u, v$  = displacements in local  $x$  and  $y$  axis directions respectively
- $V$  = shear force
- $V_d$  = dowel force
- $V_o$  = ultimate shear force capacity
- $V_{po}$  = plastic shear force
- $v$  = uniform wall shear stress
- $W_{av}$  = average crack width
- $\Sigma Z_y$  = twice the sum of yield forces of longitudinal reinforcement in weaker flange

- $\sigma$  = direct stress
- $\sigma_p$  = ultimate concrete compressive strength
- $\epsilon$  = direct strain
- $\epsilon_c$  = concrete centroidal strain perpendicular to crack direction
- $\epsilon_p$  = concrete strain corresponding to  $\sigma_p$
- $\lambda'$  = constant
- $\alpha$  = ratio of orthogonal stress to stress in direction considered
- $\theta_{zi}$  = rotation at node i about Z axis
- $\phi_i$  = shape function for node i
- $\eta, \xi$  = orthogonal dimensionless coordinates
- $\nu$  = poisson ratio
- $\Delta_{crack}$  = shear displacement across crack
- $\alpha_s$  = angle of inclination of concrete compression struts
- $\cot\alpha_t$  = variable associated with ratio of longitudinal to transverse reinforcement areas

CHAPTER I  
-INTRODUCTION

1.1 Need for Research

Cellular construction in reinforced concrete is commonplace in current civil engineering practice as this method of construction is both functional and economically competitive. In addition, the flexibility permitted by the cast-in-situ technique enables box girders to assume any desired alignment, as illustrated by the varied configurations of the large number of skew and curved highway bridges. Where large structures are exposed to public scrutiny, the aesthetic appearance of box girder design is an especially valuable asset.

As the application of concrete box girder design becomes more diverse, greater demands are made of the civil engineer in the design of structures of increasing complexity. Thus, the incentive for research in the obscure fields of structural and material behaviour has gained momentum. An example of two such fields of research that have attracted international interest in the past decade is the torsion and shear strength of reinforced and prestressed concrete members.

The complexity of box girder behaviour that has frustrated designers of the past has gradually been diffused since the advent of computer technology. The evolution of computer-orientated analytical design methods has developed rapidly to the current level of sophistication where the capabilities of structural analysis are bounded by few

4.

restrictions. The elastic analysis of concrete box girder structures is now well refined, and research effort is presently being focused on the non-linear, post-cracking region of behaviour.

To this point in time, non-linear analytical methods of analysis have been developed to trace the complete load deformation path from the elastic uncracked state through to failure. However, the constituent behaviour of concrete in its cracked form has only come under close scrutiny in recent years, and a reasonably comprehensive understanding of its behaviour is only beginning to emerge. Thus, the logical progression is the development of an improved analytical computer model that incorporates and reflects the more accurate representation of material behaviour.

## 1.2 Thesis Objective and Scope

The principal objective of this thesis is the development of an analytical computer model that can analyze a prestressed concrete box girder of arbitrary cross-section for any loading combination of bending moment, torque, and shear. In addition to estimating cracking and ultimate loads, the complete stress-deformation description of the box girder is provided at any load level in the pre-cracked or post-cracked condition.

To assist in the assessment of the analytical model performance, seven prestressed double-cell concrete box girders were cast and tested under varying load combinations of torque, bending moment, and shear. Subsequently, each beam was analyzed by the computer model for the same

respective loading conditions. The accuracy of the analytical modelling was evaluated upon comparison of the computer model results with the corresponding experimental test results and available theoretical predictions.

## CHAPTER 2

### RESEARCH EVOLUTION

#### 2.1 Introduction

This section is not an exhaustive state of the art presentation, but simply an overview of research developments demonstrating the evolutionary progression that has occurred in experimentation and analysis in fields of study pertaining to this thesis topic. The five associated fields of research encompassed are the three loading types of bending moment, torque, and shear force, together with the nature of prestressed concrete and the characteristics of box girder behaviour.

#### 2.2 Review of Developments to Current State of Art

##### 2.2.1 Experimental Approach

In the infancy of examination of reinforced concrete behaviour, the complexity involved in formulating rational analytical solutions prompted an empirical approach. Detailed experimental programs were undertaken to develop an understanding of behavioural characteristics, and the recorded test data was used to develop and test methods of analysis and design.

The elastic performance and ultimate strength of reinforced concrete in bending have been investigated upon numerous occasions in the testing of scale models of geometrically complex structures. In certain instances, actual structures have been loaded to determine service load response. An example of a bending test to destruction of



a complex scale model is the experimental study of Bouwkamp, Scordelis, and Wasti<sup>1</sup>, in which a replica of a typical two-lane reinforced concrete bridge was cast and tested to failure.

An excellent example of a field of research where extensive experimental testing has been undertaken because of the difficulty in developing a rational analytical model, is the study of the shear strength of reinforced concrete members. Widespread interest in this topic has been sustained as the "shear failure" mechanism causes a reduction in the strength of structural elements below flexural capacity and a diminution of element ductility. To this point in time, the phenomenon is still not clearly understood, and consequently code provisions have been structured to prevent such a failure. In the past ten years, investigators have turned their attention away from the shear failure mechanism as an entity in itself, and have directed their research effort toward closer examination of the contributing shear components present across a concrete crack; aggregate interlock and dowel action. The aggregate interlock effect<sup>2,3,4</sup> has been researched extensively as has dowel action<sup>4,5,6,7</sup>, and a better understanding of the physical mechanics of shear transfer has now emerged. However, the scope of experimentation in examination of the latter two phenomena has been restricted in several respects, and the numerous publications of experimental results and interpretation are not in complete agreement. A relatively recent state of the art paper on the shear strength of reinforced concrete members is that of the joint ASCE-ACI Task Committee 426<sup>8</sup>, wherein all aspects of shear transfer are reviewed. Formulae in the latter paper, as well as those in the shear provisions of most building codes for reinforced concrete, have a purely empirical basis,

thus demonstrating the valuable contribution of experimental research in complex structural fields.

Closely associated with the study of shear is that of torsion of reinforced concrete members. Only in the last ten years has this avenue of research attracted considerable attention. Indeed, the dramatic explosion in technological advance in this area is evident upon comparison of the torsion provisions of the 1963 ACI Code to those of the 1971 ACI Code and CSA Standard A23.3. In a similar procedure to that adopted for shear, the development of torsion code provisions of the 1971 ACI Code was partially dependent upon experimental results<sup>9,10,11</sup>. The corresponding torsion clauses in the more recently published CSA Standard A23.3 are quite dissimilar, a different theoretical model having been adopted as a basis for torsion derivations. The respective theories for the two codes will be addressed in the following section. From an experimental aspect, test results that were used to substantiate the two theories were in reasonable correspondence but were interpreted differently.

Of paramount importance to the designer is the nature of interaction of all three loading types bending, torsion, and shear. As in the case of shear and torsion, comprehensive experimental programs<sup>11</sup> were undertaken to establish interaction curves for torsion and bending, and torsion and shear. The only interaction formulae for torsion and bending that were developed on a purely theoretical basis are those of Lampert<sup>12</sup>, and the ensuing discussion<sup>13</sup> of the proponents of the empirical and theoretical approach highlights the current state of the art of this topic.

Experimental programs<sup>14, 15, 16</sup> devoted to prestressed concrete research have been conducted in the same manner as that adopted for reinforced concrete. Essentially, the performance of the two reinforced concrete types is quite similar in that beams of concentrically prestressed and symmetrically reinforced concrete are analogous in behaviour, as are eccentrically prestressed and unsymmetrically reinforced concrete beams. Code provisions for torsion and shear of prestressed concrete members are empirically derived, and bear a close resemblance to the corresponding reinforced concrete clauses.

Behaviour of box girder members has come under closer scrutiny in recent years as a large percentage of concrete bridges are of the multi-cell box girder type. The box section has been favoured by many designers because of its aesthetic appearance, efficiency of cross-section, and high torsional rigidity. Since the experimental research of solid and single-celled reinforced concrete members is applicable in most facets of behaviour to box girder structures, research of multi-celled, hollow members has primarily been directed toward those behavioural aspects<sup>17</sup> peculiar to concrete box girder bridges. Such aspects include cross-section distortion, warping, shear lag<sup>18</sup>, and diaphragm action. Invariably, these aspects have not been isolated and studied individually, but have simply been incorporated collectively in the testing of scale models of concrete bridges<sup>1, 19</sup>.

2.2.2 Development of Theoretical Analyses

Up to the onset of cracking, stresses and deformations in a determinate prestressed concrete box girder of simple cross-section are readily evaluated for any loading combination. The assumptions that

the uncracked concrete behaves as a homogeneous, isotropic, elastic material, and the contribution of the reinforcement to the girder stiffness is small, do not constitute a severe approximation of the actual structural behaviour. However, if the cross-section is more complex (multi-celled), longitudinal warping restraint is present (boundary conditions or diaphragm action), or the structure is indeterminate, the simplified approach using classical elastic theory is not accurate, or may indeed be non-applicable. For such a situation, a more sophisticated solution procedure is required, often in the form of a computer-orientated method of analysis.

Upon the onset of cracking, the reinforcement assumes a vital role in carrying tensile stresses and achieving stress redistribution. Of the three loading types, bending, torsion, and shear, only bending action can presently be analyzed theoretically to yield complete deformation behaviour. At the current state of knowledge, shear still defies rational theoretical analysis, whereas several theoretical postulates have been presented to predict torsional behaviour.

The first recognized theoretical model to predict the torsional strength of reinforced concrete was that of Rausch<sup>20</sup>, whose model consisted of a network of bars to represent the action of reinforced concrete: compression concrete bars and tension bars for reinforcement. All reinforcement was assumed to yield simultaneously at failure. In time, this model was modified by Cowan<sup>21</sup> and Anderson<sup>22</sup> in assuming that the concrete carried a torque at failure equal to the cracking strength of an unreinforced beam. Subsequently, this approach was questioned by Hsu<sup>23</sup>, who maintained that real behaviour lay between the two extremes of that proposed by Cowan and Anderson and 1958 German Code approach

that assumed zero cracked concrete torsional strength. The basis of Hsu's research was the development of a modified skew bending model.

The first skew bending model was proposed by Lessig<sup>24</sup>, and is illustrated in Fig. 2.1. The depicted failure surface is comprised of an inclined compression zone and a warped failure plane delineated by a diagonally inclined crack connecting compression zone ends, the inclination of the compression zone being dependent on cross-sectional geometry and ratio of longitudinal to transverse steel areas. In proposing his modified skew bending model, Hsu drew attention to the fact that the Lessig theory, being an upper bound solution, considerably overestimated ultimate strength. Hsu's principal modifications were adjusting the shorter sides of the failure surface to intersect the flange-web interface at 90°, and neglecting the torsional contribution of the shorter stirrup legs. Criticism<sup>50</sup> of Hsu's skew bending theory stemmed from three reservations:

1. Several constants were difficult to evaluate.
2. Theory had to be adjusted for square beams.
3. Dowel action of longitudinal bars was indeterminable.

In recognizing that the skew bending theory was an upper bound solution that more accurately predicted ultimate bending strength rather than ultimate torsional strength, several researchers directed their efforts toward refining the space truss theory postulated by Rausch. To this point in time, the most widely accepted space truss theory is that developed by Lampert<sup>12</sup>, the theory presented in a form directly applicable to design by Collins and Lampert<sup>25</sup>. The space truss model adopted by Lampert is shown in Fig. 2.2, consisting of intermediate shear

walls and longitudinal reinforcement considered to be concentrated into stringers at the hoop reinforcement corners. In the shear walls, the stirrups act as posts and the concrete between the inclined cracks provides the compression diagonals. The angle of the diagonals with respect to the beam axis is assumed to be constant for each side. In the walls that govern failure, the angle is such that both the longitudinal and stirrup reinforcement reach their respective yield points simultaneously. For this reason, the model is a space truss of variable diagonal inclination. The most attractive feature of Lampert's space truss theory is the simplicity of the design equations<sup>25</sup> that now form the basis of the torsion sections in the Canadian Code, CSA Standard A23.3. However, the theory is not completely general as

1. cross-section must be underreinforced,
2. model cannot accommodate shear,
3. only St. Venant torsion can be modelled (no support or load warping restraint)

Criticism of the Collins and Lampert theory is summarized comprehensively in the discussion<sup>13</sup> of the authors' paper<sup>26</sup> wherein they stated that the problem of torsion and bending was basically solved.

Thus far, only the strength predictions of theoretical analyses have been reviewed. The aspects of post-cracking stiffness and inelastic member deformation have not been addressed. The importance of these two latter aspects is paramount since the calculation of equilibrium torsional moments in a statically indeterminate structure requires not only statics but also compatibility conditions. As a point<sup>25</sup> of clarification, an equilibrium torque is one required to

maintain equilibrium in a structure, in contrast to a compatibility torque that maintains structural compatibility. Both Hsu<sup>27</sup> and Collins and Lampert<sup>25</sup> have proposed post-cracking stiffness formulae that are derived on the basis of their respective theories. Two important qualifications of Hsu's theoretical approach are that the analysis hinges on the empirical derivation of an equivalent wall thickness for solid and "thick walled" cross-sections, and applicability of the theory to non-rectangular sections is not verified.

The theories of both Hsu and Lampert are restricted to the pure torsion condition.

### 2.2.3 Analytical Computer Solutions

In the study of complex modern structures such as box girder bridges, dams, and prestressed concrete nuclear containment vessels, the experimental approach adopted in the past is becoming an increasingly expensive method of investigation. Thus, the empirical approach is gradually being superseded by refined analytical computer-orientated methods. Not only does the analytical method offer a considerable saving in terms of time, but the progressive improvement in computer technology permits the development of computer programs of increasing complexity.

In the context of the analysis of box girder bridges, the numerous analytical methods and models that have been developed fall into two categories; those that model behaviour prior to cracking, and those that model the complete structural behaviour to failure.

Of those methods that have been developed for the uncracked section, approximate methods of analysis based on simplified structural behaviour, such as the equivalent beam grillage or anisotropic slab methods,

have been used to model structural systems. Of a more precise nature, elaborate methods based on folded plate theory have been developed by several researchers, the most prominent sustained research program having been conducted by Scordelis et alia<sup>28,29</sup> at the University of California, Berkeley. In the adaptation of the folded plate theory to the analysis of box girder bridges, each component plate of the box girder is considered as an assemblage of individual elements, the bending of each plate normal to its plane being analyzed by plate flexure theory, and the in-plane bending analyzed by plane stress theory. These classical theories necessitate the representation of the applied loading by a Fourier Series, with the result that computational effort is considerable though less than that of a finite element solution. In an effort to reduce the number of equations and thus reduce computing time and programming effort, the 'finite strip method' has been proposed by Cheung<sup>30</sup>. In this method, the behaviour of each plate is approximated by an assemblage of longitudinal finite strips for which selected displacement patterns are assumed to represent the behaviour of the strip in the total structure. An additional advantage of this simplified method is that more complex material properties such as concrete anisotropy can be readily introduced. However, both the folded plate and finite strip methods are very much more restricted in their range of application than the finite element method as the two methods can only be applied to box girders of constant cross-sectional geometry. The greater flexibility is achieved at the expense of computational effort. In finite element studies, it should be recognized that the accuracy achieved is dependent upon assumptions of material properties and fineness of the structural mesh subdivisions. Generally, results closely satisfy compatibility, but not necessarily equilibrium in the continuum unless a sufficiently



fine mesh is used. An array of computer programs<sup>31</sup> has been developed at the University of California, Berkeley, to analyze box girder bridges of arbitrary plan and general cross-section.

Beyond cracking, material behaviour and structural interaction are complex. Consequently, analysis is almost exclusively performed by the finite element method. Accurate analytical determination of the stress-deformation condition of a reinforced concrete structure at a certain stage of cracking is complicated by

1. Structural response is governed by the interaction of two component materials - steel and concrete.
2. Stress-strain relationships for concrete and reinforcement are non-linear, with the concrete exhibiting anisotropy.
3. Shear transfer phenomena of aggregate interlock and dowel action together with bond slip must be considered.
4. Failure criteria for concrete under biaxial stress conditions, dowel action, and bond slip have to be established.
5. Because of non-linear material properties, equilibrium is not easily maintained, and considerable iteration must be performed within load increments.
6. Transverse rigidity and warping resistance of actual diaphragms, as well as the intrinsic transverse rigidity of the box section, must be included.
7. Dramatic load reversal can occur upon application of the first load increment after prestress transfer.

The initial development of the application of the finite element method to the analysis of reinforced concrete beam behaviour


was undertaken at the University of California. In the earliest publication of the application of the finite element method, Ngo and Scordelis<sup>32</sup> analyzed simple beams in which the concrete and steel reinforcement were represented by two-dimensional triangular finite elements, and special bond linkage elements were used to connect reinforcement to concrete. Linear elastic analyses were performed on the beams with predefined crack patterns to determine principal stresses in the concrete, and stress levels in the reinforcement and bond linkages. Since the initial publication of Ngo and Scordelis, the flexibility and capability of the finite element method in this particular application has advanced dramatically<sup>33</sup> to the point where most of the seven stipulated complications have now been successfully incorporated. Such an analytical computer model is that developed by Trikha and Edwards<sup>34</sup>.

## 2.3 Definition of Thesis Approach

### 2.3.1 Analytical Model Aspect

In recognition of the complexity encountered in the analysis of prestressed concrete box girders in the uncracked and cracked states, a finite element analytical approach has been adopted in determination of both strength and deformation characteristics. In addition to evaluating strength-deformation values at both the cracking and ultimate loads, the analytical model yields a comprehensive description of the structural behaviour for the complete load range. Generality of loading is assured in that the external loads can reflect any ratio of bending moment to torque to shear, and the nature of the loading pattern can be altered at any point in the loading sequence.

Analytical flexibility of the proposed model in a structural mechanics context is exemplified by its ability to simulate:

1. Interaction between the two material components - steel and concrete. 
2. Any reinforcement pattern of conventional steel and prestress strand.
3. Non-linear material behaviour.
4. Presence of diaphragms and the cross-sectional shear rigidity of the box girder section.
5. Shear transfer across concrete cracks.

In essence, the strength of the computer model approach is its comparative freedom from analytical and structural constraint.

#### 2.3.2 Experimental Aspect

To evaluate the analytical model performance, a limited experimental program was undertaken in which the test specimens were subjected to varying combinations of bending moment, torque, and shear. To be more representative of concrete box girders employed in practice, all test specimen cross-sections were multi-celled, and of either rectangular or trapezoidal shape. The higher degree of complexity of test specimen cross-sectional geometry also provided a more rigorous basis of comparison for the computer model.

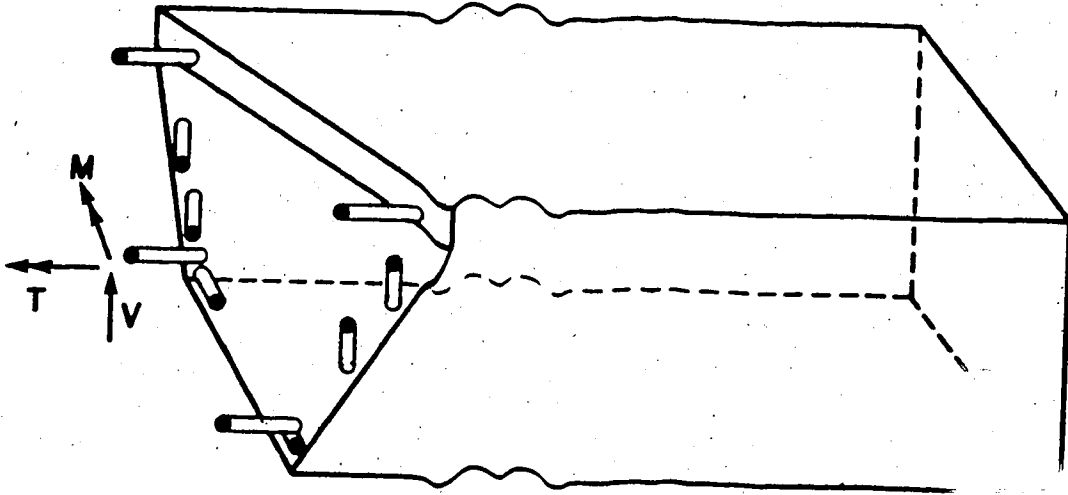


FIG. 2.1 SKEW BENDING MODEL

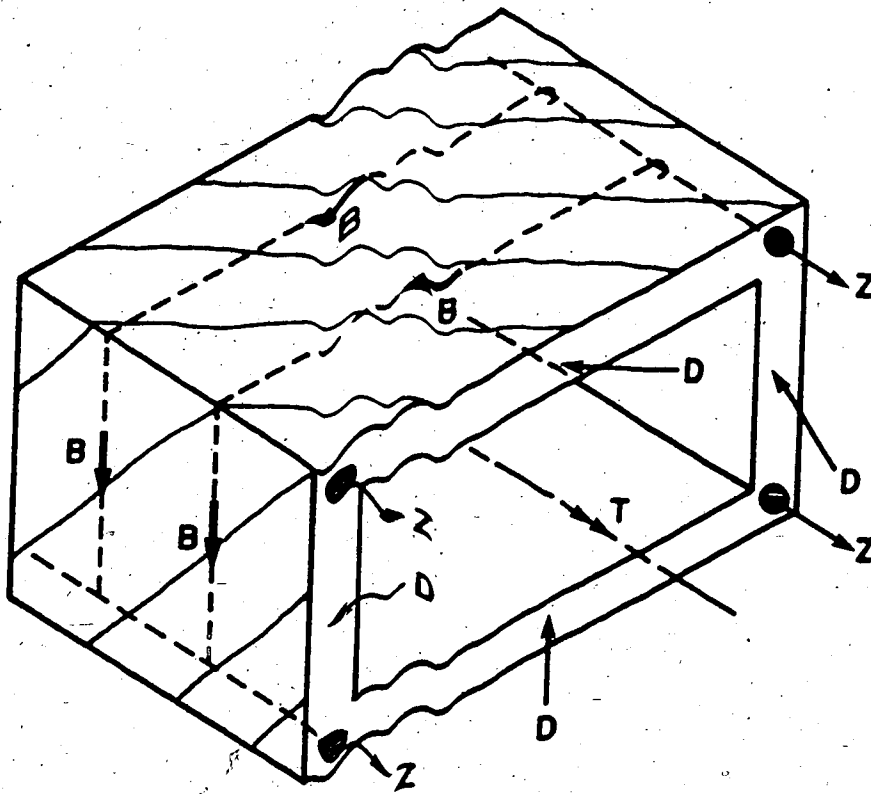


FIG. 2.2 SPACE TRUSS MODEL

## CHAPTER 3

### ANALYTICAL COMPUTER MODEL

#### 3.1 Introduction

As the complexities of structural behaviour have come under closer scrutiny, more exacting analytical methods have been developed in an effort to overcome past analytical failings or restrictions. Research in structural engineering has often turned to the analytical model as the most appropriate method of investigating complex structural behaviour. Such is the approach in this thesis to the study of the action of prestressed concrete box girders under the combined loading of torque, bending moment, and shear.

Of the analytical methods that are most commonly used in the analysis of concrete box girders, only four are capable of representing the most important characteristics of box girder behaviour, those characteristics being longitudinal bending, St. Venant torsion, transverse distortion, longitudinal warping, and shear lag. Folded plate theory, finite strip theory, finite element theory, and shell theory all yield satisfactory results in an elastic analysis, but only the finite element method is capable of simulating the inelastic behaviour of concrete in its uncracked and cracked states. Primarily for this reason, a finite element approach has been adopted. A simplified finite element mesh similar to those employed in this analysis is exhibited in Fig. 3.1.

In the development of the computer model, the following capabilities have been incorporated:

1. Representation of any general, thin-walled cross-section comprised of linear segments.
2. Representation of any in-plane loading system (prestressing included).
3. Complete description of beam behaviour in the elastic and inelastic regions up to ultimate failure.
4. Accurate portrayal of material response to the action of torsion, bending, and shear in both uncracked and cracked concrete regimes.
5. Ability to model both diaphragm action and the transverse rigidity of a box girder without diaphragms.

The coding of the analytical computer model whose main program and subroutines are listed in Appendices B and C respectively, is written in the Fortran IV language compatible with IBM System/360 and System/370. All computer analyses were achieved through the use of the Amdahl 470 computer at the University of Alberta Computing Centre, and the several system subroutines utilized by the program are public library routines.

### 3.2 Finite Element Types Employed

#### 3.2.1 Concrete Wall Element

The principal design characteristic of concrete box girders is the structural efficiency achieved by the absence of the central concrete core, thus significantly reducing the member's dead weight with a small loss of strength. As a consequence of the void, the thickness of concrete walls that define the girder's cross-sectional geometry is

usually moderately small compared with the member's depth and width. When the wall thickness is comparatively small such that it can be defined as being "thin", the box girder cross-section can be envisaged as an assemblage of flat plates, or in the analytical model as a mesh of appropriate plane stress finite elements.

Since it is most desirable for the sake of economy and efficiency that the concrete box girder walls be modelled by plane stress elements, the classification as to whether a wall thickness is "thick" or "thin" is a prime concern. Thus, it is most appropriate that this issue be examined in detail. In the following derivation, a single cell, uniformly thick box girder will be considered, as exhibited in Fig. 3.2(a).

For a thin-walled single cell, the uniform shear flow is given by

$$q = \frac{T}{2A'} \quad (3.1)$$

in which  $T$  = applied torque, and  $A'$  = area enclosed by corner longitudinal bars.

Consequently, the uniform wall shear stress is defined by

$$v = \frac{T}{2A't} \quad (3.2)$$

in which  $t$  = wall thickness.

However, the St. Venant torsion constant  $K_s$  for a closed cell is comprised of two components; i.e.,

$$K_s = K_{s1} + K_{s2} \quad (3.3)$$

in which  $K_{s1}$  = torsion constant for the equivalent open cell, and  $K_{s2}$  = torsion constant proportional to the additional torque arising from closing an open cell.

Referring to Eq. 3.3, the St. Venant torsion constant for the uniform shear flow of the closed cell is expressed by

$$K_s = \frac{(2A')^2}{\oint \frac{ds}{t}} \quad (3.4)$$

in which  $s$  = perimeter length coordinate for the closed cell cross-section, and

$$K_{s1} = \frac{1}{3} \int bt^3 \quad (3.5)$$

in which  $b$  = cross-sectional segment length of thickness  $t$ .

Therefore, for the closed single cell shown in Fig. 3.2(a), the St. Venant torsion resultant for the equivalent open cell is given by

$$T_{s1} = \frac{K_{s1} T}{K_s} \quad (3.6a)$$

Substituting for  $K_{s1}$  and  $K_s$ ,

$$\begin{aligned} T_{s1} &= \frac{\frac{1}{3} \int t^3 ds \oint \frac{ds}{t} T}{(2A')^2} \\ &= \frac{t^2 (b+d)^2 T}{3b^2 d^2} \end{aligned} \quad (3.6b)$$

in which  $b$  and  $d$  are the cross-sectional dimensions as shown in Fig. 3.2(a).

With reference to Fig. 3.2(b), the torque per unit length developed by the equivalent open cell shear stress distribution is given by



$$\Delta T_{sl} = \frac{\Delta v t^2}{6} \quad (3.8)$$

in which  $\Delta v$  = variation in wall shear stress from mid-thickness to surface.

For the complete cell,

$$\begin{aligned} T_{sl} &= \frac{1}{6} \phi \Delta v t^2 ds \\ &= \frac{1}{3} \Delta v t^2 (b+d) \end{aligned} \quad (3.9)$$

Equating the right hand sides of Eq. 3.7 and Eq. 3.9 yields

$$\Delta v = \frac{(b+d) T}{b^2 d^2} \quad (3.10)$$

From Eq. 3.2,

$$v = \frac{T}{2bd t} \quad (3.11)$$

Therefore, the ratio of the variation in the wall shear stress distribution from the mid-thickness to the surface, to the uniform shear stress is given by

$$\begin{aligned} \frac{\Delta v}{v} &= \frac{2(b+d) t}{bd} \\ &= \frac{A_c}{A^*} \end{aligned} \quad (3.12)$$

where  $A_c$  = cross-sectional area of cell.

Thus, the definition of a "thin-walled" box girder hinges on the degree of variation in the shear stress distribution that is acceptable. Many authorities postulate a threshold value of 10% that distinguish a "thick" from a "thin" box girder wall.

In employing plane stress rather than three-dimensional finite elements, the total number of degrees of freedom, and thus equations of equilibrium, is reduced considerably. As the computer model will be used to analyze only uniform beams of rectangular and trapezoidal cross-sections in this particular study, a rectangular finite element was chosen as the basic concrete wall element. The higher order rectangular finite element has three degrees of freedom per node, namely two in-plane translational degrees of freedom and a rotational degree of freedom orthogonal to the element plane.

To reduce computing costs, the behaviour of each rectangular concrete finite element is characterized by the stress-strain condition at the centroid of the element. Although this simplification approximates real behaviour, the degree of the approximation will be demonstrated to be of minor significance.

A detailed description of the rectangular finite element chosen for this analytical model is given in Section 3.3.

### 3.2.2 Reinforcement Element

The three distinct types of reinforcement represented in the computer model are:

1. Prestress reinforcement.
2. Conventional bar reinforcement.
3. Bond spring linkage.

All three are modelled by a one-dimensional constant strain finite element whose equations of equilibrium are given below:

$$\begin{pmatrix} R_i \\ R_j \end{pmatrix} = \begin{bmatrix} K' & -K' \\ -K' & K' \end{bmatrix} \begin{pmatrix} r_i \\ r_j \end{pmatrix} \quad (3.13)$$

where  $R_i, R_j$  = forces at nodes  $i$  and  $j$  respectively,  $K'$  = stiffness term, and  $r_i, r_j$  = displacements at nodes  $i$  and  $j$  respectively.

The nature and derivation of the reinforcement element stiffness elements  $K'$  will be treated in detail in Section 3.4.2.1.

### 3.2.3 Diaphragm Elements

Since the inception of box girder design, the need was recognized for the provision of transverse plates to strengthen the girders' cross-sectional rigidity, distribute shears from webs to bearings over supports, and to prevent excessive cross-sectional distortion. In practice, all box girders have diaphragms over supports, while the number of intermediary diaphragms varies considerably depending upon the span and cross-sectional shape.

Since the prime function of the diaphragm finite element in the analytical model is to provide cross-sectional shear rigidity, a lower-order element is quite satisfactory. To accommodate both the rectangular and trapezoidal cross-sectional shapes, the diaphragm element chosen is a bi-linear isoparametric serendipity element, as shown in Fig. 3.3. This element possesses two translational degrees of freedom per node, eight degrees of freedom in all per element, with the displacement vector defined by:

$$\begin{pmatrix} u \\ v \end{pmatrix} = \begin{bmatrix} \langle \phi \rangle & 0 \\ 0 & \langle \phi \rangle \end{bmatrix} \begin{pmatrix} \underline{u} \\ \underline{v} \end{pmatrix} \quad (3.14)$$

$$\text{where shape function } \phi_i = \frac{1}{4} (1+\eta_i \eta) (1+\xi_i \xi) \quad (3.15)$$

where  $i$  is the node number and  $(\xi_i, \eta_i)$  are the non-dimensional nodal coordinates.

The geometric coordinates  $(x, y)$  are mapped in the  $x$ - $y$  plane using the same shape functions as above.

$$\langle x \ y \rangle = \langle \phi \rangle_g [\underline{x} \ \underline{y}] \quad (3.16)$$

where

$$\phi_{ig} = \frac{1}{4} (1+\eta_i \eta) (1+\xi_i \xi) \quad (3.17)$$

Thus, the analytical model is capable of representing the stiffness for a diaphragm of any quadrilateral geometry. Derivation of the stiffness of a bi-linear isoparametric serendipity element is detailed by Zienkiewicz<sup>35</sup>. In the course of the computer program logic, the stress-strain condition of the diaphragm elements is not monitored as all diaphragm elements are assumed to remain elastic. A listing of the coding of the appropriate subroutines is given in Appendix D.

In accurately representing diaphragm action, three distinct behavioural aspects are addressed. Firstly, the in-plane action of actual diaphragms is incorporated through the use of the bilinear finite element with a full concrete constitutive matrix. Secondly, the transverse rigidity of a box girder length without diaphragms is represented by equivalent diaphragm elements similar to the above, the distinguishing feature being that only a shear stiffness term is present in the constitutive matrix. This aspect is treated in detail in Section 3.4.2.9. The third and last aspect of diaphragm action introduced into the analytical model is the out-of-plane warping restraint developed by actual diaphragms. Within the computer model, those serendipity

elements representing actual diaphragm segments contribute predetermined longitudinal stiffness terms to the total beam stiffness matrix at each of the element's four corner nodes. However, derivation of the warping restraint at the corner nodes is dependent upon the classification of the diaphragm thickness as being "thick" or "thin". The two respective warping derivations are fully treated in Sections 3.4.2.7 and 3.4.2.8.

### 3.3 Choice of Plane Stress Concrete Wall Element

Three plane-stress rectangular finite elements were conspicuous in a literature search for an appropriate concrete finite element to be utilized in the analytical model; the element's prerequisites were established in 3.2.1. The three elements were:

1. McCleod element<sup>36</sup>
2. Scordelis element<sup>37</sup>
3. Sisodiya and Ghali element<sup>38</sup>

Of the three plane-stress elements represented in the Sisodiya and Ghali paper<sup>38</sup>, parallelogram element PQC3 was chosen for this comparative investigation.

The method of comparison adopted in choosing the most suitable element simply involved the modelling of identical single-cell concrete girders using each of the above elements, the box girders being subjected to loading patterns of torque, bending moment, and shear. The analysis was strictly elastic, with material behaviour simplified by omitting reinforcement and approximating concrete stiffness as being linear and isotropic. To assess convergence and accuracy, three finite element meshes of varying degrees of refinement, as shown in Fig. 3.4, were used.

As a basis of comparison, both stress-strain and deformation predictions were considered. The stress predictions for the application of a simple bending moment and a pure St. Venant torque, both uniform over the central length of the beam, are plotted in Figs. 3.5(a) and 3.5(b) respectively. All three elements perform equally well in both estimating direct stress and shear stress levels, and converging to the respective theoretical values. The vertical deflection of the central beam cross-section arising from the application of bending moment, and the differential rotation of the central beam length subjected to a uniform St. Venant torque, are given in Table 3.1 for each of the three element types. As in the first basis of comparison, no particular element was significantly superior to another in its accuracy.

In a closer scrutiny of the results, the Sisodiya-Ghali element was observed to have yielded an upper bound estimate to the theoretical bending deformation. Since deformation characteristics are of prime concern in the principal analytical model, this element was considered the least preferable. In choosing between the Scordelis and McCleod elements, inter-element displacement compatibility was the criterion selected as a basis of comparison. Whereas the Scordelis element does not consistently exhibit complete displacement compatibility<sup>37</sup>, the choice of the nodal rotational degrees of freedom and the displacement functions for the McCleod element is such that full boundary compatibility is achieved. Thus, the McCleod element was chosen as the marginally preferable plane stress finite element for this application.

To satisfy the requirement of complete displacement compatibility, two McCleod finite element types are employed. For each element type, the rotational degrees of freedom are defined alternately as either

$\theta_{z1} = \left(\frac{\partial v}{\partial x}\right)_1$  or  $\theta_{z1} = \left(\frac{-\partial u}{\partial y}\right)_1$ , the rotation at node 1 of element type 1 being defined as  $\theta_{z1} = \left(\frac{\partial v}{\partial x}\right)_1$ , and the rotation at node 1 of element type 2 defined as  $\theta_{z1} = \left(\frac{-\partial u}{\partial y}\right)_1$ . By allocating element types such that adjacent elements have different type designations, each element node will have a unique rotation. Figures 3.6(a) and 3.6(b) illustrate element types 1 and 2 respectively, and an element assemblage for a two dimensional beam is displayed in Fig. 3.6(c).

The McCleod displacement functions chosen to satisfy boundary compatibility are

$$u = A_4 + A_7x + A_6y + A_{12}xy + A_1y^2 + A_{10}xy^2 \quad (3.18)$$

$$v = A_5 + A_8x + A_2y + A_3xy + A_9x^2 + A_{11}x^2y \quad (3.19)$$

in which  $A_i$  = coefficients numbered in such an order to facilitate inversion of [A] matrices.

Maintenance of boundary compatibility is demonstrated as follows. For  $y = \text{constant} = k$ , the displacements will have the form

$$u = (A_4 + kA_6 + k^2A_1) + (A_7 + kA_{12} + k^2A_{10})x \quad (3.20)$$

$$v = (A_5 + kA_2) + (A_8 + kA_3)x + (A_9 + kA_{11})x^2 \quad (3.21)$$

In this example,  $u$  is a linear function of  $x$  and can be defined by 2 nodal translations in the  $x$  direction, and  $v$  is a quadratic function of  $x$  and can be defined by two nodal translations in the  $y$  direction together with the single edge rotation  $\theta = \frac{\partial v}{\partial x}$ . Similarly, nodal displacements are uniquely defined along  $x = \text{constant}$  boundaries. Thus, displacement compatibility is maintained across element boundaries and throughout the structure.

The stiffness formulation of the McCleod finite element chosen differs from the original derivation through shifting the origin of the element's local axes to the centroid, and changing the node numbering sequence. In adopting these two changes, the matrices  $[A]^{-1}$  for element types 1 and 2 (Table 1)<sup>36</sup> have had to be reformulated. The redefined matrices are given in Table 3.2. It should be noted that the element dimensions have been redefined as  $(2A \times 2B)$  as illustrated in Figs. 3.6(a) and 3.6(b).

The plane stress constitutive relationship is defined as

$$\{\sigma\} = [D]\{\epsilon\} \quad (3.22)$$

Thus, the element stiffness matrix  $[k]$  is given by the relationship

$$[k] = [A^{-1}]^T [\bar{k}] [A^{-1}] \quad (3.23)$$

in which

$$[\bar{k}] = \int_{vol} [B]^T [D] [B] dx dy dz \quad (3.24)$$

$[B]$  is the matrix relating element strains to element nodal displacements.

### 3.4 Computer Program Description

#### 3.4.1 General Characteristics

This finite element computer program has been developed as an analytical model to predict the behaviour of prestressed or reinforced concrete box girders subjected to torsion, bending, and shear. Complete stress-strain and deformation information is provided at any specified load level in both the uncracked and cracked states up to the point of girder failure.



Finite elements employed in the program consist of rectangular plane stress concrete elements, one-dimensional reinforcement elements, and plane stress quadrilateral diaphragm elements. Provision is included within the program to represent the presence of a reinforcing steel mesh within any of the concrete elements. Those reinforcement elements whose bond with the adjoining concrete elements is suspect to deterioration during loading, are connected to adjacent concrete nodes through bond spring linkages whose stiffnesses are modified as loading progresses. At every beam cross-section delineated by concrete element nodes, equivalent diaphragm elements are introduced to simulate the box beam's transverse cross-sectional rigidity.

Any loading pattern can be superimposed upon the analytical model through the judicious choice of nodal force combinations, the only restriction being that force directions cannot be orthogonal to plane stress concrete elements. The presence of prestress forces is readily accommodated.

To accurately reproduce concrete behaviour, the program is capable of modelling non-linear material characteristics. Naturally, non-linearity is not restricted solely to concrete, as the prestress and conventional reinforcement and bond spring linkages all exhibit non-linear behaviour. The loading sequence is an incremental one consisting of the superposition of successive load increments. Following the application of each load increment, all material elements are checked for deviation from their pre-defined behavioural paths, the probability of deviation occurring being reduced through the use of the Runge-Kutta method. If significant deviation is detected, equilibrium

is restored using the modified Newton-Rapson iterative method. Probability of material deviation within a subsequent load increment is reduced by modifying all element stiffnesses at the end of the current load increment using a tangent stiffness formulation. A detailed description of the latter method of stiffness adjustment and the Runge-Kutta method is given in Section 3.4.4.

To solve the large set of equilibrium equations efficiently, a banded-block solution process has been adopted. At any instant of the solution process, only two stiffness blocks of half-band width are stored in core. Efficient transmission of the stiffness blocks in and out of core storage is achieved through the use of public library system subroutines provided by the University of Alberta Computing Services.

The non-linear behaviour of a rectangular concrete element under bi-axial stresses is characterized by the stress-strain condition at the centroid of the element. Once the principal tensile centroidal stress exceeds the concrete tensile strength, the concrete element is designated as cracked, the crack direction thereafter remaining fixed. The crack inclination is derived from the centroidal stress conditions at cracking. If the monitored crack width should close immediately following prestress transfer, the element is once again designated as an uncracked element. In reconstituting the stiffness of the concrete element following cracking, the aggregate interlock and dowel effects are taken into account in determining the shear rigidity across the crack. At all but the lowest stress levels, concrete behaves as an anisotropic material.

At the conclusion of each load increment, all elements are checked to detect local failure. Structural failure occurs when one of the principal prestress strand elements fails in tension or a concrete element crushes. In reality, the modelled structure might well not have failed under the above circumstances, but its full load carrying capacity will have been attained and its subsequent highly inelastic behaviour will indicate imminent collapse. Should failure not have occurred following the application of the load increment, a comprehensive summary of stress, strain, and deformation values will be printed out.

To enable large program runs to be monitored during their execution, several duplicate print statements were inserted in the output subroutine. The fully comprehensive output for each load increment is assigned to a high speed printing device, whereas simultaneously, a dramatically smaller representative output is viewed on a terminal screen that can subsequently assume the role of the controlling device. Termination of execution of the program can be prompted once irregular behaviour is observed.

### 3.4.2 Simulation of Material Behaviour

#### 3.4.2.1 Concrete Stiffness Under Bi-axial Stresses:

Derivation of the concrete constitutive matrix under bi-axial stress conditions closely follows the research of Liu, Nilson, and Slate<sup>39</sup>. The form of the stress-strain equations for concrete under uniaxial or biaxial stress conditions, and the resulting constitutive matrix proposed by the above authors are easily incorporated in an incremental iterative finite element analysis as developed in this thesis.

The stress-strain relationship for concrete under biaxial stresses is given by the equation

$$\sigma = \frac{\epsilon E}{(1-\nu\alpha) \left[ 1 + \left( \frac{1}{1-\nu\alpha} \frac{E}{E_s} - 2 \right) \left( \frac{\epsilon}{\epsilon_p} \right) + \left( \frac{\epsilon}{\epsilon_p} \right)^2 \right]} \quad (3.25)$$

in which  $\sigma$  = stress in direction considered,  $\epsilon$  = strain in direction considered,  $E$  = initial modulus,  $\nu$  = Poisson's ratio,  $\alpha$  = ratio of orthogonal stress to stress in direction considered,  $\sigma_p$  = ultimate compressive strength,  $\epsilon_p$  = strain at point of ultimate strength, and  $E_s = \frac{\sigma_p}{\epsilon_p}$ .

Liu, Nilson, and Slate state that the equation is applicable to concrete in biaxial compression only, but in this analysis, the equation is used in biaxial compression and compression-tension conditions, where in the latter state the orthogonal principal stress is tensile.

For uniaxial loading, the above equation simplifies to:

$$\sigma = \frac{\epsilon E}{1 + \left( \frac{E}{E_s} - 2 \right) \left( \frac{\epsilon}{\epsilon_p} \right) + \left( \frac{\epsilon}{\epsilon_p} \right)^2} \quad (3.26)$$

This theoretical equation was compared to the experimental results of a concrete cylinder tested during the experimental program. The two curves exhibited in Fig. 3.7 correspond closely, demonstrating the reasonably accurate approximation of the above equation to real behaviour.

The two distinct load conditions encountered in the analytical model are the incremental and total load cases. In the formulation of the concrete constitutive matrix, the stiffnesses in the two orthogonal principal directions are derived on a tangent moduli basis for incremental

loading, and a secant moduli approach during the iterative process when the total loading condition prevails. Thus, the concrete constitutive matrix is expressed in the form:

$$\begin{bmatrix} \sigma_1 \\ \sigma_2 \\ \sigma_{12} \end{bmatrix} = \begin{bmatrix} \lambda' \frac{E'_{1b}}{E'_{2b}} & \lambda' \nu_1 & 0 \\ \lambda' \nu_1 & \lambda' & 0 \\ 0 & 0 & \frac{E'_{1b} E'_{2b}}{E'_{1b} + E'_{2b} + 2E'_{2b} \nu_1} \end{bmatrix} \begin{bmatrix} \epsilon_1 \\ \epsilon_2 \\ \epsilon_{12} \end{bmatrix} \quad (3.27a)$$

in which

$$\lambda' = \frac{E'_{1b}}{\left(\frac{E'_{1b}}{E'_{2b}} - \nu_1^2\right)} \quad (3.27b)$$

and where in the total loading condition,

$$E'_{1b} = \frac{E}{1 + \left[\frac{1}{(1-\nu\alpha_1)} \frac{E}{E_s} - 2\right] \left(\frac{\epsilon_1}{\epsilon_p}\right) + \left(\frac{\epsilon_1}{\epsilon_p}\right)^2} \quad (3.27c)$$

for biaxial compression and compression tension. However, in a uniaxial compression state

$$E'_{1b} = \frac{E}{1 + \left(\frac{E}{E_s} - 2\right) \left(\frac{\epsilon_1}{\epsilon_p}\right) + \left(\frac{\epsilon_1}{\epsilon_p}\right)^2} \quad (3.27d)$$

while for biaxial tension, tension compression, and uniaxial tension conditions,

$$E'_{1b} = E \quad (3.27e)$$

During the application of load increments,

$$E'_{1b} = \frac{E[1 - (\frac{\epsilon_1}{\epsilon_p})^2]}{\{1 + [\frac{E}{(1 - \nu\alpha_1)E_s} - 2] (\frac{\epsilon_1}{\epsilon_p}) + (\frac{\epsilon_1}{\epsilon_p})^2\}^2} \quad (3.27f)$$

for biaxial compression and compression tension. For the uniaxial compression state

$$E'_{1b} = \frac{E[1 - (\frac{\epsilon_1}{\epsilon_p})^2]}{[1 + (\frac{E}{E_s} - 2)(\frac{\epsilon_1}{\epsilon_p}) + (\frac{\epsilon_1}{\epsilon_p})^2]^2} \quad (3.27g)$$

while for biaxial tension, tension compression, and uniaxial tension conditions,

$$E'_{1b} = E \quad (3.27h)$$

$E'_{2b}$  is defined in a similar manner to  $E'_{1b}$ .

In defining concrete moduli under biaxial stress conditions, the nature of the two associated orthogonal principal stresses is the criterion used in establishing the biaxial state. However, such a definition is misleading if one principal compressive stress is much larger than its orthogonal compressive stress such that the strain in the orthogonal direction is tensile. Since the behaviour of concrete is characterized in such a conflicting situation by its strain state, not stress state, a condition of biaxial compression only prevails when the strain in the two principal strain directions is compressive. In its application to the analytical model, use of a principal strain rather than principal stress criterion changes the concrete moduli little, as the tangent stiffness of concrete in compression at low stress levels is close to the initial tangent modulus.

3.4.2.2 Concrete Crack Width: Janjua and Welch<sup>4v</sup> propose that the concrete crack width be given by:

$$W_{av.} = L_{av.} \cdot \frac{(f_s - 3)}{E_s} \cdot R \quad (3.28)$$

where  $L_{av.}$  = average crack spacing,  $R$  = ratio of extreme fibre distance from neutral axis to distance of steel centroid to neutral axis,  $f_s$  = steel stress, and  $E_s$  = steel elastic modulus.

$$L_{av.} = 1.5t + 3D \quad (3.29a)$$

in which  $t$  = concrete cover and  $D$  = bar diameter.

All the above variables are in kip and inch units.

Unfortunately, the above formulation does not lend itself readily to inclusion within the analytical model logic as the term  $R$  is not easily determined. Moreover, the average crack spacing expression shown above does not accurately predict the test beam observations. Consequently, elaborate formulations were discarded in preference for the simple expression:

$$W_{av.} = \epsilon_c \cdot L'_{av.} \quad (3.29b)$$

in which  $\epsilon_c$  = finite element centroidal direct strain perpendicular to crack direction and  $L'_{av.}$  = observed average crack spacing.

3.4.2.3 Aggregate Interlock: Once plain concrete cracks, shear is still able to be transmitted across the crack through interlock of the two adjacent rough surfaces. The level of shear that can be transferred, however, has been a subject of constant conjecture and

research in the development of analytical models. The wide diversity of opinion is reflected in the two opposing schools of thought that support the Space Truss and Skew Bending Analogies.

Whereas a common approach<sup>41</sup> has been to assume that a constant percentage of the concrete shear strength is retained after cracking, the treatment of the aggregate interlock effect in this analytical model is based on the research conducted by Houde and Mirza<sup>4</sup>. The influence of the three parameters of crack width, concrete strength, and maximum aggregate size on the shear rigidity modulus was examined, and the results lead to the development of the relationship:

$$A = 57 \cdot \left(\frac{1}{c}\right)^{3/2} \cdot \sqrt{\frac{f_c'}{5000}} \quad (3.30)$$

where A = shear rigidity modulus and c = crack width.

All of the above variables are expressed in inch pound units. As observed in the above expression, the effect of aggregate size was found to be negligible.

The expression above was derived from experimental measurements made in the range of crack widths of  $2 \times 10^{-3}$  to  $20 \times 10^{-3}$  inches. Crack widths smaller than  $2 \times 10^{-3}$  were difficult to accurately control. In the uncertain region beyond  $\frac{1}{c} = 500$ , the authors have suggested that the curve for the rigidity modulus is asymptotic to the line  $A = G$  (shear modulus of uncracked concrete) for large values of  $\frac{1}{c}$ . Such a supposition does seem severe, however, and thus the equation for A has been applied to the range of  $\frac{1}{c} > 500$  in the absence of research that indicates otherwise. The curve for the rigidity modulus intersects the line  $A = G$  close to  $\frac{1}{c} = 1000$ .



3.4.2.4 Dowel Effect: In bridging across the concrete crack, reinforcement not only restricts the widening of the crack such that substantial aggregate interlock can develop, but also offers shear resistance normal to its axis. This shear resistive force developed in the reinforcement is termed the "dowel force". Since the dowel effect is only significant across cracks that have experienced considerable shear displacement, reinforcement must be highly stressed in tension to develop dowel action. Principal longitudinal tension reinforcement in an underreinforced beam is such an example.

The research of Houde and Mirza<sup>4</sup> is used in quantitatively defining dowel stiffness. The dowel load-displacement relationship is given by:

$$V_d = 2000 \cdot D_f \cdot \Delta_{\text{crack}} \quad (3.31)$$

where  $V_d$  = dowel force,  $\Delta_{\text{crack}}$  = shear displacement across crack, and  $D_f$  = dowel failure force.

$$D_f = 40 b_n (f'_c)^{1/3} \quad (3.32)$$

in which  $b_n$  = net beam width.

All units are in pounds and inches. Embedment length, bar size or arrangement, and axial stress in reinforcement below yield do not have a pronounced effect upon dowel action.

Appraisal of the effect of parameters in addition to those already mentioned is given in other publications. The effect of inclination of reinforcement to crack direction on dowel strength was investigated by D. Ska... and although an expression was derived for

the dowel failure force, a simple theoretical relationship could not be found for deformations. Bauman's<sup>42</sup> research demonstrated that positioning of stirrups between a diagonal crack and the support did not increase the dowel strength if the distance between crack and stirrup exceeded 2.5 cms. Also, the same author stated that dowel action was not influenced by crack width or concrete cover.

Upon the commencement of splitting along the reinforcement, dowel action deteriorates. The level of residual dowel action in such circumstances is very much dependent on stirrup spacing, but the precise behaviour is difficult to define. In this analytical model, dowel strength after splitting is considered negligible. Dowel failure occurs when the dowel displacement  $\Delta_{\text{crack}}$  exceeds  $5 \times 10^{-4}$  inches.

3.4.2.5 Cracked Concrete Stiffness: The concrete constitutive matrix for a cracked finite element is of the form:

$$\begin{pmatrix} \sigma_1 \\ \sigma_2 \\ \sigma_{12} \end{pmatrix} = \begin{bmatrix} 0 & 0 & 0 \\ 0 & E_2 & 0 \\ 0 & 0 & G' \end{bmatrix} \begin{pmatrix} \epsilon_1 \\ \epsilon_2 \\ \epsilon_{12} \end{pmatrix} \quad (3.33)$$

where  $\sigma_1$  is the principal tensile stress that acts in the direction normal to the crack. Since the concrete stiffness in this direction has been set to zero, the stress in the direction of  $\sigma_1$  will consequently be zero. In the direction of the principal compressive stress, the stress-strain relationship is given by Equations 3.27d and 3.27g in 3.4.2.1 as a uniaxial loading condition now prevails.

The cracked shear modulus  $G'$  is comprised of two contributions;

the aggregate interlock and dowel stiffnesses. The former is readily evaluated at the centroid of a concrete element as described in Sections 3.4.2.2 and 3.4.2.3. In its form presented in the preceding section, the dowel force stiffness developed in the reinforcement is not in the units of shear modulus. Therefore, the following procedure has been adopted. Upon calculation of the crack width and centroidal shear strain parallel to the crack, the dowel displacement  $\Delta_{\text{crack}}$  is evaluated. The subsequently calculated dowel force  $V_d$  is then considered uniformly distributed over the element's cracked concrete surface whose area is given by the product of the element thickness and the length of the inclined crack that passes through the centroid and extends from element boundary to boundary. The equivalent dowel shear modulus is added to the aggregate interlock rigidity modulus to define the equivalent cracked concrete shear modulus  $G'$ .

In the formulation of  $G'$ , the presence of stirrups is neglected, and all dowel stiffness contributions are calculated disregarding deviation from perpendicular inclination of reinforcement to the crack direction.

3.4.2.6 Warping Resistance of Thin Concrete Diaphragms: The out-of-plane warping resistance at the corners of a thin concrete plate is derived in most theory of elasticity texts<sup>43</sup>. For a square diaphragm element, the out-of-plane warping stiffness matrix is of the form below:

$$\begin{pmatrix} R_{1x} \\ R_{2x} \\ R_{3x} \\ R_{4x} \end{pmatrix} = \begin{bmatrix} X & -X & X & -X \\ -X & X & -X & X \\ X & -X & X & -X \\ -X & X & -X & X \end{bmatrix} \begin{pmatrix} r_{1x} \\ r_{2x} \\ r_{3x} \\ r_{rx} \end{pmatrix} \quad (3.34)$$

where  $R_{1x}$  = force at node 1 in a direction perpendicular to the element's plane,  $X$  = corner warping stiffness, and  $r_{1x}$  = displacement at node 1 corresponding to force  $R_{1x}$ .

$$X = \frac{Et^3}{3(1 + \nu) k^2} \quad (3.35)$$

in which  $E$  = concrete elastic modulus,  $t$  = thickness, and  $k$  = length of element's diagonal.

The off-diagonal stiffness terms in Eq. 3.34 have the same magnitude as the main diagonal terms since the plate was visualized as being simply supported at each of its four corners in the derivation of the warping restraint forces. Rectangular or quadrilateral diaphragm elements are treated as square elements of the same area in computing warping restraint.

#### 3.4.2.7 Warping Restraint of Thick Concrete Diaphragms:

Since the classical theory of plates formulation for diaphragm warping resistance given in the preceding section is valid only for "thin" plates, the distinction between "thick" and "thin" plate thicknesses must be made. Theoretically, no method of distinction is currently available. An additional qualification of the classical approach is that the derivation is developed for a square plate. Thus, an approximation is immediately introduced if the formulation is applied to non-square diaphragm shapes.

To analytically simulate actual diaphragm action, a finite element model was developed that permitted complete generality of diaphragm shape and thickness. To accommodate a complete range of possible diaphragm thicknesses, an assemblage of three dimensional

bi-quadratic serendipity finite elements was used to represent the presence of diaphragms. Upon comparing the corner end warping displacements of two identical double cell box beams (illustrated in Fig. 3.8), one beam being restrained longitudinally by end diaphragms, the diaphragm warping stiffness at its four corners was derived as a function of the box beam warping resistance. The warping resistance equation is of the form:

$$R_{wd} = \left( \frac{w_b}{w_d} - 1 \right) R_{wb} \quad (3.36)$$

where  $R_{wd}$  = corner warping stiffness of diaphragm,  $w_b$  = warping displacement of unrestrained box beam corner,  $w_d$  = corresponding warping displacement of box beam corner restrained by diaphragm, and  $R_{wb}$  = corner warping stiffness of unrestrained box beam.

The analytical model results and the corresponding classical plate derivations for a particular test beam are illustrated in Fig. 3.9. As expected, the classical approach dramatically overestimates the warping resistance for thick diaphragms, but even for smaller thicknesses, there is not good agreement between the two formulations. For thicknesses smaller than 2 inches, the dramatic divergence of the approaches is not significant as both predict negligible diaphragm warping restraint compared with that of the box beam. For thicknesses exceeding 2 inches, it is apparent that the classical approach does not give accurate correspondence with actual diaphragm behaviour as represented with a reasonable degree of accuracy by the finite element method. Consequently, for the beam cross-sectional geometry used in this comparison, the geometry being that of the five rectangular beams tested

in the experimental program, the finite element approach is the more preferred method for modelling diaphragm behaviour.

The diaphragm corner out-of-plane warping stiffnesses derived by the above approach are readily incorporated in the principal analytical computer model. Throughout the analysis, it is assumed that the diaphragms behave elastically.

3.4.2.8 Shear Rigidity of Equivalent Diaphragms: In modelling a rectilinear box girder cross-section as an assemblage of plane stress finite elements, no account has been taken of the girder's intrinsic cross-sectional distortion rigidity. At a cross-section in the analytical model where an actual diaphragm is not provided, externally applied loads will not be distributed correctly unless an equivalent diaphragm is introduced. Evaluation of the shear rigidity of an equivalent diaphragm is treated in detail by Sawko and Cope<sup>44</sup>. In the formulation of the element stiffness matrix, the only non-zero term in the constitutive matrix is the shear modulus. Thus, the function of the equivalent diaphragm is twofold in preserving both cross-sectional geometry and real structural performance.

3.4.2.9 Concrete-Reinforcement Bond: Assumption of perfect bond between reinforcement and concrete can result in significant error<sup>45</sup> in analytical modelling. Thus, the concept of bond spring linkages connecting reinforcement and concrete elements was developed, wherein the loss of adhesion between concrete and steel is represented by a softening of the spring stiffness. Nilson<sup>45</sup> was the first to introduce a non-linear bond-slip relationship into a finite element analysis, and subsequent extensive research investigations in this field, as that

conducted by McCutcheon, Mirza and Mufti<sup>49</sup>, used similar modelling systems to that of Nilson. The adopted equation relating bond stress to bond spring elongation used in stiffness formulation is that given by Houde and Mirza<sup>4</sup>. In both the incremental and total load cases, the bond spring linkage stiffness is the product of the bond stress curve slope<sup>4</sup> and the contributing circumferential area of the reinforcement bar to which the bond linkage is attached. Failure of the bond spring occurs when the spring elongation exceeds .0012 inches.

3.4.2.10 Reinforcement Stiffness: To simplify the analytical representation of reinforcement bars, bi-linear stress-strain curves have been assumed for both conventional and prestress reinforcement, as shown in Fig. 3.10.

Below yield, the stiffness of both reinforcement types in the incremental and total load cases is given by the respective moduli of elasticity. Beyond yielding, the slope of the strain hardening segment of the stress-strain curve defines the incremental reinforcement stiffness. However, in the total load condition that prevails in the iterative process, the method of stiffness derivation for the conventional and prestress reinforcement differs. Since the slope of the strain hardening section of the conventional reinforcement stress-strain curve is highly inelastic, an excessive number of modified Newton-Rapson iterations are often required to restore equilibrium. If the set of equations were large, this approach could be highly impractical. Therefore, once a conventional reinforcement bar has yielded in the total load condition, it is represented in the analytical model by a bar of zero stiffness, the load carried by the bar being represented by equivalent external loads applied at the bar nodes. Following such a stiffness change,

The strain in the yielding bar will increase as the load is maintained, but the magnitude of the equivalent bar loads will increase only slightly. Thus, at a particular load level, no iteration is required to restore an acceptable degree of equilibrium to the yielding bars. This approach cannot be applied, however, to the yielding of the prestress reinforcement. Prestress reinforcement constitutes the underreinforced beam's last reserve of strength, and setting of its stiffness to zero will immediately produce instability. Thus, the modified Newton-Rapson method is retained for modelling yielding prestress reinforcement in the total load condition. Use of a relaxation factor has been introduced to improve the rate of convergence of prestress strand deviation.

#### 3.4.3 Failure Criteria

Of the two material constituents, concrete and reinforcing steel, the failure characteristics of concrete are complex and warrant clarification. In establishing the tensile and compressive strengths of concrete under biaxial stress conditions, Kupfer, Hilsdorf, and Rüschi<sup>4,6</sup> have postulated a biaxial stress envelope illustrated in Fig. 3.11. In addition to specifying biaxial stress failure combinations, the authors also established that the Poisson ratio in biaxial tension, biaxial compression, and tension-compression were .18, .2, and an average value of .19 respectively. The simplified envelope used in the analytical model is shown in Fig. 3.12. Beyond cracking, the shear rigidity across a concrete crack is developed by the aggregate interlock and dowel mechanisms. In the absence of relevant information, the failure stress level for the aggregate interlock mechanism has been set equal to the uniaxial concrete compressive strength. Under actual test conditions, the evaluated aggregate interlock stress has not been found



to rise beyond 750 p.s.i.<sup>4</sup>. Dowel linkage and the concrete-related bond spring linkage failure criteria are specified in preceding Sections 3.4.2.6 and 3.4.2.9 respectively.

In a total structure context, failure in the analytical model is defined as having occurred when a concrete element has crushed or a major prestress reinforcement element has failed in tension.

#### 3.4.4 Numerical Methods

The three numerical methods that perform vital functions in the analytical model are the block-by-block gaussian elimination solution process, Runge-Kutta, and modified Newton-Rapson methods.

To reduce the size of the allocated core storage area used in the equation solution process, only two stiffness blocks are retained in core at any one time. After a stiffness block has been reduced by gaussian elimination, it is written onto auxiliary disc storage, and the following unreduced stiffness block is subsequently read into core. If an efficient method of transfer of the large data sets in and out of core storage is used, this block-by-block solution process is ideally suited to the solution of large equation systems. Logic details are given in the listing of subroutine SOLVE in Appendix D.

The area of application of the Runge-Kutta method is the progressive adjustment of the structural stiffness as the external loads are applied incrementally. Figure 3.13(a) illustrates the procedure. Using the stiffness of the material element in the previous (n-1)th. load increment, defined by the slope of line AB, the stress-strain state upon application of half of the current nth. load increment is calculated,

denoted by point C. The tangent stiffness at the corresponding point D on the predefined stress-strain curve for the material is subsequently adopted as a reasonable prediction of the average material element stiffness for the nth. load increment. Upon superposition of the full nth. load, the stress-strain state at the end of the nth. increment is established, denoted by point E. Thus, the Runge-Kutta method of stiffness prediction improves program efficiency through minimizing the need for the time-consuming iterative process that must be invoked if significant material non-linearity occurs.

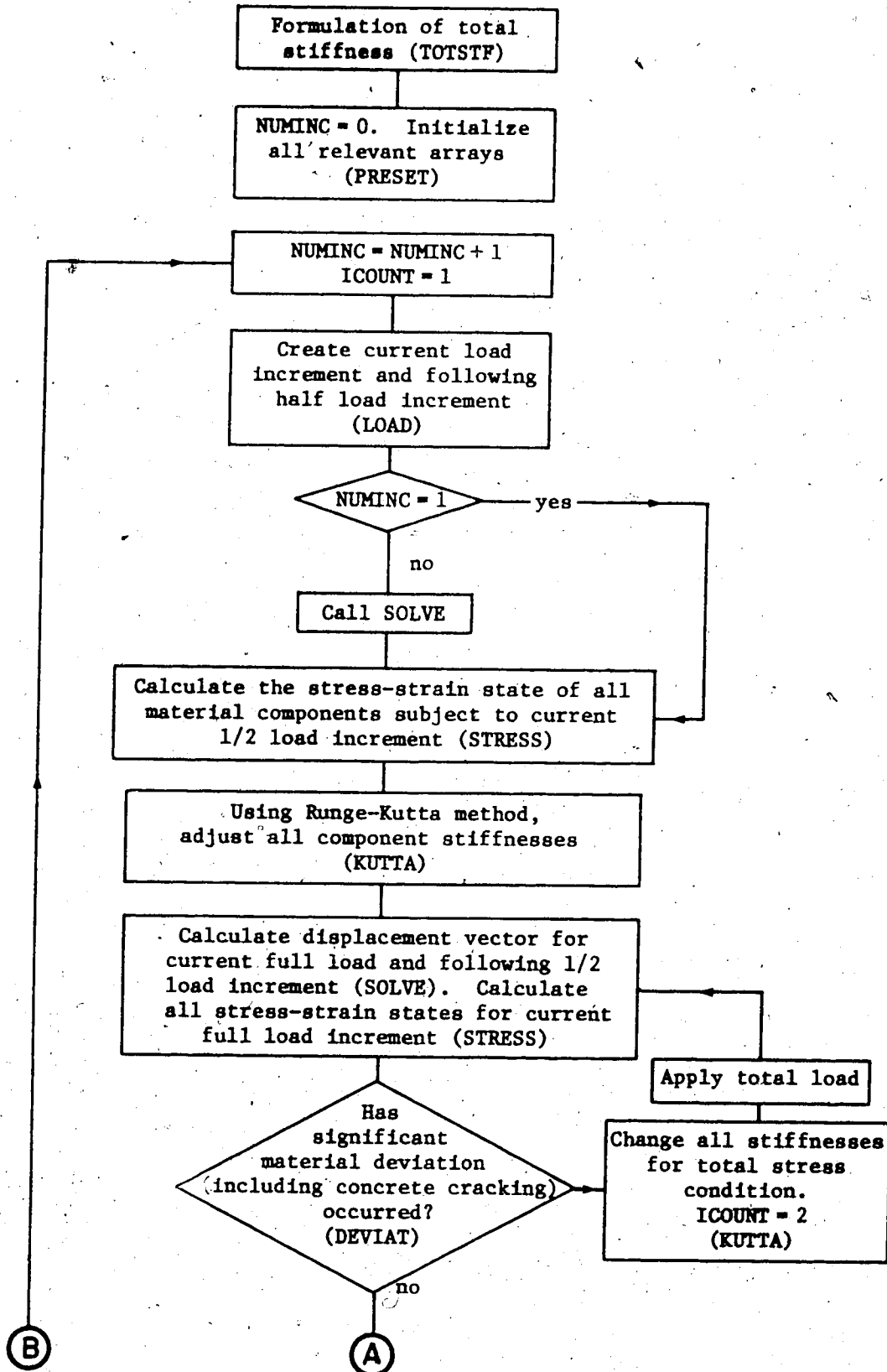
Should deviation at the end of a load increment be significant, equilibrium is restored by employing the iterative modified Newton-Rapson method. After reducing the deviation of point Q in Fig. 3.13(b) to an acceptable level, denoted by point R, the tangent stiffness at point S is the initial estimate of increment stiffness used in the Runge-Kutta stiffness adjustment for the nth. load increment.

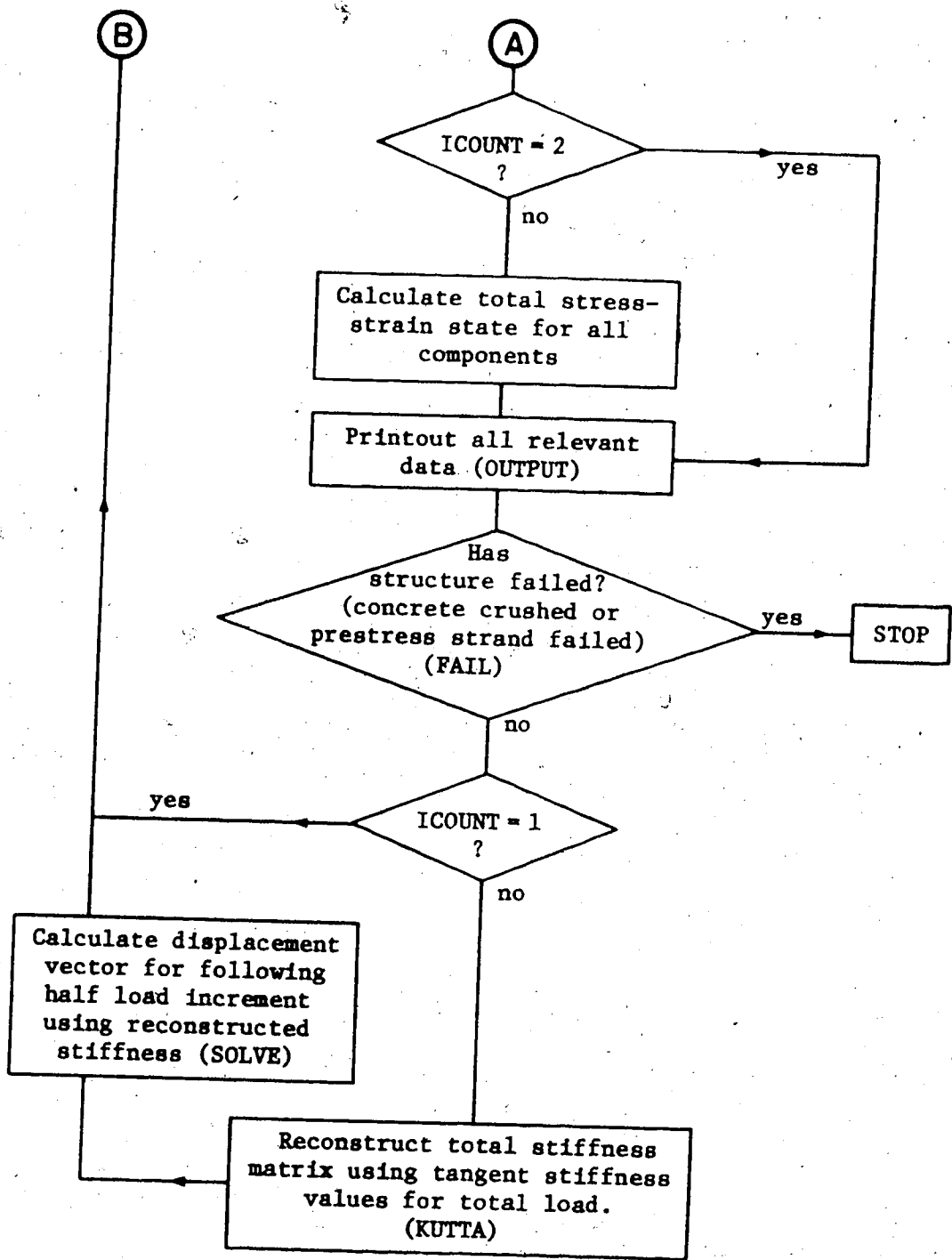
Both the Runge-Kutta and modified Newton-Rapson techniques are treated in detail in most applied mechanics texts<sup>47</sup> that address non-linear behaviour.

#### 3.4.5 Flow Chart for Main Program

In the flow chart that follows, the logic skeleton of the main program is presented, the symbolic names in brackets designating the subroutines that accomplish the defined logic steps. Further logic clarification is supplied by the numerous comment cards distributed through the main program, whose listing is given in Appendix C.

## FLOW CHART FOR MAIN PROGRAM





### 3.4.6 Derivation of Subroutine Logic

Logic development notes of the more complex subroutines comprise Appendix E.

## 3.5 Program Usage

### 3.5.1 Capabilities and Restrictions

#### (A) Beam Geometry

The program has been developed for the analysis of concrete box girder structures with modest wall thicknesses, but any wall thickness can be accommodated with the qualification that accuracy of solution will be prejudiced for "thick" walls, as detailed in 3.2.1. Cross-sectional geometry can assume any form that can be represented by linear segments, but in the program's present form, no geometry change is permitted along the beam's length. Such a shortcoming can be remedied by replacing the rectangular concrete finite element by a general quadrilateral element<sup>38</sup>.

#### (B) Material Behaviour

To reduce computational effort, the behaviour of a concrete element is characterized by the stress-strain condition at the element's centroid. For modestly fine meshes of high order elements, this approach is an acceptable approximation. Uncracked concrete is modelled as a heterogeneous, anisotropic, non-linear material, but cracking introduces two phenomena associated with the definition of shear rigidity across a crack, namely aggregate interlock effect and dowel action. As cracking progresses, the stiffness of these two contributions are modified in addition to the concrete stiffness in the parallel crack

direction. The closing of cracks produced by dramatic load reversal in the load increment following prestress transfer, and the superposition of a different loading type (torque upon bending load) is also within the program's capability.

The two principal reinforcement types, conventional steel and prestress strand, are modelled by one-dimensional finite elements. Consequently, a continuous reinforcement bar is represented by a series of segments of constant stress, producing a step-like variation in bar force. In direct contrast, steel mesh reinforcement is considered to be uniformly distributed throughout a concrete element, and its stiffness is formulated in an identical manner to that for a rectangular concrete finite element. The stress-strain curves for all three reinforcement types are approximated by multi-linear functions.

In the development of the finite element mesh, the mechanism of force transfer at the steel-concrete interface is simulated by bond spring linkages connecting adjacent steel and concrete nodes. As loading progresses, the stiffness of the bond spring is adjusted to reflect the gradual deterioration in concrete bond.

Should significant material behavioural deviation be detected within a load increment, an iterative process is automatically initiated, and proceeds until equilibrium is restored.

### (C) Loading and Boundary Conditions

Any loading or boundary condition combination can be imposed upon the analytical model provided that the appropriate degrees of freedom are present. In specifying load magnitudes, the subsequent number of load increments should not be small such that the computationally

expensive iterative process is invoked frequently. Provision for application is not restricted to external test loads, since both prestressing and post-stressing techniques can be represented by equivalent model forces.

#### (D) Diaphragms

The presence of diaphragms of any thickness and the intrinsic cross-sectional deformation resistance of the hollow beam are two important components of box girder behaviour, and both characteristics are incorporated in the program logic. Throughout the entire load range, diaphragm action is assumed to be elastic.

#### (E) Printout Information

Through the use of output control parameters, the precise nature of the printed output can be specified in a selective qualitative and quantitative manner, as detailed in 3.5.4.

#### (F) Program Monitoring

Provision is made within the program for transmission of output information to a monitoring device such as a CRT display terminal. In the running of large problems, the user has the option of observing program progress and controlling the rate of execution in the event that erroneous results may prompt run termination, thus reducing unnecessary complete run expense.

### 3.5.2 Structure Discretization

Figure 3.13 illustrates the finite element mesh chosen to model three double-cell prestressed concrete rectangular box beams tested in the experimental program. In specifying structural geometry, the global x axis must be parallel to the beam's longitudinal centroidal axis.

### 3.5.3 Input Specifications

In the preparation of the input data file, reference should be made to Appendix H in which a detailed card-by-card description of the input data is given, together with implicit logic assumptions that have a direct bearing on data activation. For ease of preparation, the input format is semi-free field, as illustrated in Appendix F which lists a sample input data file.

### 3.5.4 Output Description and Interpretation

The form of the printed output is governed by the choice of the output control variables described in Appendix H. Independent of specified controls, increment headings are printed, together with local material failure messages and progressive CPU and program cost estimates. For each load increment, structure deformations, concrete centroidal stresses and strains in the global and principal axes directions, steel mesh and bar reinforcement stresses and strains, and increment and total load levels can be selectively printed on an element or category basis. Units of pounds wt., inches, and radians are used throughout.

In the interpretation of output deformations, all values correspond to displacements in structural degree of freedom directions. The results must be processed further to determine cross-sectional rotation, beam curvature, and other such descriptive deformations.

For both concrete and steel mesh elements, all stress and strain estimates are derived for the centroidal element location. Since the reinforcement bar element is one-dimensional, the respective stress-strain values are constant for the element's length. Structural failure is defined as occurring when a concrete element crushes or a prestress strand fails in tension. Thus, the failure statement that immediately



precedes run termination is only of two possible forms. However, structural failure can develop through instability, such a failure mode resulting in the formation of an ill-conditioned set of equilibrium equations. Under such a situation program progress ceases when a negative term is encountered on the main diagonal of the total stiffness matrix during the reduction process.

Since the success of the finite element method of analysis is reflected in the quality of the program input, careful consideration should be given to the evaluation of the numerous strength of materials parameters, in particular those that have a strong influence on post-cracking behaviour.

Element Type	McCleod	Scordelis	Sisodiya-Ghali
% Below Theoretical Bending Deflection	+1.55	+ .6	-3.43
% Rotation Variation w.r.t. Theoretical Value	1.97	1.04	2.0

TABLE 3.1 DEFORMATIONS CONSIDERED IN CONCRETE FINITE ELEMENT SELECTION

$\frac{1}{8B^2}$		$-\frac{1}{8B^2}$	$-\frac{1}{4B}$	$\frac{1}{8B^2}$	$-\frac{1}{8B^2}$	$\frac{1}{4B}$
	$-\frac{3}{8B}$	$-\frac{A}{4B}$	$\frac{1}{8B}$	$\frac{3}{8B}$	$-\frac{A}{4B}$	$-\frac{1}{8B}$
	$\frac{1}{4AB}$		$-\frac{1}{4AB}$	$\frac{1}{4AB}$		$-\frac{1}{4AB}$
$\frac{1}{8}$		$\frac{3}{8}$	$\frac{B}{4}$	$\frac{1}{8}$		$\frac{3}{8}$
	$\frac{3}{8}$	$\frac{A}{4}$	$\frac{1}{8}$	$\frac{3}{8}$	$-\frac{A}{4}$	$\frac{1}{8}$
$-\frac{1}{4B}$		$\frac{1}{4B}$		$\frac{1}{4B}$		$-\frac{1}{4B}$
$-\frac{1}{8A}$		$-\frac{3}{8A}$	$-\frac{B}{4A}$	$\frac{1}{8A}$		$\frac{3}{8A}$
	$-\frac{1}{4A}$		$-\frac{1}{4A}$	$\frac{1}{4A}$		$\frac{1}{4A}$
	$-\frac{1}{8A^2}$	$-\frac{1}{4A}$	$\frac{1}{8A^2}$	$-\frac{1}{8A^2}$	$\frac{1}{4A}$	$\frac{1}{8A^2}$
$-\frac{1}{8AB^2}$		$\frac{1}{8AB^2}$	$\frac{1}{4AB}$	$\frac{1}{8AB^2}$		$-\frac{1}{8AB^2}$
	$-\frac{1}{8A^2B}$	$\frac{1}{4AB}$	$\frac{1}{8A^2B}$	$-\frac{1}{8A^2B}$	$\frac{1}{4AB}$	$-\frac{1}{8A^2B}$
$\frac{1}{4AB}$		$-\frac{1}{4AB}$		$\frac{1}{4AB}$		$-\frac{1}{4AB}$

TABLE 3.2(A). [A]<sup>-1</sup> FOR ELEMENT TYPE 1

$\frac{-1}{8B^2}$	$\frac{1}{4B}$	$\frac{1}{8B^2}$	$\frac{-1}{8B^2}$	$\frac{-1}{4B}$	$\frac{1}{8B^2}$
	$\frac{-1}{8B}$		$\frac{3}{8B}$	$\frac{A}{4B}$	$\frac{1}{8B}$
	$\frac{1}{4AB}$		$\frac{-1}{4AB}$		$\frac{1}{4AB}$
$\frac{3}{8}$	$\frac{-B}{4}$	$\frac{1}{8}$	$\frac{3}{8}$	$\frac{B}{4}$	$\frac{1}{8}$
	$\frac{1}{8}$		$\frac{3}{8}$	$\frac{A}{4}$	$\frac{1}{8}$
$\frac{-1}{4B}$		$\frac{1}{4B}$	$\frac{1}{4B}$		$\frac{-1}{4B}$
$\frac{-3}{8A}$	$\frac{B}{4A}$	$\frac{-1}{8A}$	$\frac{3}{8A}$	$\frac{B}{4A}$	$\frac{1}{8A}$
	$\frac{-1}{4A}$		$\frac{-1}{4A}$		$\frac{1}{4A}$
	$\frac{1}{8A^2}$		$\frac{-1}{8A^2}$	$\frac{-1}{4A}$	$\frac{1}{8A^2}$
$\frac{1}{8AB^2}$	$\frac{-1}{4AB}$	$\frac{-1}{8AB^2}$	$\frac{-1}{8AB^2}$	$\frac{-1}{4AB}$	$\frac{1}{8AB^2}$
	$\frac{-1}{8A^2B}$		$\frac{-1}{8A^2B}$	$\frac{-1}{4AB}$	$\frac{1}{8A^2B}$
$\frac{1}{4AB}$		$\frac{-1}{4AB}$	$\frac{1}{4AB}$		$\frac{-1}{4AB}$

TABLE 3.2(B)  $[A]^{-1}$  FOR ELEMENT TYPE 2

DOUBLE CELL  
TRAPEZOIDAL  
BOX BEAM

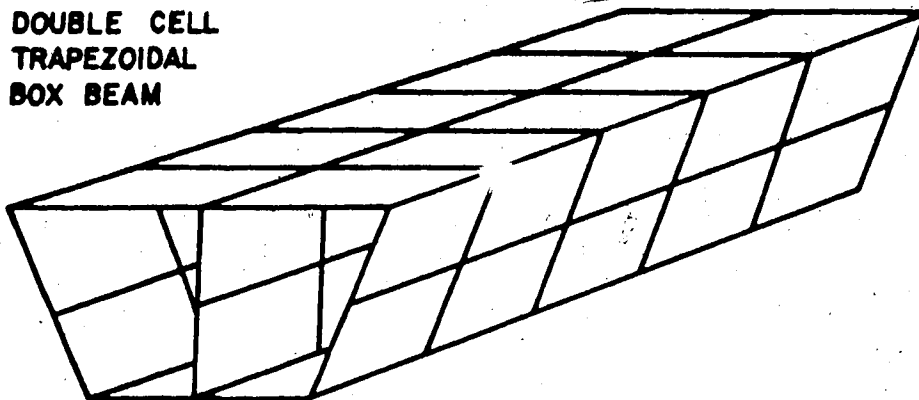
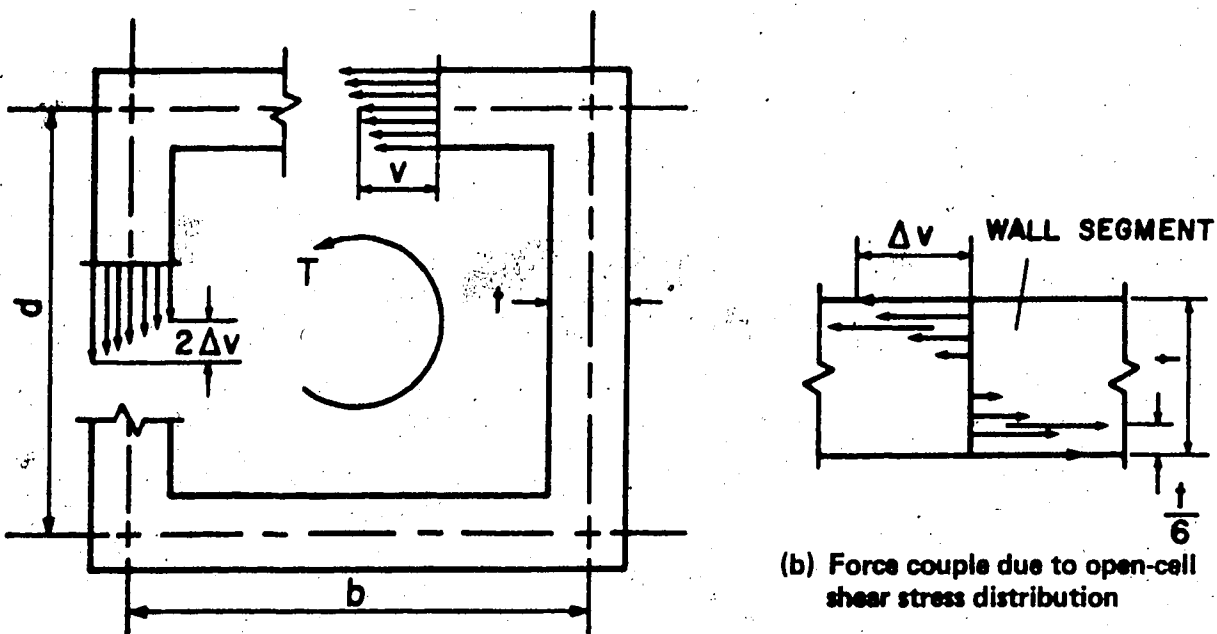


FIG. 3.1 SIMPLIFIED REPRESENTATIVE FINITE ELEMENT MESH



(a) Single-celled box girder

(b) Force couple due to open-cell shear stress distribution

FIG. 3.2 NOTATION FOR DERIVATION OF ST. VENANT SHEAR STRESS DISTRIBUTION

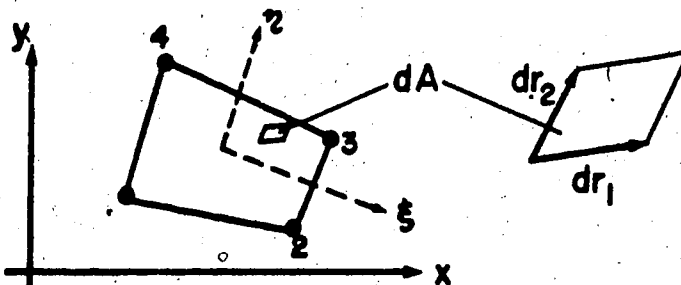
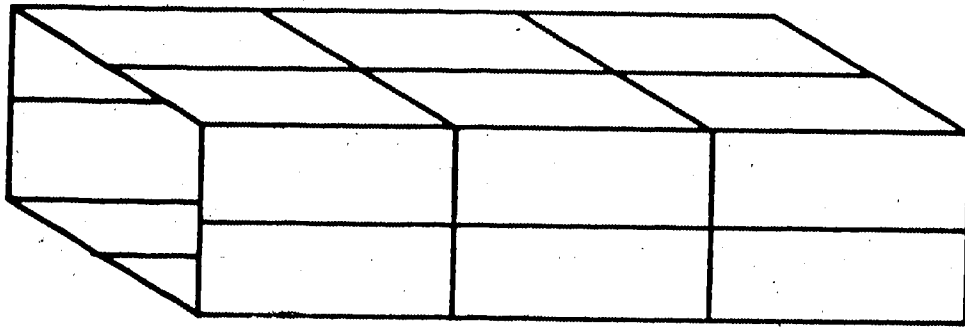
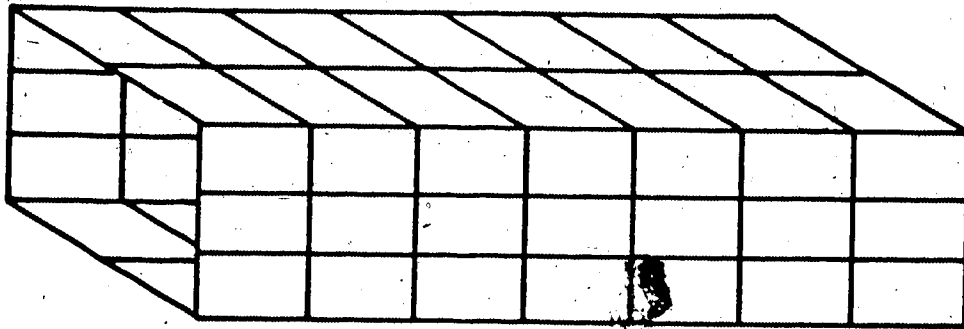


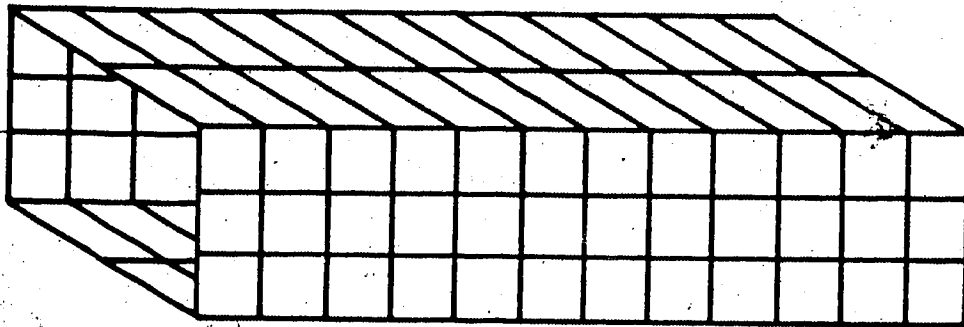
FIG. 3.3 BI-LINEAR ISOPARAMETRIC SERENDIPITY FINITE ELEMENT



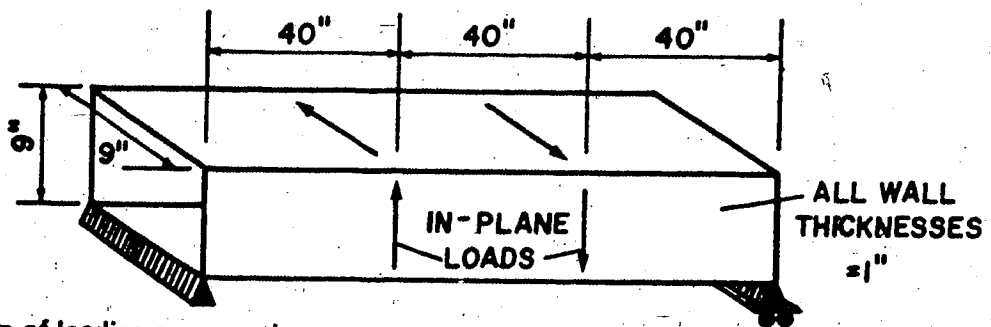
(a) Coarse mesh



(b) Finer mesh



(c) Finest mesh



(d) Location of loading cross-sections

**FIG. 3.4 THREE FINITE ELEMENT MESHES USED IN CONCRETE SELECTION PROCESS**

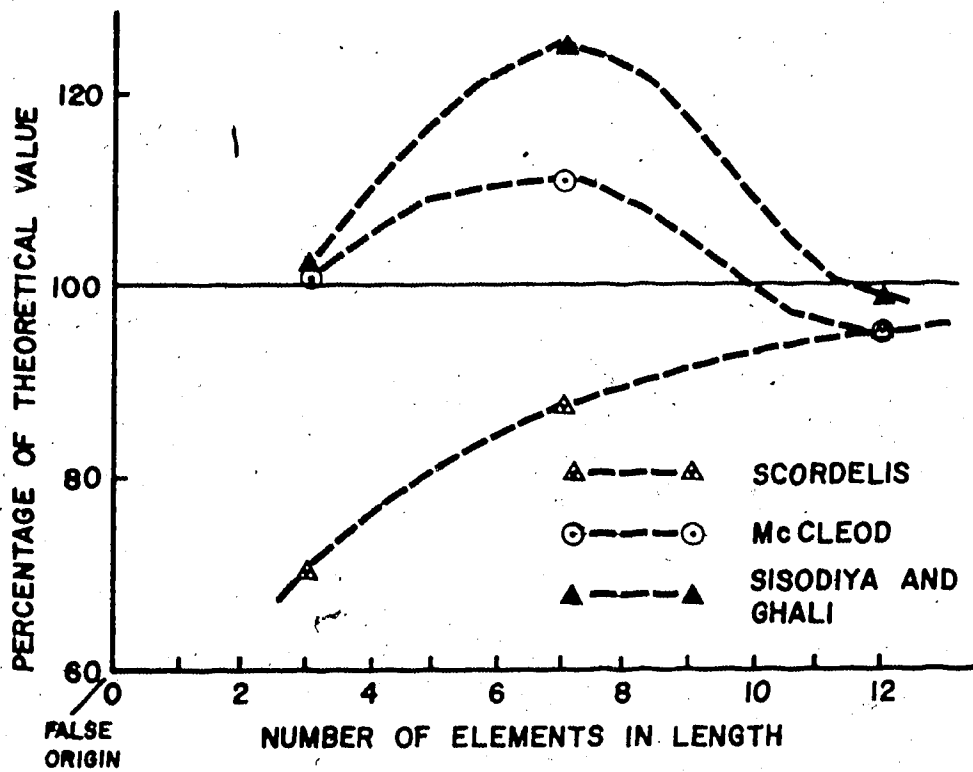


FIG. 3.5(A) DIRECT BENDING STRESSES FOR THREE CONCRETE FINITE ELEMENTS

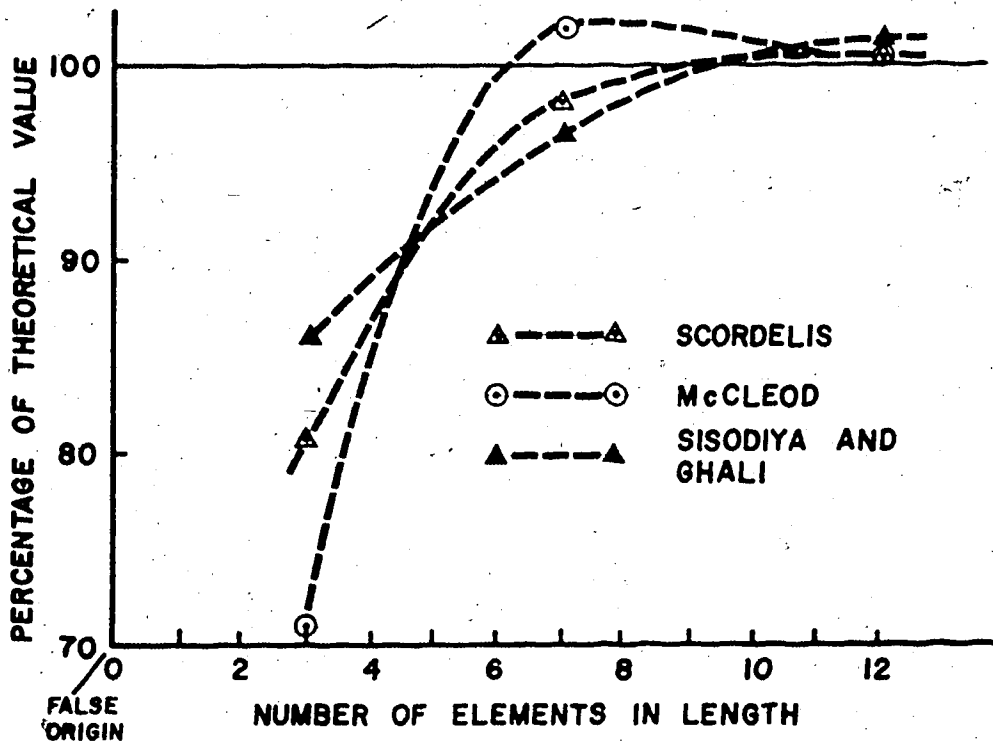


FIG. 3.5(B) ST. VENANT TORSION SHEAR STRESSES FOR THREE CONCRETE FINITE ELEMENTS

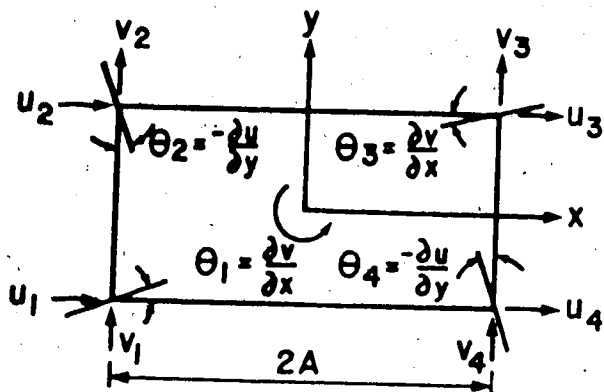


FIG. 3.6(A) ELEMENT TYPE 1

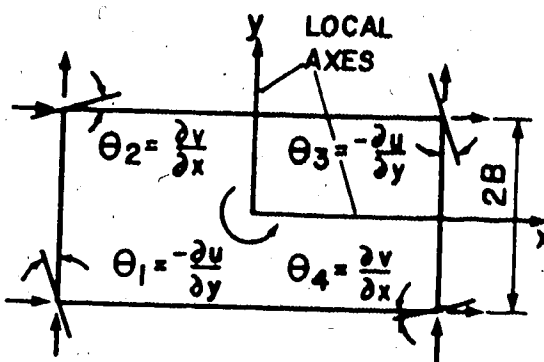


FIG. 3.6(B) ELEMENT TYPE 2

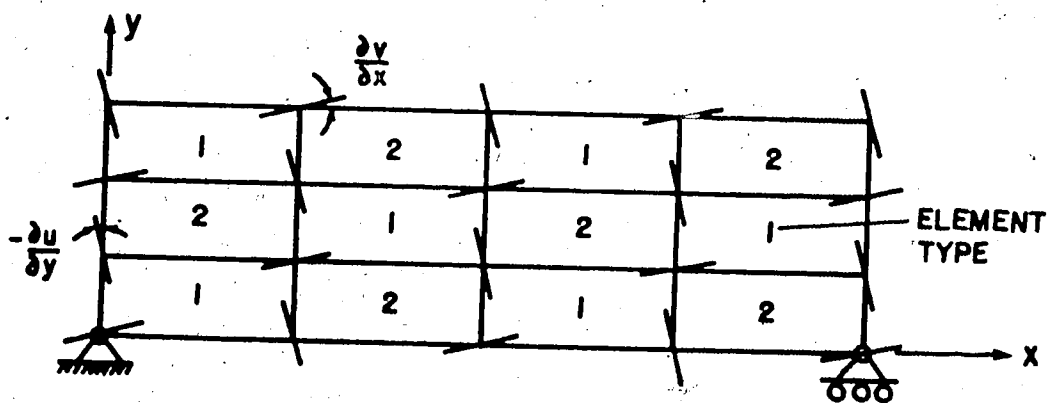


FIG. 3.6(C) TWO-DIMENSIONAL BEAM ASSEMBLAGE OF McCLEOD FINITE ELEMENTS

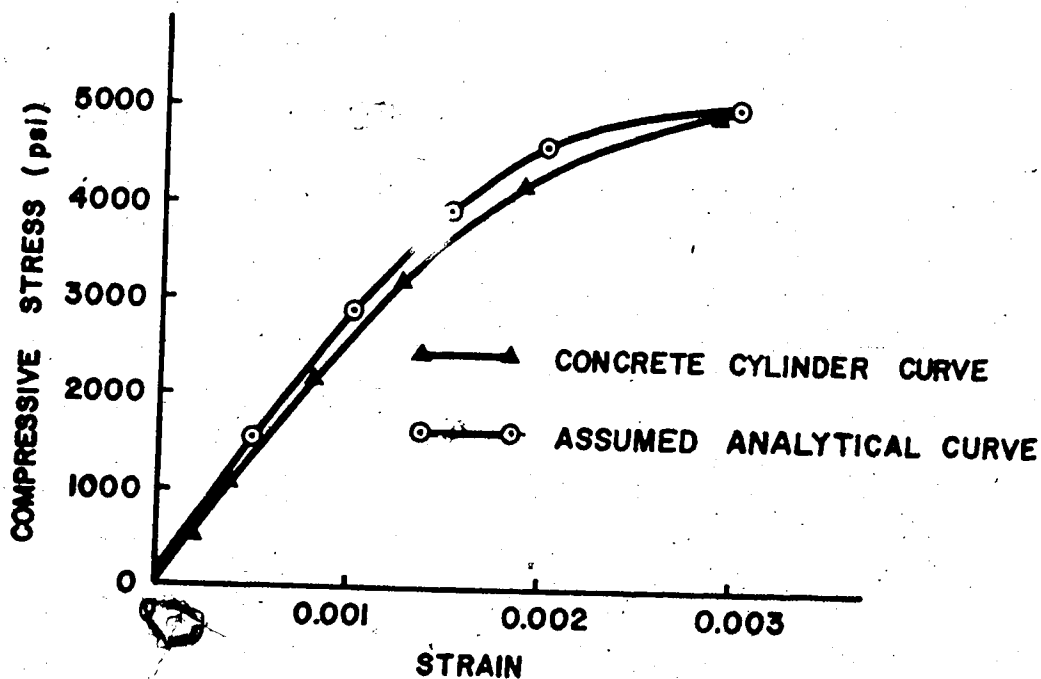


FIG. 3.7 THEORETICAL AND EXPERIMENTAL CONCRETE COMPRESSION STRESS-STRAIN CURVES

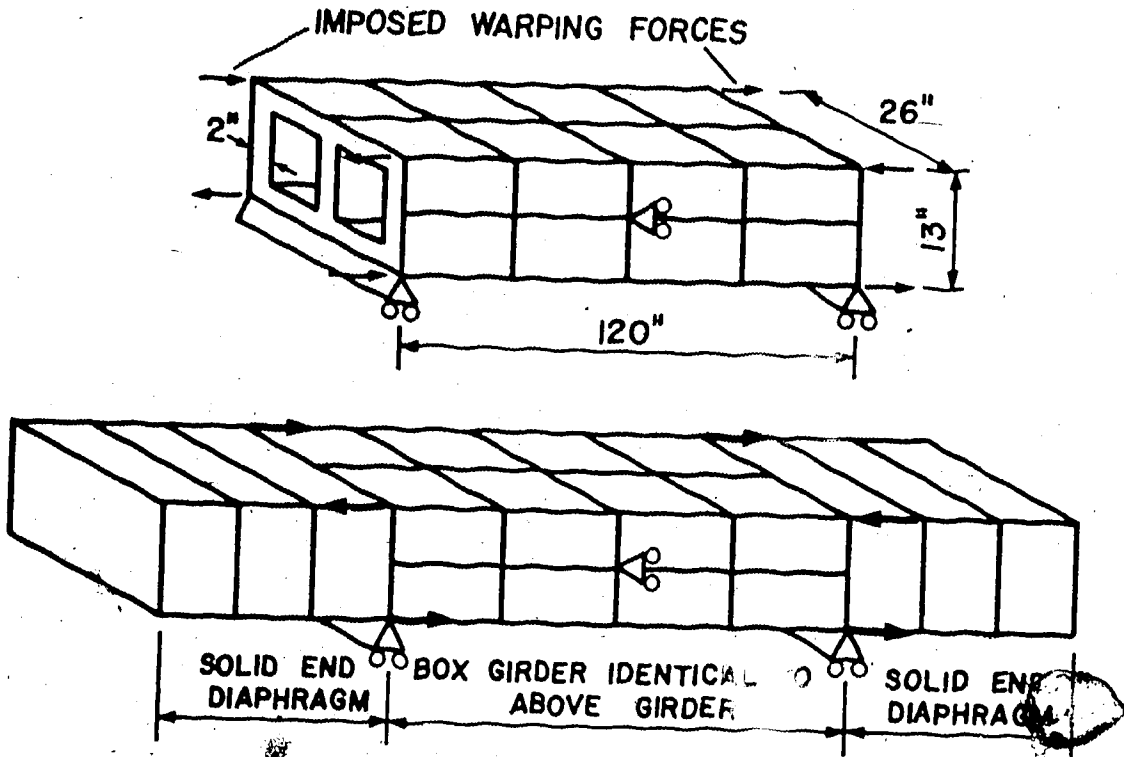


FIG. 3.8 BOX BEAM MODELS WITH THICK DIAPHRAGMS

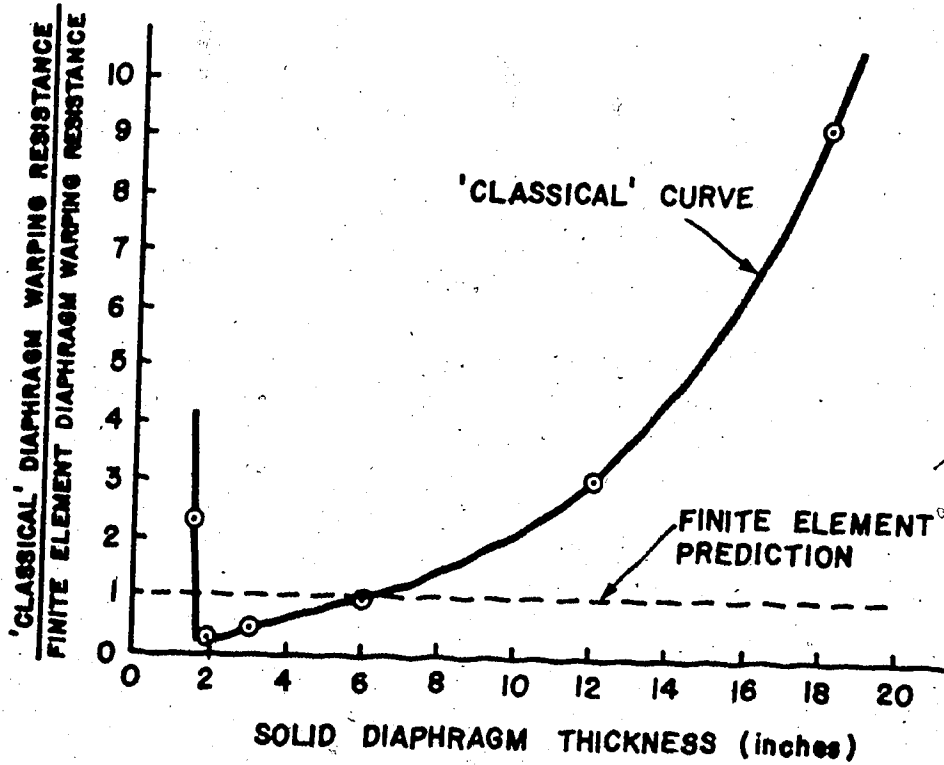


FIG. 3.9 DIAPHRAGM WARPING RESTRAINT CURVES



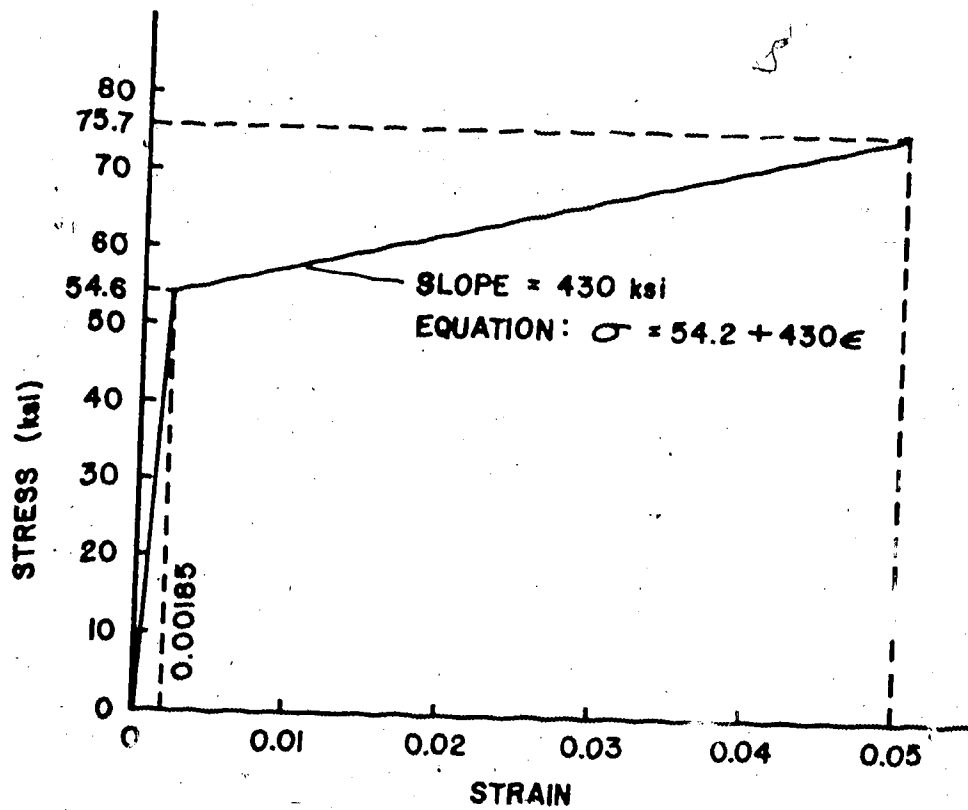


FIG. 3.10(A) CONVENTIONAL REINFORCEMENT STRESS-STRAIN CURVE

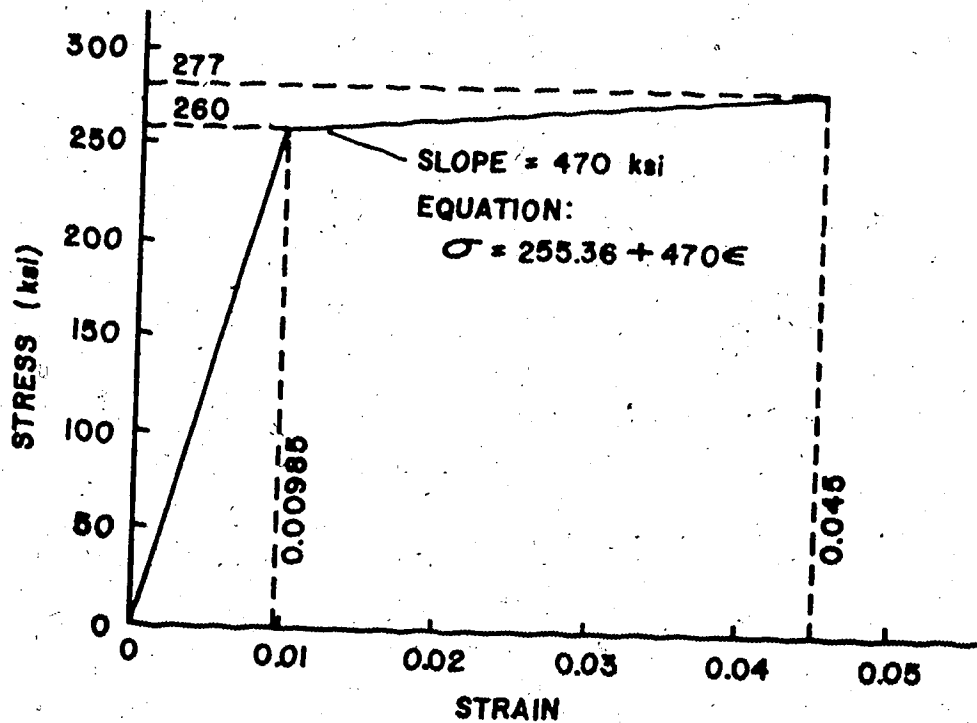


FIG. 3.10(B) PRESTRESS REINFORCEMENT STRESS-STRAIN CURVE

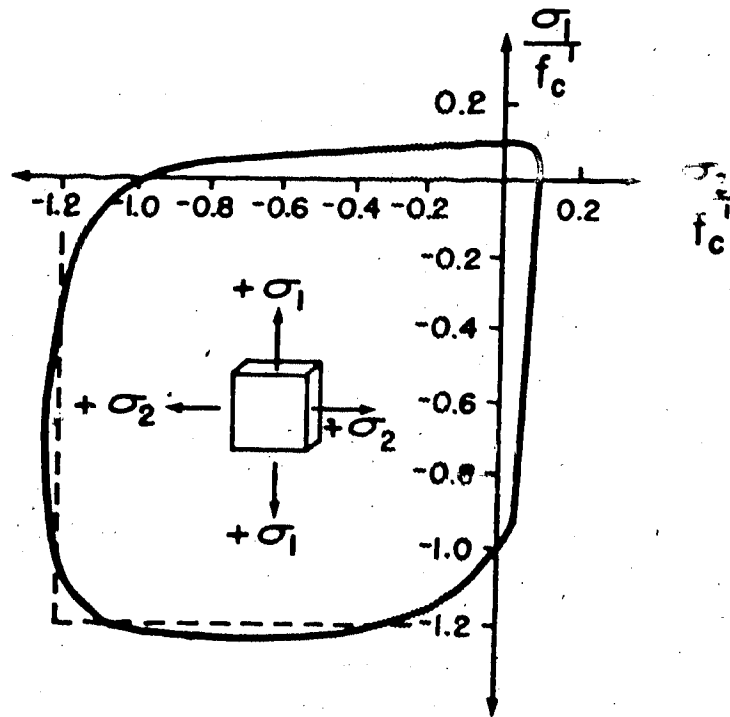


FIG. 3.11 KUPFER, HILSDORF, RUSH BIAxIAL STRESS ENVELOPE

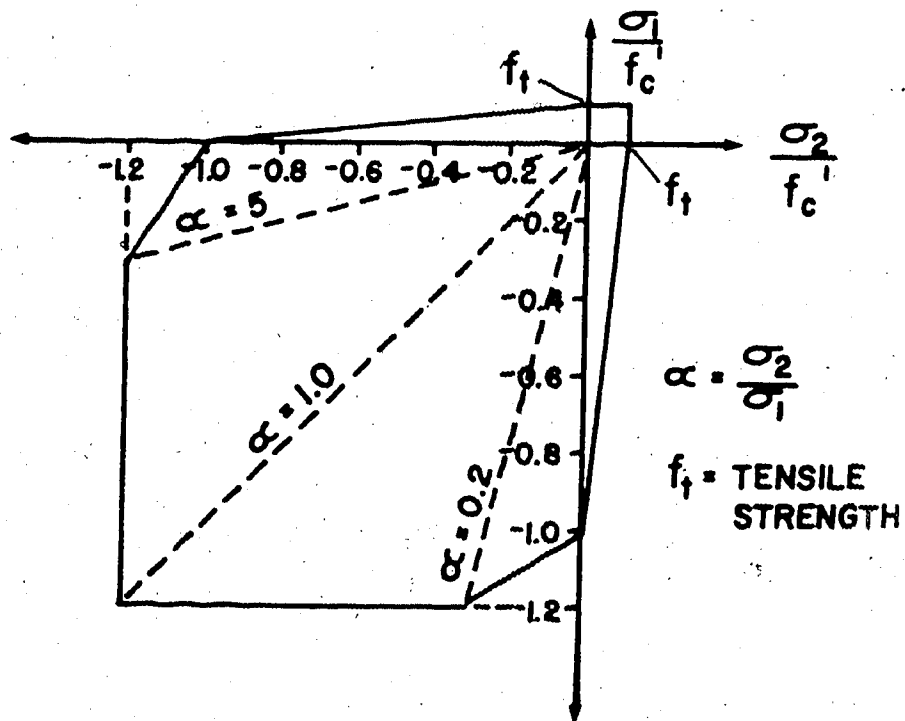


FIG. 3.12 SIMPLIFIED ANALYTICAL MODEL BIAxIAL STRESS ENVELOPE

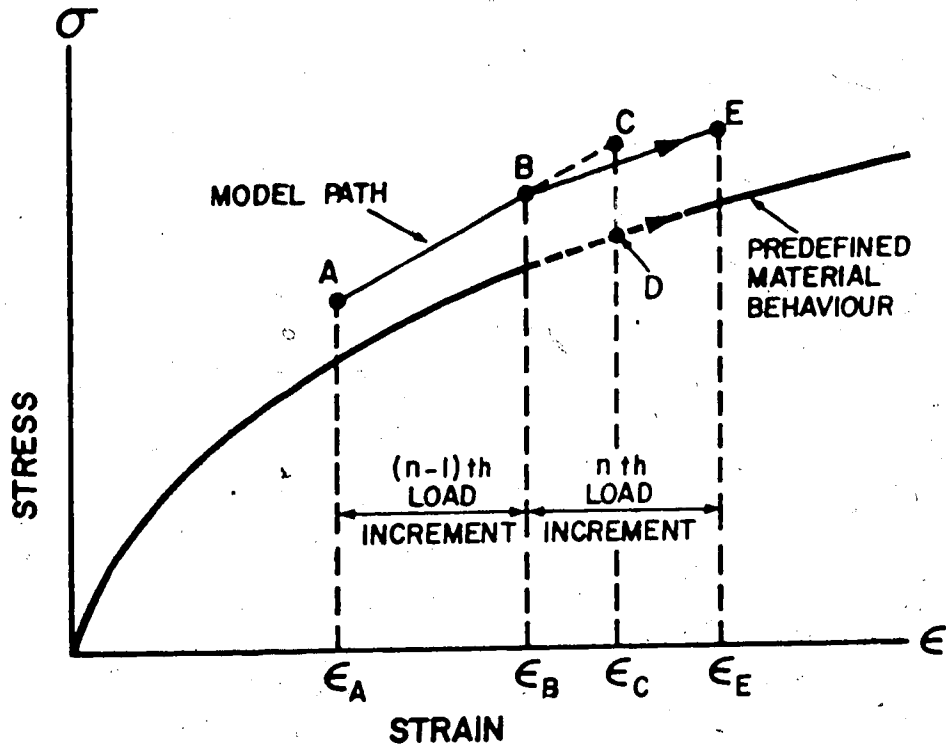


FIG. 3.13(A) RUNGE-KUTTA METHOD

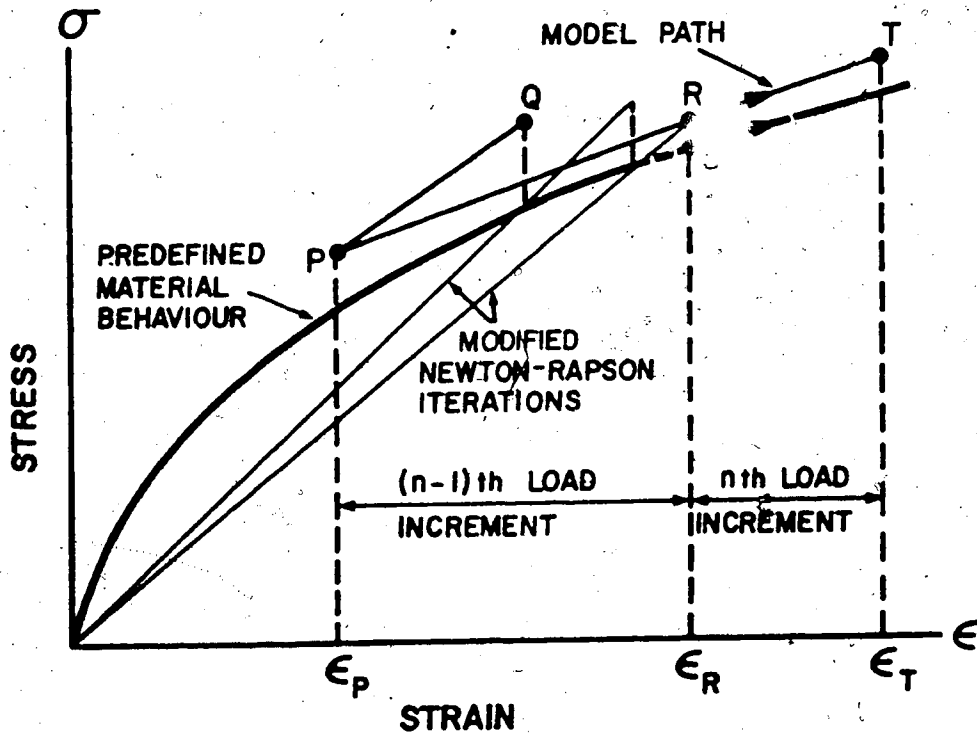


FIG. 3.13(B) MODIFIED NEWTON RAPSON METHOD

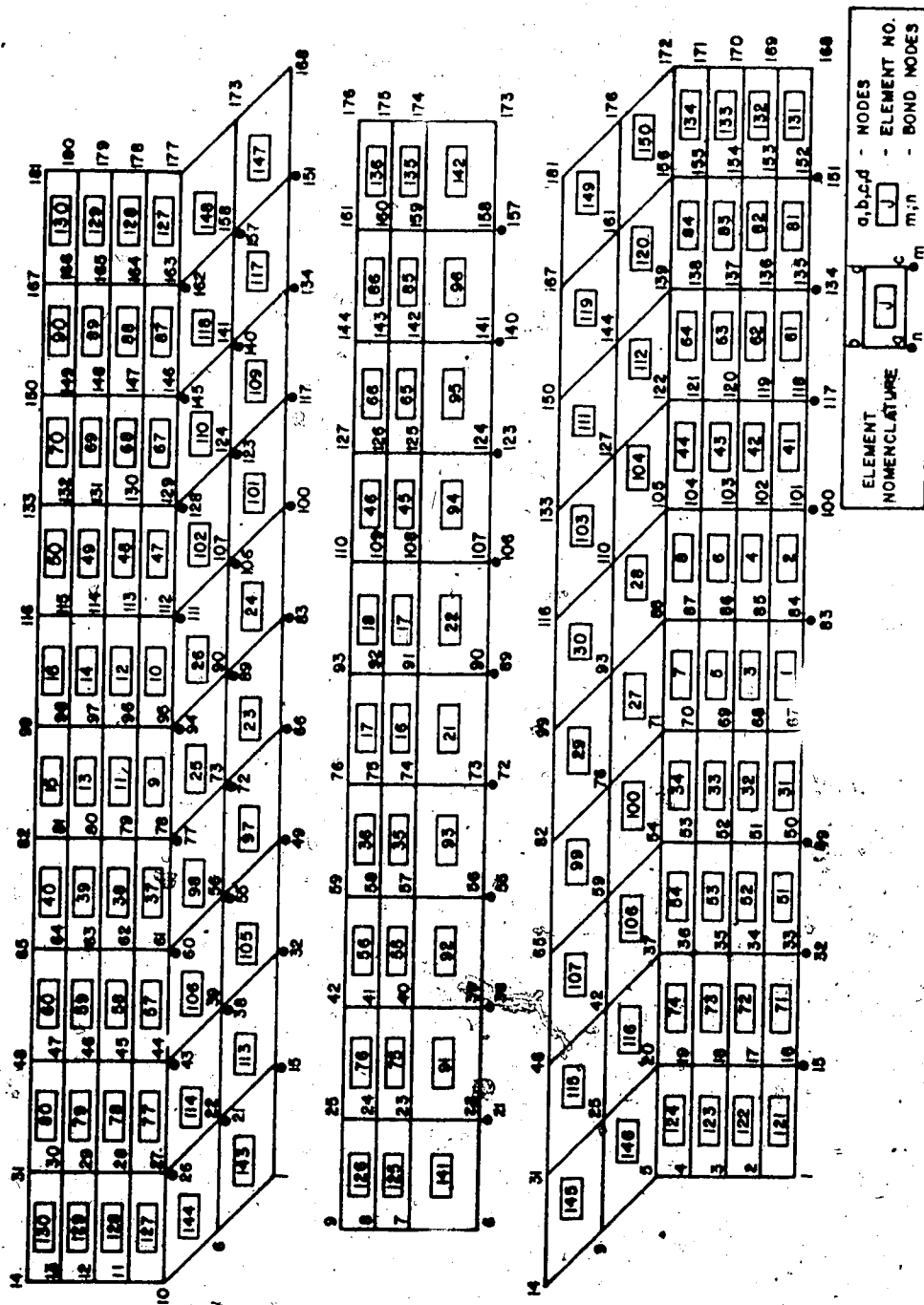


FIG. 3.14 FINITE ELEMENT MESH DISCRETIZATION

## CHAPTER 4

### EXPERIMENTAL PROGRAM

#### 4.1 Introduction

Consistent with the defined scope, the scale of the experimental program was modest in the number of beam specimens tested and the degree of parameter variation. In all, seven prestressed box beams were cast and tested to failure, with each beam subjected to different ratios of torque to bending moment to shear. All facets of the experimental program are dealt with in this chapter, and the results are presented in the following chapter.

#### 4.2 Definition of Basic Experimental Parameters

In essence, all the test beam specimens were hollow, precast, prestressed concrete members. At the preliminary design stage, it was recognized that, if the analytical model was to be tested rigorously, complex beam cross-sections of more than one cell should be tested. An extensive literature survey revealed that little if any experimental research had been conducted on the post-cracking behaviour of multi-celled members under the action of torsion, bending, and shear. From an analytical stance of generality, little benefit would have been derived in having more than two cells per beam, and practical expedience in the casting and testing sequences dictated against an excessive number of voids. Thus, the decision was made that all beams would be cast with two closely spaced voids.

Since the experimental tests were to be used strictly for comparative purposes, the number of beams cast for the testing program was small. The only principal experimental parameter whose variation was investigated in the series of tests was the load parameter. The more significant aspect of this parameter was not the level of individual loads, but the ratio of bending moment to torque to shear. In all, seven beams were cast, with five beams being subjected to varying ratios of torque to bending moment with little shear present. The remaining two beams were subjected to significant levels of shear, in conjunction with the more predominant torque-bending moment loading combination.

The primary region of concern in the full range of test beam behaviour was the post-cracking region. Thus, the initial design of the test specimens had to meet the important prerequisite that the inelastic behavioural path beyond cracking was of reasonable length compared with the respective elastic path. This condition was assured by not permitting the ratio of ultimate strength to cracking strength to fall much below the value of two.

To introduce a degree of generality of cross-sectional shape in the experimental study, two geometrical shapes were adopted in the beam design; rectangular and trapezoidal. Of the total of seven beams, five were cast with rectangular sections.

The one overriding consideration in the selection of void sizes was that all wall segments must be classified as "thin". The need for thin wall segments arose from the use of plane stress finite elements to model the beam walls. The theoretical classification as to whether a beam cross-section is "thick" or "thin", is treated in detail in 3.2.1.

### 4.3 Design of Test Specimens

All beams in the test program were precast, prestressed concrete members with modest conventional reinforcement present. Beams were categorized as belonging to either of the two test beam series according to their cross-section shape, those rectangular beams belonging to the "R" series and those trapezoidal assigned to the "T" series.

In all seven beams, a design concrete strength of 5,000 p.s.i. was adopted. To achieve the appropriate workability that would allow the small wall thicknesses to be cast free of air voids, the mix design was made considerably richer than was generally required, the actual concrete component proportions being given in Table 4.1. The respective compressive and tensile concrete strengths for the seven beams are given in Table 4.2. The load versus elongation curves for the remaining two material components, the prestress strand and the conventional reinforcement, are displayed in Figures 4.1 and 4.2 respectively. As a point of clarification, the prestress strand was 250K grade, 1/4" diameter seven strand stress relieved cable, whereas the conventional reinforcement used throughout was #3 deformed mild steel.

In defining full beam geometry, beam length, wall thickness, number of cells, cross-sectional shape and dimensions have to be specified. Of the three variables that are dimensionally functions of length, the independent variable was the wall thickness. This beam dimension had to be sufficiently large such that the prestress and conventional reinforcement could be accommodated without drastically impeding the flow of concrete during casting. As mentioned previously,

a wall thickness of 2" was chosen for all beams. Having specified the wall thickness, the dependent variables of cross-section dimensions and beam length were determined upon recognition of their respective constraints. The web height and flange width had to be a considerable order of magnitude larger than the wall thickness to ensure a reasonable degree of plane-stress action of the concrete beam walls, and the beam length such that a central test section for deformation measurement and the appropriate loading and support apparatus could be accommodated. The remaining two geometrical variables of cross-sectional shape and number of cells have been treated in Section 4.2. Complete beam dimensioning is given in Figures 4.3 and 4.4.

In design, the appropriate level of prestress was chosen such that, at transfer four days after casting, the maximum allowable tensile stresses were developed in the top flange. In all beam designs, the bottom flange compressive stresses did not approach the allowable limits.

In the calculation of the ultimate bending moment capacity, the level of reinforcement was such that the concrete crushed just prior to the prestress strand developing its ultimate strength. In establishing the ultimate torsional capacity, the space truss analogy equations as presented by Collins and Eampert,<sup>25</sup> were used to estimate beam strength.

As mentioned in the previous section, the three distinct loading types represented in this experimental program were bending moment, torque, and shear. Of the five rectangular beams cast, three were subjected to combined bending and torsion only, the remaining two acted



upon by complete bending-torsion-shear loading combinations. The two trapezoidal beams were restricted to bending and torsion loads. In predicting beam strength under combined loading, the interactive equations given in the Collins and Lampert<sup>25</sup> paper were utilized, such equations given in Fig. 4.5 together with the design curves for the rectangular and trapezoidal beams. The predicted beam strengths and failure loads are given in Table 4.3.

Premature shear failure was prevented in the beam length outside the central test section by the provision of substantial shear reinforcement, achieved in most beams by extending torsion hoop reinforcement beyond the central test section. Reinforcement details are provided in Figures 4.3 and 4.4. Also shown in the latter figures are the locations of the points of application of the bending, torsion and shear loads.

#### 4.4 Specimen Fabrication

To enable both rectangular and trapezoidal beams to be cast with the same forming unit, the timber formwork consisted of two identical reversible form segments placed adjacent to one another, as shown in Fig. 4.6.

Provision of the two adjacent cells within each beam was simply achieved by the use of styrofoam blocks held in place by the reinforcement cage. In previous research conducted at this university, the styrofoam was removed by piping acetone into the interior of the cast beams. This added precaution, however, was not deemed necessary as the styrofoam strength contribution was negligible compared with

that of the prestressed beam. In all beams, the void lengths did not extend as far as the points of support, as exhibited in Figure

4.4.

As indicated above, the presence of the reinforcement cage was utilized to maintain the positions of the styrofoam blocks. To prevent the styrofoam blocks from floating during cast, restraining beams were placed across the top of the forms to inhibit upward cage movement. Since the cage tolerances were quite small arising from the selection of narrow wall thicknesses, the reinforcement bars and hoops were lightly tack-welded in position to minimize movement and facilitate handling. As a matter of necessity, the two top corner longitudinal bars had to be moved 1" from their corner positions to allow a small vibrating needle to pass down the outside web walls during casting.

Despite the small wall thickness, the rich concrete mix whose proportioning is given in Table 4.1 did exhibit good workability with the result that very few air voids were evident upon examination after formwork stripping.

The complete casting bed before concrete pouring is shown in Plate 4.1.

#### 4.5 Loading Apparatus Design

##### 4.5.1 Beam Supports

In addition to their customary role of simple supports, the beam reactions permitted the development of a uniform St. Venant torque applied across the central test section. Consequently, each support had to allow the beam to rotate freely about its centre of rotation. Lateral

stability of the beam was ensured by the very nature of the torsion loading arms, as described in Section 4.5.3. Figure 4.7 illustrates all end support details. The roller housing shown in this figure was bolted to the top of the conventional roller and hinge supports to achieve the desired beam support conditions.

#### 4.5.2 Application of Bending Moment and Shear

Both bending moment and shear force were developed by the application of downward vertical concentrated loads applied by 50 ton Amsler jacks. If a vertical concentrated load was not to create secondary torsion during the course of a beam test, the centre line of the Amsler jack had to pass through the shear centre of the beam. This alignment was achieved through incorporating a design that was identical to that of the rotational end support, with the apparatus simply inverted. The one additional design provision not present in the end support design was the roller housing bracing whose sole function was to provide horizontal stability to the roller housing under all loading extremes. As the beam deflected under load, the bracing arms attached to the housing by a central pin maintained their horizontal posture upon adjustment of the bracing jack. The apparatus is displayed in Fig. 4.8.

#### 4.5.3 Application of Torque

Only the central test section was subjected to torque, more specifically a uniform St. Venant torque developed by a pair of equal and opposite forces whose placement along the test beam delineated the central test section. Each torsion force was applied by a cable that draped over a curved torsion arm (as in Fig. 4.9) and passed through the testing floor where it was anchored by a hydraulic jack

loading system. The curved arm geometry ensured that the torsion lever arm dimension remained constant as the beam rotated. Stability of a test beam, once the beam was placed in the testing arrangement, was provided by minimal tension in the torsion cables.

#### 4.6 Instrumentation

To plot beam behaviour throughout the test program, both stress and deformation data were recorded. As the seven strand prestress cable was of small diameter (1/4"), strain gages were difficult to attach securely, and thus could not be relied upon to accurately monitor prestress strain levels. However, the strain states of the conventional longitudinal and central transverse hoop reinforcement were monitored by strain gages to yield a representative record of stress versus load behaviour.

More emphasis was placed in the instrumentation phase on the accurate measurement of cross-section deformation within the central test section rather than extensive monitoring of reinforcement strain. By surveying the vertical and horizontal deflections of three cross-sections within the central test section, the central vertical deflection, beam curvature, and rate of twist were able to be evaluated. To facilitate fast test measurement recording, linear displacement transducers were used in preference to conventional dial gages. Plate 4.2 displays several linear displacement transducers operating under test conditions.

In recognition of the fact that the number of both load increments and individual instrument readings was large, an automatic data-recording system was used. The electrical signals from the linear

displacement transducers and the strain gages were monitored, translated, and stored on disc by a Data General Corporation Nova 210E Computer. During testing, the depression of a console key prompted the complete data set of load increment measurements to be recorded and written on disc.

All locations of strain gages and linear displacement transducers are described in Chapter 5.

#### 4.7 Testing Procedure

Upon application of each load increment, the entire regime of instrument measurement was recorded automatically as described in the preceding section. If cracking had commenced, crack propagations were clearly marked and the load intensity indicated at the furthest point of crack propagation, as seen in the following chapter's photographic plates of tested beams. As a precautionary measure, the transverse alignment of the Amsler jacks was checked at regular intervals and corrected when necessary by adjustment of the bracing turnbuckles and jacks. All cracking patterns and mode of failure were photographed upon completion of the test.

Ingredient	Wt. in lbs./batch
Cement	211
Sand	420
Coarse Aggregate (3/8")	540
Water	120

Approximate batch volume = 10 ft.<sup>3</sup>  
slump = 3" + 4"

TABLE 4.1 CONCRETE MIX PROPORTIONS

Beam Designation	Concrete Compressive Strength (psi)	Concrete Tensile Strength (psi)	Concrete Young's Modulus (psi)
R1	4816	396	2.36 x 10 <sup>6</sup>
R2	4580	462	2.133 x 10 <sup>6</sup>
R3	4545	479	2.6 x 10 <sup>6</sup>
R4	4362	288	2.69 x 10 <sup>6</sup>
R5	4562	329	1.84 x 10 <sup>6</sup>
T1	3985	354	3.0 x 10 <sup>6</sup>
T2	4262	338	2.79 x 10 <sup>6</sup>

TABLE 4.2 CONCRETE STRENGTH

Beam Designation	R1	R2	R3	R4	R5	T1	T2
Initial Prestress	79.2	79.2	79.2	79.2	79.2	72	72
Final Prestress	61.3	61.3	61.3	61.3	61.3	58.2	58.2
Cracking Bending Moment	715	715	715	715	715	429	429
Cracking Torque	454	454	454	454	454	229	229
Ultimate Bending Capacity	1515	1515	1515	1515	1515	985	985
Ultimate Torsion Capacity	380	380	380	380	380	246	246
Average Values Over Central Test Section at Failure	1010	1250	960	1150	680	618	811
Bending Moment	500	372	450	250	639	304	200
Torque	0.0	0.0	±11	±18	0.0	0.0	0.0
Shear	2.02	3.36	2.13	4.6	1.064	2.03	4.05
Ratio of $\frac{\text{Bending Moment}}{\text{Torque}}$							

Note: All units are in Kips and inches.

TABLE 4.3 BEAM DESIGN TABULATION

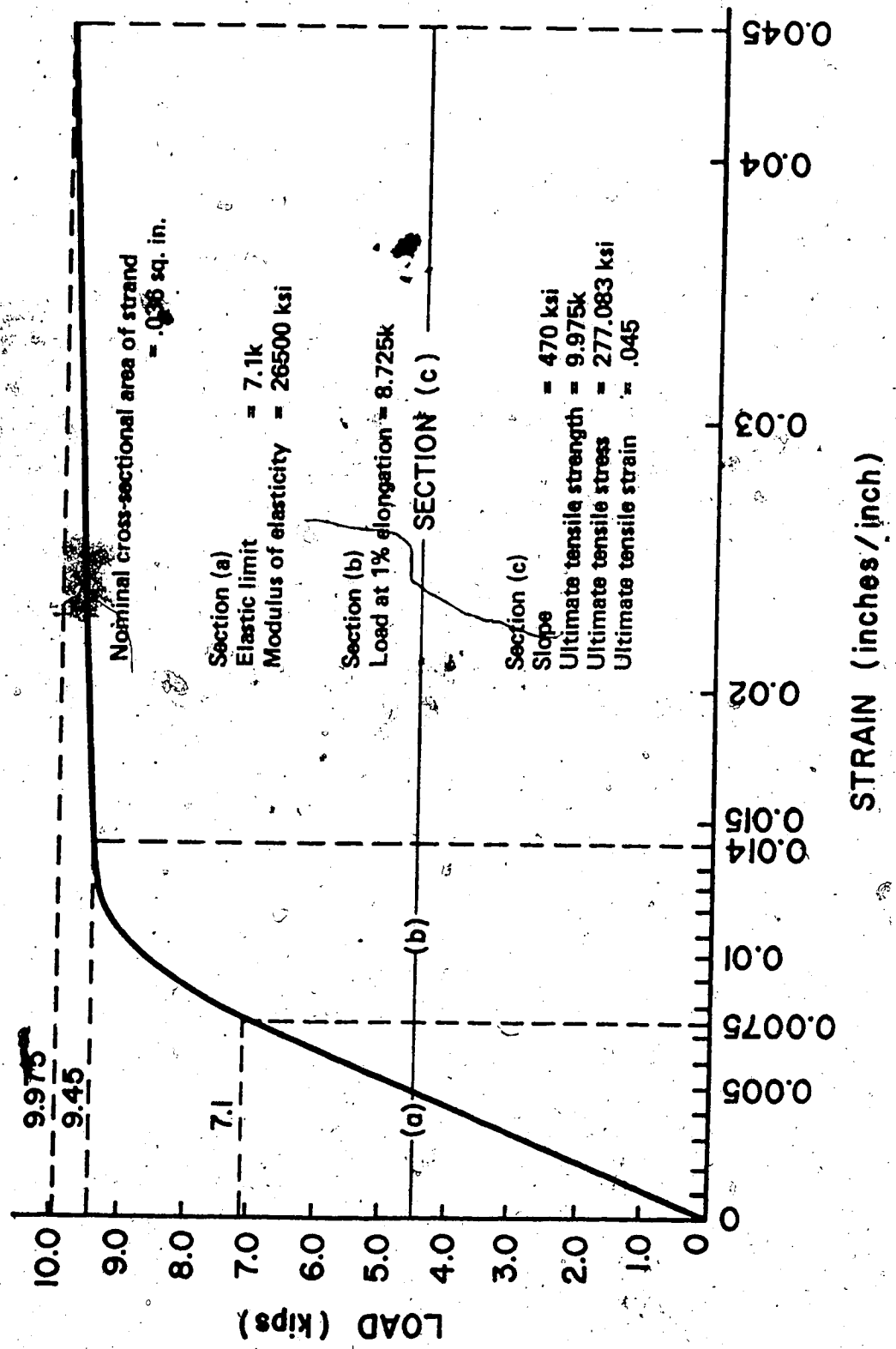


FIG. 4.1 LOAD-ELONGATION CURVE FOR PRESTRESS STRAND



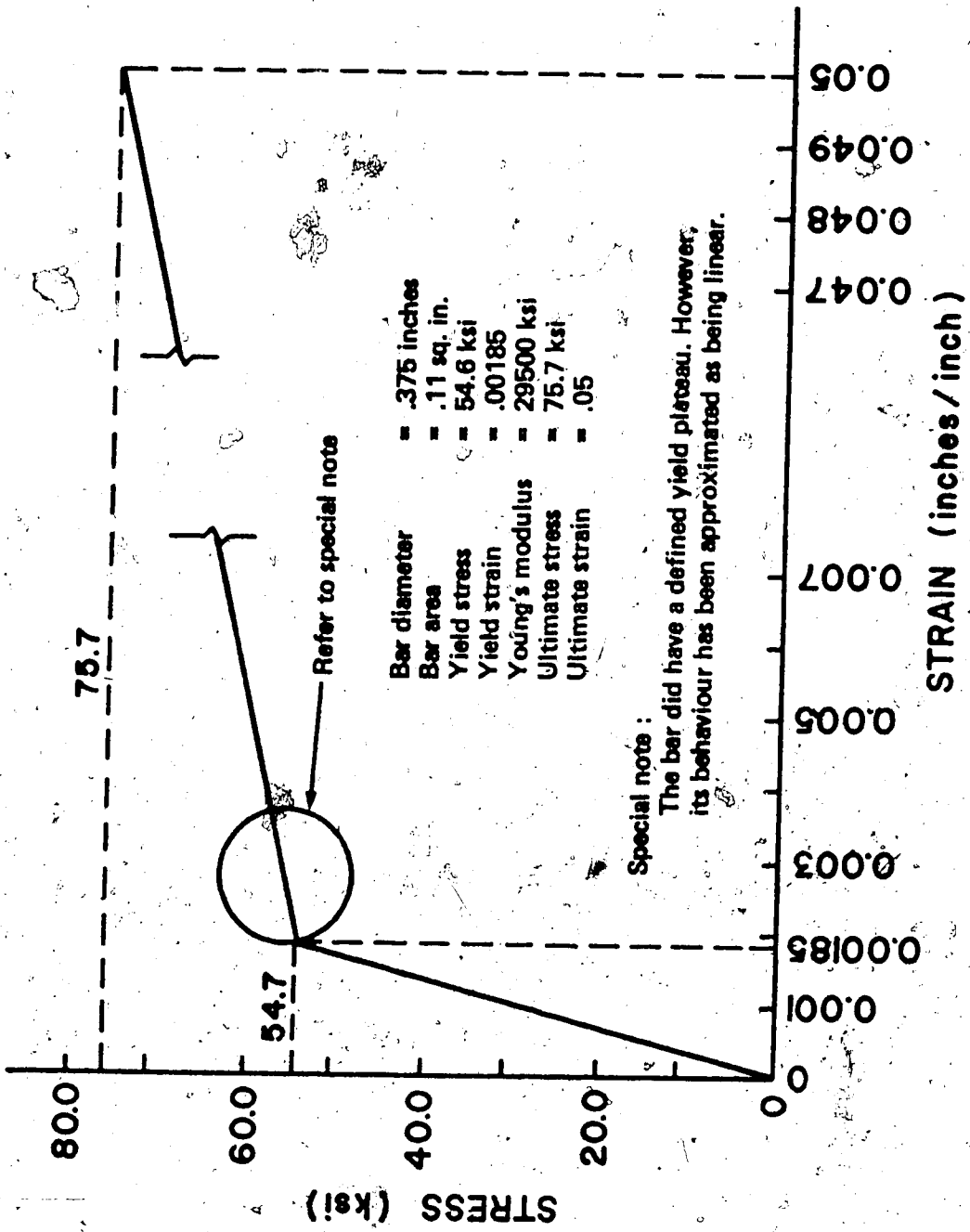


FIG. 4.2 STRESS-STRAIN CURVE FOR #3 DEFORMED BAR REINFORCEMENT

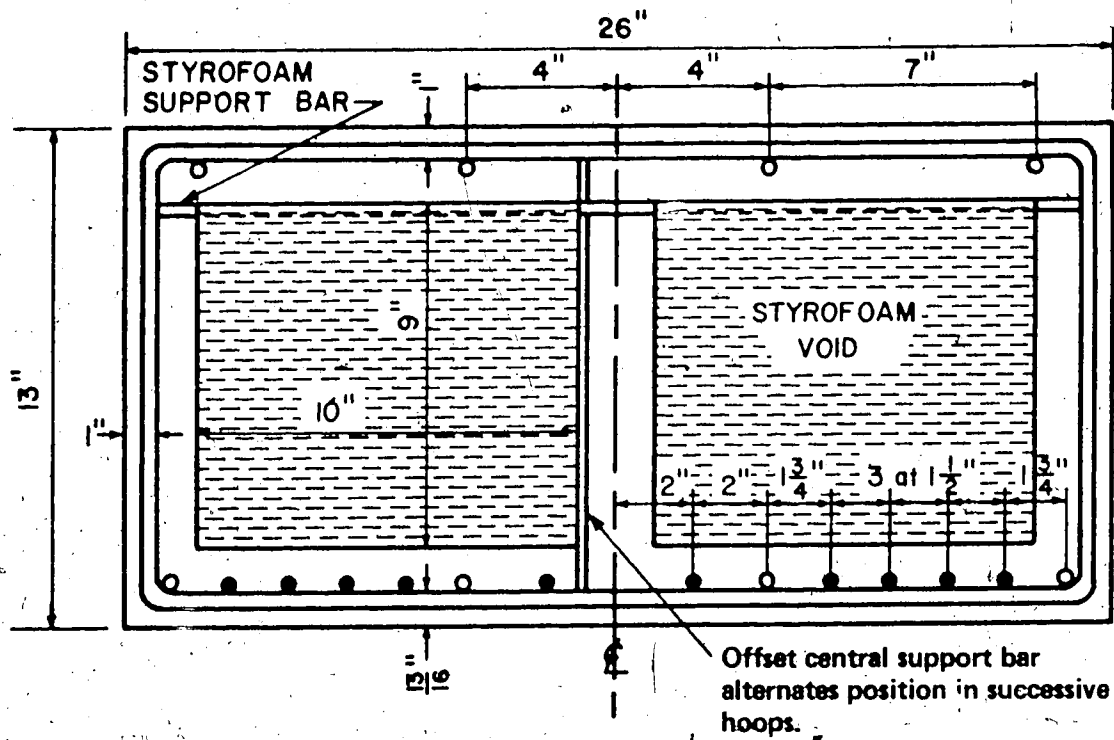


FIG. 4.3(A) RECTANGULAR BEAM CROSS-SECTION

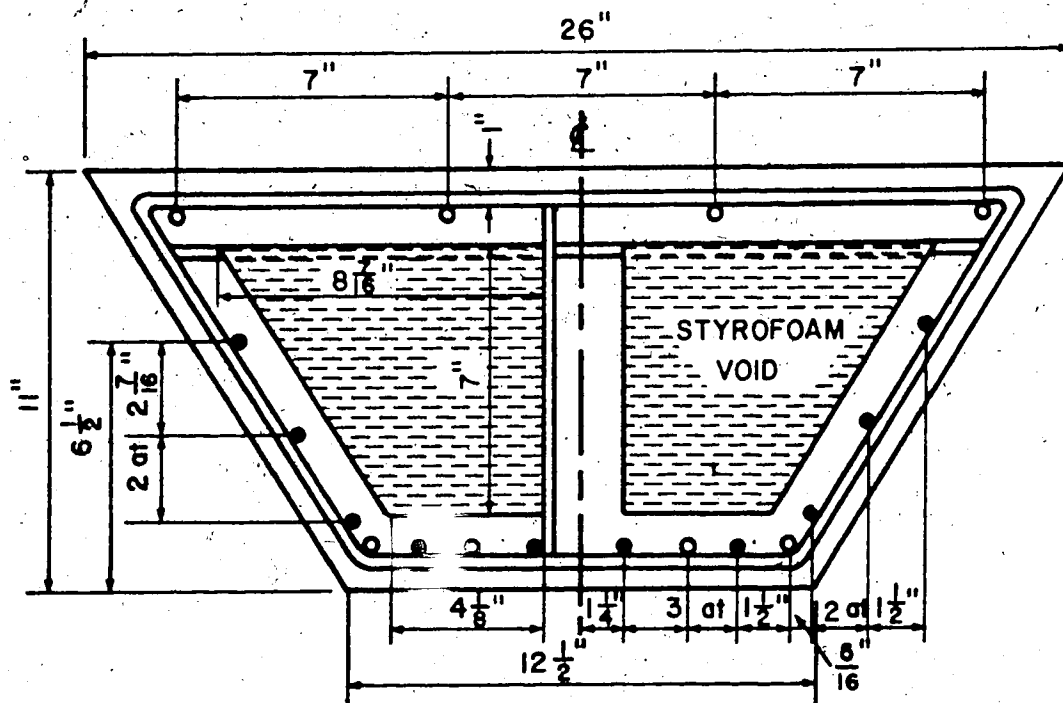


FIG. 4.3(B) TRAPEZOIDAL BEAM CROSS-SECTION

- Notes: (1) All wall thicknesses = 2"  
 (2) ○ Conventional #3 bar ● .25" Prestress strand  
 (3) All beams are symmetrical w.r.t. vertical centreline

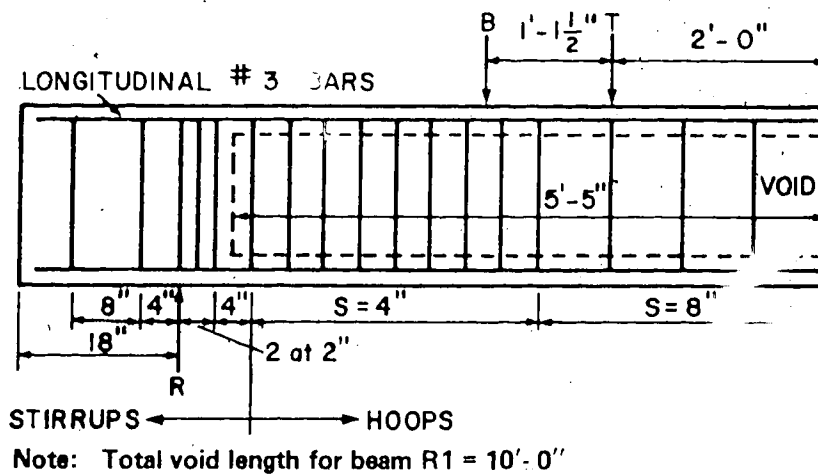


FIG. 4.4(A) REINFORCEMENT FOR BEAMS R1 AND R2

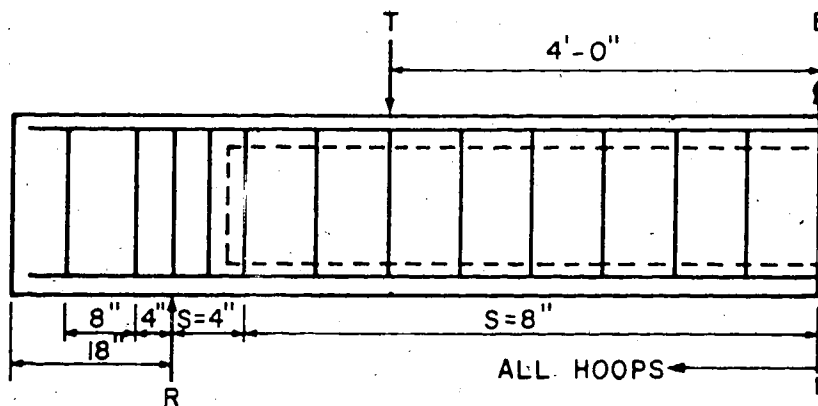


FIG. 4.4(B) REINFORCEMENT FOR BEAMS R3, R4, R5

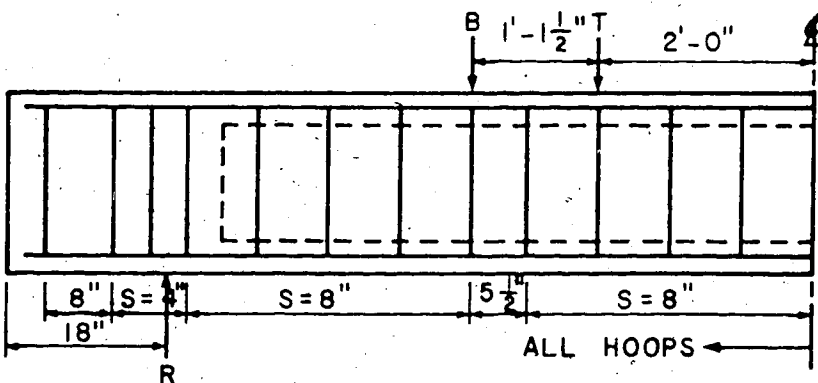


FIG. 4.4(C) REINFORCEMENT FOR BEAMS T1 AND T2

- Notes: (1) All bars are #3  
 (2) All half beam lengths = 7'-7.5"  
 (3) R = support B = jack T = torsion  
 (4) All void lengths = 11'-0" unless noted otherwise  
 (5) All longitudinal steel is 1.5" short of beam ends  
 (6) Drawings are not to scale

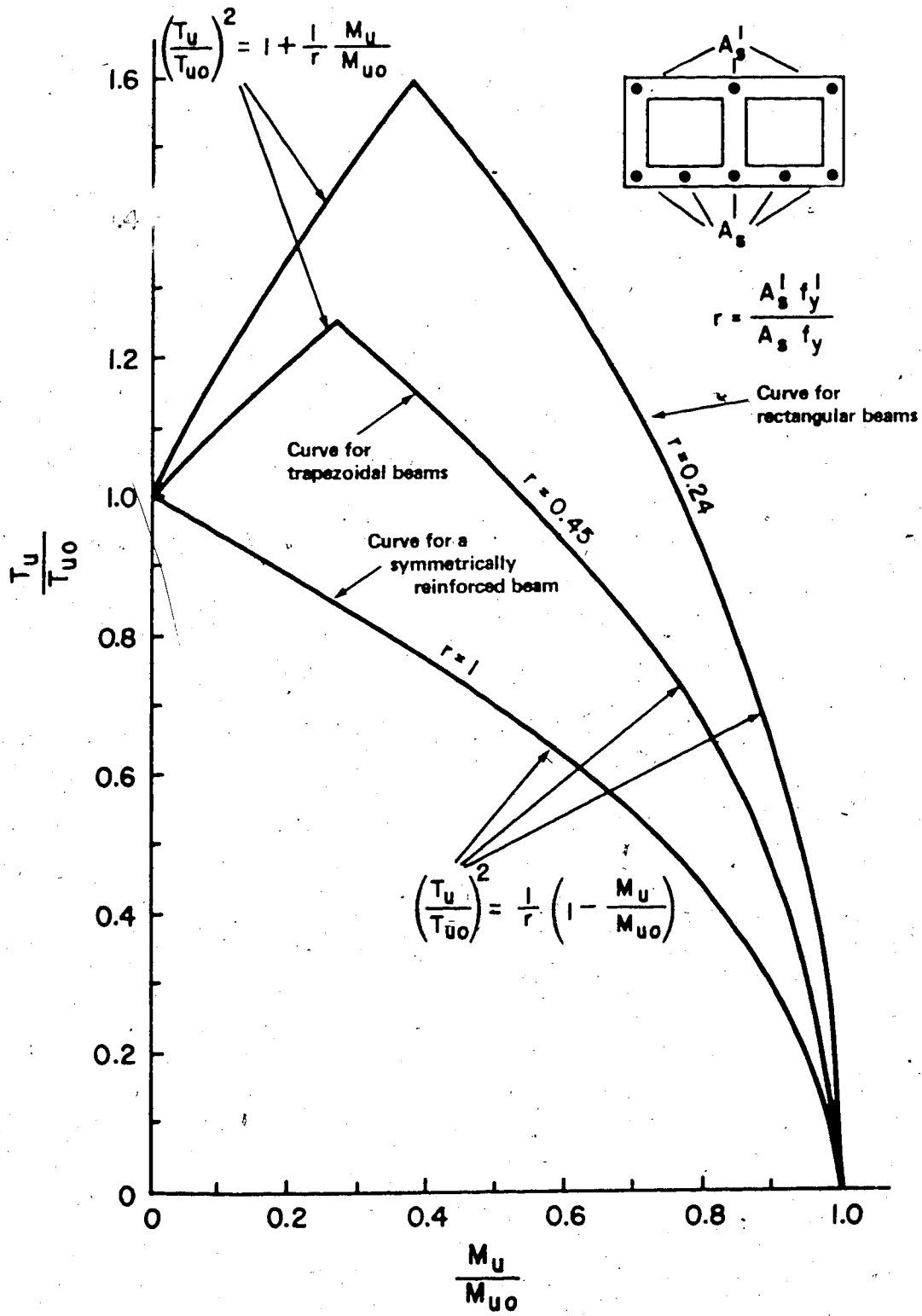
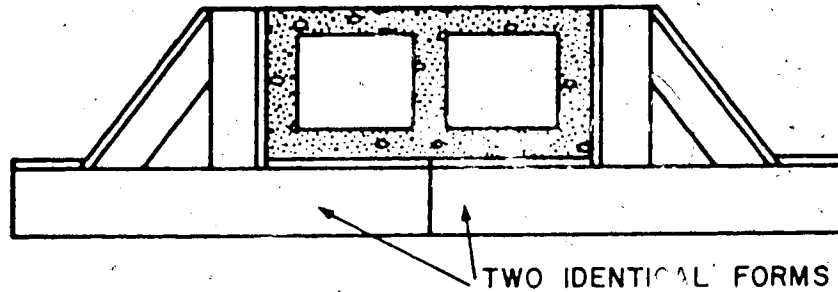


FIG. 4.5 INTERACTION EQUATIONS FOR TEST BEAMS UNDER COMBINED BENDING AND TORSION

Juxtaposition for casting rectangular beams



Juxtaposition for casting trapezoidal beams.

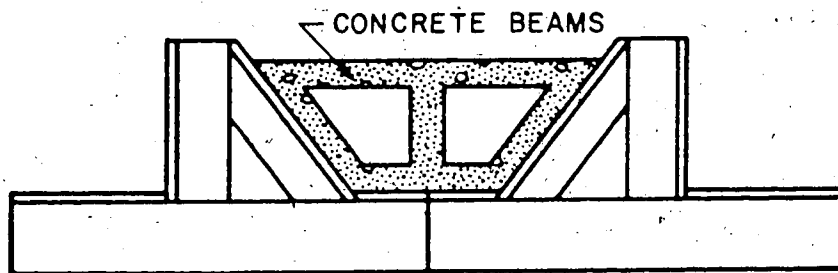


FIG. 4.6 FORMWORK SECTION

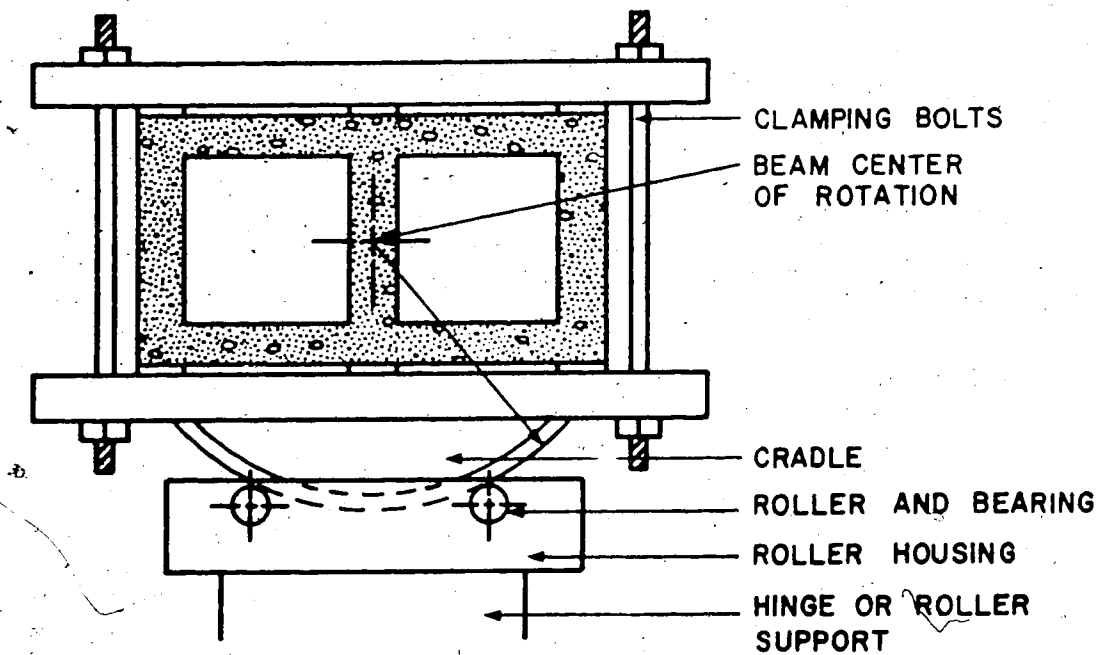


FIG. 4.7 TEST BEAM SUPPORTS

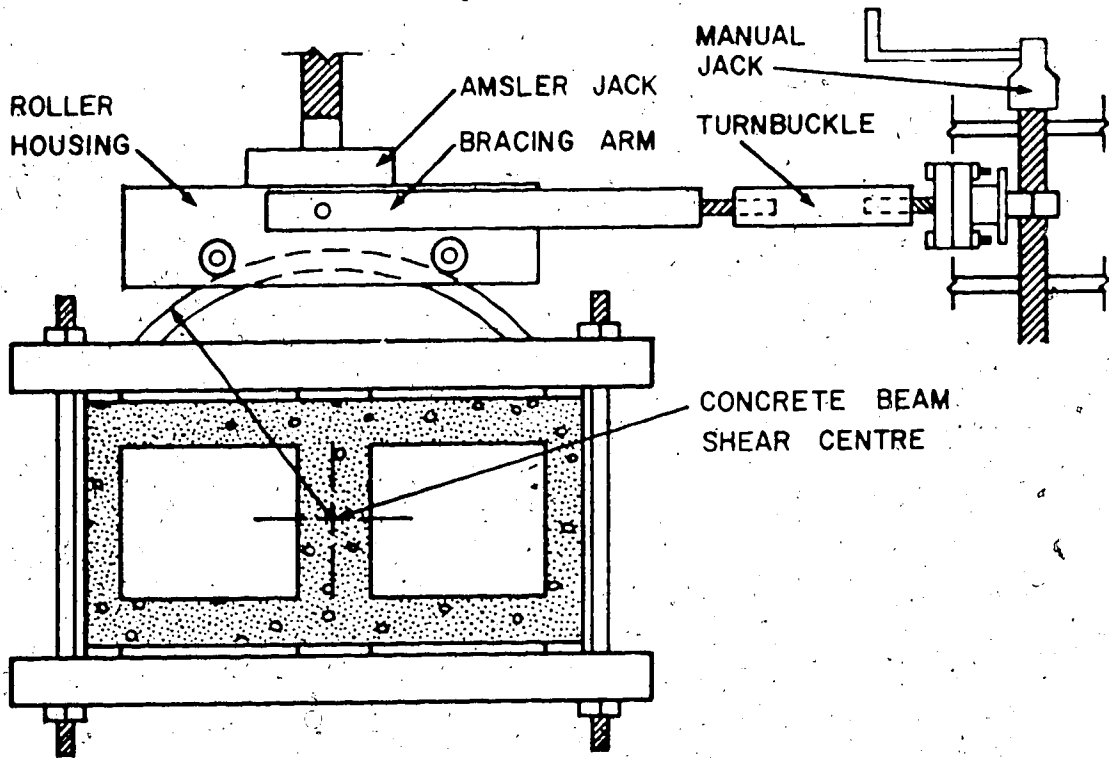


FIG. 4.8 POINT LOAD APPARATUS WITH ROLLER HOUSING

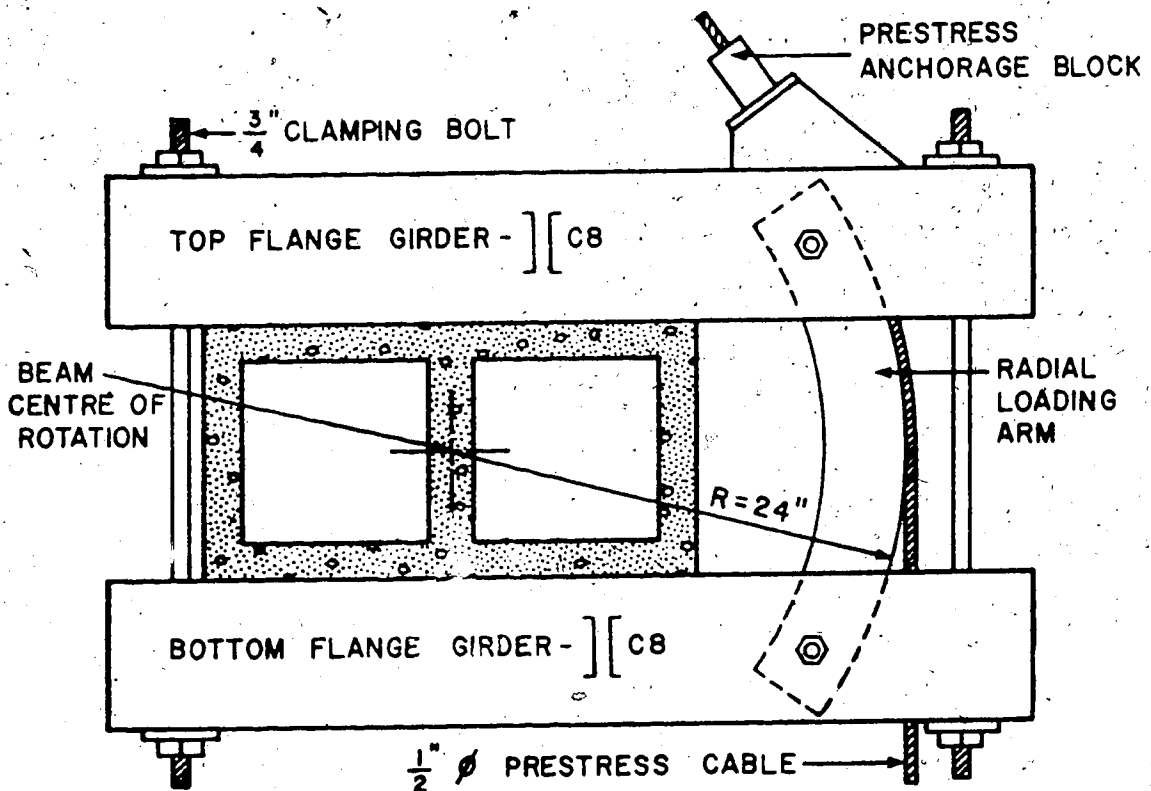


FIG. 4.9 TORSION LOAD ARM

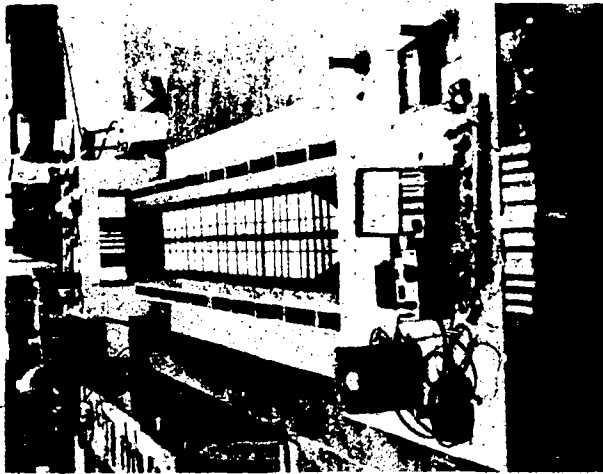


PLATE 4.1 FORMWORK BEFORE CASTING



PLATE 4.2 LINEAR DISPLACEMENT TRANSDUCERS

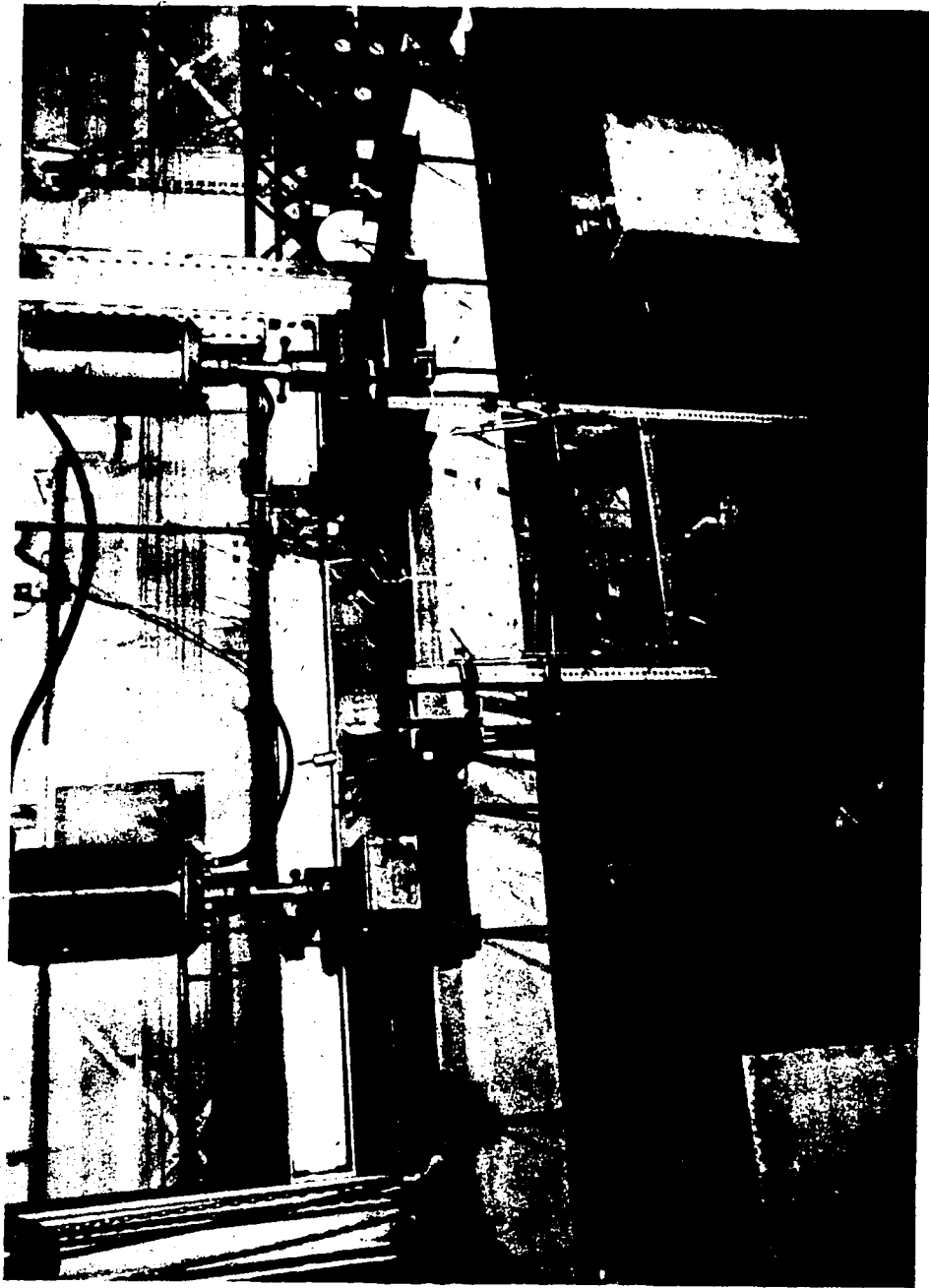


PLATE 4.3 COMPLETE EXPERIMENTAL TESTING SETUP



## CHAPTER 5

### EXPERIMENTAL RESULTS

#### 5.1 Format of Presentation of Results

The complete spectrum of experimental results for the seven beams tested is presented in this chapter. The two distinct aspects of the testing program, test measurements and observed behaviour, are treated separately in the following Sections 5.2 and 5.3.

In the measurement of beam response, greater emphasis was placed on the recording of member deformation than reinforcement stress levels. For each beam, graphs of torque versus differential rotation and bending moment versus central deflection describe complete deformation characteristics. In the only representation of monitored stresses, stress levels of the longitudinal and transverse conventional reinforcement at the central cross-section are presented in the respective plots. Beam strength is tabulated fully in the specification of prestress levels, elastic stiffness, cracking and failure loads.

Experimental observations are confined to modes of failure and distinctive cracking patterns.

In the concluding section of this chapter, the potential sources of experimental error and irregularities in the experimental program are identified and evaluated.

A complete detailed tabulation of experimental results is provided in Appendix I.

## 5.2 Test Measurements

The recorded numerical data in its processed form is presented under the three categories of beam strength, beam stiffness, and reinforcement stress.

The beam strength components of initial level of prestress, final level of prestress, cracking load, and loading combination at failure are summarized in Table 5.1. At both the cracking and failure values the bending moment specified is the total bending moment arising from the torsion arm and Amsler jack loads.

To provide a suitable basis of comparison with analytical model results, the load-deformation relationships for each test specimen have been plotted for the complete loading range. Beam response in the pre-cracked state is elastic to within a reasonable degree of accuracy, and the respective torsion and bending stiffness constants for the seven beams are given in Table 5.2. Beyond cracking, beam behaviour is highly inelastic as exhibited in Figures 5.1 to 5.5. The torque versus rotation curve for beam R4 is not presented as it closely retraces the appropriate segment of the curve for beam R3. In Figures 5.1, 5.2, and 5.3, the abscissa is the differential rotation over the central 30 inch length of the beam. The deflection ordinate of the moment-deflection curves is the vertical displacement of the central cross-section due to bending action only. Thus, in all tests where torque was present, the initial deflection measurements had to be appropriately adjusted to reflect pure bending behaviour.

In monitoring reinforcement stress levels, strain gages were attached only to the longitudinal and transverse conventional rein-

forcement at the beam's central cross-section. In most cases, the bottom and top longitudinal reinforcement stress values are averages of three readings, whereas the hoop stress levels are derived from single gage measurements. In the test setup, the beams were aligned longitudinally close to a north-south direction. Thus, differentiation of the beam's east and west sides in elevation was established. The respective stress plots are illustrated in Figures 5.6 to 5.12, with identifying curve nomenclature given in Table 5.3. All stress levels are tensile with the exception of those of the top longitudinal bars.

### 5.3 Observed Behaviour

In almost all cases, beams were not tested to complete destruction, but were loaded just beyond their observed maximum load carrying capacity. Upon approaching the load capacity of all beams, primary cracks widened markedly, especially in those tests where there was a high ratio of bending moment to torque. Thus, failure appeared to be precipitated by excessive yielding of conventional reinforcement, yielding being most pronounced in the bottom tension flange. In the testing of beam R1 to destruction, failure occurred upon the crushing of a compression diagonal across the width of the top flange. As indicated by gaping crack widths, the strands had undergone considerable inelastic strain, but complete disintegration of the beam was prevented by the ductility of the bottom prestress strands. Close to the failure of beam R4, the test in which the highest ratio of bending moment to torque was applied, a similar mode of failure was observed, but well defined splitting cracks at the level of the bottom longitudinal reinforcement were also apparent, as shown in Plate 5.1. The only beam failure that differed from this general mode of

failure was that of beam T1. Excessive local crushing and a punching shear effect became apparent beneath one torsion arm as displayed in Plate 5.2. Initiation of the local failure was primarily due to the absence of the plaster of paris pad between beam and torsion arm, thus resulting in extremely severe load stress concentrations. However, the load at failure was close to the predicted level.

Representative cracking patterns for two of the beams are illustrated in Fig. 5.13. Beams R4 and R5 were selected as they represented the extremes of highest and lowest ratio of bending moment to torque respectively. The numbering adjacent to the crack paths in Fig. 5.13 corresponds to the torsion load at which the particular crack was formed. The suffix B designates a bending load. In the testing of beam R4, the ratio of bending moment to torque at failure was close to five, and thus the resultant cracking pattern is much as expected. At the other end of the testing spectrum, the ratio of bending moment to torque for beam R5 was slightly greater than one. Consequently, the formation of parallel compression diagonals is well defined. Generally, most primary cracks were 7 to 8 inches apart, with secondary cracks more closely spaced at 2 to 4 inches.

#### 5.4 Potential Sources of Anomalies

In the casting of test specimens, dimensional tolerances are inevitably introduced, and their severity must be accounted for in the estimation of accuracy of strength and deformation predictions. The most significant source of potential dimensional inaccuracy unique to the seven beams cast was the presence of the styrofoam voids. Any substantial movement of the styrofoam blocks during casting would have

introduced dramatic variation in the thickness of the thin concrete flanges and webs. Presence of the closed torsion hoop reinforcement was used to advantage to secure the position of the voids, and post-test examination revealed that little variation in wall thickness was apparent.

The nature of the beam supports was such that a uniform St. Venant torque could be accommodated along any length of the beam. However, the presence of the 18 inch long solid beam ends beyond the supports offered longitudinal warping restraint to the small out-of-plane warping displacements that were generated at the beam ends during torsion tests. As a result, the beam length along which deformation measurements were taken was centrally located such that the influence of the solid ends would have diminished to a negligible level.

For the sake of expediency in ease of handling and positioning, the hoops and bars were lightly tack-welded during construction of the reinforcement cages. The welding was sufficiently light such that no brittle joints would be formed. The rigidity thus introduced into the cages had no effect on the pre-cracked beam stiffness, and contributed little to the post-cracked stiffness. Of greater significance concerning the reinforcement cage design was the location of the top longitudinal bars one inch in from the hoop corners. This feature was necessary to facilitate casting. Although Collins and Lampert<sup>25</sup> state that the positions of the corner longitudinal bars define cross-section geometry of the cracked concrete beam subjected to torsion, the movement of the top corner bars did not have a marked effect on the torsion failure loads for the seven beams tested. This was primarily due to the ratio of bending moment to torque remaining sufficiently high such that

the uncracked state of the top flange was preserved up to failure in most instances.

The presence of the clamping bolts that secured the torsion arms, Amsler point loading and beam support apparatus did restrain the propagation of cracking beyond the central test section in each beam. Individual bolts were  $3/4$ " in diameter and effectively acted as oversized stirrups.

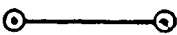

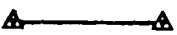







In the lower range of elastic behaviour where beam deformations were small, the linear displacement transducers did not yield consistently accurate results in the calculation of beam twist. This inaccuracy arose partly through the method of attaching to the concrete the smooth metal plates on which the transducer needles impinged, and partly because the measuring instrument was being used at the lower limit of its range of accuracy.

		Beams									
		R1	R2	R3	R4	R5	T1	T2			
At Cracking	Initial Prestress	74.4	75.8	72	72.9	71.6	65.8	65.73			
	Final Prestress	63.4	64.1	61.1	62.9	63.7	56	56.2			
At Failure	Torque	200	100	140	140	270	130	75			
	Bending Moment	460	660	760	820	330	300	300			
	Shear	0.0	0.0	10.0	10.0	0.0	0.0	0.0			
	Torque	520	372	532	336	614	290	196.5			
	Bending Moment	1080	1291	1357	1624	640	598	801			
	Shear	0.0	0.0	11.0	18	0.0	0.0	0.0			

TABLE 5.1 BEAM STRENGTH

Bending Stiffness*	4485.5	3560	4950	6340	2280	2531	2092
Torque Stiffness**	13.76 x 10 <sup>6</sup>	-	-	-	5.184 x 10 <sup>6</sup>	4.91 x 10 <sup>6</sup>	-

TABLE 5.2 PRE-CRACKED BEAM STIFFNESS  
 \* Units of Kips (inch K/inch)  
 \*\* Units of inch Kips/radian/in.

 	<p>Experimental Bottom Longitudinal Steel</p> <p>Model Bottom Longitudinal Steel</p>
 	<p>Experimental* Top Longitudinal Steel</p> <p>Model* Top Longitudinal Steel</p>
 	<p>Experimental West Hoop Leg</p> <p>Model West Hoop Leg</p>
 	<p>Experimental East Hoop Leg</p> <p>Model East Hoop Leg</p>
 	<p>Experimental Bottom Hoop Leg</p> <p>Model Bottom Hoop Leg</p>

\* Note: In Figures 5.6 and 5.12, the designation for the ordinates of the experimental top longitudinal steel curves is the symbol ▲

**TABLE 5.3 NOMENCLATURE FOR CONVENTIONAL REINFORCEMENT STRESS-LOAD CURVES**



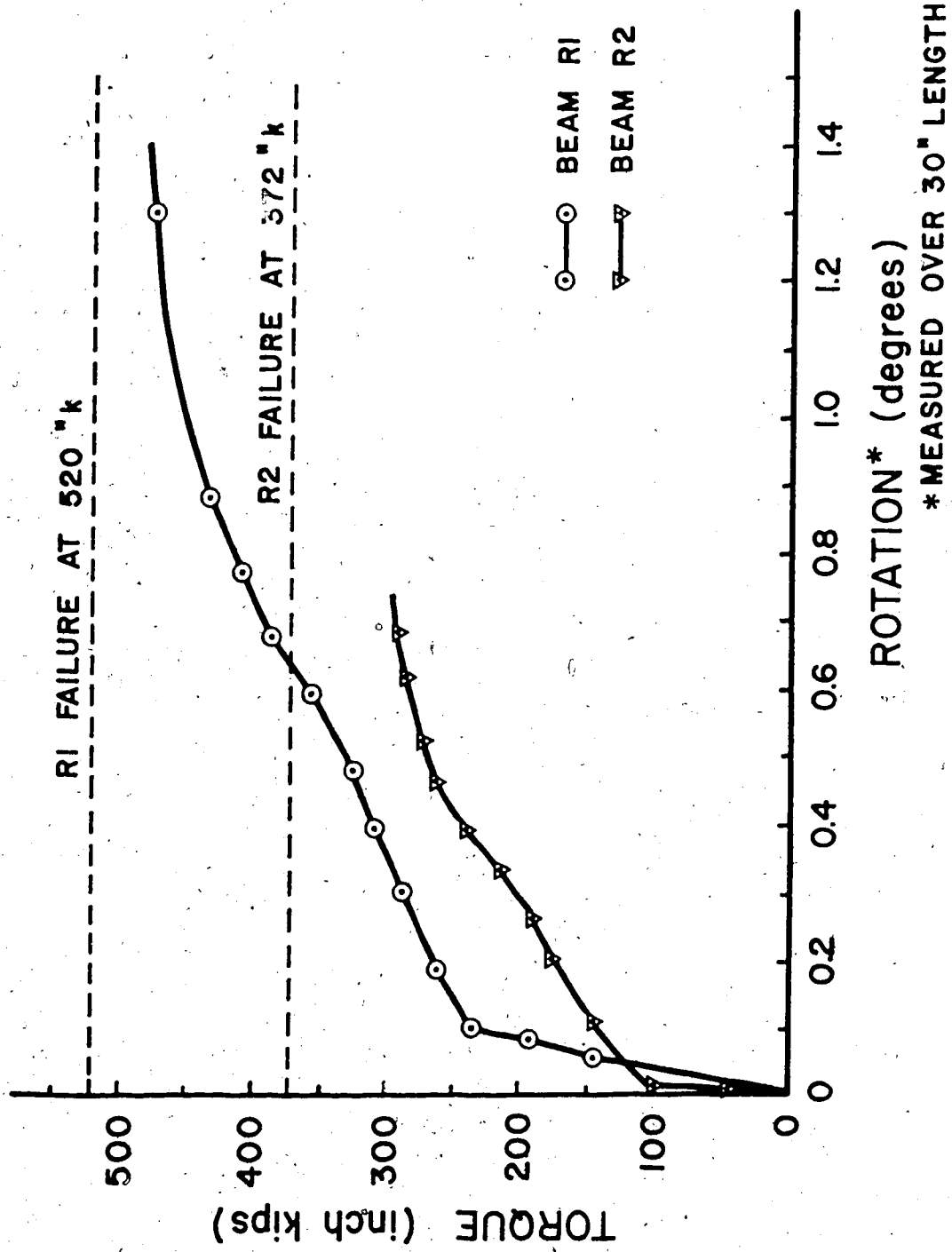


FIG. 5.1 TORQUE-ROTATION CURVES FOR BEAMS R1 AND R2

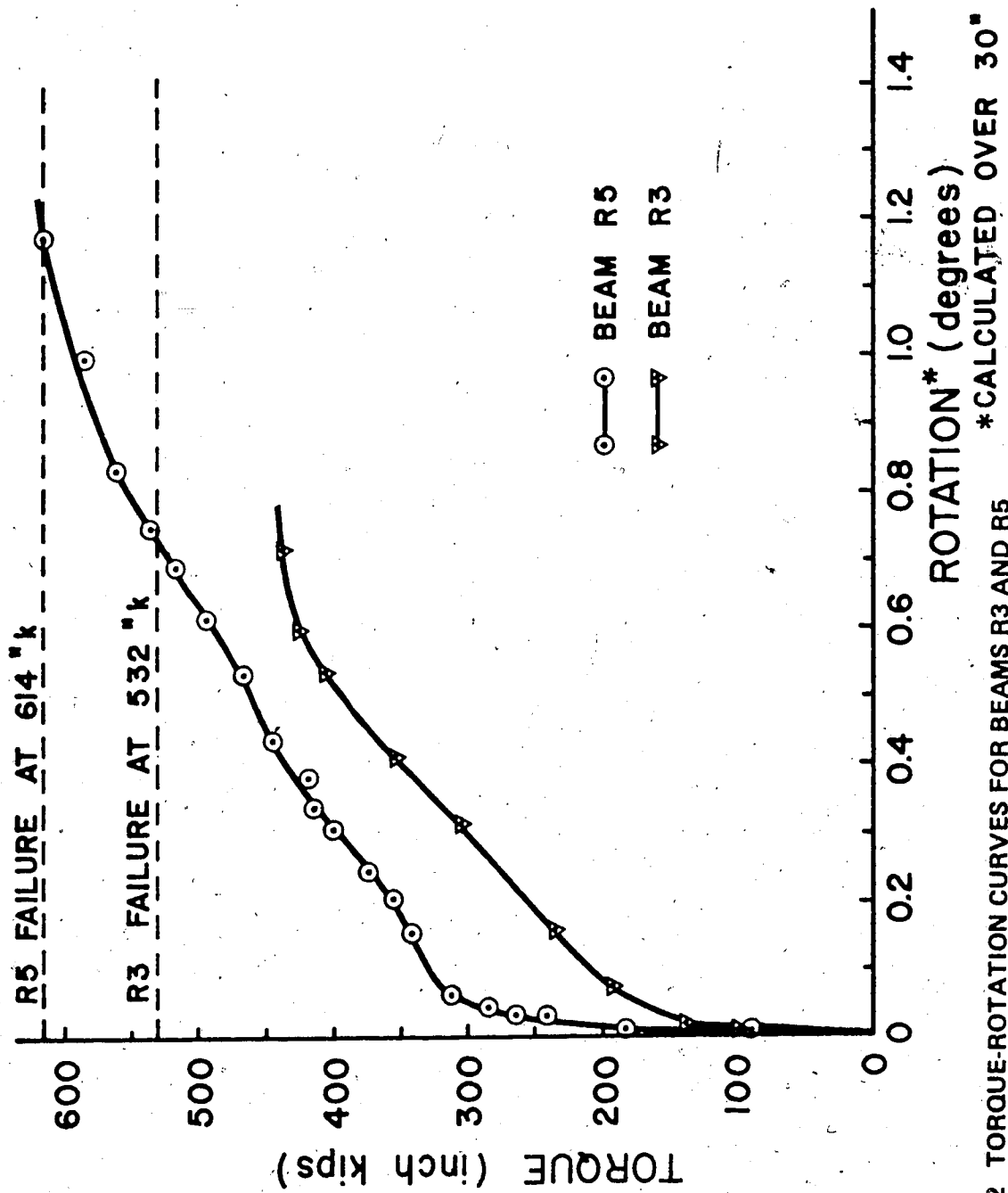


FIG. 5.2 TORQUE-ROTATION CURVES FOR BEAMS R3 AND R5

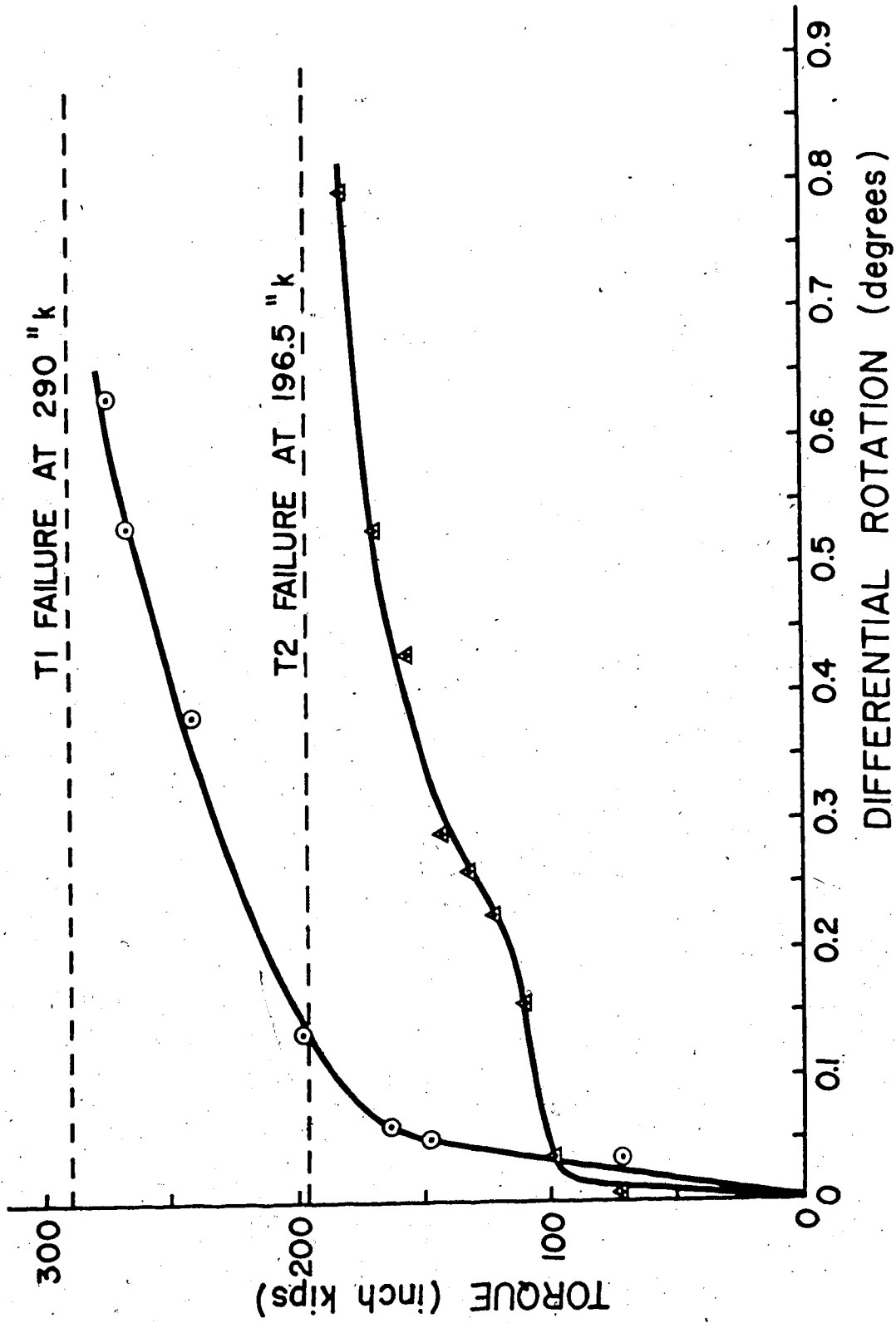


FIG. 5.3 TORQUE-ROTATION CURVES FOR BEAMS T1 AND T2

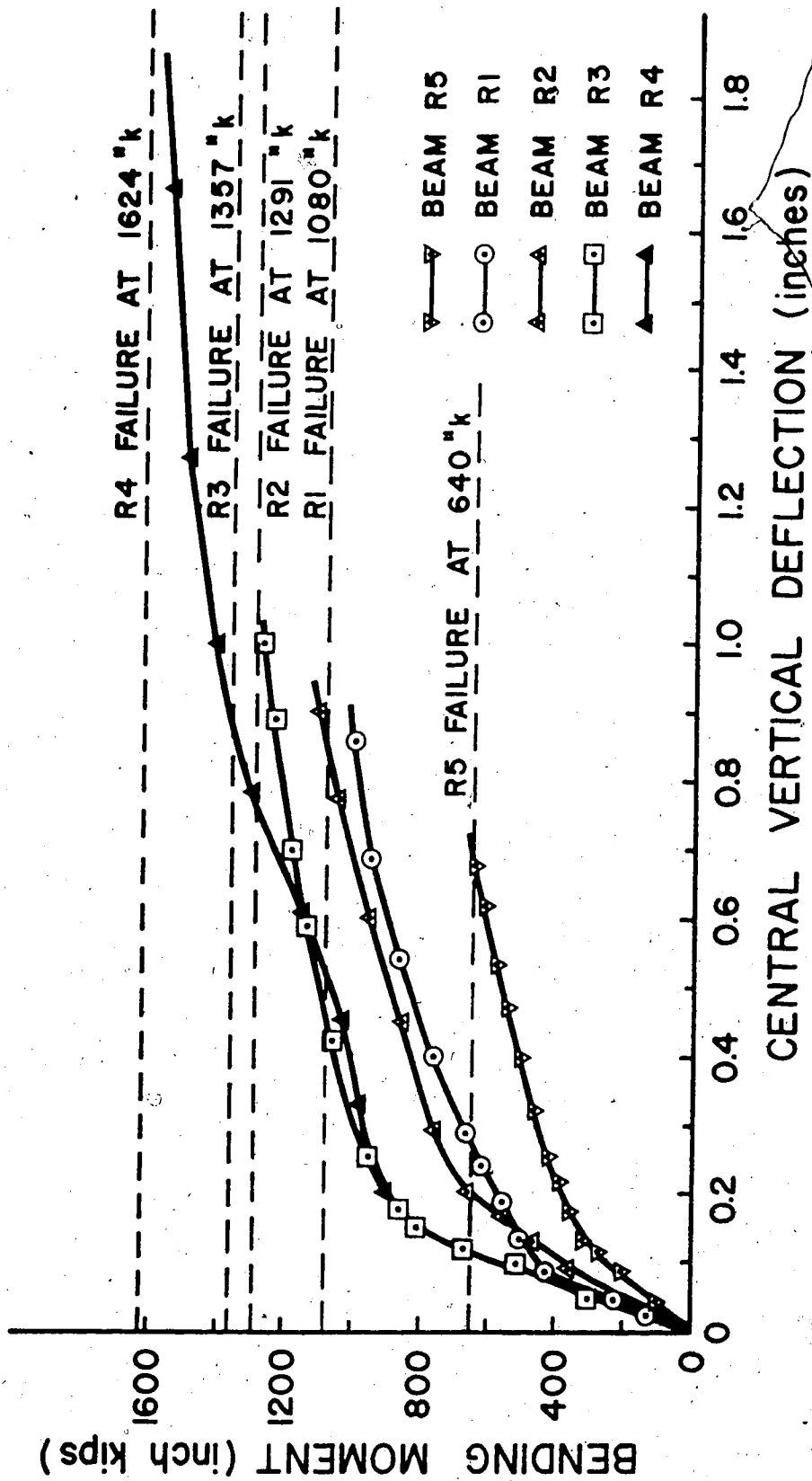


FIG. 5.4 MOMENT DEFLECTION CURVES FOR BEAMS R1, R2, R3, R4, R5

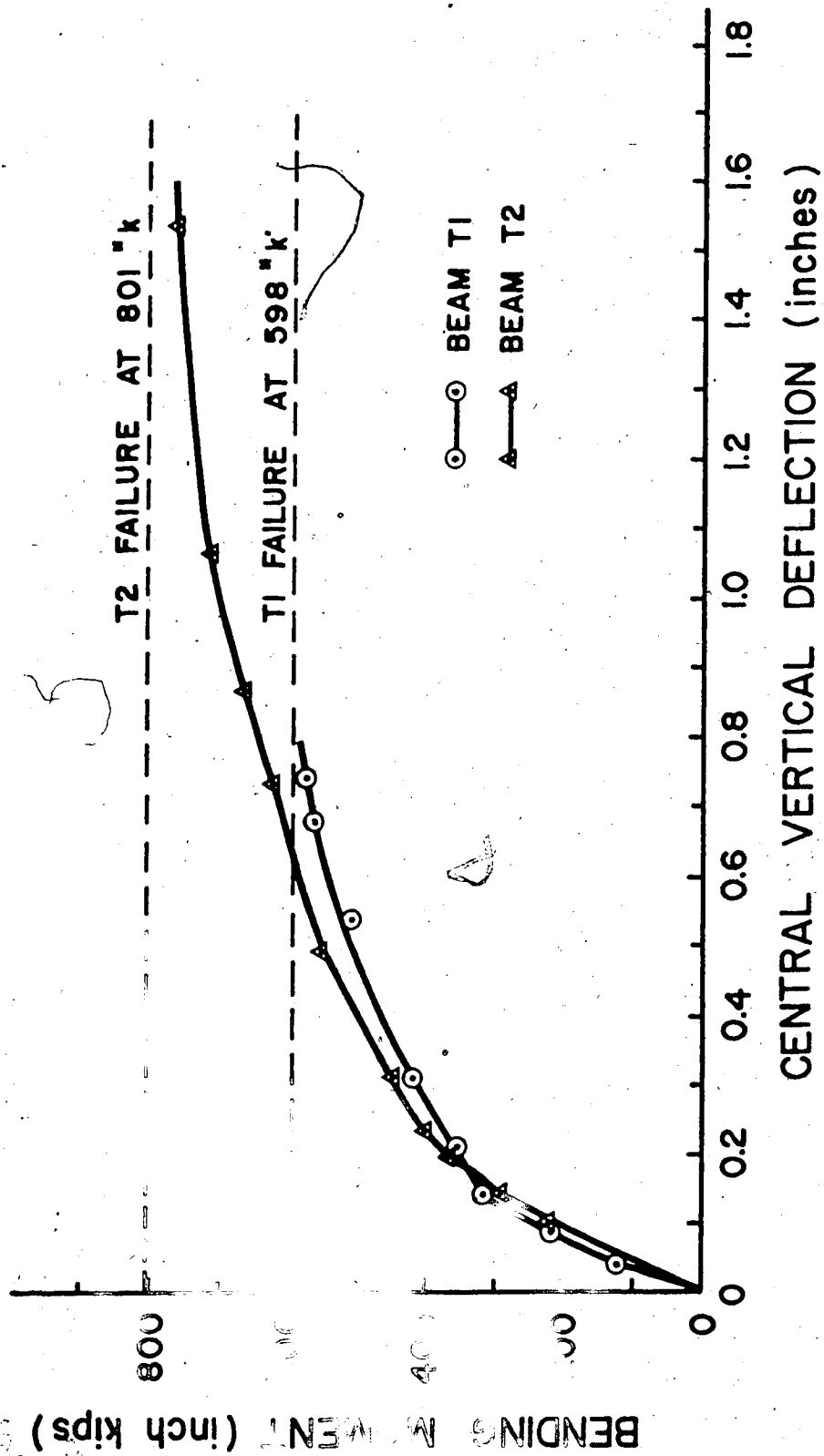


FIG. 5.5 MOMENT DEFLECTION CURVES FOR BEAMS T1 AND T2

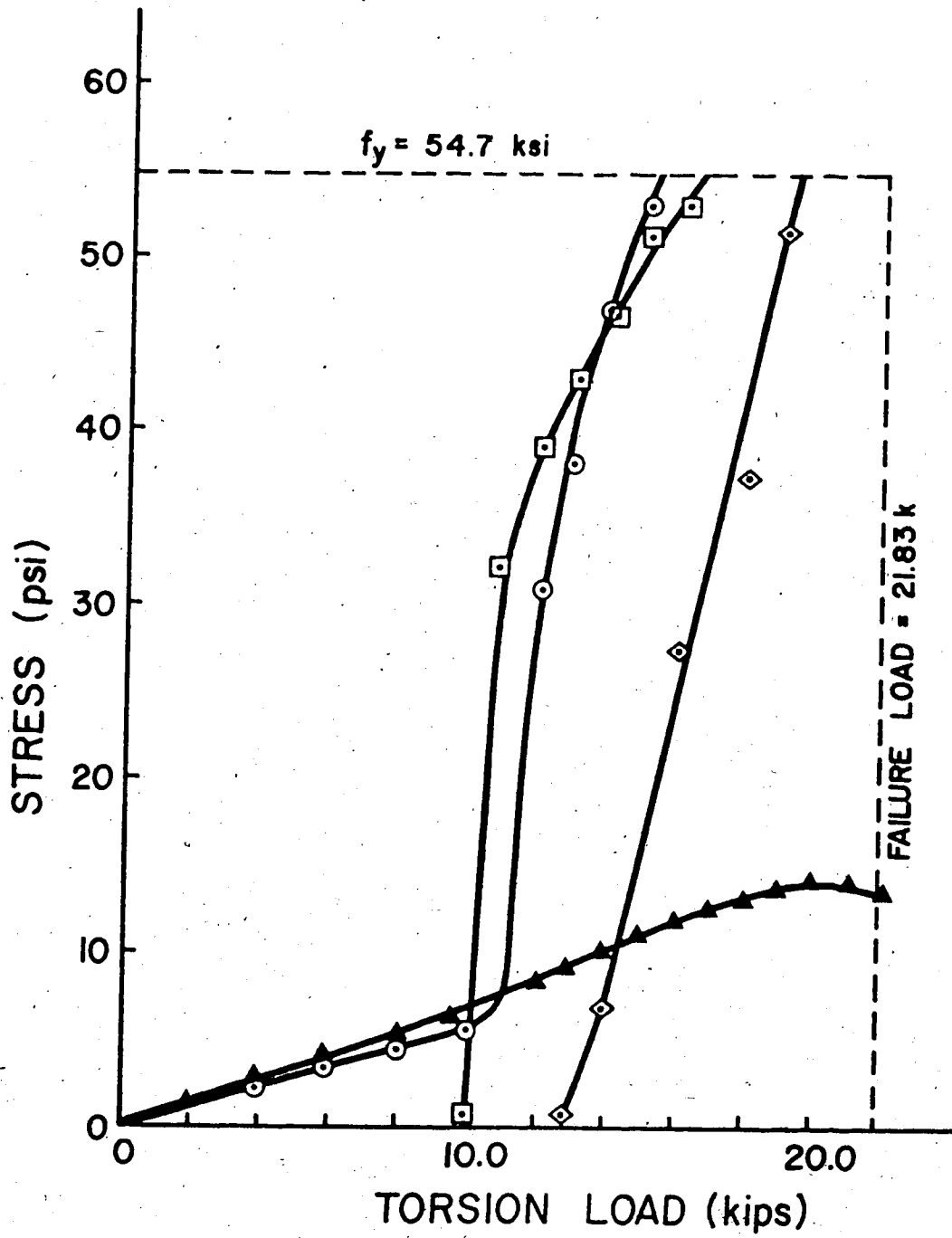


FIG. 5.6 STRESS-LOAD CURVES FOR BEAM R1 REINFORCEMENT

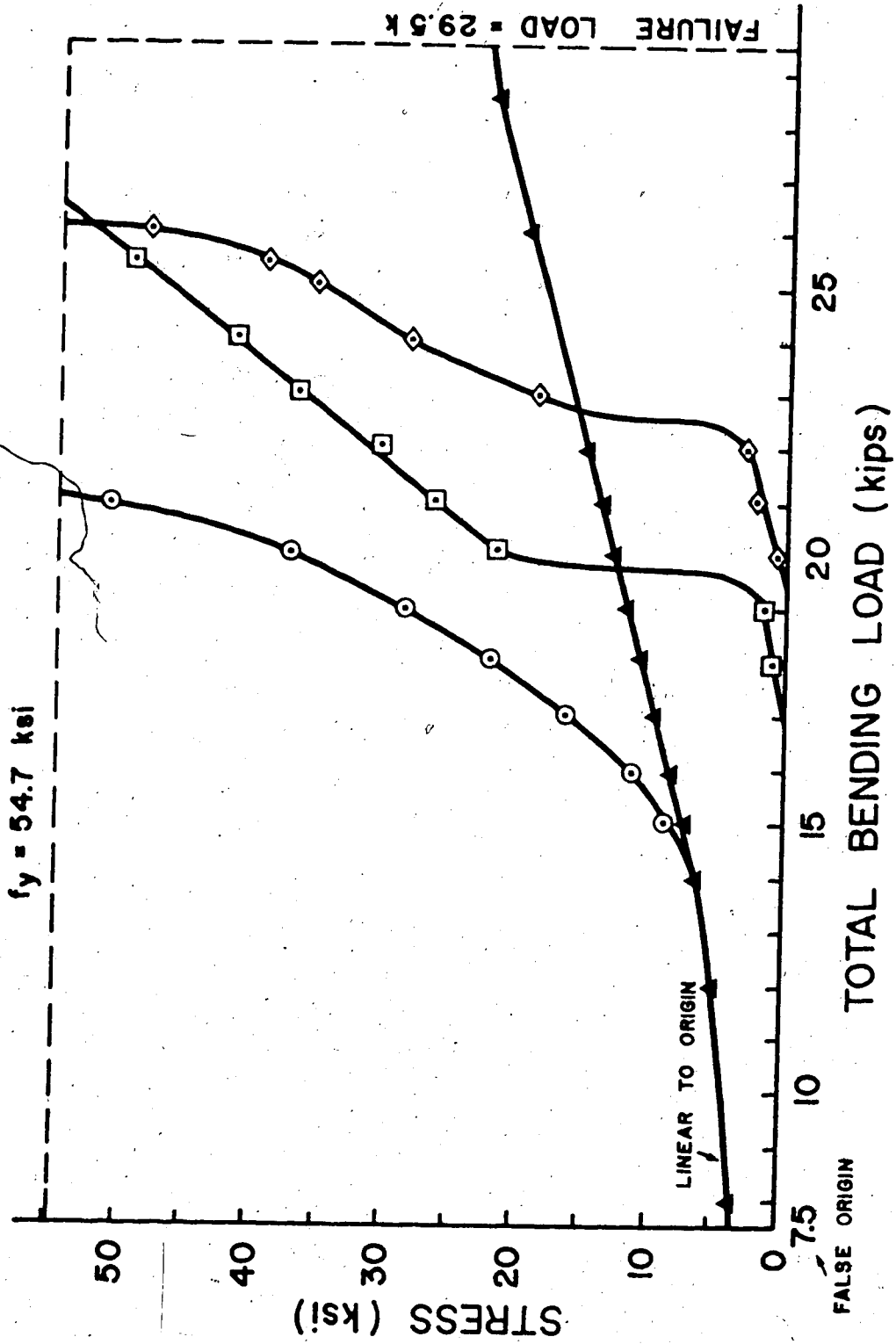


FIG. 5.7 STRESS-LOAD CURVES FOR BEAM R2 REINFORCEMENT

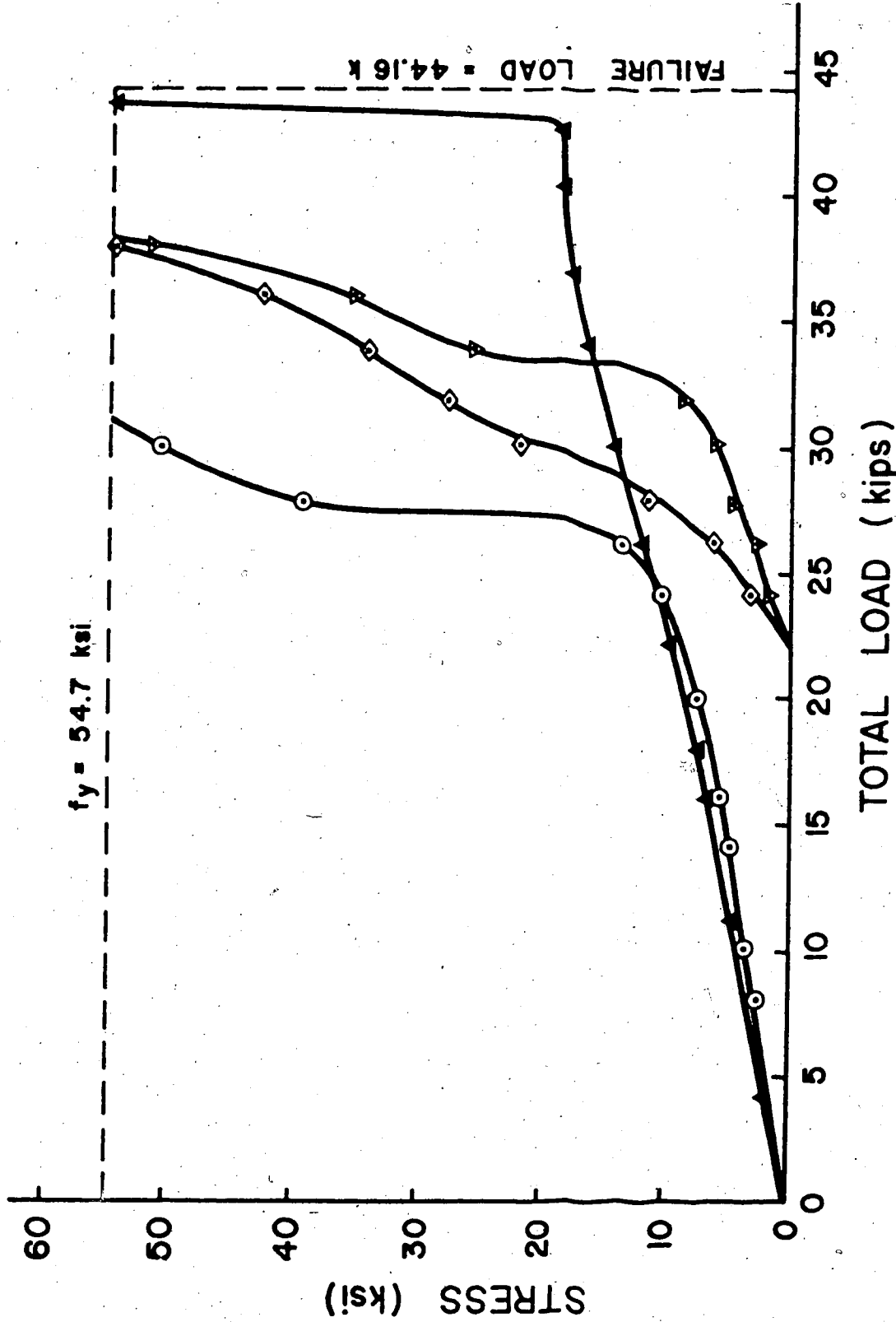


FIG. 5.8 STRESS-LOAD CURVES FOR BEAM R3 REINFORCEMENT



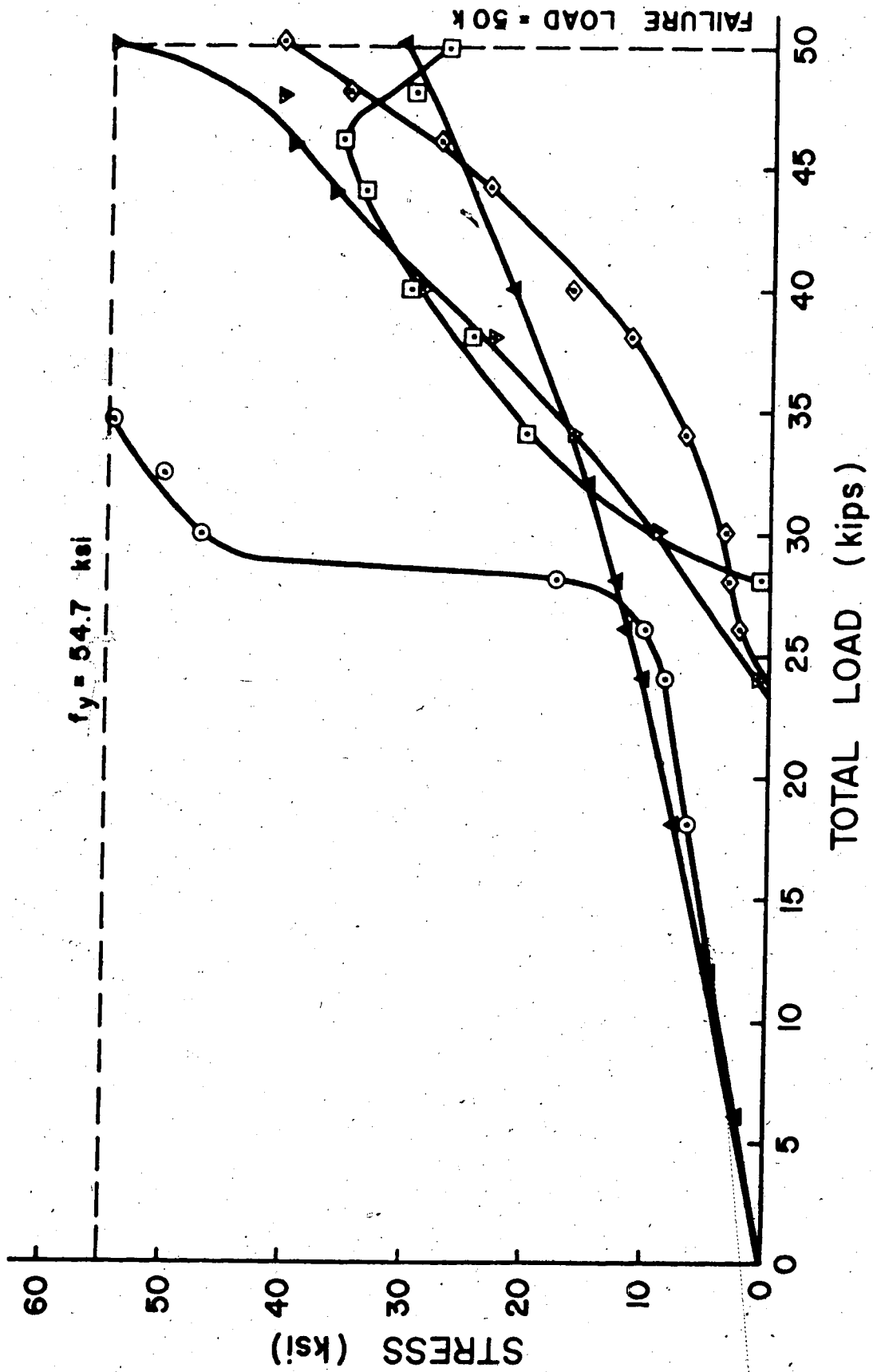


FIG. 5.9 STRESS-LOAD CURVES FOR BEAM R4 REINFORCEMENT

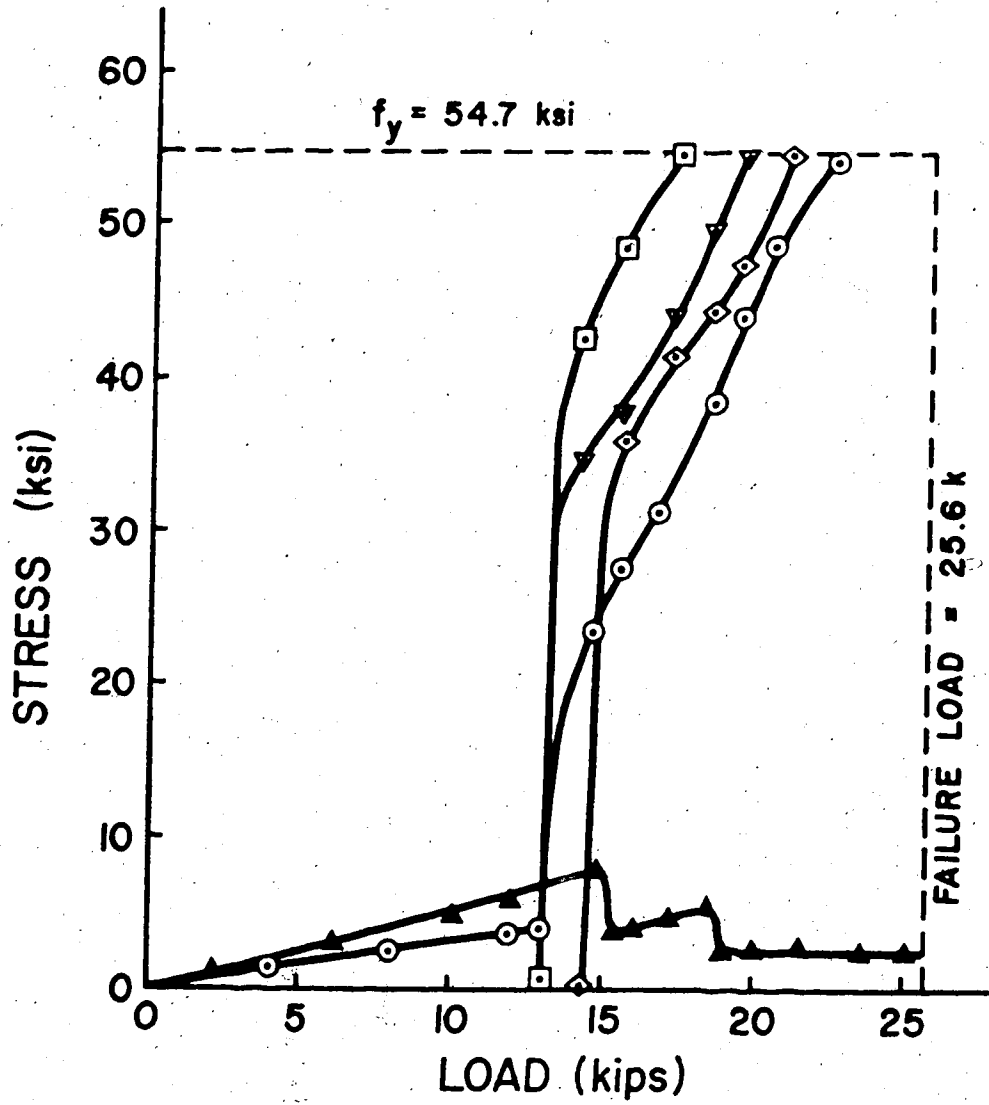


FIG. 5.10 STRESS-LOAD CURVES FOR BEAM R5 REINFORCEMENT

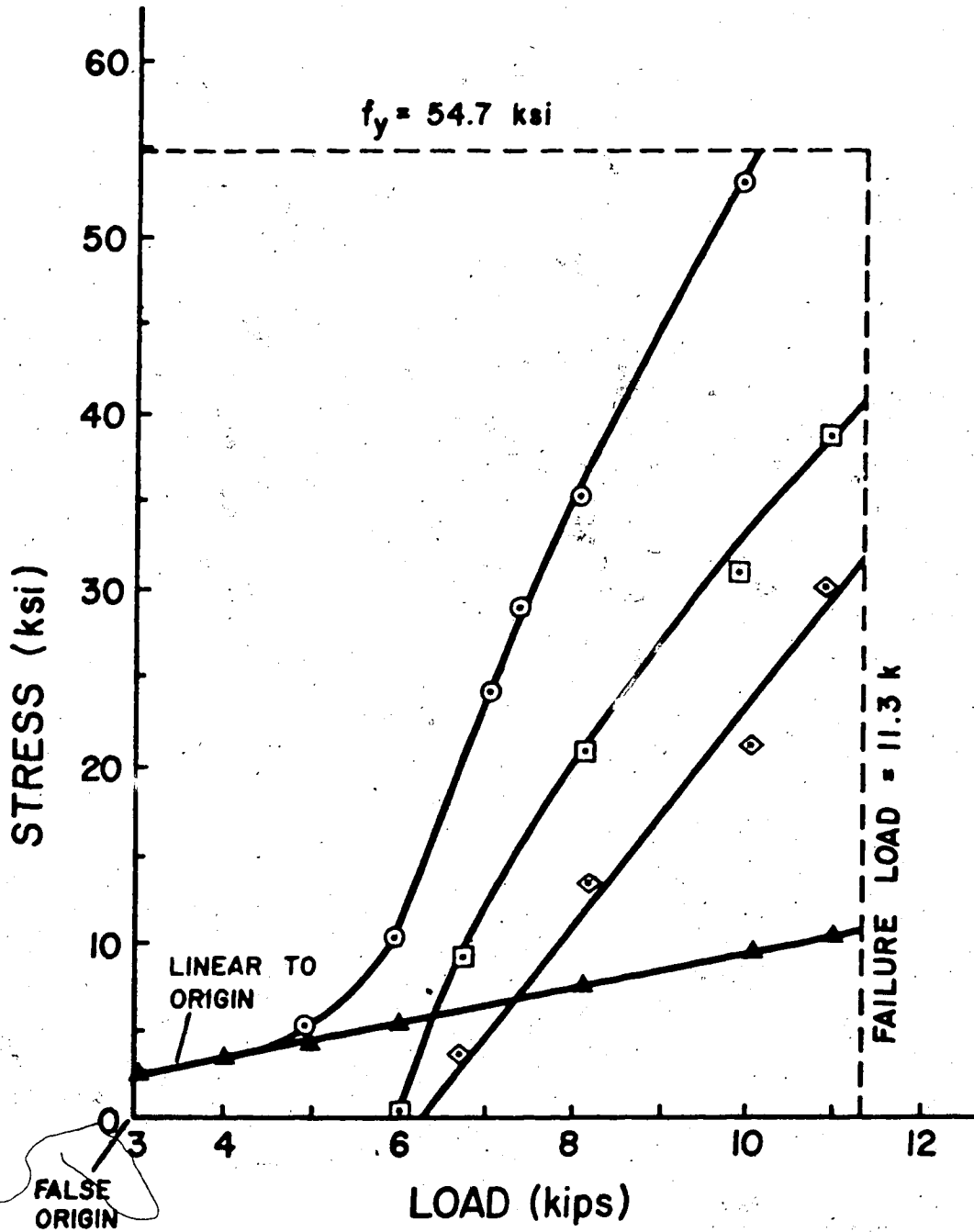


FIG. 5.11 STRESS-LOAD CURVES FOR BEAM T1 REINFORCEMENT

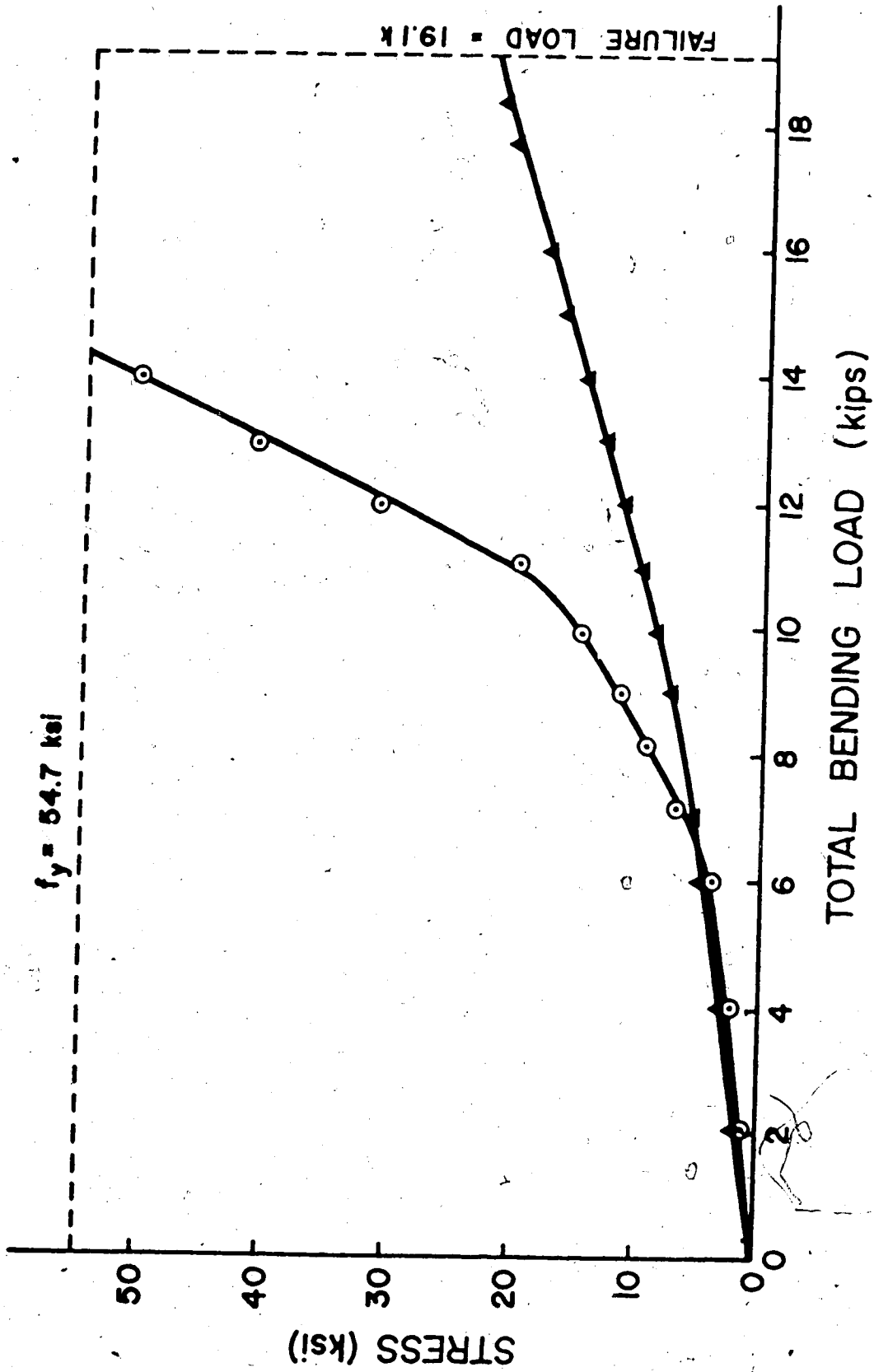


FIG. 5.12 STRESS-LOAD CURVES FOR BEAM T2 REINFORCEMENT



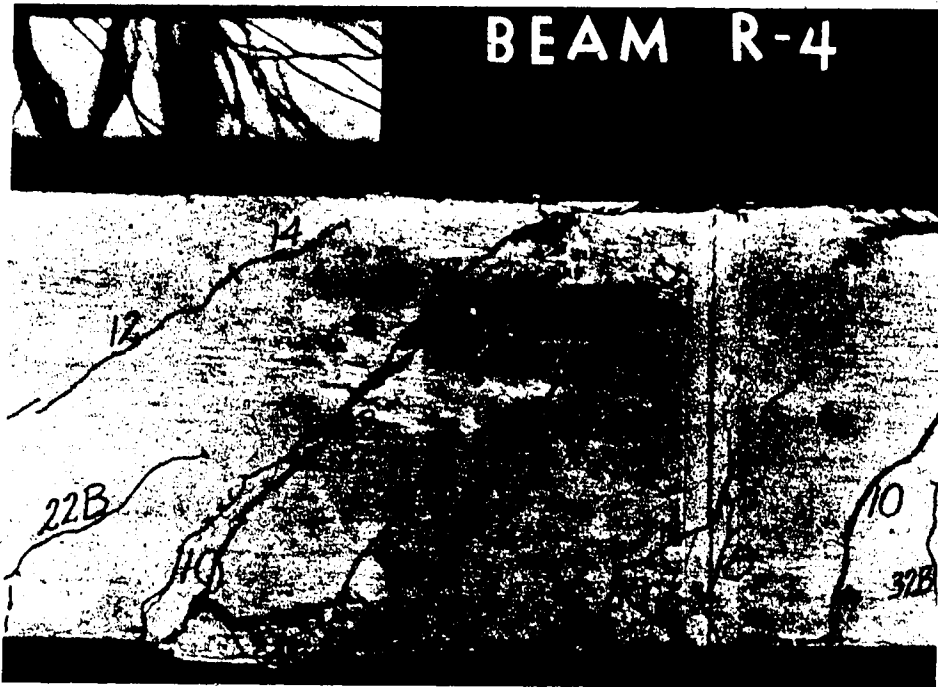


PLATE 5.1 FAILURE MODE OF BEAM R4



PLATE 5.2 LOCAL FAILURE OF BEAM T1

## CHAPTER VI

### EVALUATION OF COMPUTER MODEL RESULTS

#### 6.1 Introduction

Motivation to develop this finite element computer model arose through the need for a flexible, precise analytical method of analysis of concrete box girders subjected to a general load condition. The principles of the mechanics incorporated in the computer model have been described in detail in Chapter 3 but performance of the assembled model was not addressed. This chapter focuses on the evaluation of the computer model results through comparison with experimental tests and related current theory.

Initially, those aspects that strongly influence the computer model response and do not represent common finite element modelling considerations, are examined to establish an insight into model behavioural characteristics revealed in the subsequent comparisons. The subject of comparison is the spectrum in behaviour of the seven prestressed concrete box girders that were tested in the experimental program described in Chapter 4. Following the presentation of the experimental test results and the corresponding computer model results in Section 6.3, theoretical estimates of ultimate beam strength and interactive response are in turn compared with the analytical model predictions in Section 6.4. Performance of the finite element model is assessed on the basis of the two comparative presentations, and is pursued in Section 6.5:

## 6.2 Extraordinary Influences on Computer Model Response

In assessing the performance of the computer model, consideration must be given to the following important aspects that both individually and collectively have a strong bearing on the model results. Several aspects are unique in the application of the analytical model to simulate the response of the seven prestressed concrete box beams tested in the experimental program. All aspects are of either a material or structural nature.

### 6.2.1 Material Behaviour Aspects

In simulating the stiffness of an uncracked reinforced concrete beam, the material property of paramount concern is the initial elastic modulus for the concrete. Since the stiffness contribution of the reinforcement in an underreinforced concrete beam is small compared with that of the concrete, an inaccurate determination of the initial concrete modulus will result in a correspondingly inaccurate prediction of beam deformations. Since concrete cylinder tests did not yield consistent results and empirical formulae were not sufficiently accurate, the initial deflection measurements of the test beams were used in precisely calculating the respective initial concrete moduli.

A significant discrepancy was observed between the average crack spacing value derived using Eq. 3.29 and the corresponding experimental value determined from the beam cracking patterns at failure. Since aggregate interlock stiffness is a function of crack width and thus of average crack spacing, adoption of the considerably smaller theoretical value would have resulted in an overestimation of post-cracking concrete stiffness.



Reconstitution of the stiffness of a reinforced concrete element beyond cracking is difficult in that the contribution of "dowel action" cannot be determined accurately. Research has not conclusively established the quantitative effect upon dowel stiffness of several layers of web reinforcement or the inclination of the crack to the reinforcement axis other than at ninety degrees. However, consequences of the lack of complete understanding and definition of this phenomenon are not of major significance since dowel action accounts for less than 20 percent<sup>3</sup> of the shear strength of a cracked reinforced concrete beam.

#### 6.2.2. Structural Aspects

Although both conventional and prestress longitudinal reinforcement are represented in the analytical model by one dimensional bar finite elements, the same method cannot be extended to the modelling of stirrup and hoop reinforcement in this computer model. This restriction has arisen through characterizing the concrete finite element behaviour by the stress-strain condition at the centroid of the element. When the principal tensile stress at the concrete element centroid exceeds the specified tensile strength of concrete, the element is designated as a cracked element. However, the element is not fractured by several parallel cracks distributed across the element, but by one crack passing through the centroid. Thus, when the vertical web reinforcement is concentrated into bars located at the vertical boundaries of an element whose aspect ratio exceeds unity, it is highly probable that the sole centroidal crack will not intersect the side boundaries of the element. Consequently, the cracked element cannot utilize its web reinforcement, and a premature shear failure will occur. To resolve this modelling difficulty, the web reinforcement is distributed throughout

the element as a uni-directional steel mesh of closely spaced bars. When cracking occurs, the complete mesh stiffness for the concrete element is engaged. Thus, modelling of the mechanics of stirrup and hoop reinforcement in the cracked concrete condition closely reflects real behaviour. Figures 6.1(a) and 6.1(b) illustrate the problem and solution of this vitally important aspect of analytical modelling.

In Section 3.2.1, an expression was derived for the variation in shear stress across a "thick" wall as a function of the uniform shear flow, in the form:

$$\frac{\Delta v}{v} = \frac{A_c}{A'} \quad (3.12)$$

Clearly, for those tubular members whose height and width dimensions are only moderately large compared with the wall thickness, the maximum shear stress at the wall surface can be considerably larger than that at the wall mid-thickness; ie. the uniform shear flow. Considering that plane stress finite elements do not permit shear stress variation across their thickness, and that such elements are located at the plates' mid-thickness, only uniform shear flows can be adequately represented. The computer model's insensitivity to shear stress variation is of concern since surface cracking in concrete will immediately propagate through the entire thickness of a tubular member's wall. Thus, if the torsional shear stresses are high at the critical cross-section of a concrete box girder, the computer model will yield underconservative estimates of cracking load and to a lesser extent post-cracking member stiffness.

A further possible consequence of the location of plane stress finite elements at wall mid-thickness is the inaccurate prediction of

the ultimate bending moment capacity of an underreinforced concrete box girder. In the analytical model, the lever arm length from the force resultant in the concrete compression flange to the tension reinforcement at ultimate load conditions is fixed by geometry. If the compression flange is thick with respect to the girder's depth, the concrete compressive force resultant will be located between the wall mid-thickness and the upper flange surface, the height of the resultant force above the compression flange mid-thickness constituting the difference between the experimental and model lever arms. Also, since the thick concrete compression flange of the computer model is too stiff close to failure, the tension reinforcement will be forced to carry a disproportionately higher load, further reducing the ultimate bending moment capacity of the girder below its actual strength.

Before a reinforced concrete beam is tested, the concrete and reinforcement are already stressed through shrinkage and creep member deformations, the effects of these phenomena being most pronounced in precast prestressed concrete beams. Failure to include the presence of the tensile concrete shrinkage stresses can result in significant overestimation of the cracking load, and a slight distortion of pre-cracked deformations.

Although the longitudinal warping restraint of beam end diaphragms is not normally of real structural significance, the modelling of the seven prestressed box beams tested in the experimental program was complicated by the presence of the 18 inch long solid beam ends extending beyond each beam support. Since the warping resistance of the solid ends was comparable to that of the box beams, accurate representation of their influence on beam behaviour was essential.

Consequently, the approach outlined in Section 3.4.2.7 was adopted, and the warping stiffnesses established in the auxiliary finite element program were read in as input in the principal analytical model.

As shown in Figures 4.7, 4.8, and 4.9, clamping bolts were used to maintain the position of testing equipment at several locations along the length of the test specimens. Verified by observations during testing, the clamping bolts and the radial torsion loading arms effectively acted as very stiff stirrups, greatly restricting the propagation of web cracking in their vicinity. Thus, their presence in the analytical model is essential from both deformation and strength aspects. In a similar manner to that adopted for conventional stirrup and hoop reinforcement, equivalent steel meshes were included in adjacent concrete elements to represent their influence.

In each of the seven test beams, the solid cross-section infringed upon the test span, the distance from the support to the commencement of the styrofoam voids varying from 7.5 to 13.5 inches (Fig. 4.4). Since the stress levels at the beam ends were not sufficient to produce cracking, the primary modelling concern was deformational accuracy, especially with respect to bending deflections. Deformation characteristics were modelled closely through the use of plane stress finite elements of an appropriate, uniform thickness such that the moment of inertia remained unchanged.

In the casting of prestressed concrete beams, small flexural cracks will often appear in the top flange after transfer. Upon the application of positive moment, these cracks will immediately close, and the subsequent beam response will not reflect their initial presence.

Provision is made within the model to reproduce such behaviour. If a model crack closes in the load increments immediately following transfer, the full concrete constitutive matrix is recovered. Should a crack close at a later stage in the loading sequence, the aggregate interlock stiffness does not increase, but is maintained at the level prior to crack closing.

### 6.3 Comparison of Computer Model and Experimental Results

In this Section, the computer model and experimental results for the seven prestressed box girders are presented in a form that facilitates a thorough comparison. Assessment of the analytical model performance on the basis of this comparison is treated in Section 6.5.1.

Since the complete spectrum of beam response from initial loading to failure is to be examined, plots of torque versus rotation, bending moment versus central beam deflection, and reinforcement stresses versus load have been prepared for every test beam, each plot displaying the corresponding model and experimental coordinates. Monitoring of reinforcement stresses embraces the behaviour of the top and bottom flange conventional reinforcement at the beam span centreline and the four legs of the centrally-located hoop. The legend for identification of the reinforcement stress plots is provided in Table 5.3.

The twenty figures displaying comparative beam plots, Figures 6.2 to 6.21, are not completely comprehensive as two plots have not been presented. Reference to the Figure List indicates that the torque versus rotation curve for beam R4 and the hoop reinforcement stresses versus load graphs for beam T2 are the two absent plots. For beam

R4, its torque-rotation curve closely follows the respective plot for beam R3 since the loading of both beams only differed significantly beyond the scope of the torsion plot of beam R4. During the test of beam T2, the central hoop strain gages exhibited erratic readings which prejudiced their experimental value. In the torque-rotation graph of the experimental results of beam T2, shown in Fig. 6.20, the initial coordinates are not plotted as they displayed considerable inconsistency. The two computer model curves for the bending moment-deflection response of beam R4 represent the two loading extremes of the heavy Amsler jack load applied at the beam centreline. If the beam failure mechanism comprised a centreline hinge in the compression flange, and the loading plate was sufficiently stiff to bridge the hinge, the loading pattern of Fig. 6.22(b) is feasible, in contrast to that illustrated in Fig. 6.22(a) where complete contact is assumed.

Two computer model graph characteristics exhibited in the majority of bending moment-deflection and torque-rotation plots require clarification. For those beams where failure of the finite element model occurred within a load increment, the model strength results are described by a band delineating the lower and upper load bounds. The second point of clarification is the significance of the "translated" computer model curve shown in those figures where there is considerable discrepancy between experimental and model cracking loads. If the computer model behaviour was adjusted such that its cracking load agreed closely with the corresponding experimental load, the projected analytical model results are represented by the "translated" computer model curve. Most importantly, the translation procedure does not entail pre-cracking or post-cracking stiffness modification. Development of the translated curve is detailed in Section 6.5.1.

The cracking and ultimate strength combined loading conditions for the experimental and the corresponding computer model beams are presented in Table 6.1. Invariably, the deformation value at the point of ultimate strength was indeterminable from both the experimental and computer model results. Consequently, there is no objective method of comparing experimental and computer model postcracking stiffnesses, and thus a subjective evaluation of the corresponding curves is the best recourse.

#### 6.4 Comparison of Computer Model Results with Current Theory

Of the vast number of research publications in the field of torsion, bending, and shear in reinforced concrete, reference has been made to Collins and Lampert<sup>25</sup> in estimating pure ultimate torsional strength, Thürliman<sup>50</sup> in the evaluation of bending moment-shear interaction and pure shear strength, and Elfgren<sup>51</sup> concerning torsion-bending and torsion-bending-shear interaction. Since current theory cannot predict post-cracking member deformations under combined loading, only ultimate strength predictions will be considered. Evaluation of cracking loads will not be treated as this area of research has been exhaustively examined in the past, and resolved to a satisfactory degree. Similar to the previous Section, this Section will only present a comparison of theoretical and model predictions, with the assessment and implications of the comparison addressed in Section 6.5.2. Since geometry, concrete strength, and reinforcement levels are almost identical within the two test beam classifications, average ultimate strengths will be presented for the rectangular and trapezoidal beam categories.

### 6.4.1 Ultimate Strength

In the application of the Space Truss Theory proposed by Collins and Lampert<sup>25</sup> to estimate the ultimate torsional capacity of a prestressed concrete box girder, the form of their equations is not modified to account for initial prestress. The prestress strand is simply considered as reinforcement of strength  $f_s^* A_s^*$ , where  $f_s^*$  is the yield stress of the prestress steel and  $A_s^*$  the area of the individual strand. For both the rectangular and trapezoidal beams, the weaker top reinforcement determines the ultimate torsional capacity of the two beam classifications. When considering the trapezoidal beams, the web prestress strand was distributed to the top and bottom flange stringers such that the ultimate bending moment capacity remained unchanged. The ultimate torsional capacity is given by

$$T_o = 2A_o \sqrt{\frac{\sum Z_y}{u} \cdot \frac{S_y}{t}} \quad (6.1)$$

where  $A_o$  = area enclosed by corner longitudinal bars,  $\sum Z_y$  = twice the sum of yield forces of longitudinal bars in the weaker flange,  $S_y$  = hoop yield force,  $u$  = corner longitudinal bar perimeter, and  $t$  = hoop spacing. The average ultimate torsional capacity of the five rectangular beams using the Space Truss Theory is 379 inch kips, and the corresponding strength for the two trapezoidal beams is 239 inch kips.

Since the Space Truss Theory cannot accurately estimate the compression zone depth, and Skew Bending Theory cannot accommodate the presence of longitudinal web reinforcement or longitudinal reinforcement of different yield strengths, classical bending theory<sup>52</sup> as currently incorporated in prestressed concrete design has been used to evaluate the ultimate bending moment capacity of the two beam types. For the



five rectangular beams, the average ultimate bending moment capacity is 1515 inch kips, and 985 inch kips for the two trapezoidal beams.

Calculation of the pure shear strength of the two box beam types follows the approach advocated by Thürliman<sup>50</sup>. On the basis of a simplified, generalized space truss model, Thürliman devised the following expression for the "plastic shear force"  $V_{po}$ :

$$V_{po} = \sqrt{2 F_{yl} \cdot S_y \cdot \frac{h}{t}} \quad (6.2)$$

where  $F_{yl}$  = yield force of bottom flange longitudinal stringers,  $S_y$  = yield force of stirrups at cross-section considered,  $h$  = ultimate bending moment lever arm, or, in the absence of an accurate estimation of this value, the centre to centre distance between the top and bottom stringers, and  $t$  = stirrup spacing.

However, since both the transverse and longitudinal reinforcement must yield simultaneously before failure for the above derivation to be valid, the variable angle of inclination of the compression concrete diagonals must lie within the range:

$$5 \leq \tan \alpha_g \leq 2 \quad (6.3)$$

where  $\alpha_g$  = angle of inclination of compression struts to horizontal.

For such an inclination range, the maximum shear resistance of a concrete beam is modified to

$$V_{pmax} = \sqrt{\frac{2}{\kappa}} \cdot V_{po} \quad (6.4)$$

where  $V_{pmax}$  = maximum shear resistance, and

$$\kappa = \frac{F_{y1} \cdot t}{S_y \cdot h} \quad (6.5)$$

In the application of the above equations to prestressed concrete (Thürliman's equations were developed for reinforced concrete), the axial force  $N$  in the equation below is not zero, and corresponds to the initial prestress force.

$$F_{y1} = \frac{M}{h} + \frac{N}{2} + \frac{V}{2} \cdot \cot \alpha_s \quad (6.6)$$

The form of the developed equations remains unaltered if the term  $F_{y1}$  is replaced by the term  $(F_{y1} + \frac{Nh'}{h})$  where  $N$  is the initial prestress force, and  $h'$  is the distance from the prestress strand to the concrete force resultant. Mostly,  $h'$  equals  $h$ . Therefore, Eq. 6.6 is valid in its original form if  $F_{y1}$  is defined as the total bottom stringer yield strength including the initial prestress force.

For the rectangular box beams, the plastic shear force is 70.7 kips and the maximum shear resistance is 49.5 kips. Similarly, for the trapezoidal box beams, the plastic shear force is 57.4 kips and the maximum shear resistance is 40.5 kips.

Since a computer model loading combination could not be devised that produced a pure shear loading similar to that considered in the preceding theory, an analytical estimate of the ultimate shear capacity could not be determined.

The experimental and corresponding computer model ultimate strengths are summarized in Table 6.3.

#### 6.4.2 Torsion - Bending Interaction

Of the seven box beams tested in the experimental program, five were subjected to torque and bending moment only, those beams being R1, R2, R5, T1, and T2.

The interaction equations of Elfgren<sup>51</sup>, in an identical form to those developed by Collins and Lampert<sup>25</sup>, are utilized to describe beam response under combined torque-bending moment load conditions. Under such combined loading, beam failure under the action of a positive bending moment can be either of two modes, mode t when failure is initiated by yielding of the bottom flange longitudinal reinforcement, or mode c when yielding of the top flange stringers precipitates beam failure.

##### Mode t

$$\frac{M}{M_o} + \left(\frac{T}{T_o}\right)^2 r = 1 \quad (6.7)$$

##### Mode c

$$\frac{M}{M_o} \left(\frac{-1}{r}\right) + \left(\frac{T}{T_o}\right)^2 = 1 \quad (6.8)$$

where r = ratio of yield forces of top and bottom flange longitudinal reinforcement.

In determining the value of term r in the above two equations, the full yield strength of the prestress strand is used. For the two trapezoidal beams that contain web prestress strand reinforcement, distribution of the longitudinal web steel to the top and bottom flange stringers is such that the ultimate bending moment capacity of the beams remains unchanged. The yield force ratio "r" is .2377 and .448 for the rectangular and trapezoidal beam categories respectively.

As a basis of comparison, the interaction Equations 6.7 and 6.8 are plotted in Fig 6.23 for both the rectangular and trapezoidal beam types, together with the corresponding computer model results for the five beams that failed under torque and bending moment loading only. The computer model results are displayed in their dimensional and non-dimensional form in Table 6.3, all results being average values for the load increment in which failure of the analytical model occurred.

#### 6.4.3 Torsion - Bending - Shear Interaction

Only two of the seven test beams were subjected to shear in addition to torque and bending moment at their critical cross-sections, the two beams being rectangular box beams R3 and R4.

The interaction equations adopted to define beam response under the combined loading of torque, bending moment, and shear are those proposed by Elfgren<sup>52</sup>. In conjunction with the two previously defined modes of failure the presence of shear introduces an additional mode of failure, mode s, where the compression zone is formed on the side of the beam. The corresponding interaction equations are as follows:

##### Mode t

$$\frac{M}{M_o} + \left(\frac{T}{T_o}\right)^2 r + \left(\frac{V}{V_o}\right)^2 r = 1 \quad (6.9)$$

##### Mode c

$$\frac{M}{M_o} \left(\frac{-1}{r}\right) + \left(\frac{T}{T_o}\right)^2 + \left(\frac{V}{V_o}\right)^2 = 1 \quad (6.10)$$

Mode s

$$\left(\frac{T}{T_0}\right)^2 \frac{2r}{r+1} + \left(\frac{V}{V_0}\right)^2 \frac{2r}{r+1} + \frac{TV}{T_0 V_0} \cdot \frac{2r}{r+1} \cdot \frac{2}{\sqrt{1+b'/h'}} = 1 \quad (6.11)$$

where  $b'$  = horizontal centre to centre distance of corner stringers in top or bottom flanges, and  $h'$  = vertical centre to centre distance of corner stringers in top and bottom flanges.

In conjunction with the above equations, Thürliman's interaction equations for bending moment and shear is also considered as an additional interactive constraint that must not be violated:

$$\frac{M_p}{M_{po}} + \left(\frac{V_p}{V_{po}}\right)^2 = 1 \quad (6.12)$$

where  $M_p$  = applied moment, and  $M_{po}$  = "plastic moment" or ultimate bending moment capacity. From earlier discussion, the applied shear  $V_p$  must not exceed the maximum shear capacity  $V_{pmax}$  established by Eq. 6.4. Similarly, as a consequence of the inclination of the compression struts being restricted to  $.5 \leq \tan \alpha_s \leq 2$ , the maximum applied bending moment must satisfy the condition:

$$\frac{M_{pmax}}{M_{po}} + \frac{V_p}{V_{po}} \cdot \frac{1}{4} \sqrt{\frac{2}{K}} = 1 \quad (6.13)$$

The interaction Eq. 6.12, together with the imposed limits of Equations 6.4 and 6.13, is shown in Fig. 6.24.

Using Eq. 6.2 to evaluate the plastic shear force  $V_0$  appearing in Equations 6.9, 6.10 and 6.11, the interaction equations for the three modes of failure of beams R3 and R4 are illustrated in Fig. 6.25. Only one set of interaction equations is shown as the respective equations

for the two beams are very similar. All three interaction equations have been simplified through the evaluation of the  $(\frac{V}{V_0})$  terms which are then transferred to the numerical right hand sides of their respective equations. Thus, three dimensional interaction is reduced to a two dimensional torque-bending moment interaction.

In Table 6.3 that displays the computer model results for beams R3 and R4, the bending moment failure loads have been adjusted to allow for the presence of the central downward vertical concentrated load illustrated in Fig. I.1(c) in Appendix I. Under such a loading system, Thürliman<sup>50</sup> has established that the principal design cross-section for shear is not located beneath the central load, but at a distance  $h$  either side of the concentrated load. Elfgrén's<sup>51</sup> examination of the effect of a concentrated load yields a similar result. Consequently, the failure bending moments for beams R3 and R4 have been altered accordingly. The adjusted computer model results for the latter two beams are plotted in Fig. 6.25.

## 6.5 Assessment of Computer Model Results

### 6.5.1 Computer Model Assessment in Light of Experimentation

6.5.1.1 Prominent Aspects of Model's Performance: In the uncracked state, the computer model yielded an accurate assessment of beam stiffness since the initial modulus of elasticity for concrete was evaluated directly from beam deformations at low load levels. This procedure in determining the concrete modulus was adopted as cylinder tests conducted for the sole purpose of modulus measurement produced a wide scatter of results. In this study the need for estimating the

modulus of concrete as accurately as possible is paramount as both deformation and strength characteristics are examined. The few instances of disparity in agreement between experimental and model behaviour in the pre-cracked condition appear in the torque-rotation relationship since the experimental deflection monitoring equipment was incapable of consistently accurate measurements of very small differential deflections of adjacent beam locations.

Although corresponding experimental and model elastic stiffnesses are in close agreement, a very discernible discrepancy is evident at the onset of cracking. For all beams where cracking occurred under a combined torque-bending moment load condition: i.e. all beams with the exception of R3 and R4; the model beam cracked at a considerably higher load than the experimental beam. The three potential sources of this deviation in behaviour are: concrete tensile strength, concrete shrinkage stresses, and variation in shear stresses across the wall thickness. Of the three potential sources, the effect of the variation in wall shear stresses is the most dominating influence on behavioural discrepancy. In Section 3.2.1, the variation in the St. Venant torsional shear stress from the wall surface to wall mid-thickness was shown to be equal to the ratio of the cross-sectional area to the area enclosed by the corner longitudinal reinforcement stringers. For the rectangular and trapezoidal beams, the ratio equals .61 and .87 respectively. Since the analytical model evaluates the torsional shear stresses at the wall mid-thickness, the maximum torsional shear stresses at the surface of the experimental beams are 61% and 87% higher than the corresponding model stresses for the rectangular and trapezoidal beams. This substantial discrepancy between mid-thickness and surface torsional shear stresses is critical as

cracks in the outer surface fibres immediately propagate through the entire wall thickness. If the shear stress variation were taken into account in the calculation of the model concrete principal tensile stresses, the discrepancy in cracking loads would be substantially reduced. However, difficulty in accurately measuring the concrete tensile strength and uncertainty in establishing concrete shrinkage stresses can collectively contribute to inaccurate cracking estimates. Thus, although the variation in torsional shear stresses can be taken into account, accurate prediction of cracking loads may not be achieved consistently.

As a result of the model's higher cracking load, a response delay is exhibited in the bending moment-deflection, torque-rotation, and reinforcement stresses-load graphs. In those moment-deformation figures where the response delay is considerable, a "translated computer model curve" has been plotted in addition to the actual model curve to illustrate the projected computer model response if the cracking load discrepancy did not occur. To define the translated curve, the post-cracking portion of the actual model curve is moved horizontally to the right until the tangent projection of the inelastic curve below its local origin intersects the elastic slope at the experimental cracking load. The prophetic significance of the translation procedure illustrated in Fig. 6.1(b) is as follows. Should a concrete box beam be modelled where no account is taken of the variation of torsional shear stresses and the presence of shrinkage stresses, the analytical load-deformation results will be of the form of curve OBC in the latter figure, where a considerable discrepancy is apparent between experimental and model cracking loads. However, if both the two previously specified



sources of error in cracking prediction are taken into account, the modified analytical results are defined by the curve OAB'C'. The stiffnesses at corresponding intermediary points along BC and B'C', points D and D' for example, correspond closely as the effects of shrinkage and torsional shear stress variation are minimal in comparison to the dramatic redistribution of stresses that follows cracking. In beam tests that exhibited considerable ductility beyond cracking, the inelastic slope up to moderate load levels exhibited little decay, and thus construction of the segment AB' is a reasonable approximation of the initial modified post-cracking response. The principal motivation in introducing the translated curves is that a closer subjective comparison can be made of experimental and model post-cracking stiffnesses, and projected member deformations are predicted more accurately.

With few exceptions model post-cracking stiffness closely follows experimental behaviour, and deformation predictions of the translated model curves are consistently accurate before entering the highly inelastic deformation regions close to ultimate failure. The less pronounced effect of the torsional shear stress variation after beam cracking arises since redistribution of forces through concrete cracking and reinforcement yielding produces large stress variations that greatly exceed the influence of surface to mid-thickness shear stress variation.

At ultimate failure load conditions, the computer model bending moments are consistently 8% to 10% below the corresponding experimental moments for those beams that were subjected to a high ratio of bending moment to torque. This modelling inaccuracy is largely due to the method of delineation of the beam cross-section in the finite element model.

In representing a concrete wall by a two-dimensional plane stress finite element located at the wall mid-thickness, the moment of inertia of the uncracked beam is accurately represented and actual reinforcement locations can usually be accommodated. However, the thickness of the concrete compression zone and the location of the compressive force resultant are fixed, effectively predefining the model bending moment lever arm independently of reinforcement levels and critical beam cross-sectional parameters. For both the rectangular and trapezoidal finite element meshes, the bending moment lever arms are 4.5% shorter than theoretical estimates at ultimate load conditions, resulting in almost a 5% reduction in the ultimate bending moment capacity. The higher stress levels in the longitudinal tension reinforcement of the computer model have little effect on post-cracking stiffness except in the region close to failure where model stiffness is invariably less than experimentation indicated.

Several less significant sources of error are introduced through selection of the geometry of the finite element mesh. Defining cross-sectional geometry by mid-thickness dimensions dictates the location of all reinforcement. However, imposed reinforcement bar movements do not exceed the magnitude of their respective diameters, thus limiting error to a minimal degree. Of a more difficult nature to evaluate objectively, the fineness of a finite element mesh can influence convergence and modelling accuracy.

The mesh size was selected in this instance as a compromise between realistic accuracy expectation and computer execution costs.

6.5.1.2 Review of Individual Beam Results: Two areas of discrepancy in the comparison of model and experimental behaviour are consistent for all beams. Model bending moments at failure underestimate experimental values, thus affecting the corresponding torques in a similar manner. At low load levels when beam deformations are small, the experimental differential rotation measurements are not reliable. In the following examination of Figures 6.2 to 6.21, the legend of graph coordinates for the reinforcement stresses-load plots is given in Table 5.3.

Beam R1: The relevant plotted relationships are illustrated in Figures 6.2, 6.3 and 6.4.

Since the ratio of torque to bending moment is moderate (.5) throughout the loading sequence, the model cracking load is significantly higher than the corresponding experimental value as anticipated in the discussion of Section 6.5.1.1. The "translated" computer model curves illustrated in Figures 6.2 and 6.3 show a reasonably close post-cracking stiffness correspondence, the exception being in the highly inelastic region of the torque-rotation relationship. During the experimental testing of beam R1, the central beam length over which the differential rotation was calculated, was further removed from the influence of the substantial stirrup-like torsion load arms than in the computer model. Consequently, average model differential rotation measurements are significantly smaller than their experimental counterparts at high load levels when the restraint of the torsion arms on crack widening is most pronounced. Difference in cracking load predictions is also exhibited in the reinforcement stress plots of Figures 6.4(a) and 6.4(b).

Beam R2: The relevant plotted relationships are illustrated in Figures 6.5, 6.6, and 6.7.

As the bending moment-deflection ratio at failure is higher for beam R2 than R1, the degree to which the model ultimate strength predictions underestimate beam capacity is more pronounced. Correspondence of the elastic and post-cracking stiffnesses is accurate in both the bending moment and torque graphs, with modest divergence occurring close to failure. The only significant difference in the reinforcement stress plots is that the eastern leg of the central hoop did not yield in the model beam, but the discrepancy is not significant.

Beam R3: The relevant plotted relationships are illustrated in Figures 6.8, 6.9, and 6.10.

For beam R3, the disproportionate underestimation of the ultimate torsional capacity compared with that of the ultimate bending moment capacity is a direct result of the loading sequence. In the load increments preceding failure, the ratio of bending moment to torque was equal to 1.06. Consequently, premature failure of the test specimen had an exaggerated influence on the accuracy of the ultimate torsional estimate. Accurate prediction of the model cracking load is expected as the beam was subjected to bending moment only at the formation of initial cracks. The reinforcement stress plots also reflect the close estimate of the cracking load.

Beam R4: The relevant plotted relationships are illustrated in Figures 6.11 and 6.12.

During testing, an unexpected increase in beam stiffness occurred beyond the applied bending moment of 1100 inch kips. In retrospect, it seems that the nature of application of the central load altered, reducing the central bending moment as illustrated in Fig. 6.22. In Fig. 6.11, the "adjusted" experimental curve represents the bending moment-deflection curve based on the assumption that the central loading plate ceased to maintain uniform contact with the concrete beam at centre span, effectively maintaining only edge contact as shown in Fig. 6.22(b). The smooth stiffness change, absence of a marked post-cracking stiffness increase, and a more realistic ultimate bending moment capacity suggest that the adjusted curve is a more reasonable representation of the actual experimental behaviour. Correspondence in post-cracking stiffness between the computer model and adjusted experimental curve is close. The disagreement between the corresponding east hoop stress curves in Fig. 6.12(b) is the result of the hoop strain gage being located above its assumed mid-depth position.

Beam R5: The relevant plotted relationships are illustrated in Figures 6.13, 6.14, and 6.15.

As illustrated in Table 4.2, the initial concrete modulus for beam R5 was considerably below the average modulus of the other six beams, despite the comparable concrete strengths obtained from cylinder tests. The low concrete modulus was undoubtedly due to inadequate vibration in the narrow web walls and bottom flange, whereas the top flange, being completely exposed, was compacted sufficiently. Thus, the modulus value in Table 4.2 slightly over-estimates the web and bottom flange stiffness, and substantially underestimates the top flange stiffness. Consequently, the post-cracking stiffness of the analytical

model is less than the corresponding experimental stiffness in the bending moment-deflection relationship where the top flange stiffness is critical, and greater in the torque-rotation relationship where web and bottom flange stiffness is influential. The top longitudinal steel strain gage was malfunctioning during the experimental test.

Beam T1: The relevant plotted relationships are illustrated in Figures 6.16, 6.17, and 6.18.

In addition to the expected prediction of a higher cracking load, the only region of significant deviation is the torque-rotation curve segment close to failure. During the latter stages of the experimental test, localized crushing commenced on a top flange corner directly beneath a torsion loading arm. The crushing was confined to the corner only, but the trapezoidal beam's torsional stiffness was undoubtedly diminished, thus contributing to the increasingly inelastic response of the experimental beam.

Beam T2: The relevant plotted relationships are illustrated in Figures 6.19, 6.20, and 6.21.

Beyond 550 inch kips in the bending moment-deflection curve, considerable discrepancy is apparent that defies explanation. Deviation of model and experimental behaviour displayed in the torque-rotation graph is exaggerated since both curves are highly inelastic immediately prior to failure and the ultimate torque at failure is small in comparison to the corresponding bending moment. Experimental coordinates were not plotted in the latter figure below a torque of 109 inch kips as the results were inconsistent.

6.5.1.3 Summary: The computer model simulation of the seven prestressed box girders tested in the experimental program satisfactorily described member deformations and evaluated ultimate strengths to within an acceptable degree of accuracy. To assess the analytical model's performance in its proper perspective, two important sources of model behavioural inadequacy must be recognized. Firstly, the computer model consistently overestimates the cracking strength of "thick" walled concrete box girders that are subjected to any loading combination that includes torque. However, this shortcoming can be overcome as the actual cracking load can be calculated accurately, and a "translated computer model curve" can be drawn to illustrate model behaviour if model and experimental cracking loads coincide. Secondly, upon development of a finite element mesh, the ultimate bending moment lever arm is fixed by geometry, resulting in an inaccurate estimate of the ultimate bending moment capacity. Axial strength under combined loading that includes bending moment is influenced in a similar manner. No corrective measures can be made in the computer model to negate the influence of the latter anomaly.

### 6.5.2 Computer Model Assessment in Light of Current Theory

#### 6.5.2.1 Ultimate Strength

Ultimate Torsional Strength: Calculation of the theoretical ultimate torsional capacity of both rectangular and trapezoidal beams has been made on the basis of the "compressive stress field theory" or space truss theory. The theory is based on a kinematic approach in the theory of plasticity where an external loading is sought at which a mechanism of deformations is formed. However, the formation of the mechanism implicitly assumes that both stirrups and longitudinal steel

yield before failure. Although the space truss model has several other inherent limitations in its application, the requirement that reinforcement proportions be such that stirrups and stringers yield prior to failure is crucial in establishing the theory's validity in this instance.

Elfgren<sup>51</sup> reports that several researchers have confirmed that the yield prerequisite is met if the ratio of longitudinal to transverse reinforcement is such that

$$0.5 < \cot \alpha_T < 2.0 \quad (6.14)$$

where

$$\cot \alpha_T = \sqrt{\frac{2A_1 \sigma_1^y}{b' + h'} \cdot \frac{t}{A_w \sigma_w^y}} \quad (6.15)$$

in which  $A_1$  = area of longitudinal reinforcement,  $\sigma_1^y$  = yield stress of longitudinal reinforcement,  $b'$  = width of beam measured between corner stringers,  $h'$  = beam depth measured from top to bottom stringer,  $t$  = stirrup spacing,  $A_w$  = stirrup area, and  $\sigma_w^y$  = stirrup yield stress.

For the five rectangular beams,  $\cot \alpha_T$  equals 1.96, and 2.05 for the two trapezoidal beams. The value of  $\cot \alpha_T$  for the trapezoidal beams is of questionable significance as Eq. 6.15 was developed for rectangular beams only.

On the basis of the theoretical verification, a valid comparison can be made of the computer model and theoretical ultimate torsional capacity estimates for the rectangular beams, and the respective values in Table 6.2 illustrate good agreement. However, Equations 6.14 and 6.15 indicate that a comparison of trapezoidal results is highly questionable and furthermore, experimental and computer model results verify that



the stirrup reinforcement in both the trapezoidal beams was not yielding at failure.

The slightly higher computer model estimate for the rectangular beams is as anticipated, since only the yield force of the reinforcement is used in the theoretical calculation. Unlike the computer model, space truss theory does not take into account reinforcement strain hardening or dowel action. The additional reserve of reinforcement strength beyond yielding does not increase the ultimate torsional capacity substantially, however, as the transfer of load from concrete to steel increases reinforcement stresses dramatically as failure is approached.

Ultimate Bending Moment Strength: Both the space truss and computer models cannot accurately estimate ultimate bending moment capacities as their respective ultimate bending moment lever arms are fixed by geometry. Although not afflicted by the latter shortcoming, the skew bending model cannot accommodate longitudinal web bars and tension reinforcement of different yield strengths. Thus, the equivalent stress block theory incorporated in prestressed concrete design is the most accurate method of evaluating the ultimate bending moment capacity. The shortcoming of the computer model in this respect is treated in detail in Section 6.5.1.1.

Ultimate Shear Strength: The approach adopted by Thürliman in formulating the theoretical shear capacity of a reinforced or prestressed concrete beam is only applicable to beams underreinforced for shear. Definition of an underreinforced beam in the context of pure shear is identical to that for pure torsion, in that both the longitudinal stringers and the transverse reinforcement must yield at failure. Should

Other reinforcement type not yield at failure, the yield criteria are violated and the theory becomes invalid.

Unfortunately, a loading pattern could not be devised to enable the computer model to predict the maximum shear resistance of rectangular beams R3 and R4. The choice of loading pattern was restricted since the beam span could not be reduced without modifying behaviour, and concentrated loads could not be located close to the critical cross-section where shear failure was anticipated as their presence altered the local shear stress distribution<sup>50,51</sup>. Recognizing these two restrictions, the only feasible load combination produced a design region of maximum shear accompanied by a large bending moment.

6.5.2.3 Combined Loading Interaction: Under combined loading conditions, the correspondence between computer model and theoretical results is difficult to analyze objectively, especially since the number of beam specimens is small and no noticeable trends of deviation are apparent. Strength comparisons for each individual load type have been made, and qualifications that arose through those comparisons are applicable to the combined loading evaluation.

Correspondence in the torque-bending moment interaction, illustrated in Fig. 6.23, is good, although it should be recognized that non-dimensional presentation of results can disguise fundamental differences in performance. For example, beams T1 and T2 are both over-reinforced for torsion, but their interaction coordinates lie close to the corresponding theoretical under-reinforced interaction curve.

Displayed in Fig. 6.25, the interaction equations for beams R3 and R4 do not significantly reflect the influence of the modest amount

of shear present in both beams. Since the degree of error that is inevitably encountered in experimentation and computer modelling is of the same order of magnitude as the adjustment of the two interaction equations for the presence of shear, little can be deduced from the proximity of the computer model coordinates to the theoretical torque-bending moment-shear interaction curve illustrated in the latter figure. In the testing of beam R3, the ratio of torque to bending moment was close to unity in the load increments preceding failure. Thus, experimental and computer modelling error would have resulted in disproportionately large changes in the torque loading at failure.

The most serious reservation concerning interactive behaviour is the obscure definition of an underreinforced beam, especially when shear is present. Current provisions proposed to prevent premature failure by crushing of concrete are conservative in the absence of a more thorough understanding of load interaction. In contrast, the computer model is a generalized analytical tool whose applicability is not restricted by loading or reinforcement limitations.

6.5.2.3 Limitations in Application of Theory: The following limitations apply to the calculation of the ultimate torsional capacity of a reinforced concrete beam using space truss theory:

1. The beam must be underreinforced: ie. longitudinal and transverse reinforcement must yield prior to failure.
2. St. Venant torsion must be dominant.
3. Along the beam length, the cross-section must be uniform.
4. Dowel action of reinforcement is neglected.

The theory adopted to calculate the ultimate bending moment strength, as described in Section 6.4.1 and 6.5.2.1, is not subjected to limitation in its applicability.

Thürliman's approach in estimating the ultimate shear capacity of a reinforced or prestressed beam is only subject to two limitations:

1. The beam must be underreinforced for shear: i.e. longitudinal and transverse reinforcement yield simultaneously at failure.
2. The top uncracked flange does not carry shear.

The interaction equations presented by Elfgren<sup>51</sup> are subject to the following qualifications in their application:

1. The beam cross-section must be consistent along its length.
2. Interaction equations for polygonal cross-sections are not verified.
3. Criteria for preventing premature failure through concrete crushing are not explicit.

The only limitation or qualification equally applicable to the computer model is that the uncracked top flange does not carry shear. One serious qualification not attributed to theory is the inaccurate length of the bending moment lever arm at failure. In conclusion, the flexibility of the computer model is characterized by several important areas of application that are beyond theoretical capabilities:

1. The member cross-section can change along its length through the use of a general quadrilateral concrete finite element.
2. Any reinforcement arrangement can be accommodated for both underreinforced and overreinforced conditions.
3. Member deformations are described comprehensively.

4. All stress-deformation information is available at any loading stage between cracking and failure.

5. Indeterminate structural analysis under any loading combination is possible.

6.5.2.4 Summary: In pure torsion, agreement between the computer model and theoretical results was satisfactory for the under-reinforced rectangular beams. However, since the two trapezoidal beams were overreinforced for torsion, a meaningful comparison could not be made. Analytical model estimates of the ultimate bending moment capacities of all beams were inaccurate since the bending moment lever arms, fixed by finite element mesh geometry, were incorrect.

Although difficult to assess objectively, torque-bending moment interaction corresponded closely. Such close correspondence was not apparent in the torque-bending moment-shear interactive behaviour of beams R3 and R4.

Objective assessment of the computer model results through comparison with the corresponding theoretical predictions was not conclusive as the theory is limited in its range of application, and complex interactive behaviour is presented theoretically in a general form that does not permit explicit comparison.

Beams	Bending Moment						Torque			Shear		
	Cracking			Ultimate			Ultimate			Ultimate		
	E	M	$\frac{M}{E}$	E	M	$\frac{M}{E}$	E	M	$\frac{M}{E}$	E	M	$\frac{M}{E}$
R1	460	570	1.24	1080	1015	.94	520	492	.95	0	0	-
R2	660	820	1.24	1291	1197	.93	372	336	.9	0	0	-
R3	760	760	1.0	1357**	1267	.93	532	432	.81	11.0	11.0	1.0
R4*	820	820	1.0	1452**	1239	.853	336	336	1.0	12	18	.67
R5	330	330	1.0	640	600	.94	614	562	.92	13	0	.72
T1	300	350	1.17	598	620	.97	290	583	.95	0	0	-
T2	300	420	1.4	801	570	.95	196.5	276	.95	0	0	-
					595	.99	180	288	.99			
					742	.93		168	.85			
					767	.96		180	.92			

Notes: (1) E = Experimental result M = Computer model result

(2) All units are in inches and kips.

\* The adjusted experimental values are given.

\*\* These are centreline moments. The design moments at "h" from centreline are plotted in interaction diagrams.

TABLE 6.1 EXPERIMENTAL AND COMPUTER MODEL CRACKING AND ULTIMATE LOADING

Beams	Ultimate Bending Moment Capacity			Ultimate Torque Capacity			Ultimate Shear Capacity		
	Space Truss Estimate	Model Estimate	Model Theory	Bending Theory Est.	Model Est.	Model Theory	Shear Theory Est.	Model Est.	Model Theory
R1, R2, R3 R4, R5	1515	1370	.905	379	390	1.029	49.5	-	-
T1, T2	985	915	.929	239	300	1.256	-	-	-

Note: All units are in inches and kips.

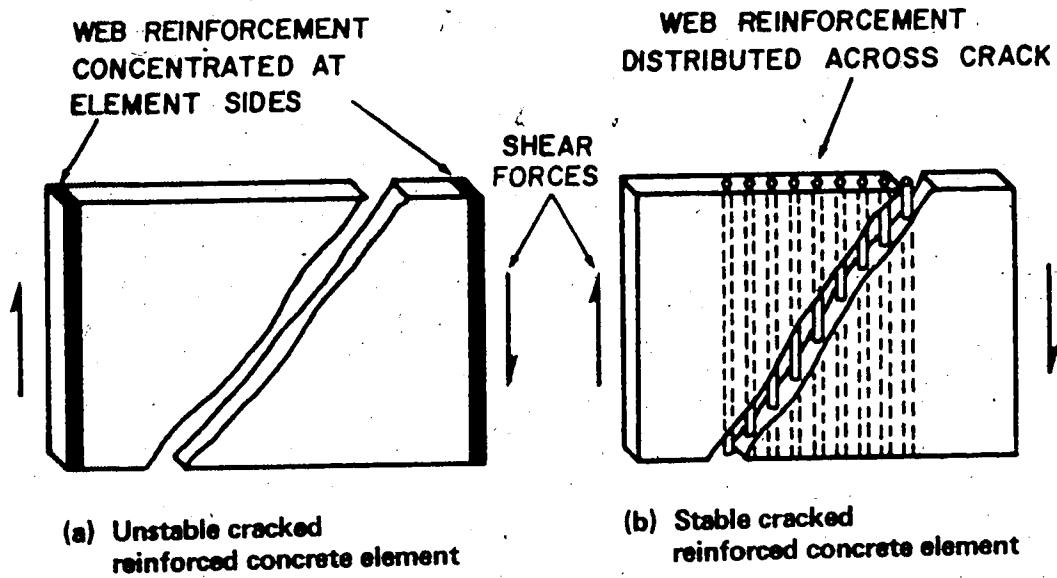
TABLE 6.2 MODEL AND THEORETICAL ULTIMATE STRENGTHS

Failure Loads	Beams													
	R1	R2	R3	R4	R5	T1	T2	R1	R2	R3	R4	R5	T1	T2
$M_u$	1015	1197	1166**	1085**	610	582.5	754.5							
$T_u$	492	336	451	336	572.5	282	177							
$V_u$	0	0	11	12.5	0	0	0							
$M_{uo}$	1370	1370	1370	1370	1370	915	915							
$T_{uo}$	390	390	390	390	390	300	300							
$V_{uo}$ **	70.7	70.7	70.7	70.7	70.7	57.44	57.44							
$M_u/M_{uo}$	.741	.874	.851	.792	.446	.637	.825							
$T_u/T_{uo}$	1.262	.862	1.157	.86	1.468	.94	.59							
$V_u/V_{uo}$	0	0	.155	.177	0	0	0							

\* All values are average values for the failure load increment  
 \*\* Bending moment values distance h (beam depth) from centre concentrated load.  
 \*\*\* Theoretical Value

Note: All units are in inches and kips

TABLE 6.3 COMPUTER MODEL RESULTS



\* Note: Web reinforcement is uniformly distributed across element, but when crack forms through centroid, the reinforcement is effectively distributed across the crack only.

FIG. 6.1(A) METHOD OF MODELLING WEB REINFORCEMENT

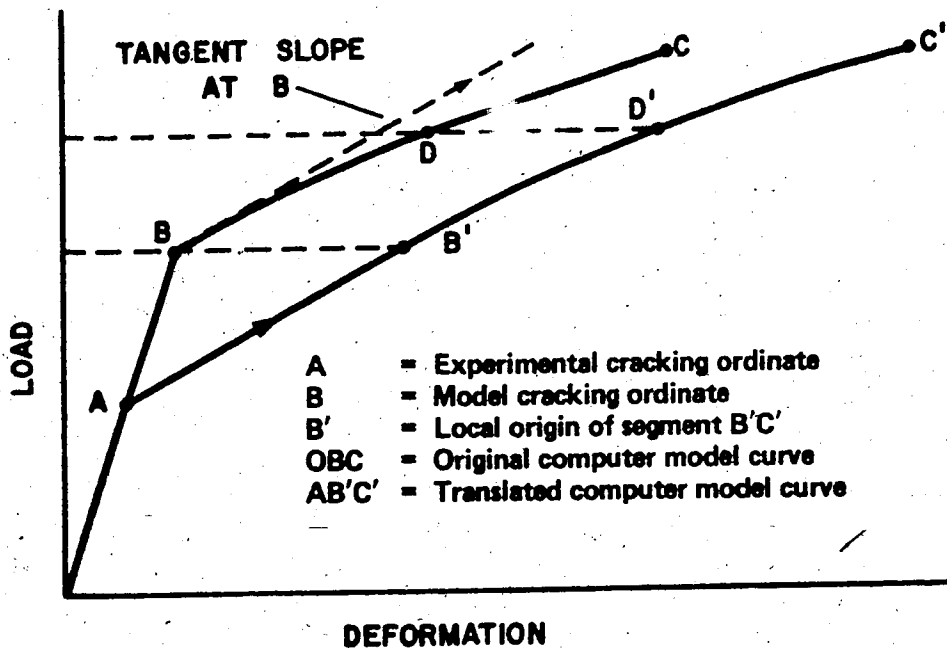


FIG. 6.1(B) TRANSLATION PROCEDURE



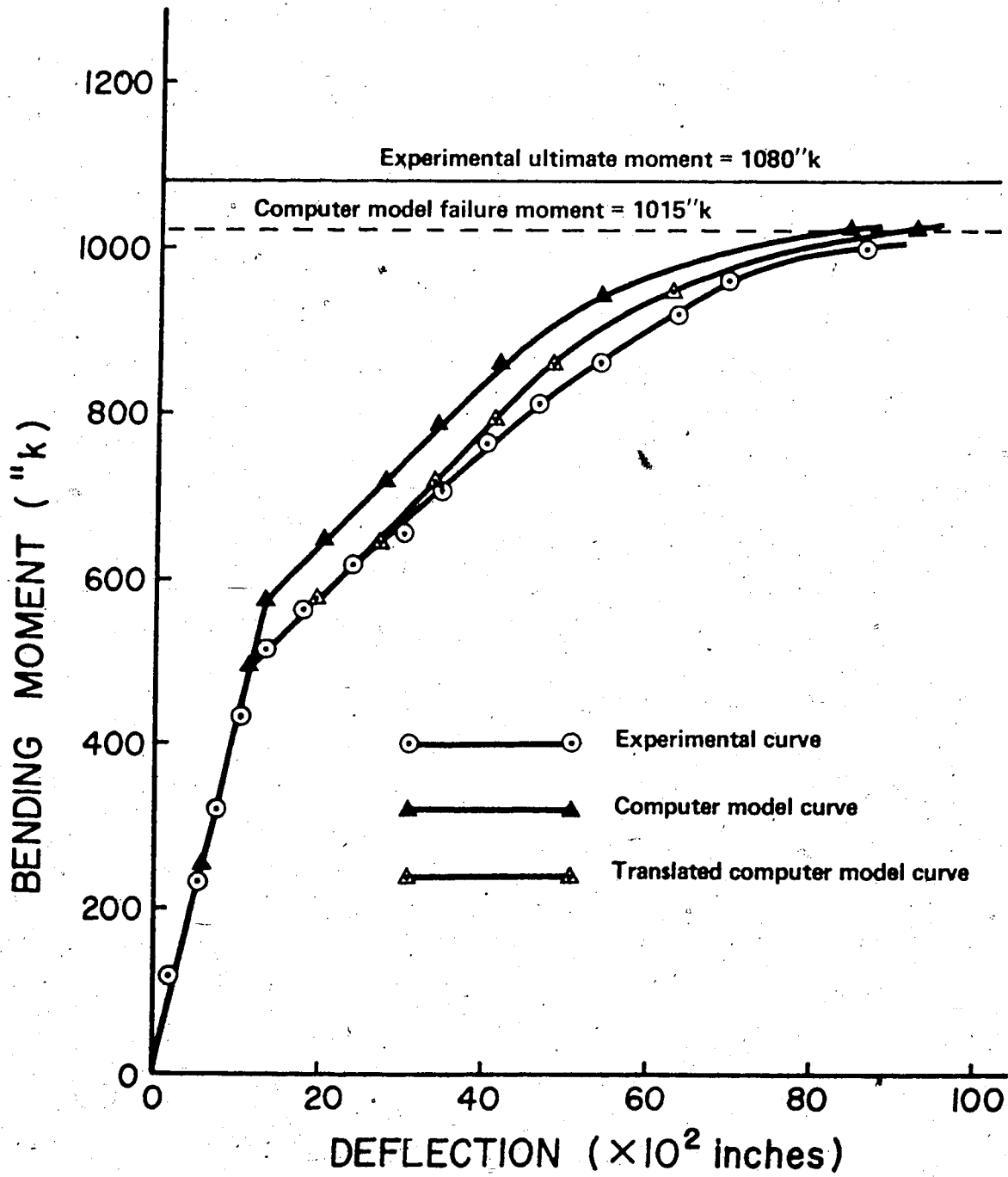


FIG. 6.2 MODEL AND TEST BENDING MOMENT-DEFLECTION CURVES FOR BEAM R1

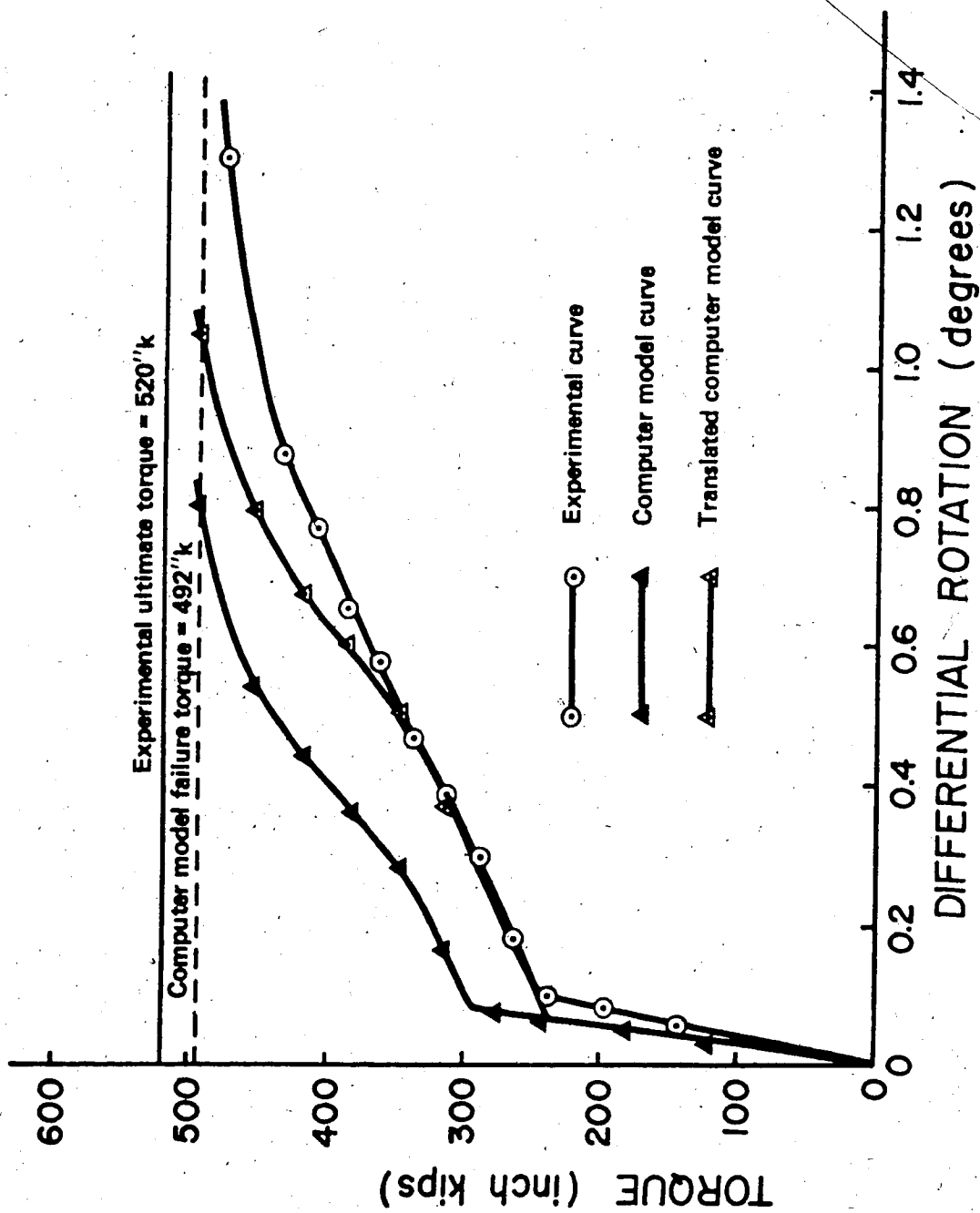


FIG. 6.3 MODEL AND TEST TORQUE-ROTATION CURVES FOR BEAM R1

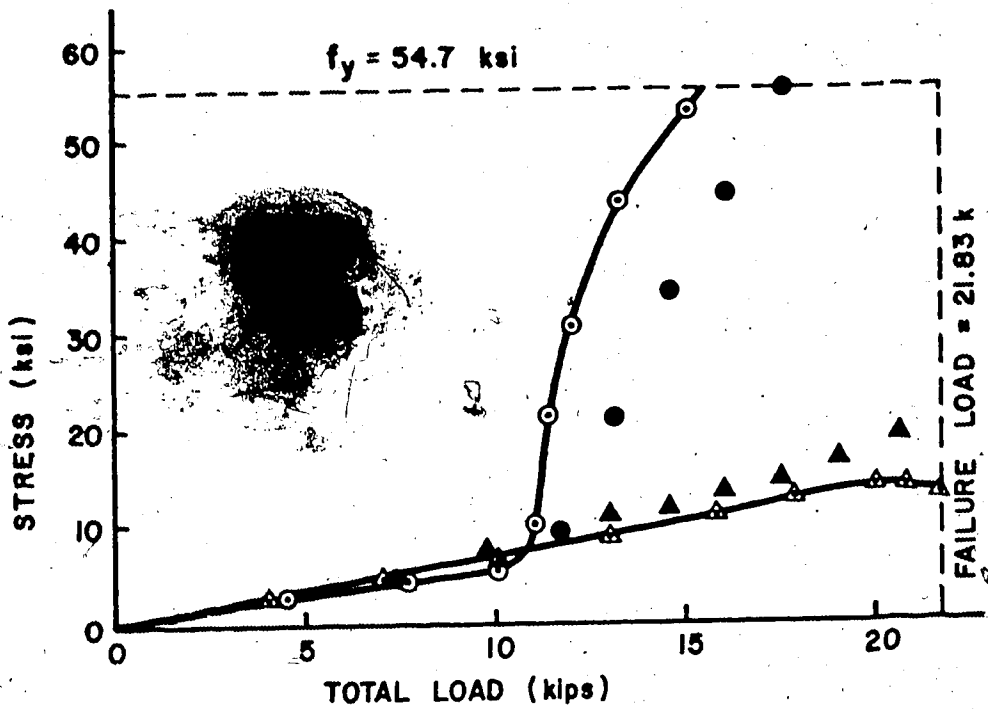


FIG. 8.4(A) TEST AND MODEL LONGITUDINAL CONVENTIONAL REINFORCEMENT STRESSES FOR BEAM R1

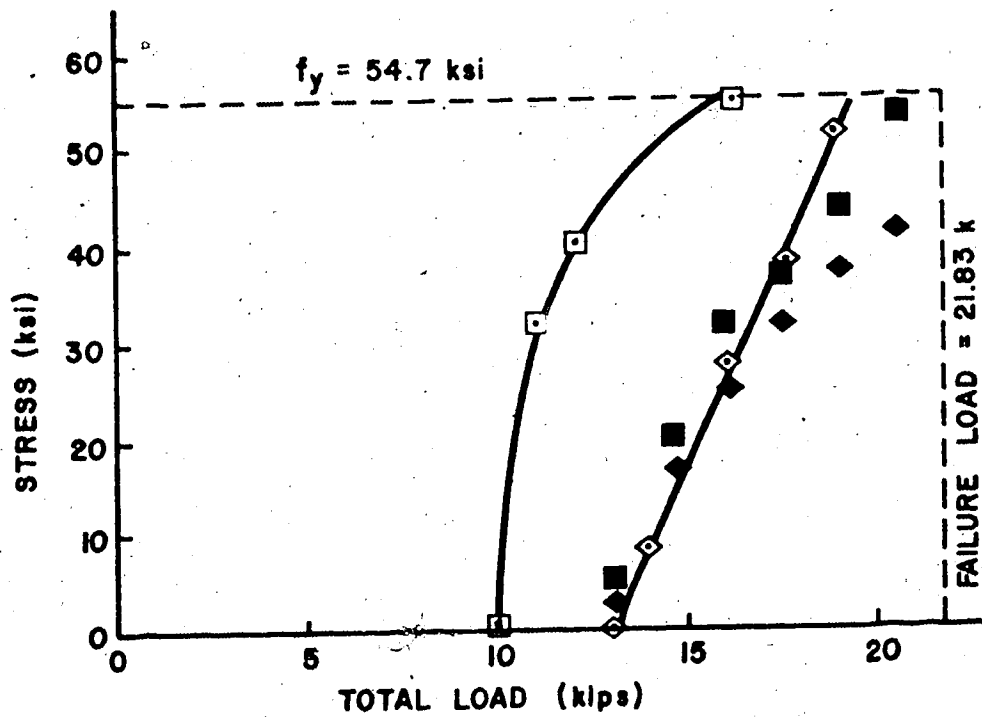


FIG. 8.4(B) TEST AND MODEL HOOP REINFORCEMENT STRESSES FOR BEAM R1

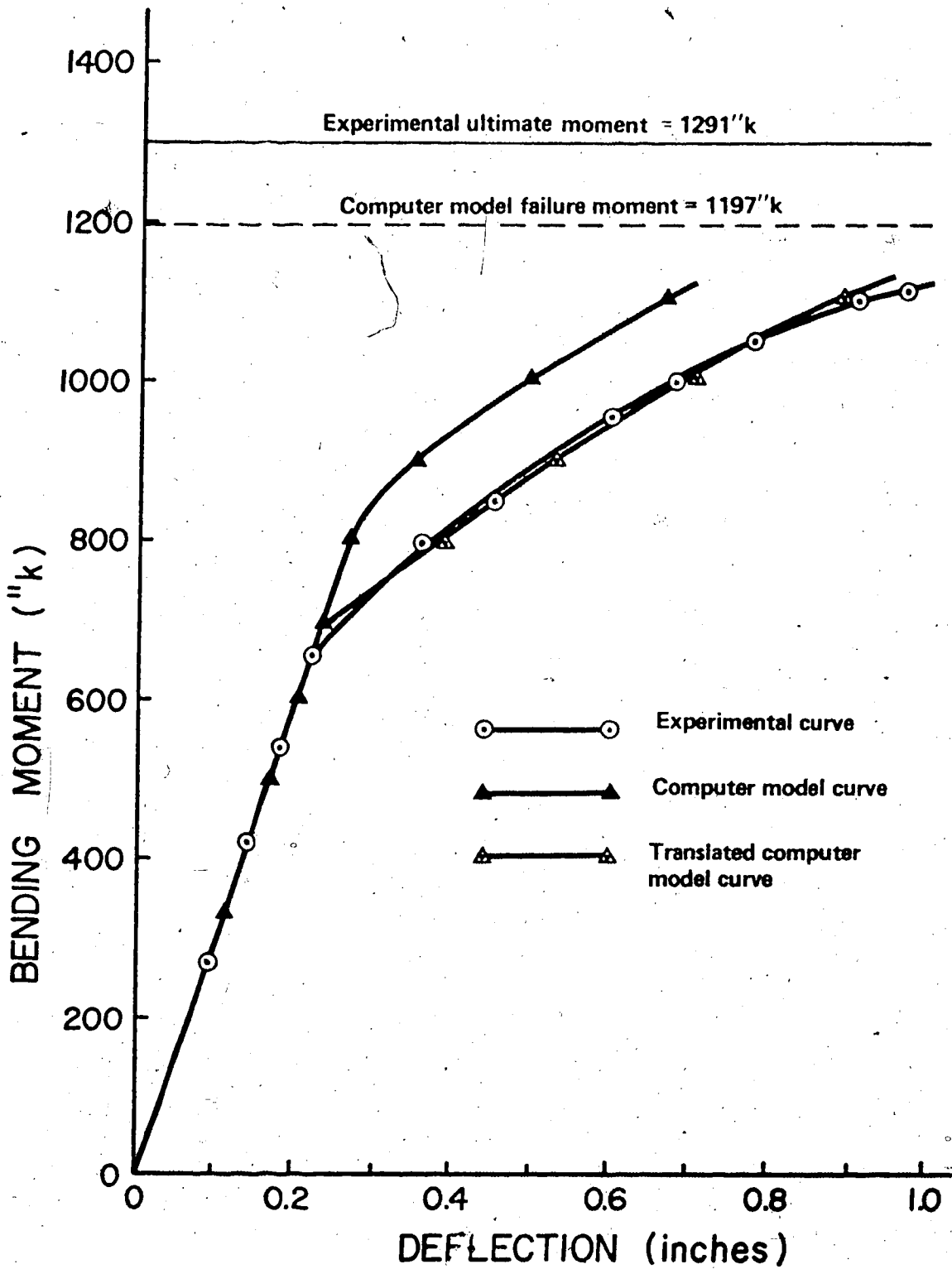


FIG. 6.5 MODEL AND TEST BENDING MOMENT-DEFLECTION CURVES FOR BEAM R2

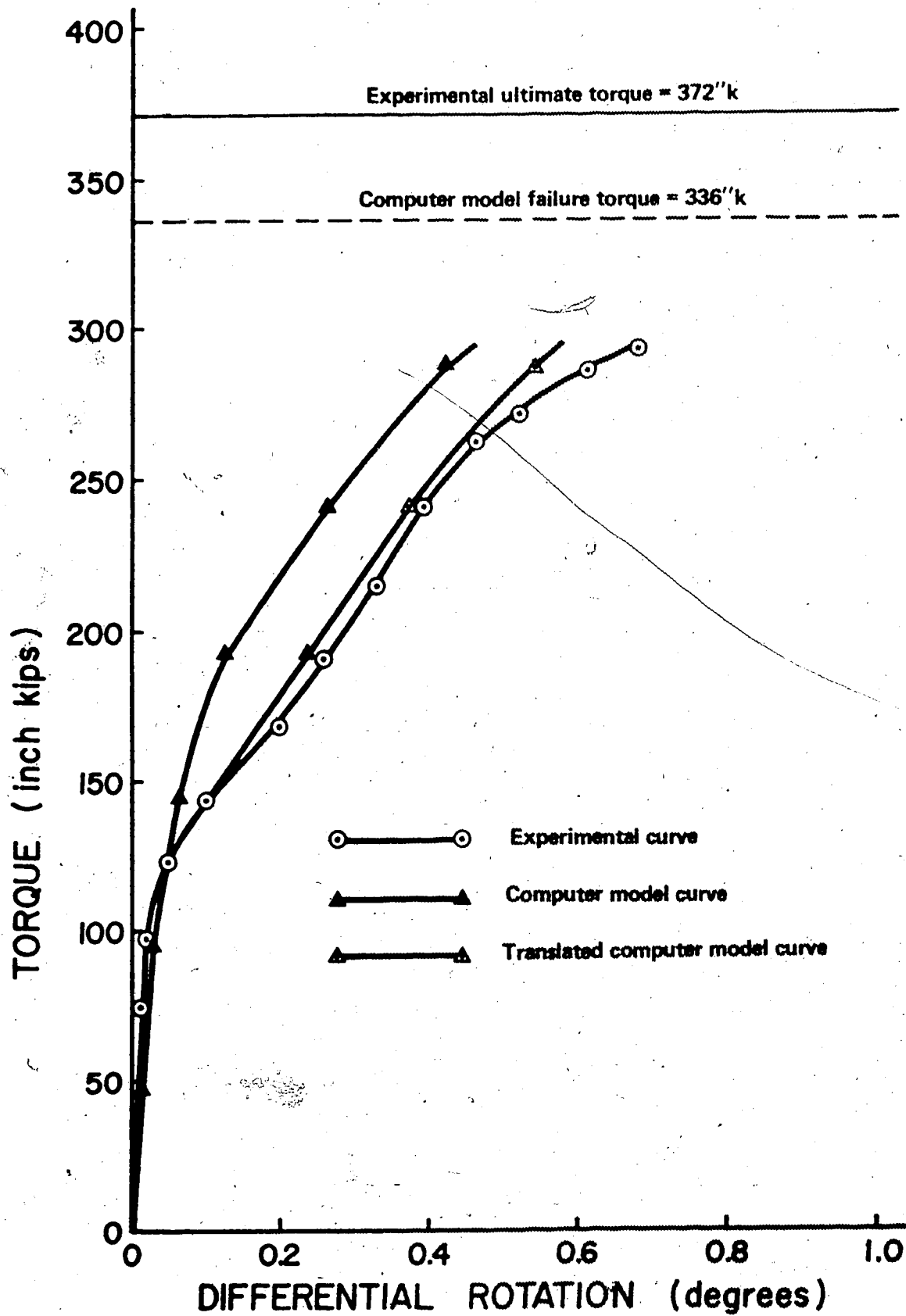


FIG. 6.6 MODEL AND TEST TORQUE-ROTATION CURVES FOR BEAM R2

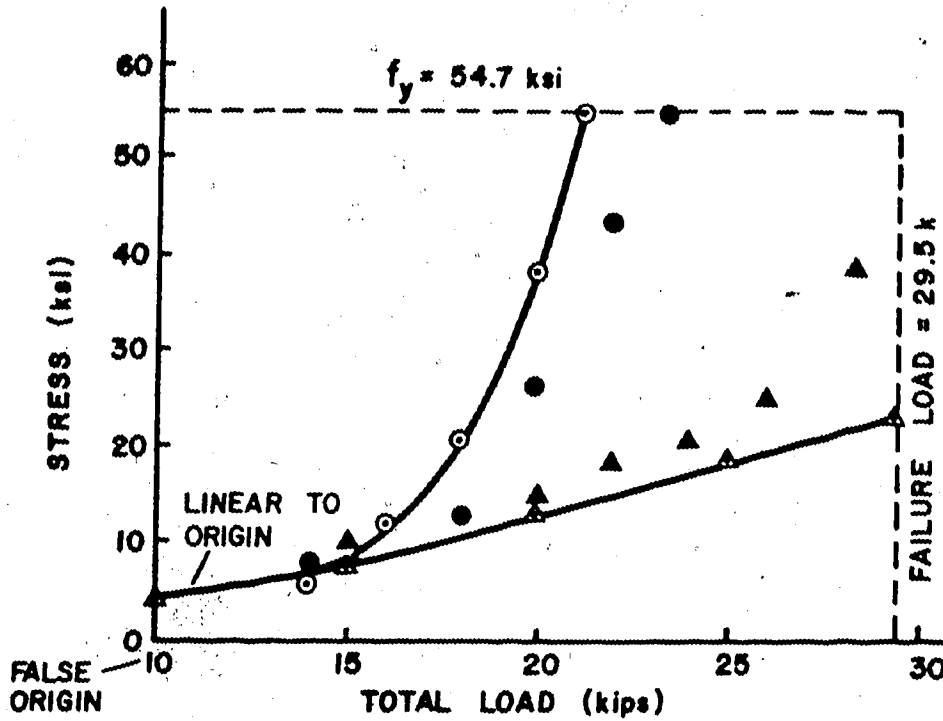


FIG. 6.7(A) TEST AND MODEL LONGITUDINAL CONVENTIONAL REINFORCEMENT STRESSES FOR BEAM R2

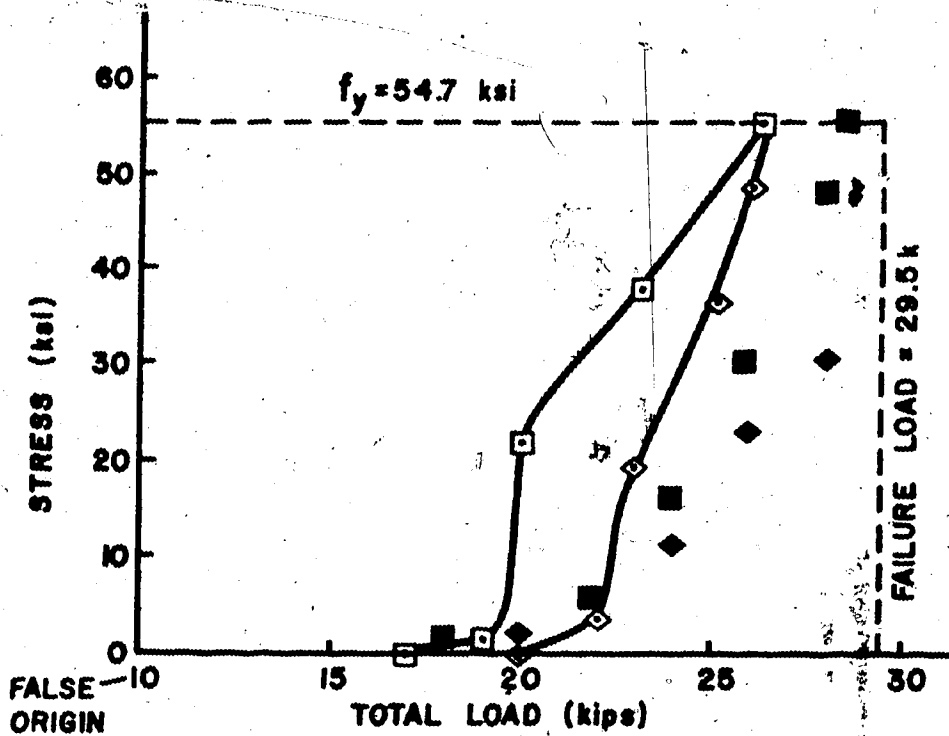


FIG. 6.7(B) TEST AND MODEL HOOP REINFORCEMENT STRESSES FOR BEAM R2

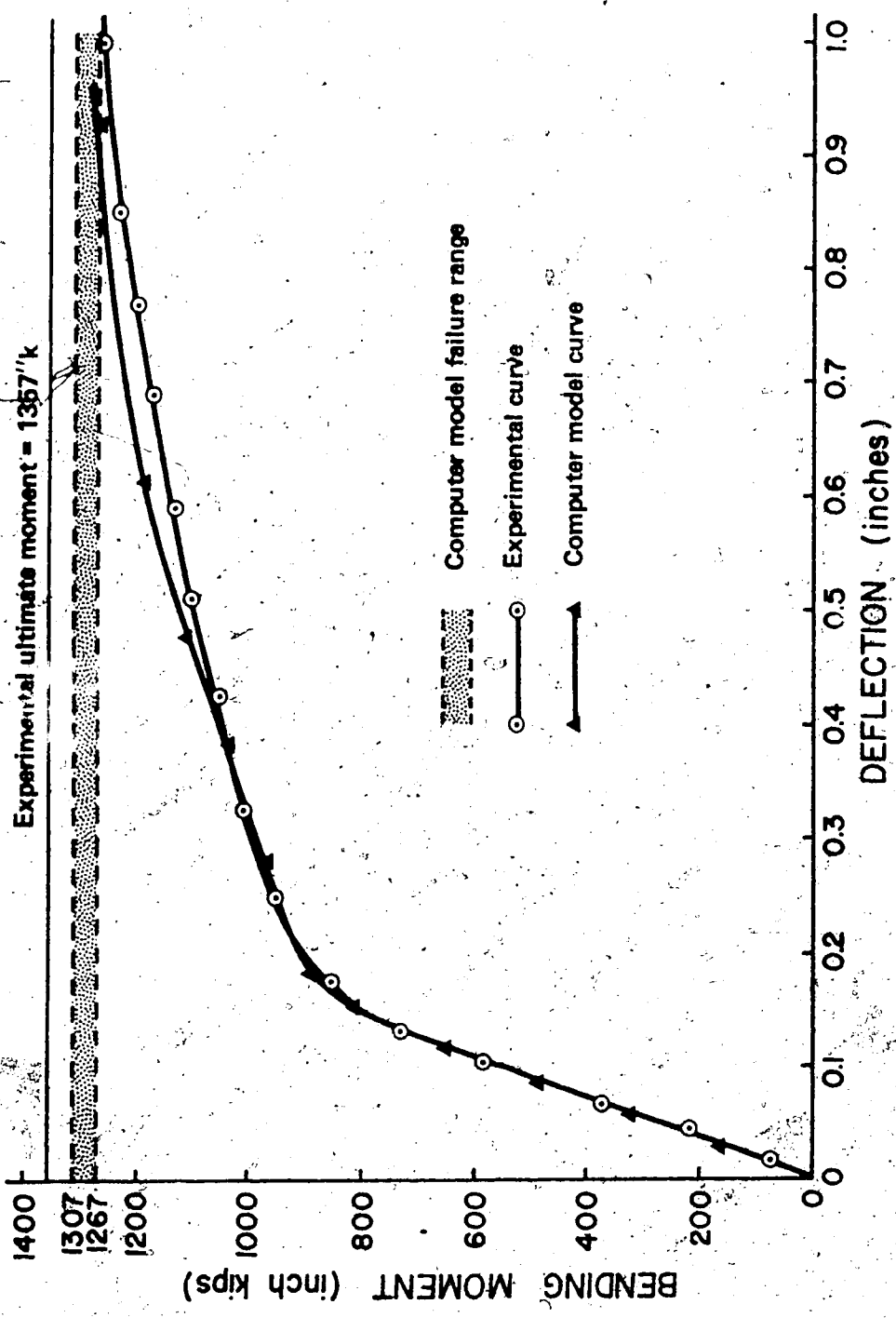


FIG. 6.8 MODEL AND TEST BENDING MOMENT-DEFLECTION CURVES FOR BEAM R3

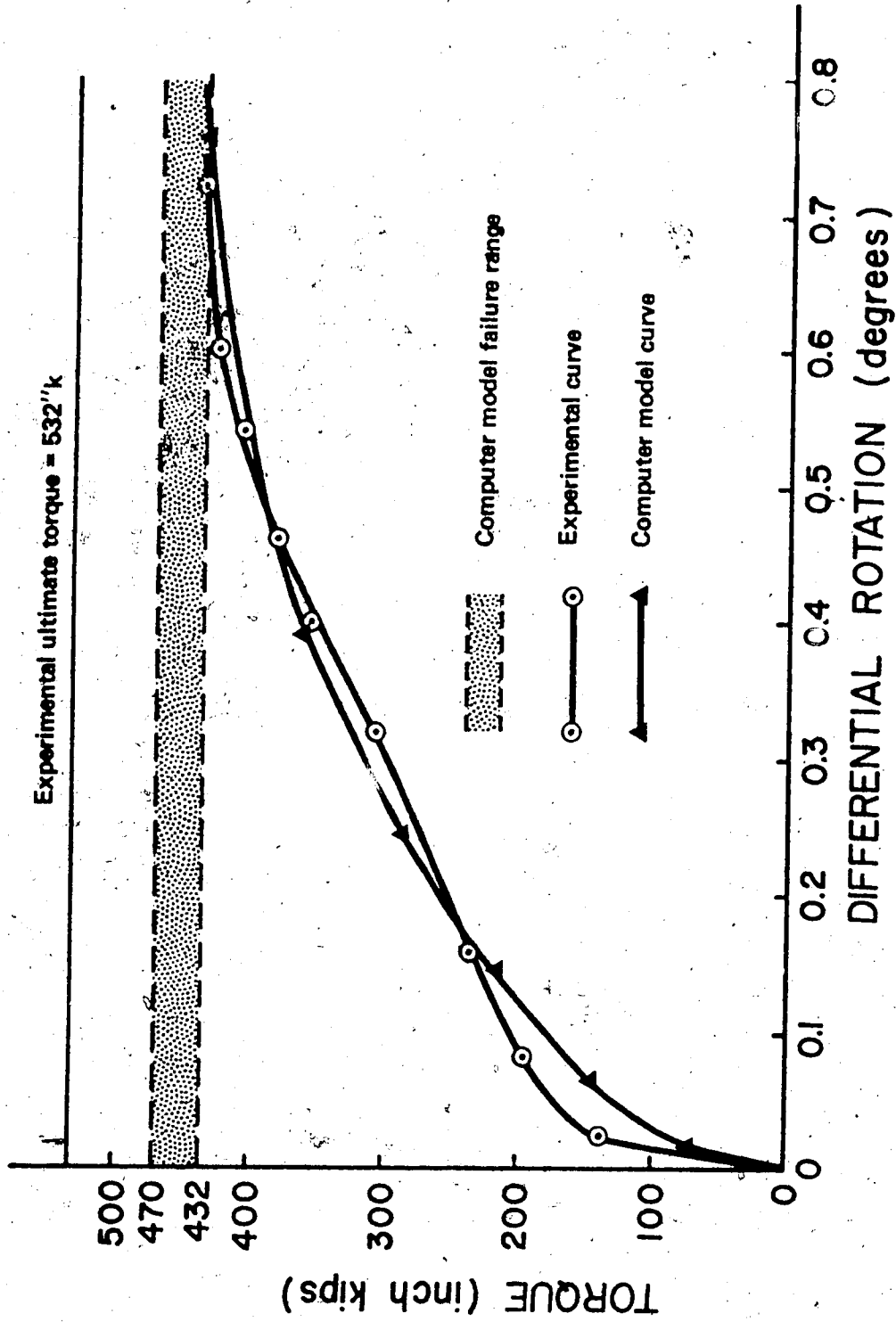


FIG. 6.9 MODEL AND TEST TORQUE-ROTATION CURVES FOR BEAM R3



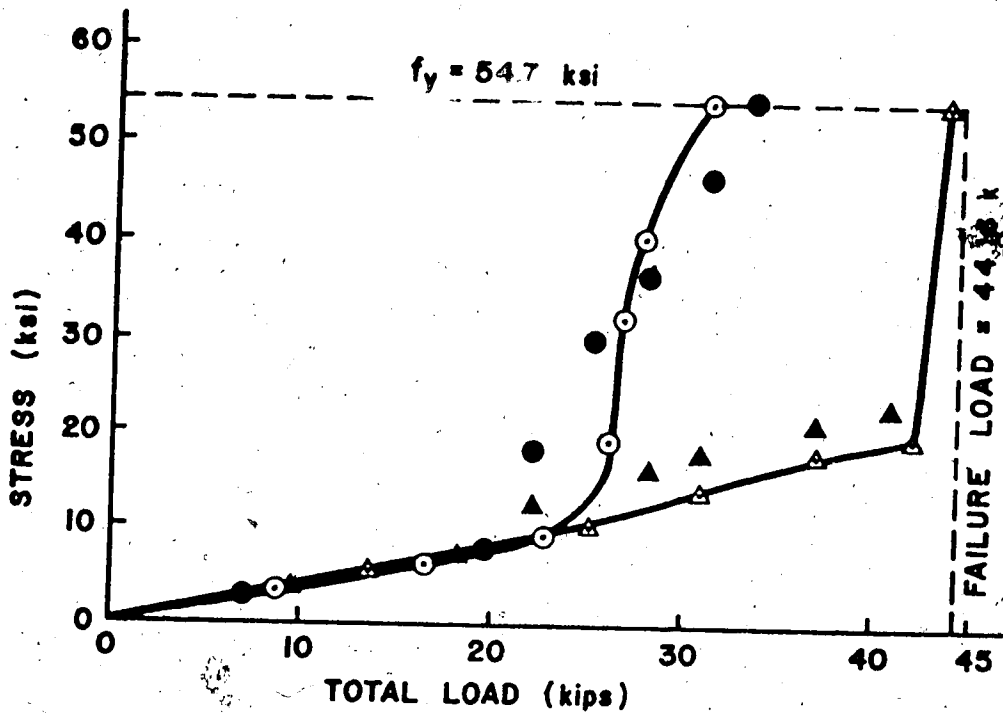


FIG. 6.10(A) TEST AND MODEL LONGITUDINAL CONVENTIONAL REINFORCEMENT STRESSES FOR BEAM R3

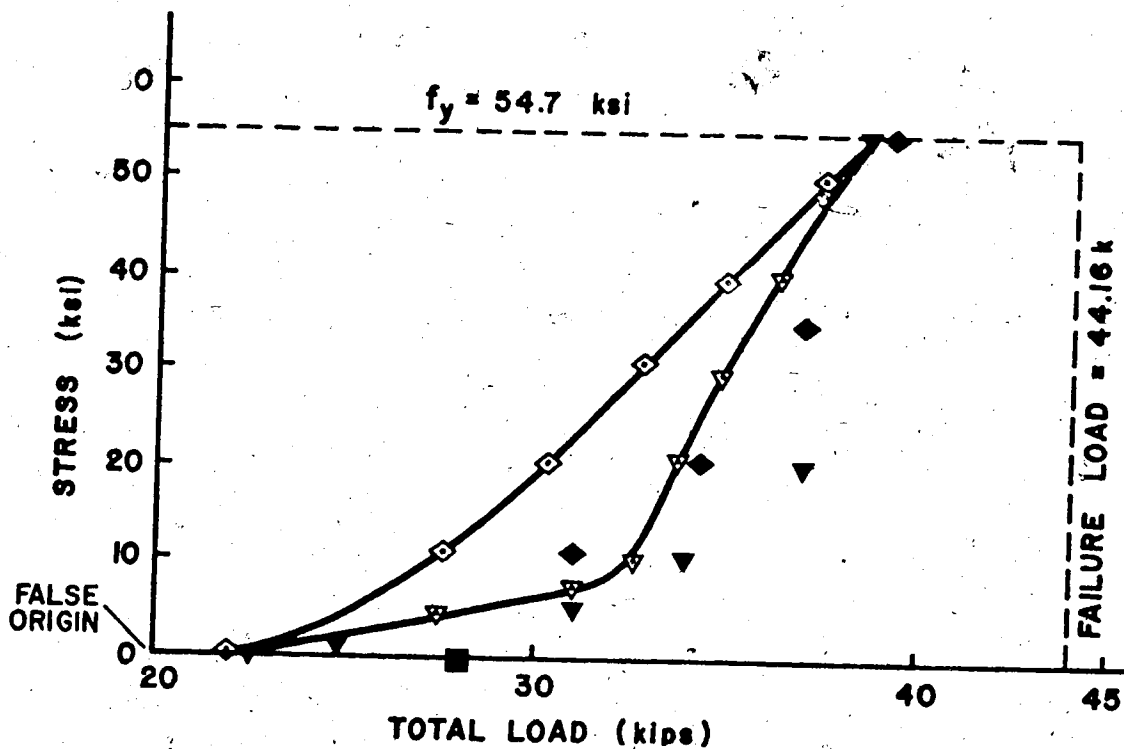


FIG. 6.10(B) TEST AND MODEL HOOP REINFORCEMENT STRESSES FOR BEAM R3

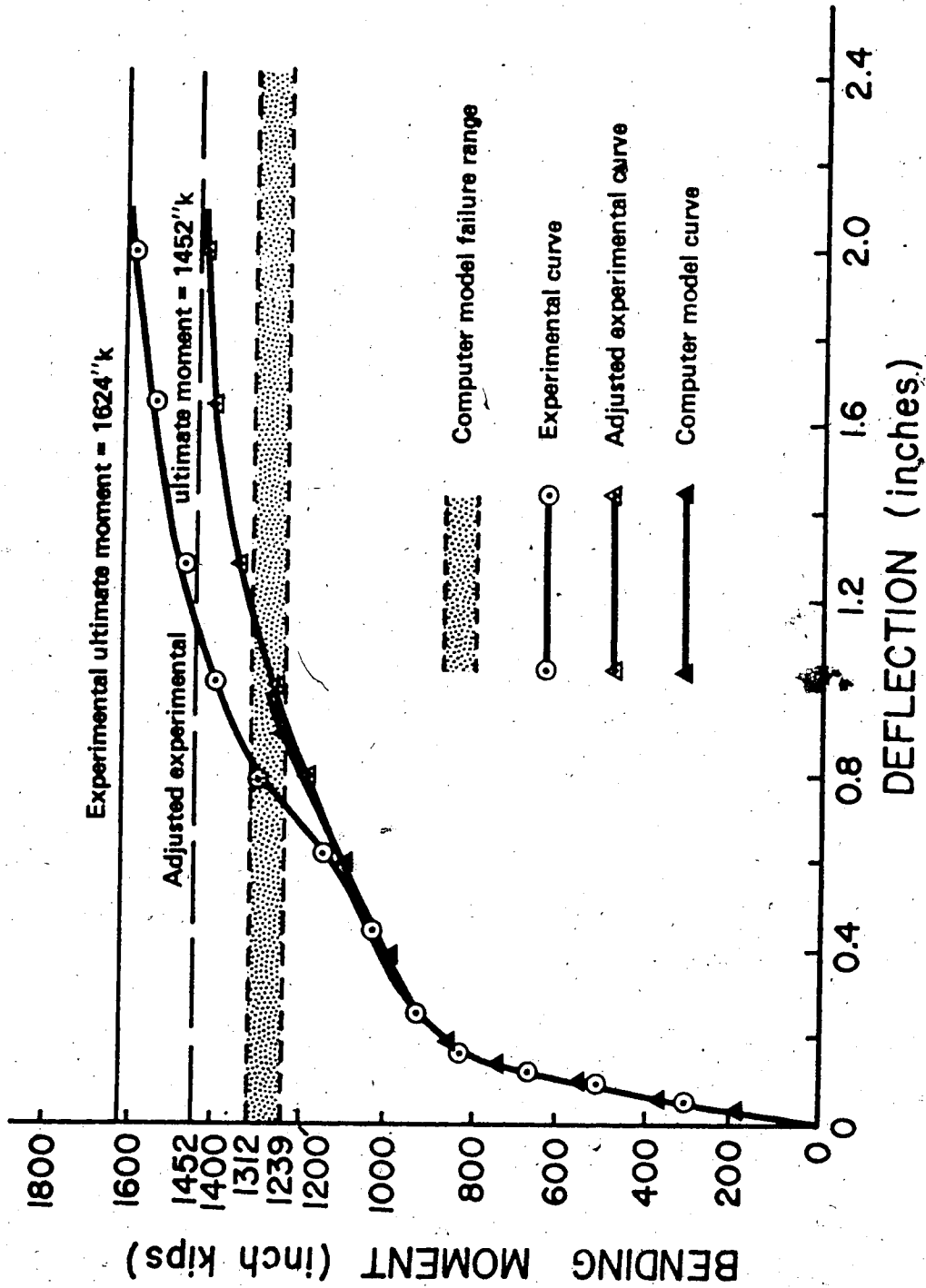


FIG. 6.11 MODEL AND TEST BENDING MOMENT-DEFLECTION CURVES FOR BEAM R4

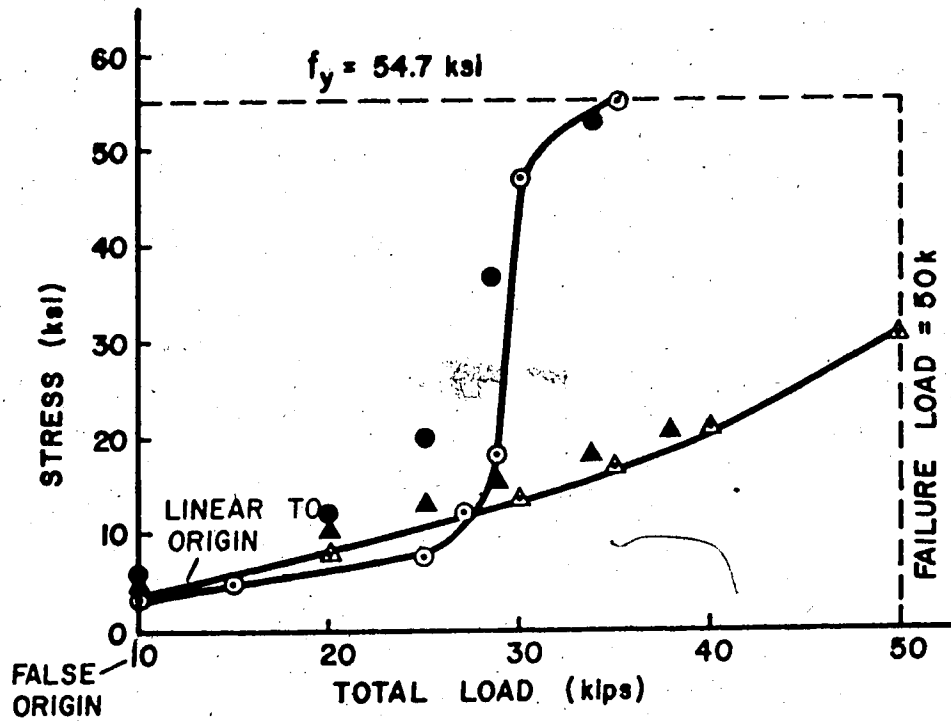


FIG. 6.12(A) TEST AND MODEL LONGITUDINAL CONVENTIONAL REINFORCEMENT STRESSES FOR BEAM R4

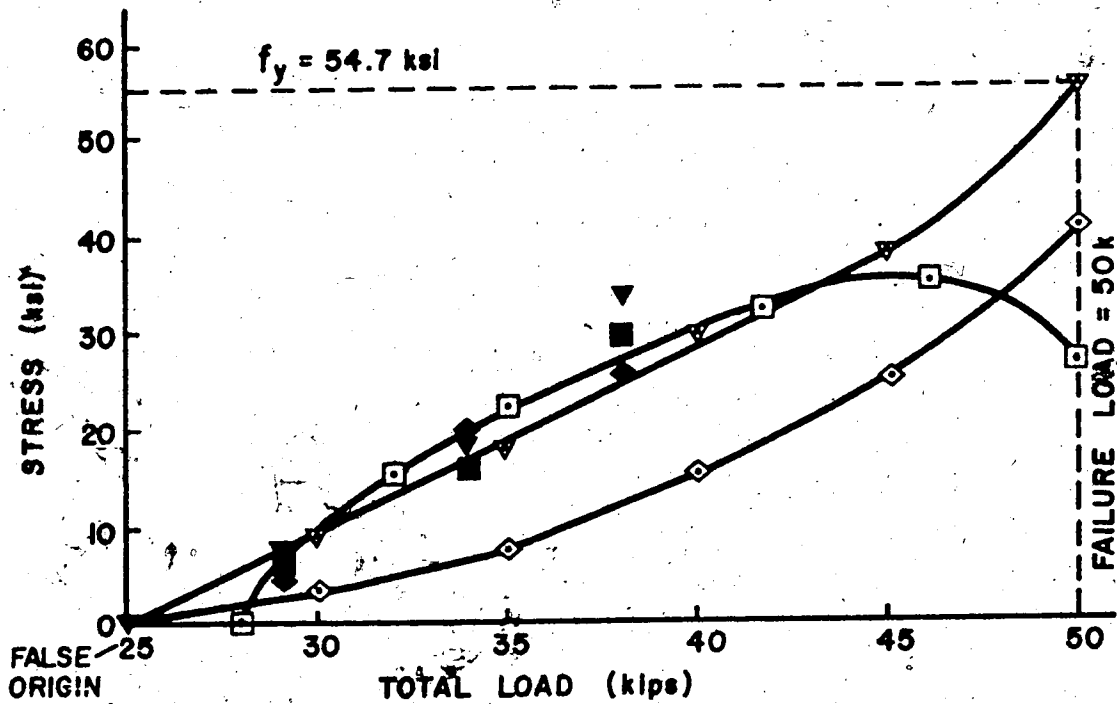


FIG. 6.12(B) TEST AND MODEL HOOP REINFORCEMENT STRESSES FOR BEAM R4

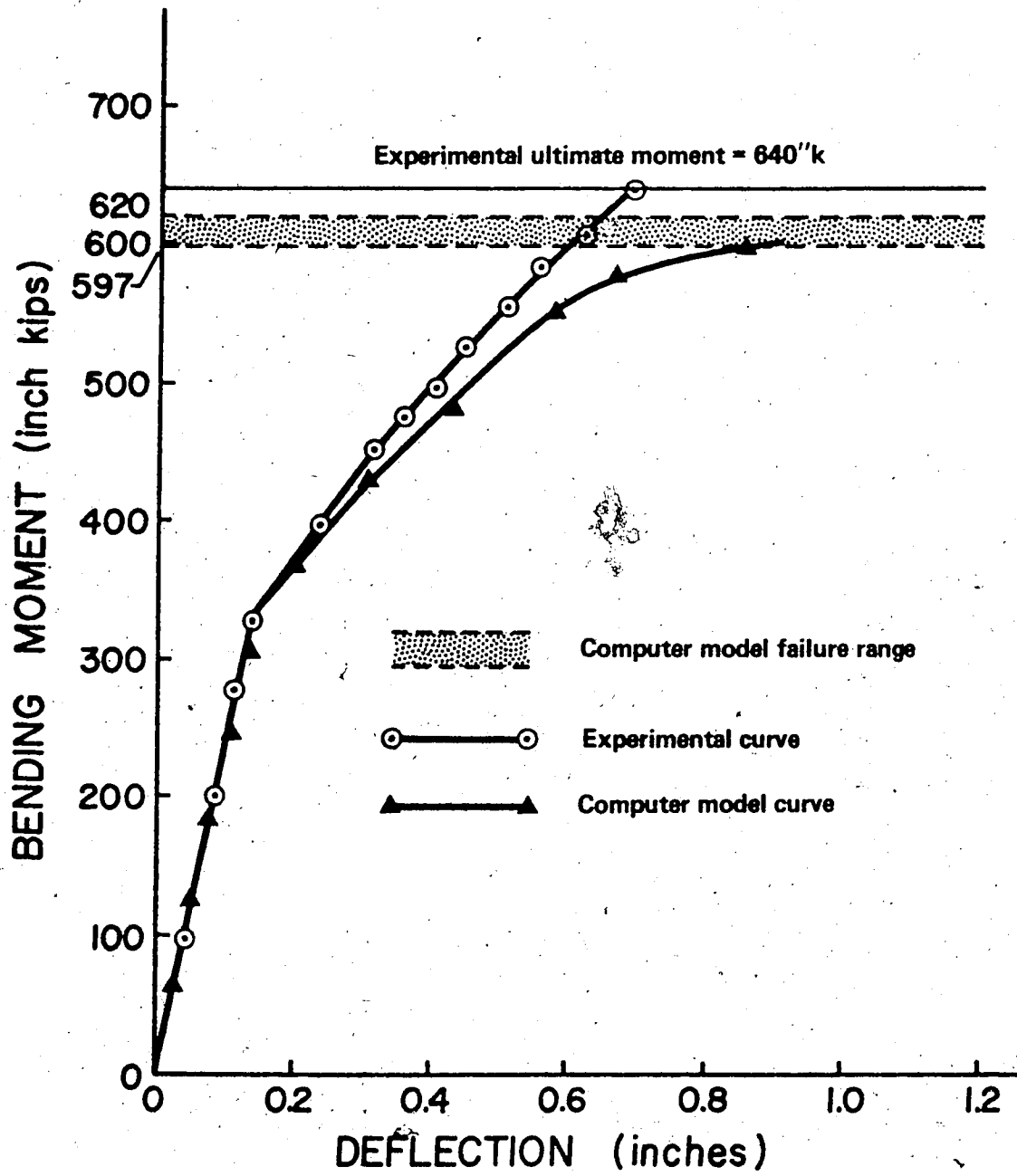


FIG. 6.13 MODEL AND TEST BENDING MOMENT-DEFLECTION CURVES FOR BEAM R5

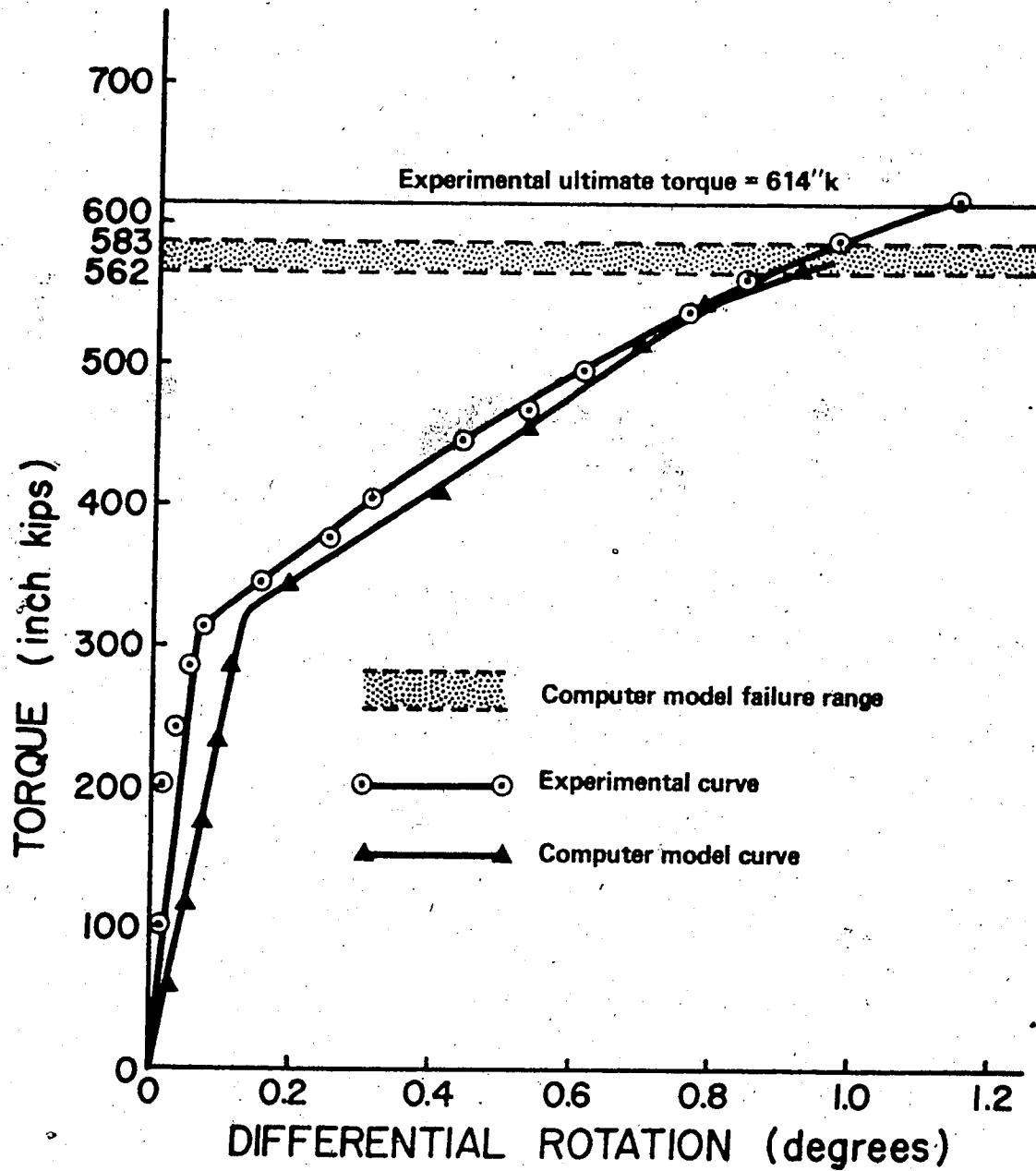


FIG. 6.14 MODEL AND TEST TORQUE-ROTATION CURVES FOR BEAM R5

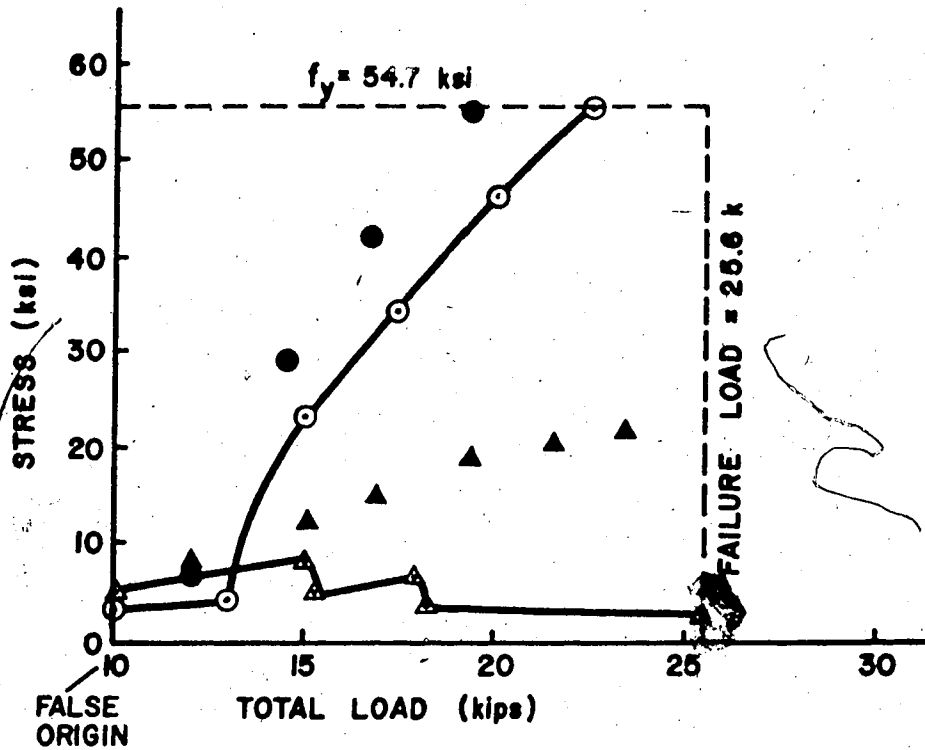


FIG. 6.15(A) TEST AND MODEL LONGITUDINAL CONVENTIONAL REINFORCEMENT STRESSES FOR BEAM R5

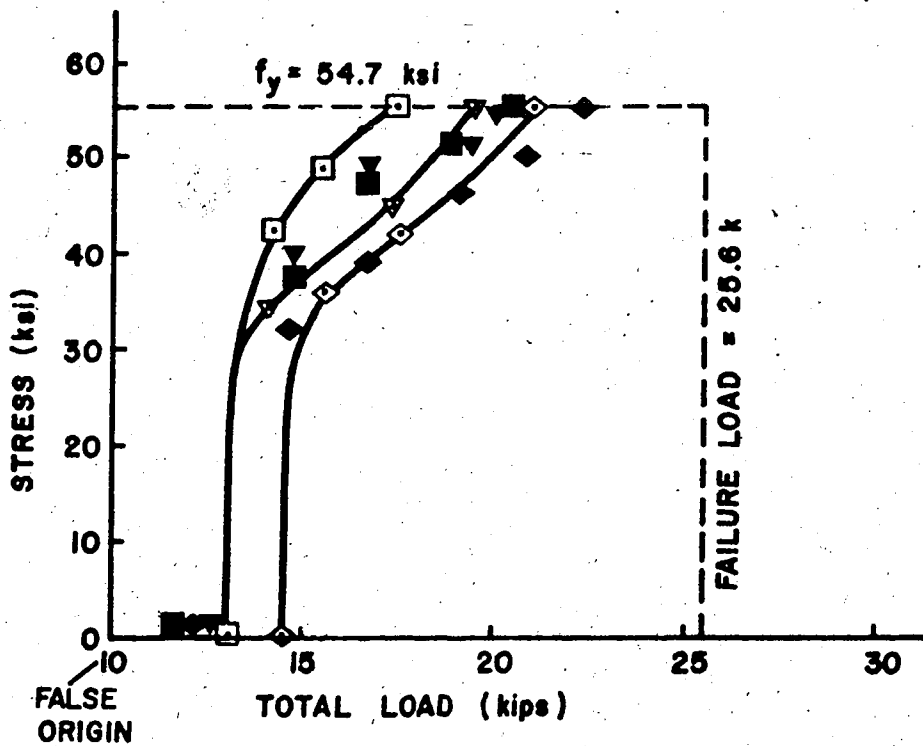


FIG. 6.15(B) TEST AND MODEL HOOP REINFORCEMENT STRESSES FOR BEAM R5

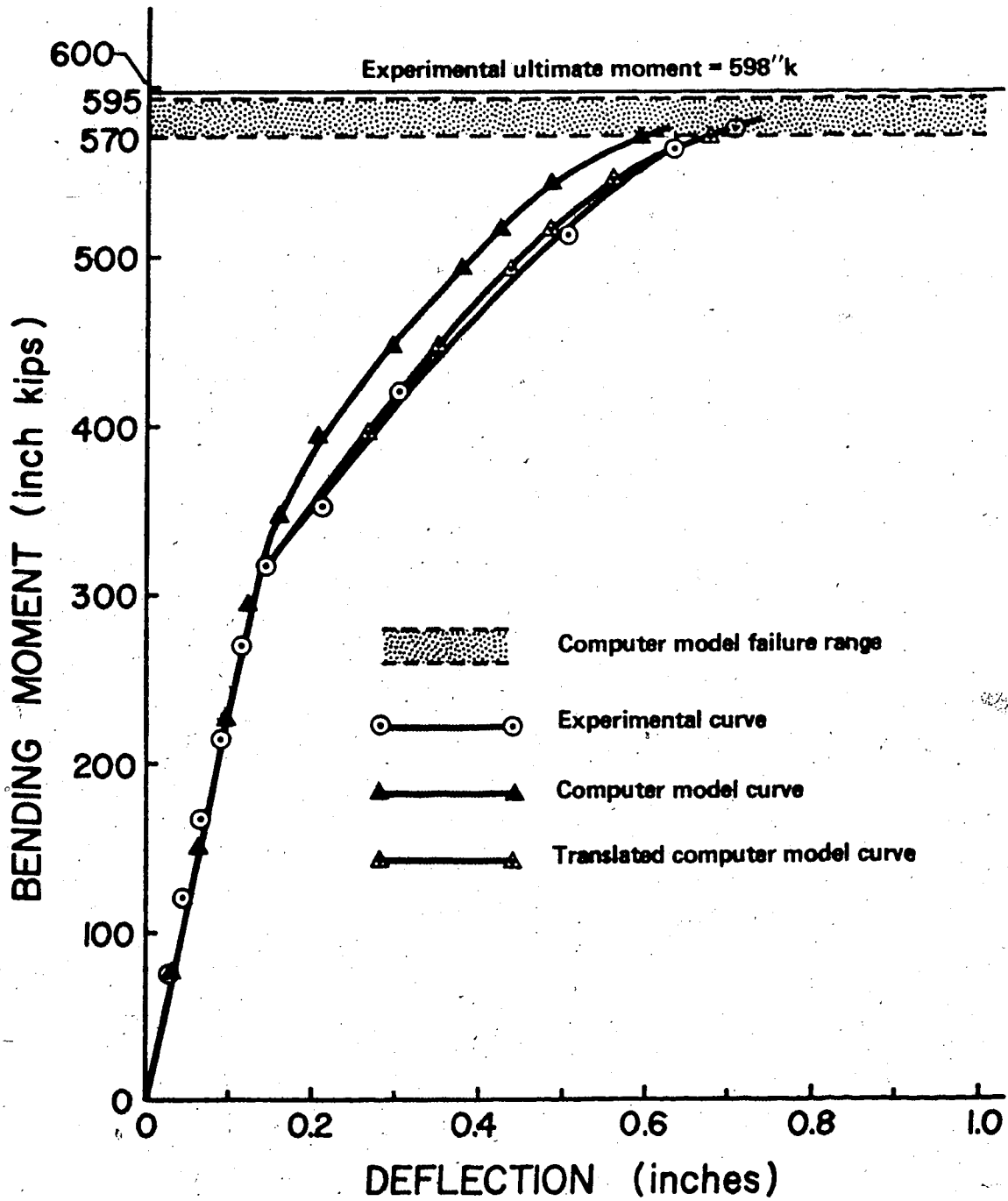


FIG. 6.16 MODEL AND TEST BENDING MOMENT DEFLECTION CURVES FOR BEAM T1

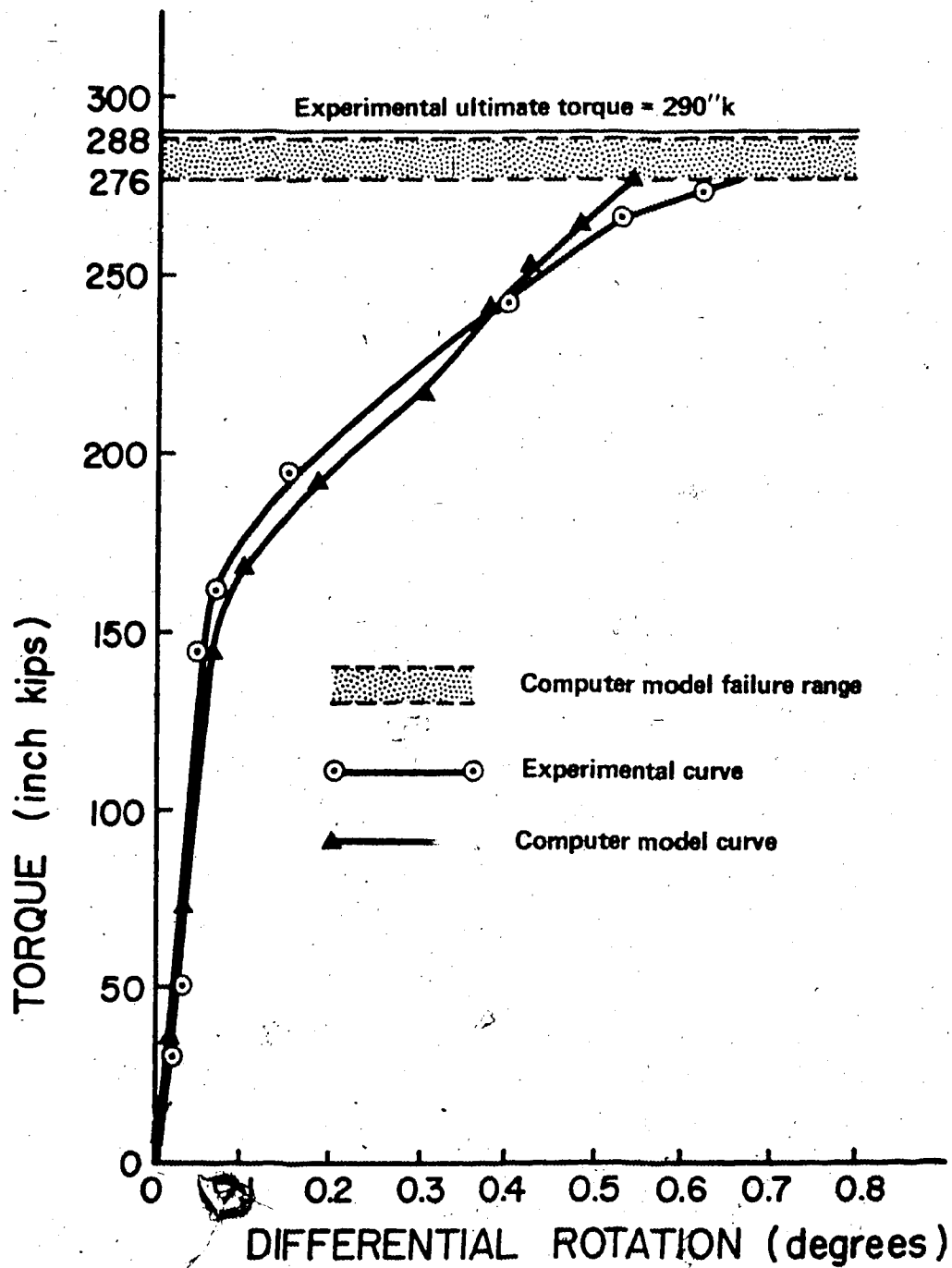


FIG. 6.17 MODEL AND TEST TORQUE-ROTATION CURVES FOR BEAM T1



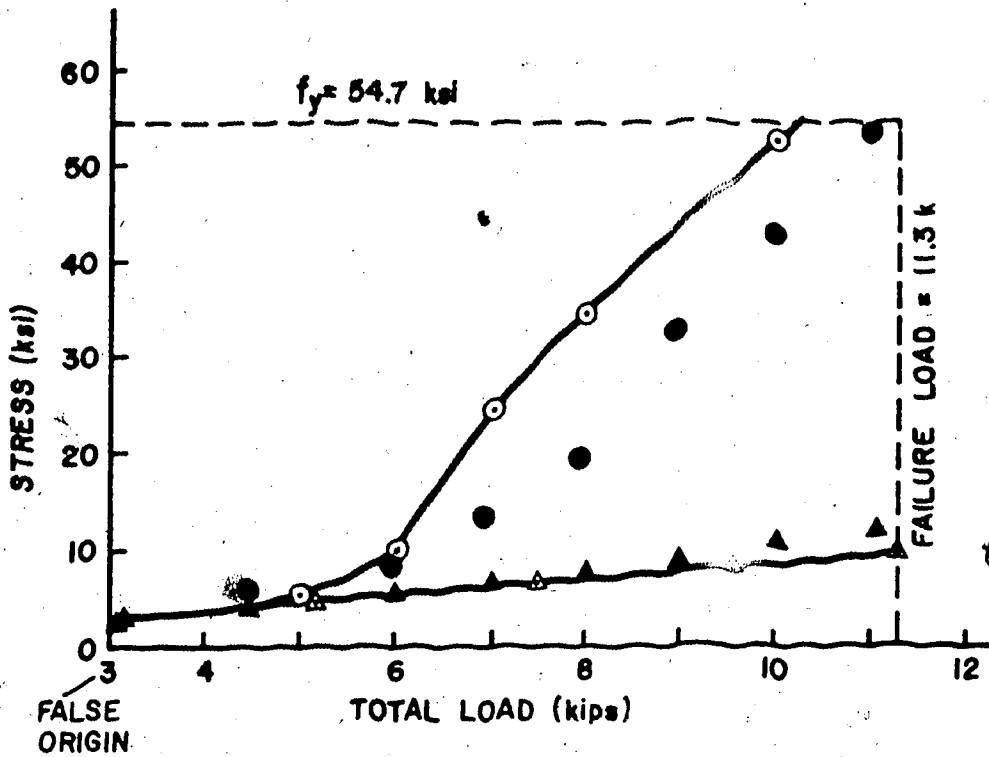


FIG. 6.18(A) TEST AND MODEL LONGITUDINAL CONVENTIONAL REINFORCEMENT STRESSES FOR BEAM T1

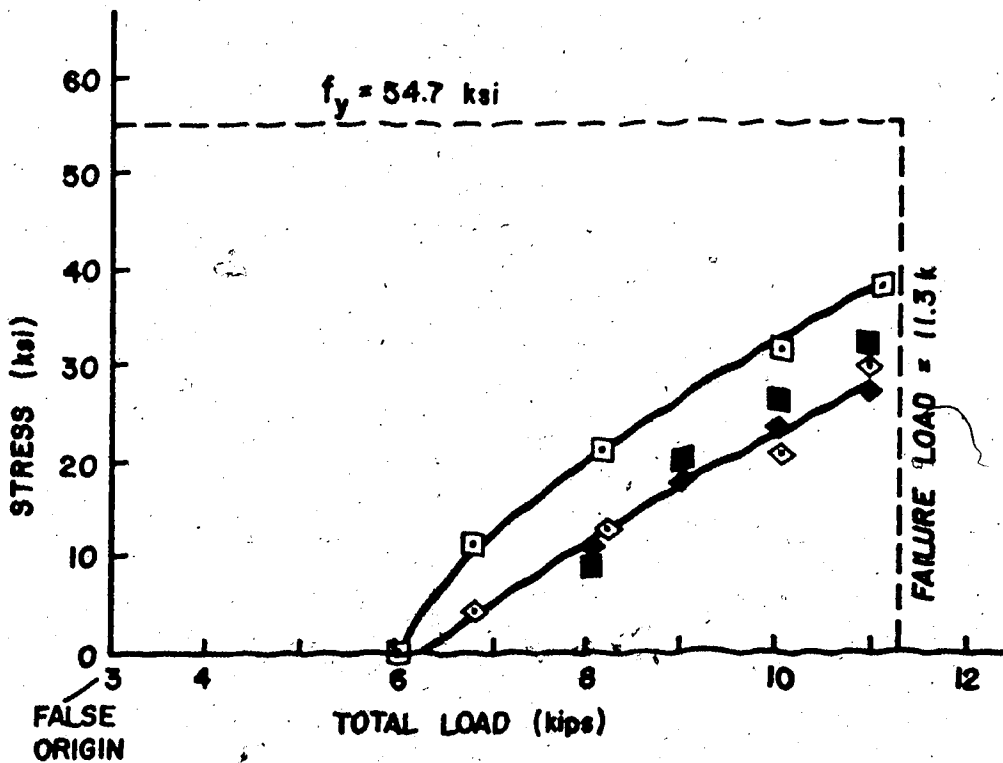


FIG. 6.18(B) TEST AND MODEL HOOP REINFORCEMENT STRESSES FOR BEAM T1

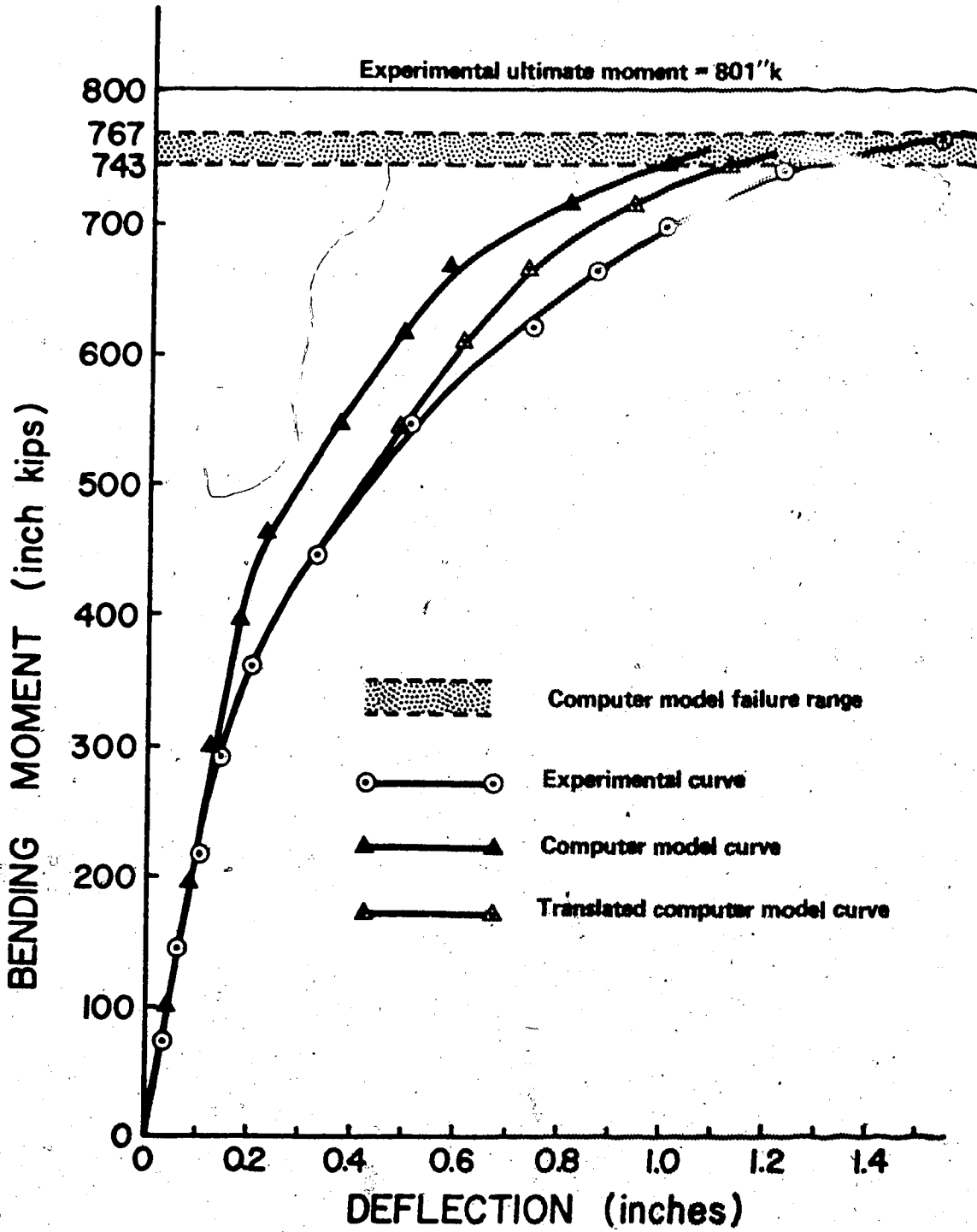


FIG. 6.19 MODEL AND TEST BENDING MOMENT-DEFLECTION CURVES FOR BEAM T2

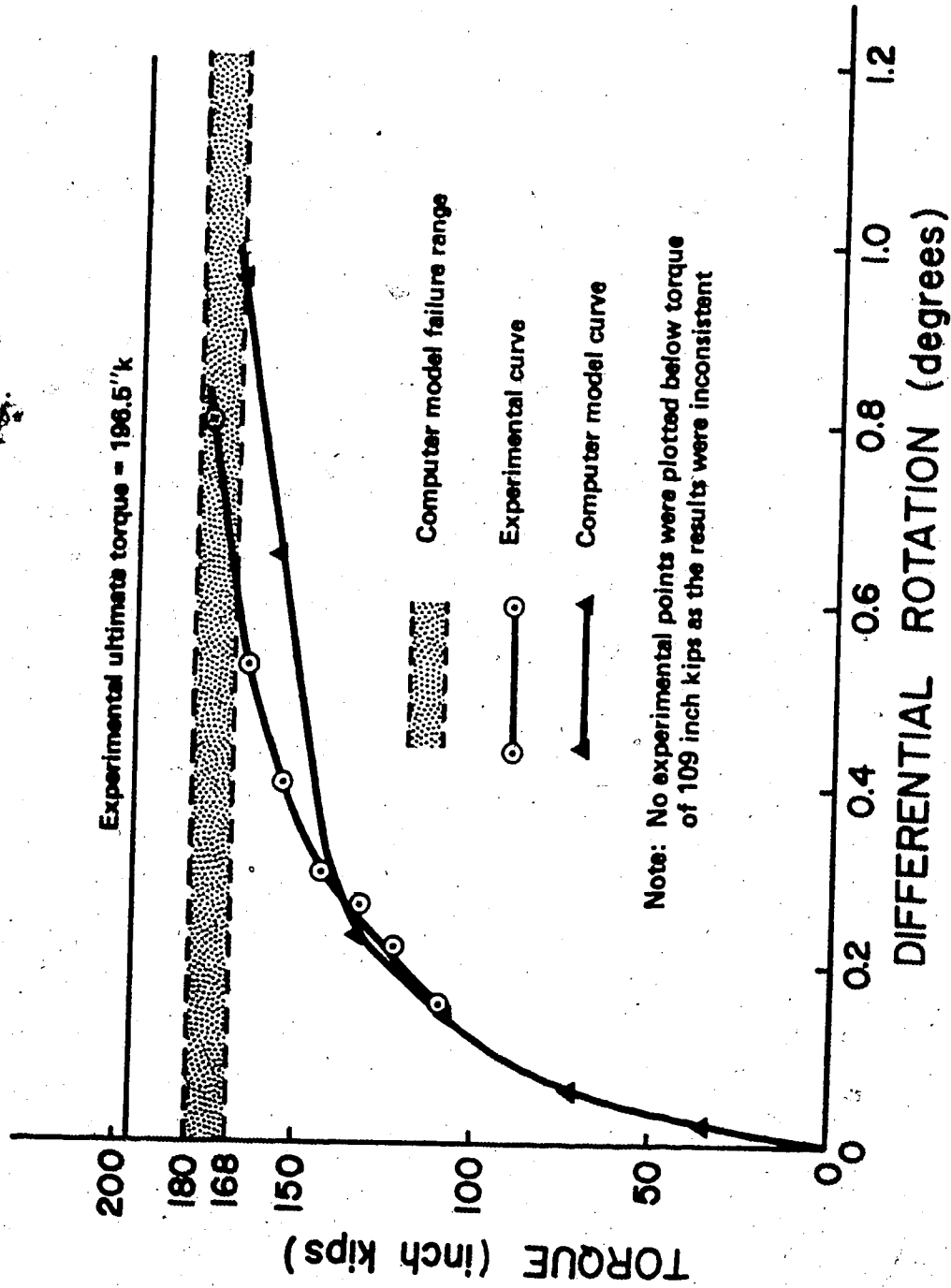


FIG. 1.20 MODEL AND TEST TORQUE-ROTATION CURVES FOR BEAM T2

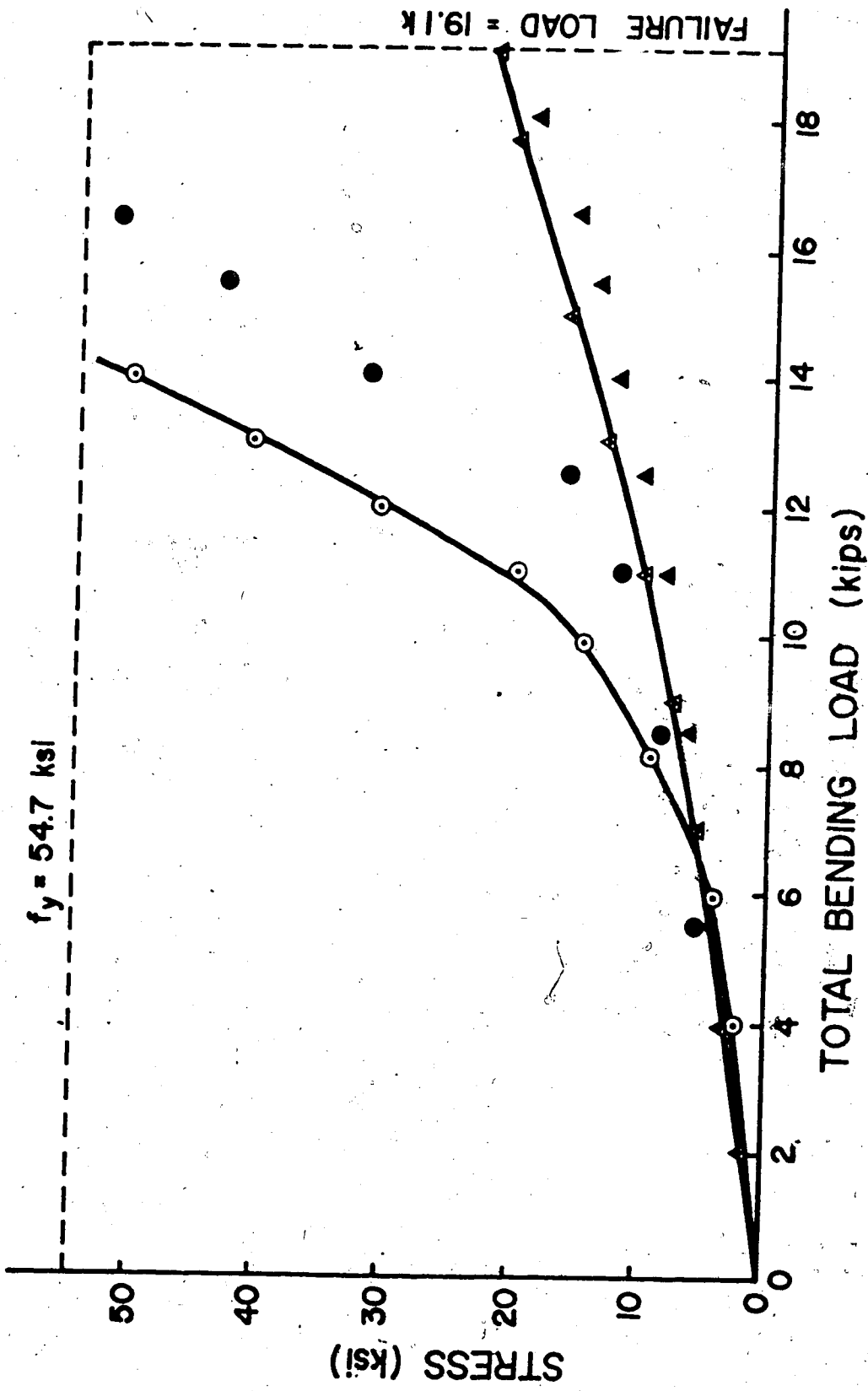
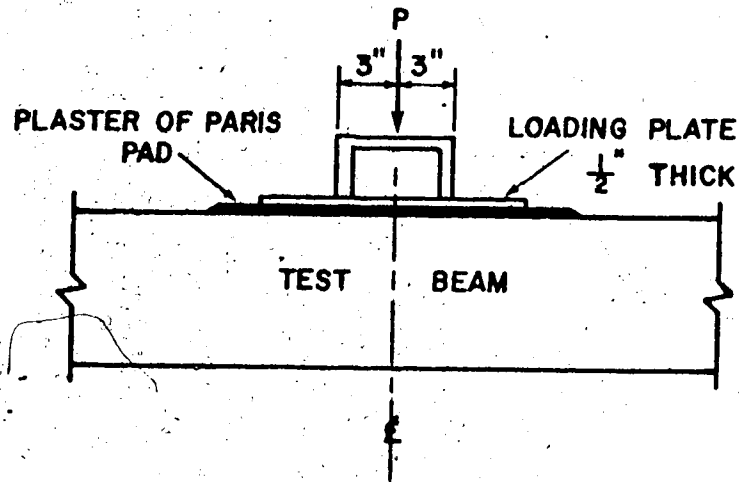
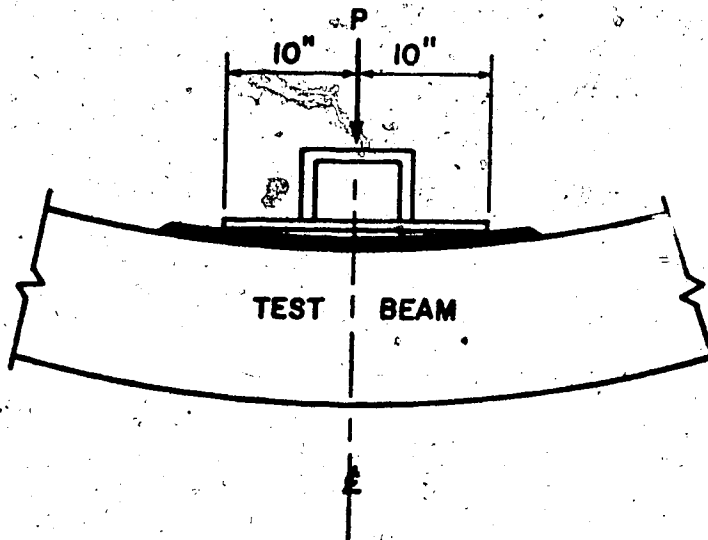


FIG. 6.21 TEST AND MODEL LONGITUDINAL CONVENTIONAL REINFORCEMENT STRESSES FOR BEAM T2



Beam span = 147"  
 Maximum moment due to  $P$  = 35.25 $P$

- (a) Complete contact of loading plate and plaster of Paris pad



Maximum moment due to  $P$  = 31.75 $P$

- (b) Edge contact of loading plate and plaster of Paris pad

FIG. 6.22 CENTRAL LOAD VARIATION FOR BEAM R4

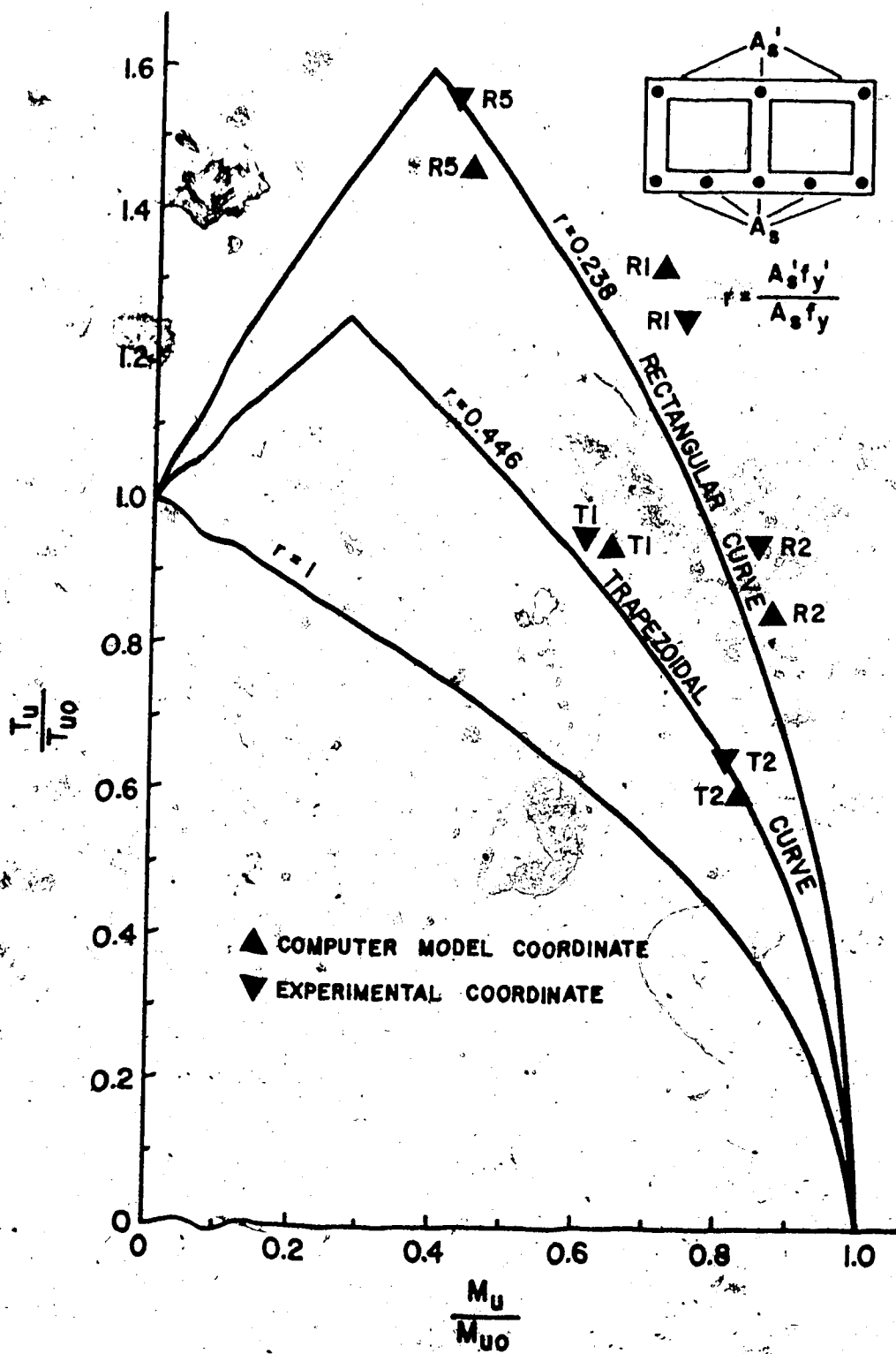


FIG. 6.23 TORQUE-BENDING MOMENT INTERACTION DIAGRAM FOR MODEL EVALUATION

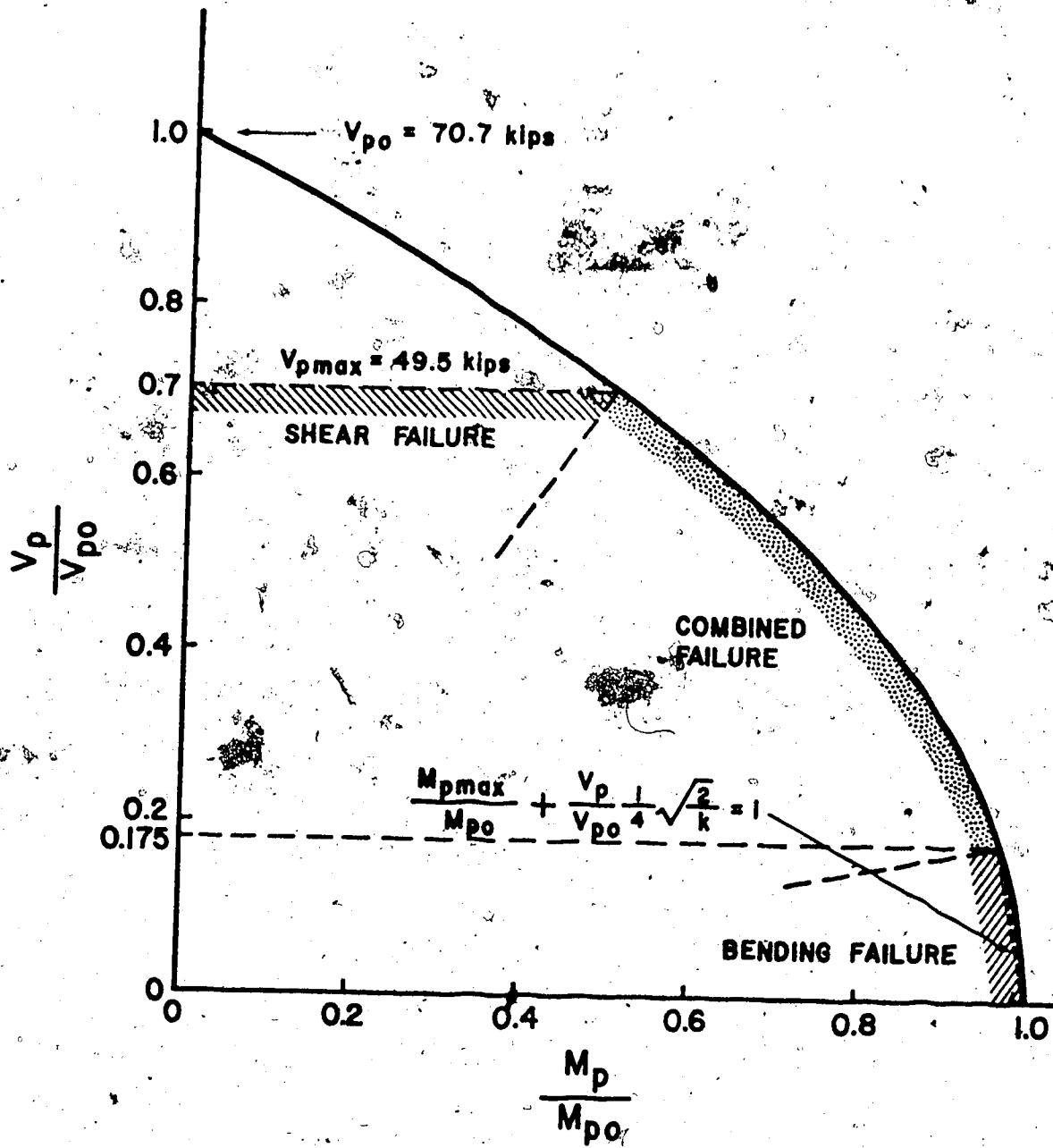
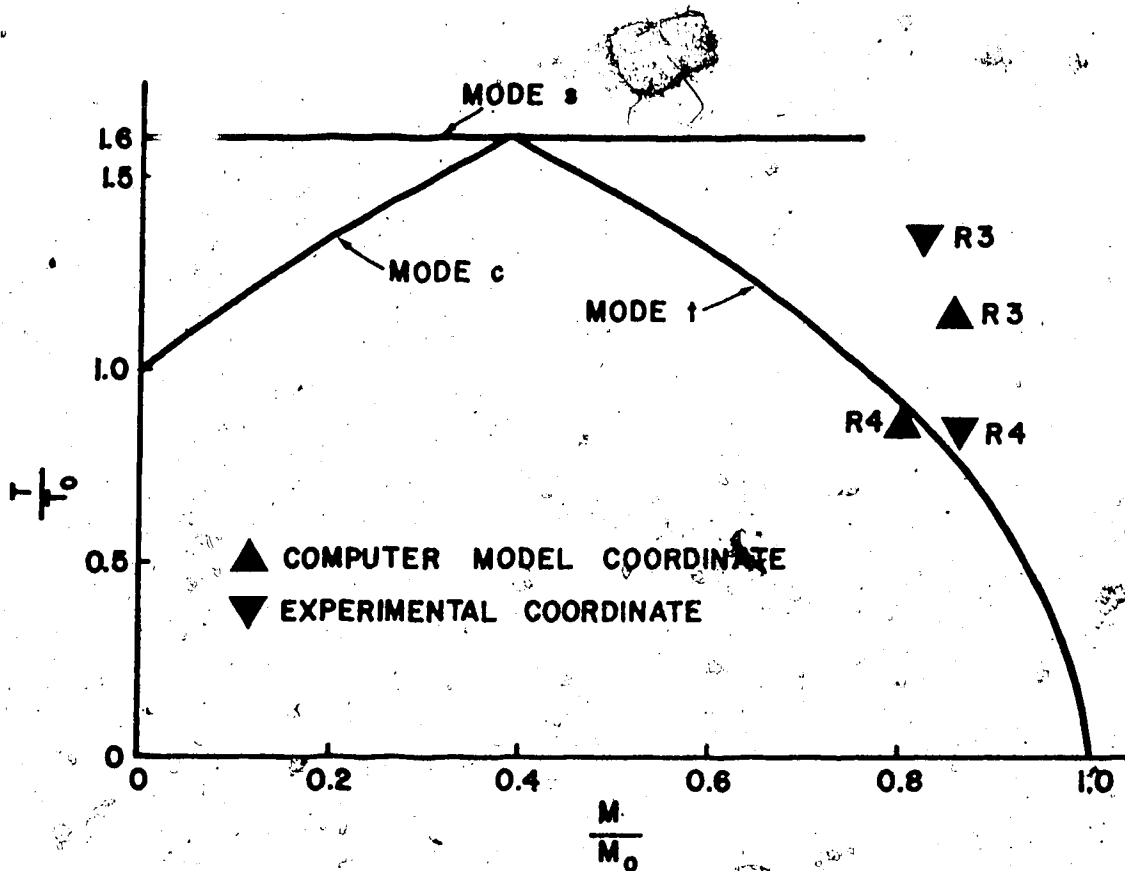


FIG. 6.24 INTERACTION DIAGRAM FOR BENDING MOMENT AND SHEAR



**INTERACTION EQUATIONS FOR BEAM R3:**

$$\text{MODE t: } \frac{M}{M_0} + 0.2377 \left( \frac{T}{T_0} \right)^2 = 0.994$$

$$\text{MODE c: } -4.207 \frac{M}{M_0} + \left( \frac{T}{T_0} \right)^2 = 0.976$$

$$\text{MODE s: } \frac{T}{T_0} = 1.6$$

**INTERACTION EQUATIONS FOR BEAM R4:**

$$\text{MODE t: } \frac{M}{M_0} + 0.2377 \left( \frac{T}{T_0} \right)^2 = 0.985$$

$$\text{MODE c: } -4.207 \frac{M}{M_0} + \left( \frac{T}{T_0} \right)^2 = 0.936$$

$$\text{MODE s: } \frac{T}{T_0} = 1.6$$

**FIG. 6.25 ADJUSTED TORQUE-BENDING MOMENT-SHEAR INTERACTION DIAGRAM FOR BEAMS R3 AND R4**



## CHAPTER VII

### CONCLUSION AND SUMMARY

#### 7.1 Principal Implications of Comparison

Of the two sources of comparison that were utilized in the evaluation of the analytical model, the results of the small, comprehensive experimental program provided the better basis for a conclusive assessment.

From experimental comparisons, two potential sources of model inaccuracy were isolated; underconservative estimation of the cracking load under torsion loading conditions, and inaccurate representation of the bending moment lever arm at ultimate failure. The former qualification of behaviour can be overcome if the variation of torsional shear stress across the wall thickness is taken into account. To reflect the more accurate prediction of cracking load, the computer model results are transformed accordingly through the translation of the post-cracking sections of the bending moment-deflection and torque-rotation curves. Inaccurate prediction of the ultimate bending moment capacity cannot be resolved as the maximum lever arm length is fixed by geometry, but this deficiency is only of significance in underreinforced beams where the ratio of compression flange thickness to beam depth is unusually high. Since the modest degree of discrepancy between experimental and model results is principally derived from the latter qualification, accurate simulation of beam behaviour can be attained for concrete box girders of lower wall thickness to depth ratios.

The principal conclusion that arose from the model assessment in light of current theory was the general applicability of the analytical model achieved through freedom from restrictive assumptions. Where valid comparisons can be made, agreement between analytical and theoretical results is good. Theoretical interactive behaviour, presented in its dimensionless equation form, does not permit an explicit evaluation of model results, and can indeed be misleading because of the dimensionless form of presentation.

Consideration of the significant aspects of the assessment procedure affirm the value of the computer model as a capable, versatile, analytical tool in its context of the analysis of concrete box girders acted upon by torsion, bending, and shear. Qualification of its accuracy is isolated to one potential source of error, and the range of application is almost without restriction. Characteristic of all finite element modelling, the reliability of output information is reflected in the quality of input specifications.

## 7.2 Application of the Analytical Model

Within their respective confines of validity determined by explicit assumptions, theoretical strength predictions discussed in Chapter 6 are not in conflict with analytical model results. The important qualification concerning the analytical value of current theory is the restrictive nature of assumptions that limit the regions of theoretical application. As specified in Section 6.5.2.3, the following computer model capabilities are beyond the range of theory application:

1. Beams may contain any level of reinforcement, to the extent of being overreinforced.
2. Cross-sectional geometry may vary along the member's length.
3. St. Venant torsion need not be dominant.
4. Member deformations are described comprehensively at all load levels from commencement of loading to failure.
5. The stress levels of all component materials are evaluated throughout the loading sequence.
6. Indeterminate analysis under any loading condition is possible.

present form, the computer model cannot permit variation in cross-sectional geometry along its length as a rectangular concrete finite element has been used. Replacement of the rectangular element with a plane stress general quadrilateral element<sup>38</sup> that has the same degrees of freedom will overcome this shortcoming.

The flexibility and fully comprehensive nature of the analytical model can be a valuable asset in the design process. Although the model is not suited to direct incorporation in preliminary design, final design proposals can be checked thoroughly through the use of the analytical model after material and geometrical parameters have been chosen. Since current practice is increasingly oriented toward ultimate strength design, a certain degree of concrete cracking is often tolerated at extreme service load conditions. Evaluation of reinforcement and concrete stress levels under such conditions, though beyond theoretical capabilities, is readily achieved by the computer model which, in addition, can provide accurate estimation of structural deformations. In statically indeterminate structures, the analytical model may well represent the only reliable method of analysis.

Enthusiastic adoption of the analytical model approach must be tempered through recognition of the inherent dependence of model accuracy on quality of input specifications. Evaluation of failure load conditions is most strongly influenced by beam geometry and reinforcement strength, the effect of concrete compressive strength being more pronounced as the overreinforced condition is approached. In the accurate determination of deformations, the initial concrete modulus is the most crucial parameter, assuming that the cracking load is estimated closely through accurate monitoring of concrete tensile strength and shrinkage stresses. Invariably, concrete strength parameters can be notoriously inconsistent if care is not exercised in their evaluation. Therefore, suitability of the computer model method must be viewed within the context of input parameter accuracy, as the highly sophisticated and comprehensive nature of finite element analysis can be completely negated by erroneous input.

### 7.3 Summary

The principal objective of this thesis topic is the development of an analytical computer model that can analyze reinforced or prestressed concrete box girders of arbitrary cross-section for any loading combination of bending moment, torque, and shear. Of the many refined capabilities of the finite element model, prediction of deformations in the post-cracking region has been chosen as the main premise on which performance of the model is evaluated.

Linear concrete segments of the box girder are represented in the model by higher-order plane stress rectangular finite elements that

are assigned twelve degrees of freedom, two translational and one rotational degree of freedom at each element node. Reinforcement is represented by one-dimensional bar elements. To enable the complete load-deformation path to be described from onset of loading through to failure, the loading sequence is an incremental, iterative one where the probability of material behavioural deviation in successive load increments is reduced by the Runge-Kutta method. Should significant material deviation be detected, the modified Newton-Rapson method restores equilibrium in an iterative procedure.

Concrete is modelled as a non-linear, anisotropic material, and following cracking, its effective shear modulus in the reformulated constitutive relationship is redefined on aggregate interlock and dowel action considerations. The important aspects of diaphragm action are treated comprehensively in the analytical model in the simulation of cross-sectional distortional stiffness, longitudinal warping restraint, and intrinsic transverse shear rigidity of box girders without diaphragms. In the absence of theoretical or experimental information, an auxiliary finite element model has been employed to investigate the longitudinal warping resistance of "thick" diaphragms.

To test the capabilities of the computer model rigorously, a literature survey was conducted to find experimental results of multi-celled box girders subjected to torsion, bending, and shear where testing was pursued to failure. No suitable reference was found, and consequently, a small experimental program was undertaken in which seven double-celled, prestressed concrete box girders, five rectangular and two trapezoidal in cross-section, were tested to failure under varying

combinations of the latter three load types.

To evaluate the accuracy of the analytical model predictions, corresponding computer model and experimental results were compared in detail through examination of the respective bending moment-deflection, torque-rotation, and reinforcement stresses-load relationships. Where applicable, the model results were also assessed in light of current theoretical predictions. From an overall perspective, performance of the analytical model was very satisfactory.

#### 7.4 Conclusion

The object of this thesis has been achieved in the development of a finite element analytical model that can analyze concrete box girders of arbitrary cross-section subjected to torsion, bending, and shear. Being afflicted by only one shortcoming that is not significant in members of common cross-sectional geometry, the computer model is a flexible, comprehensive mode of analysis whose range of application is limited by few constraints. Of the numerous material parameters that govern the model's behaviour, only the phenomenon of dowel action is ill-defined as certain aspects of its contribution to shear strength have not as yet been clarified. In the research of concrete box girder behaviour, exhaustive time-consuming experimental test programs are now superseded in almost every respect by the analytical model. Considering the restrictive assumptions in current theory, the computer model greatly increases the analytical scope and design capability in this field of study.

## REFERENCES

1. Bouwkamp, J.G., Scordelis, A.C., and Waste, S.T., "Ultimate Strength of Concrete Box Girder Bridge", Journal of Structural Division, ASCE, Vol. 100, No. ST1, January, 1974, pp. 31-49.
2. Hofbeck, J.A., Ibrahim, I.O., and Mattock, A.H., "Shear Transfer in Reinforced Concrete", Proc. ACI, Vol. 66, No. 2, February, 1969, pp. 119-128.
3. Fenwick, R.C., and Paulay, T., "Mechanisms of Shear Resistance of Concrete Beams", Journal of Structural Division, ASCE, Vol. 94, No. ST10, October, 1968, pp. 2325-2350.
4. Houde, J., and Mirza, M.S., "A Finite Element Analysis of Shear Strength of Reinforced Concrete Beams", Symposium on Shear in Reinforced Concrete, ACI Special Publication, SP-42, 1974.
5. Dulacska, H., "Dowel Action of Reinforcement Crossing Cracks in Concrete", Proc., ACI, Vol. 69, No. 70, December, 1972, pp. 754-757.
6. Taylor, H.P.J., "Investigation of the Dowel Shear Forces Carried by the Tensile Steel in Reinforced Concrete Beams", Cement and Concrete Association, Technical Report TRA 431, November, 1969.
7. Bauman, T., "Experiments to Study the Doweling Action of Flexural Tensile Reinforcement in a Reinforced Concrete Beam", Portland Cement Association, Foreign Literature Study No. 612, October, 1969.
8. ASCE-ACI Committee 426, "The Shear Strength of Reinforced Concrete Members", Journal of Structural Division, ASCE, Vol. 99, No. ST6, June, 1973, pp. 1091-1187.
9. Hsu, T.T.C., "Torsion of Structural Concrete - Behaviour of Reinforced Concrete Rectangular Members", Torsion of Structural Concrete, American Concrete Institute, Special Publication SP-18, 1968, pp. 261-306.
10. Hsu, T.T.C., and Kemp, E.L., "Background and Practical Application of Tentative Design Criteria for Torsion", Proc. ACI, Vol. 66, No. 1, January, 1969, pp. 12-23.
11. Zia, P., "What Do We Know About Torsion in Concrete Members", Journal of Structural Division, ASCE, Vol. 96, No. ST6, June, 1970, pp. 1185-1199.

12. Lampert, P., "Ultimate Strength of Reinforced Concrete Beams in Torsion and Bending", Dissertation No. 4445, Institut für Baustatik, ETH Zurich, 1970, 190 pp.
13. Discussion of paper by Lampert, P., and Collins, M.P., "Torsion, Bending and Confusion - An Attempt to Establish the Facts", Proc. ACI, Vol. 70, No. 2, Disc. No. 69-45, February, 1973, pp. 156-166.
14. Cowan, H.J., and Armstrong, S., "Experiments on the Strength of Reinforced and Prestressed Concrete Beams and of Concrete-Encased Steel Joists in Combined Research", Magazine of Concrete Research, Vol. 7, No. 19, London, March, 1955, pp. 3-20.
15. Gardner, R.P.M., "The Behaviour of Prestressed Concrete I-Beams Under Combined Bending and Torsion", Technical Report TRA/329, Cement and Concrete Association, London, February, 1960.
16. Swamy, N., "The Behaviour and Ultimate Strength of Prestressed Concrete Hollow Beams Under Combined Bending and Torsion", Magazine of Concrete Research, London, Vol. 14, No. 40, March, 1962.
17. Maisel, B.I., Rowe, R.E., and Swann, R.A., "Concrete Box-Girder Bridges", Proc. The Structural Engineer, Vol. 51, No. 10, October, 1973, pp. 363-376.
18. Malcolm, D.J., and Redwood, R.G., "Shear Lag in Stiffened Box Girders", Journal of Structural Division, Vol. 96, No. ST7, July, 1970, pp. 1403-1419.
19. Kashima, S., and Breen, J.E., "Construction and Load Tests of a Segmented Precast Box Girder Bridge Model", Centre for Highway Research, Research Report 121-5, University of Texas, Austin, February, 1975.
20. Rausch, E., "Berechnung des Eisenbetons gegen Verdrehung und Ascheren (Design of Reinforced Concrete for Torsion and Shear)", Springer Verlag, Berlin, Germany, 1929.
21. Cowan, H.J., "Elastic Theory for Torsional Strength of Rectangular Reinforced Concrete Beams", Magazine of Concrete Research, Vol. 2, No. 4, London, England, July, 1950, pp. 3-8.
22. Andersen, P., "Experiments with Concrete in Torsion", Transactions, ASCE, Vol. 100, Paper No. 1912, 1935, pp. 949-983.
23. Hsu, T.C., "Ultimate Torque of Reinforced Rectangular Beams", Journal of Structural Division, ASCE, Vol. 94, No. ST2, February, 1968, pp. 485-510.



24. Lessig, N.N., "Determination of Load Carrying Capacity of Reinforced Concrete Elements Subjected to Flexure and Torsion", Trudy, No. 5, Institution Betona, Zhelezobetona (Concrete and Reinforced Concrete Institute), Moscow, 1959, pp. 5-28, P.C.A. Foreign Literature Studies No. 371.
25. Collins, M.P., and Lampert, P., "Designing for Torsion", Structural Concrete Symposium, Department of Civil Engineering, University of Toronto, 1971, pp. 38-79.
26. Collins, M.P., and Lampert, P., "Torsion, Bending, and Confusion - An Attempt to Establish the Facts", Proc. ACI, Vol. 69, No. 8, August, 1972, pp. 500-504.
27. Hsu, T.T.C., "Post-Cracking Torsional Rigidity of Reinforced Concrete Sections", Proc. ACI, Vol. 70, No. 5, May, 1973, pp. 352-360.
28. Scordelis, A.C., "Analysis of Simply Supported Box Girder Bridges", University of California, Berkeley, Structural Engineering and Structural Mechanics Report No. SESM 66-17. October, 1966.
29. Scordelis, A.C., and Davis, R.E., "Stresses in Continuous Concrete Box Girder Bridges", Second International Symposium on Concrete Bridge Design, American Concrete Institute, Chicago, April, 1969.
30. Cheung, Y.K., "Analysis of Box Girder Bridges by the Finite Strip Method", Second International Symposium on Concrete Bridge Design, American Concrete Institute, Chicago, April, 1969.
31. Scordelis, A.C., "Analytical Solutions for Box Girder Bridges", Proc. International Conference on Developments in Bridge Design and Construction, Cardiff, Wales, April, 1971, pp. 200-216.
32. Ngo, D., and Scordelis, A.C., "Finite Element Analysis of Reinforced Concrete Beams", Proc. ACI, Vol. 64, No. 3, March, 1967.
33. Scordelis, A.C., "Finite Element Analysis of Reinforced Concrete Structures", Proc. Speciality Conference on the Finite Element Method in Civil Engineering, McGill University, Montreal, June, 1972, pp. 71-113.
34. Trikha, D.N., and Edwards, A.D., "Analysis of Concrete Box Girders Before and After Cracking", Proc. Institute of Civil Engineering, Vol. 53, Part 2, December, 1972, pp. 515-528.
35. Zienkiewicz, O.C., "The Finite Element Method in Engineering Science", McGraw Hill, London, 1971.

36. McCleod, I.A., "New Rectangular Finite Element For Shear Wall Analysis", Journal of Structural Division, ASCE, Vol. 95, ST3, March, 1969, pp. 399-409.
37. Meyer, C., and Scordelis, A.C., "Computer Program for Prismatic Folded Plates with Plate and Beam Elements", University of California, Berkely, Structural Engineering and Structural Mechanics Report No. SESM 7-3, February, 1970.
38. Sisodiya, R.G., and Ghali, A., "Analysis of Box Girder Bridges of Arbitrary Shape", Publications, International Association of Bridge and Structural Engineering, Vol. 33-I, 1973, pp. 203-217.
39. Liu, T.C.Y., Nilson, A.H., and Slaté, F.O., "Biaxial Stress-Strain Relationships for Concrete", Journal of Structural Division, ASCE, Vol. 98, No. ST5, Proc. Paper 8905, May, 1972, pp. 1025-1034.
40. Janjua, M.A., and Welch, G.B., "Magnitude and Distribution of Concrete Cracks in Reinforced Concrete Flexural Members", Unicity Report No. R78, University of New South Wales, Australia, July, 1972.
41. Salem, M.H., and Mohray, B., "Nonlinear Analysis of Planar Reinforced Concrete Structures", Report No. 74-2022, Structural Eng. Series No. 410, University of Illinois, July, 1974.
42. Bauman, T., "Experiments to Study the Doweling Action of Flexural Tensile Reinforcement in a Reinforced Concrete Beam", Portland Cement Association, Foreign Literature Study No. 612, October, 1969.
43. Timoshenko, S.P., and Woinowsky-Krieger, S., "Theory of Plates and Shells", Engineering Societies Monographs, McGraw-Hill, 2nd Edition, 1959.
44. Sawko, F., and Cope, R.G., "Analysis of Multi-Cell Bridges Without Transverse Diaphragms - A Finite Element Approach", Proceedings, The Structural Engineer, No. 11, Vol. 47, November, 1969, pp. 455-460.
45. Nilson, A.H., "Nonlinear Analysis of Reinforced Concrete by the Finite Element Method", Journal of American Concrete Institute, Vol. 65, September, 1968, pp. 757-766.
46. Kupfer, H., Hilsdorf, H., and Rüsich, H., "Behaviour of Concrete Under Biaxial Stress", Proceedings, ACI, Vol. 66, August, 1969, pp. 656-666.
47. Desai, C.S., and Abel, J.F., "Introduction to the Finite Element Method", Van Nostrand, New York, 1972.

48. Discussion of paper of Hsu, T.C., "*Ultimate Torque of Reinforced Rectangular Beams*", Proc. Paper 6203, Journal of Structural Division, ASCE, Vol. 94, No. ST11, November, 1968, pp. 2645-2647.
49. Mufti, A.A., Mirza, M.S., McCutcheon, J.O., and Houde, J., "*A Study of the Behaviour of Reinforced Concrete Elements Using Finite Elements*", Structural Concrete Series No. 70-5, McGill University, Montreal, September, 1970.
50. Thürlimann, B., "*Shear Strength of Reinforced and Prestressed Concrete Beams - CEB Approach*", ACI Symposium, Philadelphia, U.S.A., 1976.
51. Elfgrén, L., "*Reinforced Concrete Beams Loaded in Combined Torsion, Bending and Shear*", Publication 71:3, Division of Concrete Structures, Chalmers University of Technology, Göteborg, Sweden, 1972.
52. Libby, J.R., "*Modern Prestressed Concrete*", Van Nostrand Reinhold, New York, 1971.

APPENDICES

APPENDIX A

SIGN CONVENTIONS AND SYSTEMS

## APPENDIX A

### SIGN CONVENTIONS AND SYSTEMS

#### (1) Global Axes Directions

The global x axis must be in the beam's longitudinal direction, and the global y axis in the upward vertical direction. Having chosen the x and y directions, the global z axis is defined by the right hand axis convention.

#### (2) Node Numbering

##### (a) Rectangular concrete elements

Refer to Figure A-1.

##### (b) Reinforcement elements

The node numbering sequence should be in the positive global axis direction. A vertical inclined bar should be numbered in the upward direction.

##### (c) Bond spring linkages

No predefined node numbering convention

#### (3) Nodal Forces and Displacements

Positive in positive global axis direction.

#### (4) Nodal Moments and Rotations

Positive when acting clockwise looking along global axis in positive direction.

(5) Stresses and Strains

(a) Direct stresses and strains

Tension positive, compression negative

(b) Shear stresses and strains

Positive when acting on a positive face in a positive global axis direction, or a negative face in a negative global axis direction.

(6) Mohr's Circle

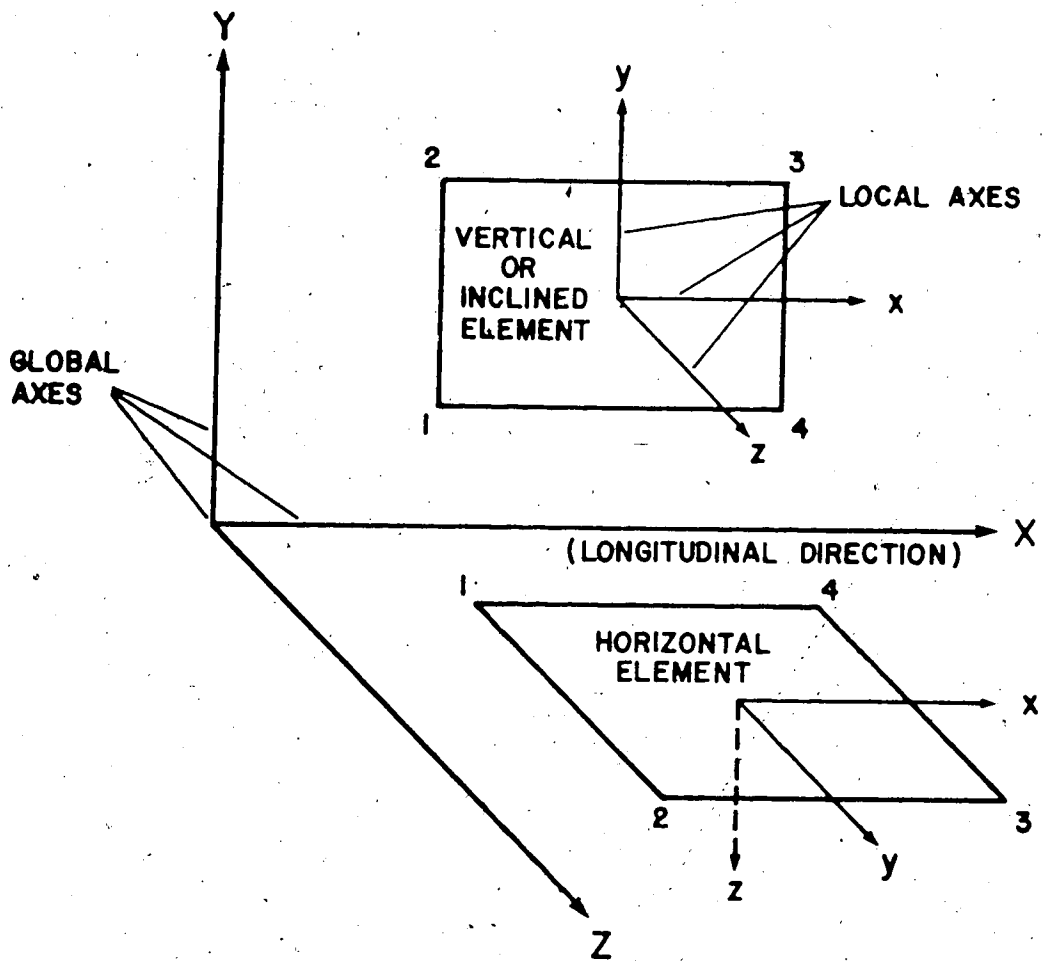
Same sign convention for direct stresses and strains as above is used. However, shear stresses and strains are positive when the couple acts in the clockwise direction.

(7) Dimensional Parameter Units

Length - inches

Force - pounds wt.

Rotation - degrees (CANGLE(NEL))



**FIG. A-1 NODE NUMBERING SEQUENCE FOR RECTANGULAR CONCRETE ELEMENTS**



APPENDIX B

SYMBOLIC NAMES

SYMBOLIC NAMES DESCRIPTION

THE CODES REFERRED TO IN THE DESCRIPTION COLUMNS BELOW ARE DEFINED AT THE BOTTOM OF THE TABLE.

SYMBOLIC NAME	DESCRIPTION
AGMOD	AGGREGATE INTERLOCK RIGIDITY MODULUS
AL (M3,3)	TOTAL STIFFNESS MATRIX MODULUS
ANGLE (MEL, 1)	ANGLE IN DEGREES OF STEEL WESH LAYER 1 TO LONGITUDINAL DIRECTIONAL
AR (M3,3)	TOTAL STIFFNESS MATRIX ARRAY
AVCSP	AVERAGE CONCRETE SPACING IN INCHES
BS (3, 3)	COMPONENT ELEMENT STIFFNESS BLOCK
CALTR (MEL)	ALTERATION INDICATOR FOR CONCRETE ELEMENT (CODE1)
CANGLE (MEL)	ANGLE OF PRINCIPAL TENSILE STRESS OR CRACK TO LONGITUDINAL DIRECTION
CARMA (M3)	CIRCUMFERENTIAL BOND AREA FOR BOND SLIP LINKAGE
CONDEV	HATCHING ALLOWABLE PERCENTAGE DEVIATION OF PRINCIPAL CONCRETE COMPRESSIVE STRESS FROM ITS STRESS-STRAIN CURVE
CONMOD	INITIAL MODULUS FOR CONCRETE
D (3, 3)	COMBINED CONSTITUTIVE MATRIX FOR CONCRETE AND STEEL WESH
D1 (M3M3)	GENERAL DISPLACEMENT VECTOR
D2 (2, M3M3)	DISPLACEMENT ARRAY FOR CURRENT LOAD INCREMENT AND FOLLOWING HALF LOAD INCREMENT
DAGG (MEL)	COMBINED AGGREGATE INTERLOCK AND DOBEL MODULUS FOR A CRACKED CONCRETE ELEMENT
DCONC (MEL, 3, 3)	CONCRETE CONSTITUTIVE MATRIX
DEVCON	HATCHING ALLOWABLE CHANGE IN CONCRETE CONSTITUTIVE MATRIX BEFORE ALTERATION IS MADE
DYVRO	SINGULARLY FOR REINFORCEMENT
DY	DOBEL LINKAGE FAILURE DISPLACEMENT
DPMOD (MEL)	DIAPHRAGM ELEMENT SHEAR MODULUS
DSH (3, 3)	STEEL WESH CONSTITUTIVE MATRIX
DST (M3M3)	TOTAL DISPLACEMENT VECTOR
ECOB (MEL, 3)	INCREMENTAL CENTROIDAL CONCRETE STRAINS (EX, EY, EXY)
ECULT	ULTIMATE CONCRETE STRAIN
EXPR	PRESTRESS REINFORCEMENT YIELD STRAIN
EXRDO	CONVENTIONAL REINFORCEMENT YIELD STRAIN
ELTRM (MEL)	CONCRETE ELEMENT THICKNESS
ES (MEL, EDIRMS)	INCREMENTAL CENTROIDAL STEEL WESH STRAINS FOR ALL WESH DIRECTIONS
ESULT	ULTIMATE STEEL WESH STRAIN
ESPLT	PRESTRESS STEEL STRAIN
ESRO (M3)	INCREMENTAL REINFORCEMENT ELEMENT STRAIN

FRULT	ULTIMATE CONVENTIONAL STEEL STRAIN
ESLIP	BOND LINKAGE STRAIN
ESTP (12, 12)	CONCRETE ELEMENT STIFFNESS MATRIX
EB1	LONGITUDINAL SHRINKAGE STRAIN IN BOTTOM FLANGE
EB2	" " " " " "
EB3	" " " " " "
EB4	" " " " " "
EB5	" " " " " "
EB6	" " " " " "
EB7	" " " " " "
EB8	" " " " " "
EB9	" " " " " "
EB10	" " " " " "
EB11	" " " " " "
EB12	" " " " " "
EB13	" " " " " "
EB14	" " " " " "
EB15	" " " " " "
EB16	" " " " " "
EB17	" " " " " "
EB18	" " " " " "
EB19	" " " " " "
EB20	" " " " " "
EB21	" " " " " "
EB22	" " " " " "
EB23	" " " " " "
EB24	" " " " " "
EB25	" " " " " "
EB26	" " " " " "
EB27	" " " " " "
EB28	" " " " " "
EB29	" " " " " "
EB30	" " " " " "
EB31	" " " " " "
EB32	" " " " " "
EB33	" " " " " "
EB34	" " " " " "
EB35	" " " " " "
EB36	" " " " " "
EB37	" " " " " "
EB38	" " " " " "
EB39	" " " " " "
EB40	" " " " " "
EB41	" " " " " "
EB42	" " " " " "
EB43	" " " " " "
EB44	" " " " " "
EB45	" " " " " "
EB46	" " " " " "
EB47	" " " " " "
EB48	" " " " " "
EB49	" " " " " "
EB50	" " " " " "
EB51	" " " " " "
EB52	" " " " " "
EB53	" " " " " "
EB54	" " " " " "
EB55	" " " " " "
EB56	" " " " " "
EB57	" " " " " "
EB58	" " " " " "
EB59	" " " " " "
EB60	" " " " " "
EB61	" " " " " "
EB62	" " " " " "
EB63	" " " " " "
EB64	" " " " " "
EB65	" " " " " "
EB66	" " " " " "
EB67	" " " " " "
EB68	" " " " " "
EB69	" " " " " "
EB70	" " " " " "
EB71	" " " " " "
EB72	" " " " " "
EB73	" " " " " "
EB74	" " " " " "
EB75	" " " " " "
EB76	" " " " " "
EB77	" " " " " "
EB78	" " " " " "
EB79	" " " " " "
EB80	" " " " " "
EB81	" " " " " "
EB82	" " " " " "
EB83	" " " " " "
EB84	" " " " " "
EB85	" " " " " "
EB86	" " " " " "
EB87	" " " " " "
EB88	" " " " " "
EB89	" " " " " "
EB90	" " " " " "
EB91	" " " " " "
EB92	" " " " " "
EB93	" " " " " "
EB94	" " " " " "
EB95	" " " " " "
EB96	" " " " " "
EB97	" " " " " "
EB98	" " " " " "
EB99	" " " " " "
EB100	" " " " " "



```

CODE 2
-1 - INCLINED CONCRETE ELEMENT
0 - HORIZONTAL CONCRETE ELEMENT
1 - VERTICAL

CODE 3
1,2 - RCLEOD CONCRETE ELEMENT TYPES
3 - ACTUAL DIAPHRAGM ELEMENT
4 - EQUIVALENT DIAPHRAGM ELEMENT
5 - WARPING RESISTANCE ELEMENT

CODE 4
-1 - X GLOBAL AXIS
0 - Y "
1 - Z "
2 - INCLINED VERTICAL DIRECTION

CODE 5
-1 - CONVENTIONAL REINFORCEMENT
0 - PRESTRESSED "
1 - BOND LINKAGE

CODE 6
1 - X GLOBAL AXIS
2 - Y "
3 - Z "
4 - THERAY GLOBAL AXIS (AXIS OF ROTATION ABOUT Y AXIS)
5 - THTETA "

CODE 7
-1 - BOND SPRING LINKAGE MODE WITH 1 DEGREE OF FREEDOM
0 - INTERNAL MODE WITH 3 DEGREES OF FREEDOM
1 - CORNER " 5
2 - SPECIAL DIAPHRAGM MODE WITH 4 DEGREES OF FREEDOM (ALL DEGREES OF FREEDOM EXCEPT THTETA)
3 - INTERNAL DIAPHRAGM MODE - 2 TRANSLATIONAL DEGREES OF FREEDOM. THIS MODE DOES NOT ADJOIN CONCRETE BOX GIRDER WALL ELEMENTS.

CODE 8
-1 - JUST CRACKED IN CURRENT LOAD INCREMENT
0 - UNCRACKED
1 - CRACKED

```

FILE

APPENDIX C  
MAIN PROGRAM LISTING



```

1780 DTOT(I)=D2(I,I)
1781 CONTINUE
1782 C CALCULATION OF ALL COMPONENT STRESSES FOR FULL LOAD VECTOR.
1783 CALL STRESS(MC)
1784 C FAILURE CHECK FOR BEAR
1785 CALL FAIL
1786 C CHECK TO DETERMINE ANY FURTHER CRACKING
1787 MC=0
1788 CALL TIER(1,0,ITIER)
1789 COSTY=COST(0)
1790 WRITE (6,330) ITIER,COSTY
1791 WRITE (7,330) ITIER,COSTY
1792 DO 69 I=1,NELE
1793 IF (BCRACK(I).EQ.1) GO TO 60
1794 STRES=PT
1795 IF (SBOCC(I).EQ.0) GO TO 58
1796 STRES=PT*(1.0-PSBOCC(I)/TC)
1797 IF (SBOCC(I).LT.SIGNAL) GO TO 60
1798 MC=MC+1
1799 MC=MC+1
1800 MC=MC+1
1801 WRITE (6,340) I
1802 WRITE (7,340) I
1803 CONTINUE
1804 C CHECK TO DETERMINE WHETHER ANY SIGNIFICANT DEVIATIONS IN MATERIAL
1805 C PROPERTIES HAVE OCCURRED.
1806 CALL DEVIA(10)
1807 IF (DEVIA(10).EQ.0) GO TO 100
1808 C ADJUSTMENT OF STRUCTURAL STIFFNESS MATRIX TO PERMIT TOTAL LOAD
1809 C IMPARTION FOR RESPONDING EQUILIBRIUM OF ALL STRUCTURAL ELEMENTS
1810 I=1
1811 CALL TIER(1,0,ITIER)
1812 COSTY=COST(0)
1813 WRITE (6,340) ITIER,COSTY
1814 MC=MC+1
1815 IF (MC.GT.HAIT) GO TO 380
1816 WRITE (6,345) MC
1817 WRITE (7,345) MC
1818 ICOUNT=2
1819 IF (MC.GT.1) GO TO 78
1820 C FOR THE FIRST ITERATION, TOTAL STRESS CONDITION IS
1821 C CALCULATED
1822 DO 65 J=1,J
1823 DO 65 I=1,NELE
1824 TSCOR(I,J)=TSCOR(I,J)+SIGCOR(I,J)
1825 TPCOR(I,J)=TPCOR(I,J)+PCOR(I,J)
1826 CONTINUE
1827 DO 70 J=1,NELE
1828 DO 70 I=1,NELE
1829 IF (EMBR(I).EQ.0) GO TO 76
1830 TORS(I,J)=TORS(I,J)+SIGS(I,J)
1831 TERS(I,J)=TERS(I,J)+ERS(I,J)
1832 CONTINUE
1833 DO 75 I=1,NELE
1834 TSCRO(I)=TSCRO(I)+SIGRO(I)
1835 TPCRO(I)=TPCRO(I)+PCRO(I)
1836 CONTINUE
1837 C DETERMINE RESTRAINT LOAD VECTOR
1838 DO 76 I=1,NELE

```

```

1800 DTOT(I)=D2(I,I)
1801 CONTINUE
1802 C CALCULATION OF ALL COMPONENT STRESSES FOR FULL LOAD VECTOR.
1803 CALL STRESS(MC)
1804 C FAILURE CHECK FOR BEAR
1805 CALL FAIL
1806 C CHECK TO DETERMINE ANY FURTHER CRACKING
1807 MC=0
1808 CALL TIER(1,0,ITIER)
1809 COSTY=COST(0)
1810 WRITE (6,330) ITIER,COSTY
1811 WRITE (7,330) ITIER,COSTY
1812 DO 69 I=1,NELE
1813 IF (BCRACK(I).EQ.1) GO TO 60
1814 STRES=PT
1815 IF (SBOCC(I).EQ.0) GO TO 58
1816 STRES=PT*(1.0-PSBOCC(I)/TC)
1817 IF (SBOCC(I).LT.SIGNAL) GO TO 60
1818 MC=MC+1
1819 MC=MC+1
1820 MC=MC+1
1821 WRITE (6,340) I
1822 WRITE (7,340) I
1823 CONTINUE
1824 C CHECK TO DETERMINE WHETHER ANY SIGNIFICANT DEVIATIONS IN MATERIAL
1825 C PROPERTIES HAVE OCCURRED.
1826 CALL DEVIA(10)
1827 IF (DEVIA(10).EQ.0) GO TO 100
1828 C ADJUSTMENT OF STRUCTURAL STIFFNESS MATRIX TO PERMIT TOTAL LOAD
1829 C IMPARTION FOR RESPONDING EQUILIBRIUM OF ALL STRUCTURAL ELEMENTS
1830 I=1
1831 CALL TIER(1,0,ITIER)
1832 COSTY=COST(0)
1833 WRITE (6,340) ITIER,COSTY
1834 MC=MC+1
1835 IF (MC.GT.HAIT) GO TO 380
1836 WRITE (6,345) MC
1837 WRITE (7,345) MC
1838 ICOUNT=2
1839 IF (MC.GT.1) GO TO 78
1840 C FOR THE FIRST ITERATION, TOTAL STRESS CONDITION IS
1841 C CALCULATED
1842 DO 65 J=1,J
1843 DO 65 I=1,NELE
1844 TSCOR(I,J)=TSCOR(I,J)+SIGCOR(I,J)
1845 TPCOR(I,J)=TPCOR(I,J)+PCOR(I,J)
1846 CONTINUE
1847 DO 70 J=1,NELE
1848 DO 70 I=1,NELE
1849 IF (EMBR(I).EQ.0) GO TO 76
1850 TORS(I,J)=TORS(I,J)+SIGS(I,J)
1851 TERS(I,J)=TERS(I,J)+ERS(I,J)
1852 CONTINUE
1853 DO 75 I=1,NELE
1854 TSCRO(I)=TSCRO(I)+SIGRO(I)
1855 TPCRO(I)=TPCRO(I)+PCRO(I)
1856 CONTINUE
1857 C DETERMINE RESTRAINT LOAD VECTOR
1858 DO 76 I=1,NELE

```

```

1859 DTOT(I)=D2(I,I)
1860 CONTINUE
1861 C CALCULATION OF TOTAL STIFFNESS MATRIX
1862 CALL KNTA(NE1,NE2,NS3,TS,AL,AR)
1863 CALL TIER(1,0,ITIER)
1864 COSTY=COST(0)
1865 WRITE (6,370) ITIER,COSTY
1866 C FIRST COLUMN OF LOAD VECTOR B2(I,2,ERQNS) IS ALTERED FOR CRACKING
1867 LOAD INCREMENT TO CURRENT TOTAL LOAD
1868 DO 80 I=1,NELE
1869 B2(I,1)=DTOT(I)+DTOT(I)
1870 CONTINUE
1871 GO TO 50
1872 IF (ICOUNT.EQ.2) GO TO 140
1873 C CALCULATION OF TOTAL STRESS CONDITION AND MODAL DEPLECTIONS OF ALL
1874 C STRUCTURAL ELEMENTS AFTER APPLICATION OF LOAD INCREMENT.
1875 DO 112 I=1,NELE
1876 DTOT(I)=DTOT(I)+D2(I,1)
1877 CONTINUE
1878 DO 115 J=1,J
1879 DO 120 I=1,NELE
1880 TSCOR(I,J)=TSCOR(I,J)+SIGCOR(I,J)
1881 TPCOR(I,J)=TPCOR(I,J)+PCOR(I,J)
1882 CONTINUE
1883 DO 120 I=1,NELE
1884 IF (EMBR(I).EQ.0) GO TO 120
1885 TORS(I,J)=TORS(I,J)+SIGS(I,J)
1886 TERS(I,J)=TERS(I,J)+ERS(I,J)
1887 CONTINUE
1888 DO 125 I=1,NELE
1889 TSCRO(I)=TSCRO(I)+SIGRO(I)
1890 TPCRO(I)=TPCRO(I)+PCRO(I)
1891 CONTINUE
1892 C PRINTOUT OF ALL RELEVANT DATA
1893 CALL OUTPOT(MCI)
1894 C FAILURE CHECK FOR BEAR
1895 CALL FAIL
1896 IF (ICOUNT.EQ.1) GO TO 20
1897 C SUBSTITUTION OF TOTAL STIFFNESS MATRIX IF NON-LINEAR ITERATIVE
1898 C PROCESS WAS USED IN LAST LOAD INCREMENT. CHANGE IS NECESSARY SINCE
1899 C THE ITERATIONAL PROCESS IS TO BE RESUMED.
1900 DO 150 J=1,J
1901 DO 150 I=1,NELE
1902 AT(I,J)=0
1903 CONTINUE
1904 DO 155 J=1,J
1905 DO 155 I=1,NELE
1906 B1(I,J)=0
1907 CONTINUE
1908 CALL KNTA(NE1,NE2,NS3,TS,AL,AR)
1909 C CALCULATION OF DISPLACEMENT VECTOR OF FOLLOWING HALF
1910 C INCREMENT USING RECONSTITUTED TOTAL STIFFNESS MATRIX
1911 CALL LOADHAIRC
1912 DO 160 I=1,NELE
1913 B2(I,1)=0
1914 CONTINUE
1915 CALL SOLVER(NE1,NE2,NS3,NS4,TS,AL,AR,B1,B2)
1916 GO TO 20

```

```

1900
1901
1902
1903
1904
1905
1906
1907
1908
1909
1910
1911
1912
1913
1914
1915
1916
1917
1918
1919
1920
1921
1922
1923
1924
1925
1926
1927
1928
1929
1930
1931
1932
1933
1934
1935
1936
1937
1938
1939
1940
1941
1942
1943
1944
1945
1946

C      FORMAT STATEMENTS
200  WRITE (6,205)
205  FORMAT('/// ** ERROR IN FIRST SYSTEM SUBROUTINE SETDSE IN MAIN PRO
      'GRAHEZ **')
      STOP
210  WRITE (6,215)
215  FORMAT('/// ** ERROR IN SECOND SYSTEM SUBROUTINE SETDSE IN MAIN PR
      'OGRAMHE **')
      STOP
220  WRITE (6,225)
225  FORMAT('/// ** ** ** ** ** ** ** ** ** * * * * *')
230  FORMAT('/// ** ** ** * * * * *')
240  FORMAT('/// ** ** ** * * * * *')
250  FORMAT('/// ** ** ** * * * * *')
260  FORMAT('/// ** ** ** * * * * *')
270  FORMAT('/// ** ** ** * * * * *')
280  FORMAT('/// ** ** ** * * * * *')
290  FORMAT('/// ** ** ** * * * * *')
300  FORMAT('/// ** ** ** * * * * *')
310  FORMAT('/// ** ** ** * * * * *')
320  FORMAT('/// ** ** ** * * * * *')
330  FORMAT('/// ** ** ** * * * * *')
340  FORMAT('/// ** ** ** * * * * *')
350  FORMAT('/// ** ** ** * * * * *')
360  FORMAT('/// ** ** ** * * * * *')
370  FORMAT('/// ** ** ** * * * * *')
380  WRITE (6,385) IC
385  FORMAT('/// ** ** ** * * * * *')
      STOP
      END

```



APPENDIX D  
SUBROUTINES LISTING

```

1 SUBROUTINE WARP(TS, NS1, NS2)
2 .....
3 THIS SUBROUTINE CALCULATES AND ADDS INTO THE TOTAL STIFFNESS
4 MATRIX, THE WARPING RESTRAINT OF THE DIAPHRAGMS.
5 .....
6 C
7 COMMON/BLOCK2/WEL, WELT, WELCHK, WELD, INDCEL(105), WELSLZ(105),
8 IINDOEL(105), WIDRHC(105), CANGLE(105), CALTER(105),
9 ZWELT(215), ELNEN(215), NODERL(215, 4), NDRFP(215),
10 CONOR/BLOCKS/WODER, ICHODR(220), I(220), Y(220), Z(220)
11 CONOR/BLOCKS/COMOD, COMOD, FERMOD, SLPDOD, SLSHOD, FC, FT,
12 IPAG, PFR, PFR, PFRS, DP, NSLP, KCOLT, FULT, SPOLT, RESULT, P1, P2, P3, P4,
13 ZPO, EREQ, EXPE, CONDEV, OYCON, DEVZEO, FREDV, SLPDEV, IDEV, AVCSF, RELAX
14 DIMENSION TS(NS1, NS2), ID(4), ID(4)
15 CALCULATION OF DIAGONAL LENGTH. A TRAPEZOIDAL ELEMENT WILL BE
16 TREATED AS A RECTANGLE OF THE SAME AREA.
17 DO 5 I=1, 4
18 ID(I)=2*(NODERL(WEL, I))
19 ID(3)=1*(NODERL(WEL, I))
20 CONTINUE
21 IAV=(ID(2)+ID(3)-ID(1)-ID(4))*0.5
22 YAV=(ID(3)+ID(4)-ID(1)-ID(2))*0.5
23 DIAG=SQRT(IAV**2+YAV**2)
24 CALCULATION OF WARPING AND ADDITION INTO TOTAL STIFFNESS MATRIX
25 ELTW(WEL) IS THE EQUIVALENT CLASSICAL DIAPHRAGM THICKNESS
26 STIP=COMOD*ELTW(WEL)**3/(3.0*(1.0*PO)*DIAG**2)
27 DO 10 I=1, 4
28 II=NODERL(WEL, I)
29 IF(ICHODR(II), EQ, 3) GO TO 10
30 DO 10 J=1, 4
31 JJ=NODERL(WEL, J)
32 CALL LOCATE(II, JJ, FROW, FCOL)
33 IF(FROW.LT.FCOL) GO TO 10
34 FROW=FCOL+1
35 NNAZ=J
36 STIP=STIP*(-1)**NNAZ
37 IZ=FCOL*TS(NS1, NS2)
38 IZ=FCOL*TS(NS1, NS2)
39 CONTINUE
40 RETURN
41 END
42 .....
43 SUBROUTINE DIAPHR(TS, NS1, NS2)
44 .....
45 THIS SUBROUTINE CALCULATES AND ADDS INTO THE TOTAL STIFFNESS
46 MATRIX, THE STIFFNESS OF BOTH ACTUAL AND PSEUDO DIAPHRAGMS
47 .....
48 C
49 COMMON/BLOCK2/WEL, WELT, WELCHK, WELD, INDCEL(105), WELSLZ(105),
50 IINDOEL(105), WIDRHC(105), CANGLE(105), CALTER(105),
51 ZWELT(215), ELNEN(215), NODERL(215, 4), NDRFP(215),
52 DIMENSION B2(2, 2), DP(6, 6), TS(NS1, NS2)
53 CALL ISOBLS(00)
54 PARTITIONING OF ELEMENT STIFFNESS INTO (2, 2) BLOCKS
55 DO 15 I=1, 4
56 II=NODERL(WEL, I)
57 DO 15 J=1, 4
58 JJ=NODERL(WEL, J)
59 IF(ICHODR(II), EQ, 3) GO TO 15
60 IF(ICHODR(JJ), EQ, 3) GO TO 15
61 IF(IINDOEL(II), EQ, 0) GO TO 15
62 IF(IINDOEL(JJ), EQ, 0) GO TO 15
63 IF(IINDOEL(II), EQ, 0) AND (IINDOEL(JJ), EQ, 0) GO TO 15
64 IF(IINDOEL(II), EQ, 0) AND (IINDOEL(JJ), EQ, 0) RETURN
65 AT LEAST ONE BLOCK MODE IS AN INCLINED ELEMENT MODE
66 DO 5 J=1, 2
67 B3(I, J)=0.0
68 CONTINUE
69 IF(WELNO(2), EQ, 0) GO TO 20
70 BL=WELNO(2)
71 CALL TSWAT(LT, BL)
72 DO 10 J=1, 2
73 DO 10 I=1, 2
74 B2(I, J)=B2(I, J)+STIP
75 B2(I, J)=B2(I, J)+STIP
76 B2(I, J)=B2(I, J)+STIP
77 B2(I, J)=B2(I, J)+STIP
78 B2(I, J)=B2(I, J)+STIP
79 B2(I, J)=B2(I, J)+STIP
80 B2(I, J)=B2(I, J)+STIP
81 B2(I, J)=B2(I, J)+STIP
82 B2(I, J)=B2(I, J)+STIP
83 B2(I, J)=B2(I, J)+STIP
84 B2(I, J)=B2(I, J)+STIP
85 B2(I, J)=B2(I, J)+STIP
86 B2(I, J)=B2(I, J)+STIP
87 B2(I, J)=B2(I, J)+STIP
88 B2(I, J)=B2(I, J)+STIP
89 B2(I, J)=B2(I, J)+STIP
90 B2(I, J)=B2(I, J)+STIP
91 B2(I, J)=B2(I, J)+STIP
92 B2(I, J)=B2(I, J)+STIP
93 B2(I, J)=B2(I, J)+STIP
94 B2(I, J)=B2(I, J)+STIP
95 B2(I, J)=B2(I, J)+STIP
96 B2(I, J)=B2(I, J)+STIP
97 B2(I, J)=B2(I, J)+STIP
98 B2(I, J)=B2(I, J)+STIP
99 B2(I, J)=B2(I, J)+STIP
100 B2(I, J)=B2(I, J)+STIP
101 B2(I, J)=B2(I, J)+STIP
102 B2(I, J)=B2(I, J)+STIP
103 B2(I, J)=B2(I, J)+STIP
104 B2(I, J)=B2(I, J)+STIP
105 B2(I, J)=B2(I, J)+STIP
106 B2(I, J)=B2(I, J)+STIP
107 B2(I, J)=B2(I, J)+STIP
108 B2(I, J)=B2(I, J)+STIP
109 B2(I, J)=B2(I, J)+STIP
110 B2(I, J)=B2(I, J)+STIP
111 B2(I, J)=B2(I, J)+STIP
112 B2(I, J)=B2(I, J)+STIP
113 B2(I, J)=B2(I, J)+STIP
114 B2(I, J)=B2(I, J)+STIP
115 B2(I, J)=B2(I, J)+STIP

```

```

56 JJ=NODERL(WEL, J)
57 DO 10 K=1, 2
58 DO 10 L=1, 2
59 LL=(L-1)*4+1
60 KK=(K-1)*4+1
61 K2(L, K)=DP(LL, KK)*DFERMOD(WEL)*ELTWR(WEL)
62 CONTINUE
63 CALL DPHADD(II, JJ, B2, TS, NS1, NS2)
64 RETURN
65 END
66 .....
67 SUBROUTINE DPHADD(II, JJ, B2, TS, NS1, NS2)
68 .....
69 THIS SUBROUTINE ADDS BLOCK B2(2,2) INTO TOTAL STIFFNESS MATRIX
70 .....
71 C
72 DIMENSION B2(2, 2), TS(NS1, NS2), BB(2), WC(2)
73 CALL LOCATE(II, JJ, FROW, FCOL)
74 LOCAL X AXIS CORRESPONDS TO GLOBAL X AXIS, AND LOCAL Y AXIS
75 CORRESPONDS TO GLOBAL Y AXIS.
76 DO 5 I=1, 2
77 BB(I)=FROW+3-I
78 FC(I)=FCOL+3-I
79 CONTINUE
80 BLOCK(2, 2) IS TRANSPORTED IF EITHER MODE IS COMMON TO AN
81 INCLINED ELEMENT.
82 CALL TSPORH(II, JJ, B2)
83 DO 10 J=1, 2
84 L=FC(J)
85 DO 10 I=1, 2
86 K=NR(I)
87 IP(K, LT, L) GO TO 10
88 KKP=L+1
89 TS(KK, LL)=TS(KK, L)+B2(I, J)
90 CONTINUE
91 RETURN
92 END
93 .....
94 SUBROUTINE TSPORH(II, JJ, B2)
95 .....
96 THIS SUBROUTINE TRANSPORTS THE DIAPHRAGM STIFFNESS BLOCK B2(2, 2)
97 IF EITHER BLOCK MODE IS ALSO AN INCLINED ELEMENT MODE.
98 .....
99 C
100 DIMENSION LT(2, 2), B3(2, 2), WELNO(2), B2(2, 2)
101 IZTPERR=4
102 REAL*4 LT
103 MODE(1)=II
104 MODE(2)=JJ
105 CALL WELLOC(MODE, WELNO)
106 IF(WELNO(1), EQ, 0) AND (WELNO(2), EQ, 0) RETURN
107 AT LEAST ONE BLOCK MODE IS AN INCLINED ELEMENT MODE
108 DO 5 J=1, 2
109 DO 5 I=1, 2
110 B3(I, J)=0.0
111 CONTINUE
112 IF(WELNO(2), EQ, 0) GO TO 20
113 BL=WELNO(2)
114 CALL TSWAT(LT, BL)
115 DO 10 J=1, 2
116 DO 10 I=1, 2

```

```

171 C..... NUMBERING IS IN THE LOCAL I-Y ORDER.
172 C.....
173 C.....
174 C.....
175 C.....
176 C.....
177 C.....
178 C.....
179 C.....
180 C.....
181 C.....
182 C.....
183 C.....
184 C.....
185 C.....
186 C.....
187 C.....
188 C.....
189 C.....
190 C.....
191 C.....
192 C.....
193 C.....
194 C.....
195 C.....
196 C.....
197 C.....
198 C.....
199 C.....
200 C.....
201 C.....
202 C.....
203 C.....
204 C.....
205 C.....
206 C.....
207 C.....
208 C.....
209 C.....
210 C.....
211 C.....
212 C.....
213 C.....
214 C.....
215 C.....
216 C.....
217 C.....
218 C.....
219 C.....
220 C.....
221 C.....
222 C.....
223 C.....
224 C.....
225 C.....
226 C.....
227 C.....
228 C.....
229 C.....
230 C.....

```

```

171 C.....
172 C.....
173 C.....
174 C.....
175 C.....
176 C.....
177 C.....
178 C.....
179 C.....
180 C.....
181 C.....
182 C.....
183 C.....
184 C.....
185 C.....
186 C.....
187 C.....
188 C.....
189 C.....
190 C.....
191 C.....
192 C.....
193 C.....
194 C.....
195 C.....
196 C.....
197 C.....
198 C.....
199 C.....
200 C.....
201 C.....
202 C.....
203 C.....
204 C.....
205 C.....
206 C.....
207 C.....
208 C.....
209 C.....
210 C.....
211 C.....
212 C.....
213 C.....
214 C.....
215 C.....
216 C.....
217 C.....
218 C.....
219 C.....
220 C.....
221 C.....
222 C.....
223 C.....
224 C.....
225 C.....
226 C.....
227 C.....
228 C.....
229 C.....
230 C.....

```

```

171 C.....
172 C.....
173 C.....
174 C.....
175 C.....
176 C.....
177 C.....
178 C.....
179 C.....
180 C.....
181 C.....
182 C.....
183 C.....
184 C.....
185 C.....
186 C.....
187 C.....
188 C.....
189 C.....
190 C.....
191 C.....
192 C.....
193 C.....
194 C.....
195 C.....
196 C.....
197 C.....
198 C.....
199 C.....
200 C.....
201 C.....
202 C.....
203 C.....
204 C.....
205 C.....
206 C.....
207 C.....
208 C.....
209 C.....
210 C.....
211 C.....
212 C.....
213 C.....
214 C.....
215 C.....
216 C.....
217 C.....
218 C.....
219 C.....
220 C.....
221 C.....
222 C.....
223 C.....
224 C.....
225 C.....
226 C.....
227 C.....
228 C.....
229 C.....
230 C.....

```

```

231 JOBIV(2,1)=JOB(2,1)/DETJ
232 JOBIV(1,2)=JOB(1,2)/DETJ
233 JOBIV(2,2)=JOB(1,1)/DETJ
234 DEFINITION OF MATRIX B(3,3)
235 AT(1)=JOBIV(1,1)*(ETA-1.0)+JOBIV(1,2)*(XI-1.0)*.25
236 AT(2)=JOBIV(1,1)*(1.0-ETA)+JOBIV(1,2)*(XI-1.0)*.25
237 AT(3)=JOBIV(1,1)*(1.0-ETA)+JOBIV(1,2)*(XI-1.0)*.25
238 AT(4)=JOBIV(2,1)*(ETA-1.0)+JOBIV(2,2)*(XI-1.0)*.25
239 AT(5)=JOBIV(2,1)*(1.0-ETA)+JOBIV(2,2)*(XI-1.0)*.25
240 AT(6)=JOBIV(2,1)*(1.0-ETA)+JOBIV(2,2)*(1.0-ETA)*.25
241 AT(7)=JOBIV(2,1)*(1.0-ETA)+JOBIV(2,2)*(1.0-ETA)*.25
242 AT(8)=JOBIV(2,1)*(1.0-ETA)+JOBIV(2,2)*(1.0-ETA)*.25
243 AT(9)=JOBIV(2,1)*(1.0-ETA)+JOBIV(2,2)*(1.0-ETA)*.25
244 J=4*XI
245 B(1,1)=AX(I)
246 B(1,2)=0.0
247 B(2,1)=0.0
248 B(2,2)=AX(I)
249 B(3,1)=AX(I)
250 B(3,2)=AX(I)
251 CONTINUE
252 C
253 DEFINITION OF UNIT CONSTITUTIVE MATRIX. THE INDIVIDUAL STIFFNESS TERMS
254 WILL BE MULTIPLIED BY THE ACTUAL SHEAR MODULUS IN ROUTINE DPRSTP.
255 DO 20 J=1,3
256 DO 20 I=1,3
257 C(I,J)=0.0
258 CONTINUE
259 IF (XNELTY(NEL),NE.3) GO TO 23
260 THE FULL CONSTITUTIVE MATRIX IS USED FOR ACTUAL DIAPHRAGMS
261 (XNELTY(NEL)=3). WHEREAS ONLY THE UNIT SHEAR TERM IS INCLUDED
262 FOR PSEUDO DIAPHRAGMS.
263 C(1,1)=2.5
264 C(2,1)=5
265 C(2,2)=5
266 C(3,3)=1.0
267 C(3,1)=1.0
268 DO 25 J=1,3
269 DO 25 I=1,3
270 A(I,J)=0.0
271 CONTINUE
272 DO 35 I=1,3
273 DO 35 J=1,3
274 DO 35 K=1,3
275 A(I,J)=A(I,J)+C(I,K)*B(K,J)
276 CONTINUE
277 DO 45 I=1,8
278 DO 45 J=1,8
279 DO 45 K=1,3
280 DP(I,J)=DP(I,J)+B(K,I)*A(K,J)+B(K,J)*DP(I,J)+B(K,I)*A(K,J)
281 CONTINUE
282 CONTINUE
283 IF (ISITP.EQ.0) RETURN
284 WRITE (6,100) NEL
285 FOREAT (//, STIFFNESS MATRIX FOR DIAPHRAGM ELEMENT NO.,13, ' ')
286 DO 120 I=1,8
287 WRITE (6,110) (DP(I,J),J=1,8)
288 FOREAT (//,5)
289 CONTINUE
290 RETURN
291
292 SUBROUTINE SRRHOD(NC)
293 C
294 THIS SUBROUTINE CALCULATES THE AGGREGATE INTERLOCK (LBS/SQ. INCH)
295 DEVELOPED ALONG A CRACK OF WIDTH WC
296 C
297 C
298 C
299 C
300 C
301 C
302 C
303 C
304 C
305 C
306 C
307 C
308 C
309 C
310 C
311 C
312 C
313 C
314 C
315 C
316 C
317 C
318 C
319 C
320 C
321 C
322 C
323 C
324 C
325 C
326 C
327 C
328 C
329 C
330 C
331 C
332 C
333 C
334 C
335 C
336 C
337 C
338 C
339 C
340 C
341 C
342 C
343 C
344 C
345 C
346 C
347 C
348 C
349 C
350 C
351 C
352 C
353 C
354 C
355 C
356 C
357 C
358 C
359 C
360 C
361 C
362 C
363 C
364 C
365 C
366 C
367 C
368 C
369 C
370 C
371 C
372 C
373 C
374 C
375 C
376 C
377 C
378 C
379 C
380 C
381 C
382 C
383 C
384 C
385 C
386 C
387 C
388 C
389 C
390 C
391 C
392 C
393 C
394 C
395 C
396 C
397 C
398 C
399 C
400 C
401 C
402 C
403 C
404 C
405 C
406 C
407 C
408 C
409 C
410 C
411 C
412 C
413 C
414 C
415 C
416 C
417 C
418 C
419 C
420 C
421 C
422 C
423 C
424 C
425 C
426 C
427 C
428 C
429 C
430 C
431 C
432 C
433 C
434 C
435 C
436 C
437 C
438 C
439 C
440 C
441 C
442 C
443 C
444 C
445 C
446 C
447 C
448 C
449 C
450 C
451 C
452 C
453 C
454 C
455 C
456 C
457 C
458 C
459 C
460 C
461 C
462 C
463 C
464 C
465 C
466 C
467 C
468 C
469 C
470 C
471 C
472 C
473 C
474 C
475 C
476 C
477 C
478 C
479 C
480 C
481 C
482 C
483 C
484 C
485 C
486 C
487 C
488 C
489 C
490 C
491 C
492 C
493 C
494 C
495 C
496 C
497 C
498 C
499 C
500 C
501 C
502 C
503 C
504 C
505 C
506 C
507 C
508 C
509 C
510 C
511 C
512 C
513 C
514 C
515 C
516 C
517 C
518 C
519 C
520 C
521 C
522 C
523 C
524 C
525 C
526 C
527 C
528 C
529 C
530 C
531 C
532 C
533 C
534 C
535 C
536 C
537 C
538 C
539 C
540 C
541 C
542 C
543 C
544 C
545 C
546 C
547 C
548 C
549 C
550 C
551 C
552 C
553 C
554 C
555 C
556 C
557 C
558 C
559 C
560 C
561 C
562 C
563 C
564 C
565 C
566 C
567 C
568 C
569 C
570 C
571 C
572 C
573 C
574 C
575 C
576 C
577 C
578 C
579 C
580 C
581 C
582 C
583 C
584 C
585 C
586 C
587 C
588 C
589 C
590 C
591 C
592 C
593 C
594 C
595 C
596 C
597 C
598 C
599 C
600 C
601 C
602 C
603 C
604 C
605 C
606 C
607 C
608 C
609 C
610 C
611 C
612 C
613 C
614 C
615 C
616 C
617 C
618 C
619 C
620 C
621 C
622 C
623 C
624 C
625 C
626 C
627 C
628 C
629 C
630 C
631 C
632 C
633 C
634 C
635 C
636 C
637 C
638 C
639 C
640 C
641 C
642 C
643 C
644 C
645 C
646 C
647 C
648 C
649 C
650 C
651 C
652 C
653 C
654 C
655 C
656 C
657 C
658 C
659 C
660 C
661 C
662 C
663 C
664 C
665 C
666 C
667 C
668 C
669 C
670 C
671 C
672 C
673 C
674 C
675 C
676 C
677 C
678 C
679 C
680 C
681 C
682 C
683 C
684 C
685 C
686 C
687 C
688 C
689 C
690 C
691 C
692 C
693 C
694 C
695 C
696 C
697 C
698 C
699 C
700 C
701 C
702 C
703 C
704 C
705 C
706 C
707 C
708 C
709 C
710 C
711 C
712 C
713 C
714 C
715 C
716 C
717 C
718 C
719 C
720 C
721 C
722 C
723 C
724 C
725 C
726 C
727 C
728 C
729 C
730 C
731 C
732 C
733 C
734 C
735 C
736 C
737 C
738 C
739 C
740 C
741 C
742 C
743 C
744 C
745 C
746 C
747 C
748 C
749 C
750 C
751 C
752 C
753 C
754 C
755 C
756 C
757 C
758 C
759 C
760 C
761 C
762 C
763 C
764 C
765 C
766 C
767 C
768 C
769 C
770 C
771 C
772 C
773 C
774 C
775 C
776 C
777 C
778 C
779 C
780 C
781 C
782 C
783 C
784 C
785 C
786 C
787 C
788 C
789 C
790 C
791 C
792 C
793 C
794 C
795 C
796 C
797 C
798 C
799 C
800 C
801 C
802 C
803 C
804 C
805 C
806 C
807 C
808 C
809 C
810 C
811 C
812 C
813 C
814 C
815 C
816 C
817 C
818 C
819 C
820 C
821 C
822 C
823 C
824 C
825 C
826 C
827 C
828 C
829 C
830 C
831 C
832 C
833 C
834 C
835 C
836 C
837 C
838 C
839 C
840 C
841 C
842 C
843 C
844 C
845 C
846 C
847 C
848 C
849 C
850 C
851 C
852 C
853 C
854 C
855 C
856 C
857 C
858 C
859 C
860 C
861 C
862 C
863 C
864 C
865 C
866 C
867 C
868 C
869 C
870 C
871 C
872 C
873 C
874 C
875 C
876 C
877 C
878 C
879 C
880 C
881 C
882 C
883 C
884 C
885 C
886 C
887 C
888 C
889 C
890 C
891 C
892 C
893 C
894 C
895 C
896 C
897 C
898 C
899 C
900 C
901 C
902 C
903 C
904 C
905 C
906 C
907 C
908 C
909 C
910 C
911 C
912 C
913 C
914 C
915 C
916 C
917 C
918 C
919 C
920 C
921 C
922 C
923 C
924 C
925 C
926 C
927 C
928 C
929 C
930 C
931 C
932 C
933 C
934 C
935 C
936 C
937 C
938 C
939 C
940 C
941 C
942 C
943 C
944 C
945 C
946 C
947 C
948 C
949 C
950 C
951 C
952 C
953 C
954 C
955 C
956 C
957 C
958 C
959 C
960 C
961 C
962 C
963 C
964 C
965 C
966 C
967 C
968 C
969 C
970 C
971 C
972 C
973 C
974 C
975 C
976 C
977 C
978 C
979 C
980 C
981 C
982 C
983 C
984 C
985 C
986 C
987 C
988 C
989 C
990 C
991 C
992 C
993 C
994 C
995 C
996 C
997 C
998 C
999 C
1000 C

```

```

351 C*****
352 C
353 COMMON/BLCK1/BEOS, BRAD, HBLK, BUNINC, ICOUNT
354 COMMON/BLCK2/HEL, HELT, BELCKE, BELD, TBCRL(195), IERLSZ(185),
355 IERDNL(185), IERFNC(185), CANGLE(185), CALTER(185),
356 ZIRHTL(215), ALTRH(215), HODREL(215, 4), HDBRP(215),
357 COMMON/BLCK3/COBMOD, SROBOD, PREBOD, SLFMOD, SHS MOD, FC, P2,
358 IYAGG, PFR, PFRS, DP, SLIP, ECULT, EBULT, EBULT, EBULT, P1, P2, P3, P4,
359 ZBR, HERRG, HERRG, CONDEV, DEVCON, DEVVRO, PFRDVI, IDRV, AVCSF, RELAI
360 COMMON/BLCK12/SIGCON(185, 3), ECOM(185, 3), SIGS(185, 4), ERS(185, 4),
361 TSCON(185, 3), TSCX(185, 3), TSCCC(185, 3), TSCGT(185, 3), TSCAGG(185, 3),
362 TSCRO(185, 3), TSCRO(185, 3), TSCRO(185, 3), TSCRO(185, 3),
363 TSCRO(185, 3), TSCRO(185, 3), TSCRO(185, 3), TSCRO(185, 3),
364 COMMON/BLCK13/STRESS(185, 4), HDOVEL(185), HCRACK(185), HYAGG(185),
365 ISTRERR=4, CALTER
366 ISTRERR=4, CALTER
367 ISTRERR=4, CALTER
368 ISTRERR=4, CALTER
369 ISTRERR=4, CALTER
370 ISTRERR=4, CALTER
371 ISTRERR=4, CALTER
372 ISTRERR=4, CALTER
373 ISTRERR=4, CALTER
374 ISTRERR=4, CALTER
375 ISTRERR=4, CALTER
376 ISTRERR=4, CALTER
377 ISTRERR=4, CALTER
378 ISTRERR=4, CALTER
379 ISTRERR=4, CALTER
380 ISTRERR=4, CALTER
381 ISTRERR=4, CALTER
382 ISTRERR=4, CALTER
383 ISTRERR=4, CALTER
384 ISTRERR=4, CALTER
385 ISTRERR=4, CALTER
386 ISTRERR=4, CALTER
387 ISTRERR=4, CALTER
388 ISTRERR=4, CALTER
389 ISTRERR=4, CALTER
390 ISTRERR=4, CALTER
391 ISTRERR=4, CALTER
392 ISTRERR=4, CALTER
393 ISTRERR=4, CALTER
394 ISTRERR=4, CALTER
395 ISTRERR=4, CALTER
396 ISTRERR=4, CALTER
397 ISTRERR=4, CALTER
398 ISTRERR=4, CALTER
399 ISTRERR=4, CALTER
400 ISTRERR=4, CALTER
401 ISTRERR=4, CALTER
402 ISTRERR=4, CALTER
403 ISTRERR=4, CALTER
404 ISTRERR=4, CALTER
405 ISTRERR=4, CALTER
406 ISTRERR=4, CALTER
407 ISTRERR=4, CALTER
408 ISTRERR=4, CALTER
409 ISTRERR=4, CALTER
410 ISTRERR=4, CALTER

```

```

411 COMMON/BLCK12/SIGCON(185, 3), ECOM(185, 3), SIGS(185, 4), ERS(185, 4),
412 TSCON(185, 3), TSCX(185, 3), TSCCC(185, 3), TSCGT(185, 3), TSCAGG(185, 3),
413 TSCRO(185, 3), TSCRO(185, 3), TSCRO(185, 3), TSCRO(185, 3),
414 TSCRO(185, 3), TSCRO(185, 3), TSCRO(185, 3), TSCRO(185, 3),
415 TSCRO(185, 3), TSCRO(185, 3), TSCRO(185, 3), TSCRO(185, 3),
416 TSCRO(185, 3), TSCRO(185, 3), TSCRO(185, 3), TSCRO(185, 3),
417 TSCRO(185, 3), TSCRO(185, 3), TSCRO(185, 3), TSCRO(185, 3),
418 TSCRO(185, 3), TSCRO(185, 3), TSCRO(185, 3), TSCRO(185, 3),
419 TSCRO(185, 3), TSCRO(185, 3), TSCRO(185, 3), TSCRO(185, 3),
420 TSCRO(185, 3), TSCRO(185, 3), TSCRO(185, 3), TSCRO(185, 3),
421 TSCRO(185, 3), TSCRO(185, 3), TSCRO(185, 3), TSCRO(185, 3),
422 TSCRO(185, 3), TSCRO(185, 3), TSCRO(185, 3), TSCRO(185, 3),
423 TSCRO(185, 3), TSCRO(185, 3), TSCRO(185, 3), TSCRO(185, 3),
424 TSCRO(185, 3), TSCRO(185, 3), TSCRO(185, 3), TSCRO(185, 3),
425 TSCRO(185, 3), TSCRO(185, 3), TSCRO(185, 3), TSCRO(185, 3),
426 TSCRO(185, 3), TSCRO(185, 3), TSCRO(185, 3), TSCRO(185, 3),
427 TSCRO(185, 3), TSCRO(185, 3), TSCRO(185, 3), TSCRO(185, 3),
428 TSCRO(185, 3), TSCRO(185, 3), TSCRO(185, 3), TSCRO(185, 3),
429 TSCRO(185, 3), TSCRO(185, 3), TSCRO(185, 3), TSCRO(185, 3),
430 TSCRO(185, 3), TSCRO(185, 3), TSCRO(185, 3), TSCRO(185, 3),
431 TSCRO(185, 3), TSCRO(185, 3), TSCRO(185, 3), TSCRO(185, 3),
432 TSCRO(185, 3), TSCRO(185, 3), TSCRO(185, 3), TSCRO(185, 3),
433 TSCRO(185, 3), TSCRO(185, 3), TSCRO(185, 3), TSCRO(185, 3),
434 TSCRO(185, 3), TSCRO(185, 3), TSCRO(185, 3), TSCRO(185, 3),
435 TSCRO(185, 3), TSCRO(185, 3), TSCRO(185, 3), TSCRO(185, 3),
436 TSCRO(185, 3), TSCRO(185, 3), TSCRO(185, 3), TSCRO(185, 3),
437 TSCRO(185, 3), TSCRO(185, 3), TSCRO(185, 3), TSCRO(185, 3),
438 TSCRO(185, 3), TSCRO(185, 3), TSCRO(185, 3), TSCRO(185, 3),
439 TSCRO(185, 3), TSCRO(185, 3), TSCRO(185, 3), TSCRO(185, 3),
440 TSCRO(185, 3), TSCRO(185, 3), TSCRO(185, 3), TSCRO(185, 3),
441 TSCRO(185, 3), TSCRO(185, 3), TSCRO(185, 3), TSCRO(185, 3),
442 TSCRO(185, 3), TSCRO(185, 3), TSCRO(185, 3), TSCRO(185, 3),
443 TSCRO(185, 3), TSCRO(185, 3), TSCRO(185, 3), TSCRO(185, 3),
444 TSCRO(185, 3), TSCRO(185, 3), TSCRO(185, 3), TSCRO(185, 3),
445 TSCRO(185, 3), TSCRO(185, 3), TSCRO(185, 3), TSCRO(185, 3),
446 TSCRO(185, 3), TSCRO(185, 3), TSCRO(185, 3), TSCRO(185, 3),
447 TSCRO(185, 3), TSCRO(185, 3), TSCRO(185, 3), TSCRO(185, 3),
448 TSCRO(185, 3), TSCRO(185, 3), TSCRO(185, 3), TSCRO(185, 3),
449 TSCRO(185, 3), TSCRO(185, 3), TSCRO(185, 3), TSCRO(185, 3),
450 TSCRO(185, 3), TSCRO(185, 3), TSCRO(185, 3), TSCRO(185, 3),
451 TSCRO(185, 3), TSCRO(185, 3), TSCRO(185, 3), TSCRO(185, 3),
452 TSCRO(185, 3), TSCRO(185, 3), TSCRO(185, 3), TSCRO(185, 3),
453 TSCRO(185, 3), TSCRO(185, 3), TSCRO(185, 3), TSCRO(185, 3),
454 TSCRO(185, 3), TSCRO(185, 3), TSCRO(185, 3), TSCRO(185, 3),
455 TSCRO(185, 3), TSCRO(185, 3), TSCRO(185, 3), TSCRO(185, 3),
456 TSCRO(185, 3), TSCRO(185, 3), TSCRO(185, 3), TSCRO(185, 3),
457 TSCRO(185, 3), TSCRO(185, 3), TSCRO(185, 3), TSCRO(185, 3),
458 TSCRO(185, 3), TSCRO(185, 3), TSCRO(185, 3), TSCRO(185, 3),
459 TSCRO(185, 3), TSCRO(185, 3), TSCRO(185, 3), TSCRO(185, 3),
460 TSCRO(185, 3), TSCRO(185, 3), TSCRO(185, 3), TSCRO(185, 3),
461 TSCRO(185, 3), TSCRO(185, 3), TSCRO(185, 3), TSCRO(185, 3),
462 TSCRO(185, 3), TSCRO(185, 3), TSCRO(185, 3), TSCRO(185, 3),
463 TSCRO(185, 3), TSCRO(185, 3), TSCRO(185, 3), TSCRO(185, 3),
464 TSCRO(185, 3), TSCRO(185, 3), TSCRO(185, 3), TSCRO(185, 3),
465 TSCRO(185, 3), TSCRO(185, 3), TSCRO(185, 3), TSCRO(185, 3),
466 TSCRO(185, 3), TSCRO(185, 3), TSCRO(185, 3), TSCRO(185, 3),
467 TSCRO(185, 3), TSCRO(185, 3), TSCRO(185, 3), TSCRO(185, 3),
468 TSCRO(185, 3), TSCRO(185, 3), TSCRO(185, 3), TSCRO(185, 3),
469 TSCRO(185, 3), TSCRO(185, 3), TSCRO(185, 3), TSCRO(185, 3),
470 TSCRO(185, 3), TSCRO(185, 3), TSCRO(185, 3), TSCRO(185, 3),

```



```

471 IF (IBRST (IBR) - EQ. 0) GO TO 220
472 IS=0.0
473 SIGR0 (IBR) = 0.0
474 IF (IBRST (IBR)) 202, 204, 206
475 TSGR0 (IBR) = PFR
476 GO TO 208
477
478 TSGR0 (IBR) = PFR
479 GO TO 208
480 TSGR0 (IBR) = 0.0
481 IF (STRAIN.LT.0.0) TSGR0 (IBR) = -TSGR0 (IBR)
482 IF (IBRST (IBR)) 210, 220, 230
483 WRITE (6, 215) IBR
484 FORMAT (/, ' *** CONVENTIONAL REINFORCEMENT ELEMENT NUMBER',
485 /, '13, ' HAS FAILED *****')
486 RETURN
487
488 IF (ICOUNT.EQ.0) GO TO 220
489 STRESS=TSGR0 (IBR) * SIGR0 (IBR)
490 STRESS=TSGR0 (IBR)
491 WRITE (6, 226) IBR
492
493
494
495
496
497
498
499
500
501
502
503
504
505
506
507
508
509
510
511
512
513
514
515
516
517
518
519
520
521
522
523
524
525
526
527
528
529
530
531
532
533
534
535
536
537
538
539
540
541
542
543
544
545
546
547
548
549
550
551
552
553
554
555
556
557
558
559
560
561
562
563
564
565
566
567
568
569
570
571
572
573
574
575
576
577
578
579
580
581
582
583
584
585
586
587
588
589
590
591
592
593
594
595
596
597
598
599
600
601
602
603
604
605
606
607
608
609
610
611
612
613
614
615
616
617
618
619
620
621
622
623
624
625
626
627
628
629
630
631
632
633
634
635
636
637
638
639
640
641
642
643
644
645
646
647
648
649
650
651
652
653
654
655
656
657
658
659
660
661
662
663
664
665
666
667
668
669
670
671
672
673
674
675
676
677
678
679
680
681
682
683
684
685
686
687
688
689
690
691
692
693
694
695
696
697
698
699
700
701
702
703
704
705
706
707
708
709
710
711
712
713
714
715
716
717
718
719
720
721
722
723
724
725
726
727
728
729
730
731
732
733
734
735
736
737
738
739
740
741
742
743
744
745
746
747
748
749
750
751
752
753
754
755
756
757
758
759
760
761
762
763
764
765
766
767
768
769
770
771
772
773
774
775
776
777
778
779
780
781
782
783
784
785
786
787
788
789
790
791
792
793
794
795
796
797
798
799
800
801
802
803
804
805
806
807
808
809
810
811
812
813
814
815
816
817
818
819
820
821
822
823
824
825
826
827
828
829
830
831
832
833
834
835
836
837
838
839
840
841
842
843
844
845
846
847
848
849
850
851
852
853
854
855
856
857
858
859
860
861
862
863
864
865
866
867
868
869
870
871
872
873
874
875
876
877
878
879
880
881
882
883
884
885
886
887
888
889
890
891
892
893
894
895
896
897
898
899
900
901
902
903
904
905
906
907
908
909
910
911
912
913
914
915
916
917
918
919
920
921
922
923
924
925
926
927
928
929
930
931
932
933
934
935
936
937
938
939
940
941
942
943
944
945
946
947
948
949
950
951
952
953
954
955
956
957
958
959
960
961
962
963
964
965
966
967
968
969
970
971
972
973
974
975
976
977
978
979
980
981
982
983
984
985
986
987
988
989
990
991
992
993
994
995
996
997
998
999
1000

```

```

C ***** UNCRACKED ELEMENT *****
C
CORRO/BLOCK1/BEOS, BRAND, BELK, BUSHIC, ICOUNT
IF (CORRO/BLOCK2/BEL, BELT, BELCHK, BELD, BDCCL (185), IBELST (185),
1RDOWL (185), WIDTCH (185), CANGLE (185), CALTR (185),
2IBELT (215), ELTH (215), BODWEL (215, 4), HDPFP (215), DPHMOD (215)
CORRO/BLOCK6/CORRO, MODOD, PREMOD, SLPMOD, SBRMOD, PC,
1PAG, PWR, PUP, PHS, OP, SLP, ECULT, REULT, REULT, REULT, P1, P2, P3, P4,
2PQ, REPO, REPR, CONDY, DTVCOR, DEVRPO, PREDR, SLPDZY, IDEV, ATCSP, REZAI
CORRO/BLOCK10/RTT (12, 12), RS (3, 3), B (3, 12, 9), B2 (3, 12, 9), D (3, 3),
1DCOR (185, 3, 3), BCRACK (185), P (86)
CORRO/BLOCK12/SIGCO (185, 3), RECO (185, 3), SIGNS (185, 4), IHS (185, 4),
1TSGCO (185, 3), TSCOH (185, 3), TSGCC (185), TSGCT (185), TSGAGG (185),
2TCC (185), TECT (185), TSGHS (185, 4), TSGCT (185), TSGAGG (185),
3REPO (190), TSGRO (190), TERZO (190)
CORRO/BLOCK13/BIRESR (185, 4), BDOWNEL (185), BCPACK (185), BIAGG (185),
1REPO (190), BICREO (190)
INTEGR4 CALTR
DIMENSION DD (3, 3), TH (3, 3), TT1 (3, 3), OTT1 (3, 3)
REAL*4 DD (3, 3)
DO 3 I=1, 3
DO 3 J=1, 3
DD (J, I) = 0.0
DD (I, J) = 0.0
OTT1 (J, I) = 0.0
CONTINUE
C ***** CALCULATION OF PRINCIPAL STRESSES AND STRAINS *****
CALL PRNCS
CALL PRNCS
IF (T-TEC) (BEL)
PC=TEC (BEL)
ST=TSGCT (BEL)
SC=TSGCC (BEL)
ES=PC/ECULT
ZEPT=ET/ECULT
ZEPG=EC/ECULT
IF (MCRAK (BEL) .NE. 0) GO TO 30
DEFINITION OF POISSON RATIO
IF (ST.GE. 0.0.AND. SC.GE. 0.0) P=P2
IF (ST.LT. 0.0.AND. SC.LT. 0.0) P=P1
IF (ST.GE. 0.0.AND. SC.LT. 0.0) P=P3
IF (ST.LT. 0.0.AND. SC.LT. 0.0) P=P3
A1=SC/ST
A2=ST/SC
IF (ST.GE. 0.0.OR. FT.GE. 0.0) GO TO 10
C ***** INCREMENTAL LOADING *****
IF (ICOUNT.PQ.2) GO TO 12
C ***** COMPRESSIVE STRESS IN PRINCIPAL DIRECTION *****
ZIB=CONROD*(1.0-ZEPT**2)/(1.0*(CONROD/RS*(1.0-PU*A1))-2.0)*
ZEPT*ZEPT**2**2
GO TO 14
C ***** TENSILE STRESS IN PRINCIPAL DIRECTION FOR BOTH INCREMENTAL AND *****
TOTAL LOADS.
ZIB=CONROD
GO TO 18
C ***** TOTAL LOADING *****
C ***** COMPRESSIVE STRESS IN PRINCIPAL DIRECTION *****
ZIB=CONROD/(1.0*(CONROD/(1.0-PU*A1)*RS)-2.0)*ZEPT*ZEPT**2
GO TO 18

```

```

201 IF (IBRST (IBR) - EQ. 0) GO TO 220
202 IS=0.0
203 SIGR0 (IBR) = 0.0
204 IF (IBRST (IBR)) 202, 204, 206
205 TSGR0 (IBR) = PFR
206 GO TO 208
207
208 TSGR0 (IBR) = PFR
209 GO TO 208
210 TSGR0 (IBR) = 0.0
211 IF (STRAIN.LT.0.0) TSGR0 (IBR) = -TSGR0 (IBR)
212 IF (IBRST (IBR)) 210, 220, 230
213 WRITE (6, 215) IBR
214 FORMAT (/, ' *** CONVENTIONAL REINFORCEMENT ELEMENT NUMBER',
215 /, '13, ' HAS FAILED *****')
216 RETURN
217
218 IF (ICOUNT.EQ.0) GO TO 220
219 STRESS=TSGR0 (IBR) * SIGR0 (IBR)
220 STRESS=TSGR0 (IBR)
221 WRITE (6, 226) IBR
222
223
224
225
226
227
228
229
230
231
232
233
234
235
236
237
238
239
240
241
242
243
244
245
246
247
248
249
250
251
252
253
254
255
256
257
258
259
260
261
262
263
264
265
266
267
268
269
270
271
272
273
274
275
276
277
278
279
280
281
282
283
284
285
286
287
288
289
290
291
292
293
294
295
296
297
298
299
300
301
302
303
304
305
306
307
308
309
310
311
312
313
314
315
316
317
318
319
320
321
322
323
324
325
326
327
328
329
330
331
332
333
334
335
336
337
338
339
340
341
342
343
344
345
346
347
348
349
350
351
352
353
354
355
356
357
358
359
360
361
362
363
364
365
366
367
368
369
370
371
372
373
374
375
376
377
378
379
380
381
382
383
384
385
386
387
388
389
390
391
392
393
394
395
396
397
398
399
400
401
402
403
404
405
406
407
408
409
410
411
412
413
414
415
416
417
418
419
420
421
422
423
424
425
426
427
428
429
430
431
432
433
434
435
436
437
438
439
440
441
442
443
444
445
446
447
448
449
450
451
452
453
454
455
456
457
458
459
460
461
462
463
464
465
466
467
468
469
470
471
472
473
474
475
476
477
478
479
480
481
482
483
484
485
486
487
488
489
490
491
492
493
494
495
496
497
498
499
500
501
502
503
504
505
506
507
508
509
510
511
512
513
514
515
516
517
518
519
520
521
522
523
524
525
526
527
528
529
530
531
532
533
534
535
536
537
538
539
540
541
542
543
544
545
546
547
548
549
550
551
552
553
554
555
556
557
558
559
560
561
562
563
564
565
566
567
568
569
570
571
572
573
574
575
576
577
578
579
580
581
582
583
584
585
586
587
588
589
590
591
592
593
594
595
596
597
598
599
600
601
602
603
604
605
606
607
608
609
610
611
612
613
614
615
616
617
618
619
620
621
622
623
624
625
626
627
628
629
630
631
632
633
634
635
636
637
638
639
640
641
642
643
644
645
646
647
648
649
650
651
652
653
654
655
656
657
658
659
660
661
662
663
664
665
666
667
668
669
670
671
672
673
674
675
676
677
678
679
680
681
682
683
684
685
686
687
688
689
690
691
692
693
694
695
696
697
698
699
700
701
702
703
704
705
706
707
708
709
710
711
712
713
714
715
716
717
718
719
720
721
722
723
724
725
726
727
728
729
730
731
732
733
734
735
736
737
738
739
740
741
742
743
744
745
746
747
748
749
750
751
752
753
754
755
756
757
758
759
760
761
762
763
764
765
766
767
768
769
770
771
772
773
774
775
776
777
778
779
780
781
782
783
784
785
786
787
788
789
790
791
792
793
794
795
796
797
798
799
800
801
802
803
804
805
806
807
808
809
810
811
812
813
814
815
816
817
818
819
820
821
822
823
824
825
826
827
828
829
830
831
832
833
834
835
836
837
838
839
840
841
842
843
844
845
846
847
848
849
850
851
852
853
854
855
856
857
858
859
860
861
862
863
864
865
866
867
868
869
870
871
872
873
874
875
876
877
878
879
880
881
882
883
884
885
886
887
888
889
890
891
892
893
894
895
896
897
898
899
900
901
902
903
904
905
906
907
908
909
910
911
912
913
914
915
916
917
918
919
920
921
922
923
924
925
926
927
928
929
930
931
932
933
934
935
936
937
938
939
940
941
942
943
944
945
946
947
948
949
950
951
952
953
954
955
956
957
958
959
960
961
962
963
964
965
966
967
968
969
970
971
972
973
974
975
976
977
978
979
980
981
982
983
984
985
986
987
988
989
990
991
992
993
994
995
996
997
998
999
1000

```

```

591 C
592 14
593
594
595
596
597
598
599
600
601
602
603
604
605
606
607
608
609
610
611
612
613
614
615
616
617
618
619
620
621
622
623
624
625
626
627
628
629
630
631
632
633
634
635
636
637
638
639
640
641
642
643
644
645
646
647
648
649
650
651
652
653
654
655
656
657
658
659
660
661
662
663
664
665
666
667
668
669
670
671
672
673
674
675
676
677
678
679
680
681
682
683
684
685
686
687
688
689
690
691
692
693
694
695
696
697
698
699
700
701
702
703
704
705
706
707
708
709
710
711
712
713
714
715
716
717
718
719
720
721
722
723
724
725
726
727
728
729
730
731
732
733
734
735
736
737
738
739
740
741
742
743
744
745
746
747
748
749
750
751
752
753
754
755
756
757
758
759
760
761
762
763
764
765
766
767
768
769
770
771
772
773
774
775
776
777
778
779
780
781
782
783
784
785
786
787
788
789
790
791
792
793
794
795
796
797
798
799
800
801
802
803
804
805
806
807
808
809
810
811
812
813
814
815
816
817
818
819
820
821
822
823
824
825
826
827
828
829
830
831
832
833
834
835
836
837
838
839
840
841
842
843
844
845
846
847
848
849
850
851
852
853
854
855
856
857
858
859
860
861
862
863
864
865
866
867
868
869
870
871
872
873
874
875
876
877
878
879
880
881
882
883
884
885
886
887
888
889
890
891
892
893
894
895
896
897
898
899
900
901
902
903
904
905
906
907
908
909
910
911
912
913
914
915
916
917
918
919
920
921
922
923
924
925
926
927
928
929
930
931
932
933
934
935
936
937
938
939
940
941
942
943
944
945
946
947
948
949
950
951
952
953
954
955
956
957
958
959
960
961
962
963
964
965
966
967
968
969
970
971
972
973
974
975
976
977
978
979
980
981
982
983
984
985
986
987
988
989
990
991
992
993
994
995
996
997
998
999
1000

```

C SIMILAR STIFFNESS DERIVATIONS FOR ORTHOGONAL DIRECTION.  
 E2B=CONMOD\*(1.0-EFPC\*\*2)/(1.0+(CONMOD/183\*(1.0-PU\*A2))-2.0)\*  
 1EFC\*EFPC\*\*2)\*\*2  
 GO TO 25  
 E2B=CONMOD/(1.0+(CONMOD/(1.0-PU\*A2)\*E3)-2.0)\*EFPC\*EFPC\*\*2)  
 GO TO 25  
 IF (SC.GE.0.0-OR.FC.GE.0.0) GO TO 20  
 IF (ICONT.EQ.2) GO TO 19  
 E2B=CONMOD\*(1.0-EFPC\*\*2)/(1.0+(CONMOD/183\*(1.0-  
 1-PU\*A2))-2.0)\*EFPC\*EFPC\*\*2)\*\*2  
 GO TO 25  
 E2B=CONMOD/(1.0+(CONMOD/(1.0-PU\*A2)\*E3)-2.0)\*EFPC\*EFPC\*\*2)  
 GO TO 25  
 E2B=CONMOD  
 DD(1,1)=DELTA\*E1B/E2B  
 DD(2,1)=DELTA\*E1P/E2B  
 DD(1,2)=DELTA\*E  
 DD(2,2)=DELTA  
 DD(3,3)=E1B\*E2B/(E1B\*E2B+2\*E2B\*E)  
 GO TO 40  
 C FORMATION OF PRINCIPAL CONSTITUTIVE MATRIX FOR A CRACKED ELEMENT  
 IP(NCRACK(NEL),LT,-1,OR,NCRACK(NEL),GT,1) GO TO 37  
 IF (SC.GE.0.0) GO TO 36  
 IF (ICONT.EQ.1) GO TO 34  
 D22=CONMOD/(1.0+(CONMOD/E3-2.0)\*EFPC\*EFPC\*\*2)  
 GO TO 38  
 D22=CONMOD\*(1.0-EFPC\*\*2)/(1.0+(CONMOD/E3-2.0)\*EFPC\*EFPC\*\*2)\*\*2  
 GO TO 38  
 D22=CONMOD/(1.0-PU\*\*2)  
 GO TO 38  
 D22=1000.0  
 NCRACK(NEL)=D22  
 DD(2,2)=D22  
 DD(3,3)=DAGG(NEL)  
 C TRANSFORMATION OF CONSTITUTIVE MATRIX , CHANGING FROM PRINCIPAL  
 STRESS AXES TO LOCAL ELEMENT AXES  
 IF (NRC.GT.99) GO TO 40  
 TERA=CANGLE(NEL)\*3.1415926/180.0  
 C=COS(TERA)  
 S=SIN(TERA)  
 DEFINITION OF TRANSFORMATION MATRICES.  
 TH(1,1)=C\*\*2  
 TH(2,1)=S\*\*2  
 TH(3,1)=2.0\*S\*C  
 TH(1,2)=S\*\*2  
 TH(2,2)=C\*\*2  
 TH(3,2)=-2.0\*S\*C  
 TH(1,3)=S\*C  
 TH(2,3)=-S\*C  
 TH(3,3)=C\*\*2-S\*\*2  
 DO 50 I=1,3  
 DO 50 J=1,3  
 DD(I,J)=DTH(I,J)+DD(K,I)\*TH(K,J)  
 DO 50 K=1,3  
 C CONTINUE  
 NOTE THAT IN ABOVE MATRIX MULTIPLICATION, MATRIX DD(3,3) IS  
 SYMMETRIC  
 DO 60 I=1,3  
 DO 60 J=1,3

```

DO 60 K=1,3
KD(I,J)=KD(I,J)+TH(K,J)*DTH(K,I)
CONTINUE
60
IF (IBD(I,I).LT.0.0) KD(I,I)=1000.0
DO 70 I=1,3
CONTINUE
70
GO TO 90
80 WRITE (6,82) BEL,EFPC
82 FORMAT('/// ***** ELEMENT NUMBER',I3,' HAS EXCEEDED ULTIMATE STRAIN
1 ****',//) EFPC =',E1A.5)
STOP
90 RETURN
END
SUBROUTINE KUTTA(N51,N52,N53,N54,N55)
C *****
C THIS SUBROUTINE ADJUSTS THE STRUCTURAL COMPONENT STIFFNESSES
FOR THE NEW LOAD INCREMENT USING THE KUTTA-RIDGE METHOD. ALSO,
FAILURE OF CONVENTIONAL REO, DORZEL AND SLIP LINKAGES IS TAKEN
INTO ACCOUNT IN STIFFNESS FORMULATION
C *****
CONMOD/BLOCK1/EQHS,EBAND,EBLK,EBREC,ICOUNT
CONMOD/BLOCK2/HEL,HELT,HELCH,HELD,INDCEL(185),IBELSI(185),
1NDOWL(185),NIDTRC(185),CANGLE(185),CALTR(185),
2IBELTY(215),ELTRN(215),MODEL(215,4),MDREF(215),DPHMOD(215)
CONMOD/BLOCK3/HELSH,HESSH(185),INSHS(185),NDIMS,ZZPSTL(185,4),
1ARGL(185,4),SHSTP(185,3,3),SHESH(185,1)
CONMOD/BLOCK4/HE,HEPO,MODES(190,2),IBRDN(190),IBRTY(190),
1BALTER(190),BARFA(190),CARFA(190),RSTP(190),TSGPZE(190),
CONMOD/BLOCK5/MODES,ICODE(220),I(220),I(220),Z(220)
CONMOD/BLOCK6/CONMOD,REKOD,PREMOD,SLPMOD,SASMOD,PC,PT,
1PAGE,POP,POPRES,DP,ESLFP,SCULT,ZPOLT,ZEGLT,RESULT,P1,Z2,PJ,PA,
2PO,ZERRO,EPPEP,CORDEV,DEYCOB,DEYREO,PREDEV,SLPDEV,IDEV,AVGSP,HELI
CONMOD/BLOCK9/LFOINBY(20,2),FOUB1,FOUB2,NURECC,
1HUBELK,ISOLVE,LEN
CONMOD/BLOCK10/ZSTP(12,12),BS(3,3),B1(3,12,9),B2(3,12,9),D(3,3),
1DCORC(185,3,3),DCRACK(185),DAGG(185)
CONMOD/BLOCK12/SIGCOF(185,3),ECOF(185,3),SIGHS(185,4),ZHS(185,4),
1TSCCO(185,3),TSCOH(185,3),TSCCC(185),TSGST(185),TSGAGG(185),
2TCCC(185),TECT(185),TSGSH(185,4),TSHS(185,4),SIGNRO(190),
3RPEO(190),TSGRZO(190),TPEO(190)
CONMOD/BLOCK13/HESSH(185,4),BDOWEL(185),NCRACK(185),NVA33(185),
1HREO(190),NCRPO(190)
DIRECTION IS (N51,N52),AL (N53),AR (N53),DCDIP(185,3,3),AS:PDCT(190),
1DSR(3,3)
FEALSS,ED(3,3)
ITERERRS=CALTER,BALTER,FOUB1,INFO(4),SALTER(185)
ITERERRS=LEN
DATA MOD/200020000/
C ***** ADJUSTMENT OF ALL CONCRETE ELEMENT CONSTITUTIVE MATRICES
DO 50 I=1,HELT
MEL=I
IF (NCRACK(I).EQ.-1) NCRACK(I)=1
SUB1=0.0
SUB2=0.0
DO 5 J=1,3
DO 5 K=1,3
KD(I,J)=0.0
CONTINUE
5
IF (NCRACK(I).EQ.0) GO TO 10

```

```

771 C AGGREGATE INTERLOCK STIFFNESS IS CALCULATED TO REDEFINE SZHAR
772 C MODULUS.
773 CALL WCRACK(WC)
774 CALL SRRHOD(WC)
775 CALL MDCONC(MD)
776 C
777 C CHECK ON ANY CHANGE IN STEEL REIN STIFFNESS. STIFFNESS OF
778 C REINFORCED CONCRETE ELEMENT WILL BE CHANGED AT EVERY LOAD
779 C INCREMENT ONCE YIELDING HAS OCCURRED.
780 IPIBRESH(MEL, EQ, 0) GO TO 30
781 SALTER(MEL)=0
782 DO 25 J=1, NDIRS
783 IF(SHRS(MEL, J).EQ.1) GO TO 25
784 IFCORR(MEL, J) GO TO 22
785 STRAIN-TRES(MEL, J)
786 GO TO 24
787 STRAIN-TRES(MEL, J)+SHS(MEL, J)
788 IFSYSTRN.GT.STRN.AND.STRN.LT.ZERO GO TO 25
789 SALTER(MEL)=1
790 GO TO 30
791 C
792 C CHECK ON, AND CALCULATION OF CONCRETE CONSTITUTIVE MATRIX
793 C CHANGE
794 DO 35 J=1, 3
795 SW1=SW1+ND(J, J)
796 SW2=SW2+DCONC(L, J, J)
797 CONTINUE
798 DO 40 K=1, 3
799 PREDV=(SUM1-SOR2)*100.0/SUM1
800 IFCORR(LT, 0.0) PREDV=-PREDV
801 IFCORR(LT, DRVCON) GO TO 48
802 CALTER(I)=1
803 DO 40 J=1, 3
804 DO 40 K=1, 3
805 C THE STIFFNESS CHANGES ADDED TO THE TOTAL STIFFNESS MATRIX ARE
806 C CALCULATED USING THE CHANGE IN THE CONSTITUTIVE MATRIX. THE
807 C CURRENT CONSTITUTIVE MATRIX DCONC(MEL, I, J) IS THEN RESET.
808 DCONC(I, K, J)=ND(K, J)+DCONC(L, K, J)
809 DCORC(I, K, J)=DB(K, J)
810 CONTINUE
811 GO TO 50
812 CALTER(I)=0
813 CONTINUE
814 C
815 C ADJUSTMENT OF ALL REINFORCEMENT ELEMENT STIFFNESSES
816 DO 60 I=1, NREMO
817 RE=I
818 IPIBRESH(I, EQ, 1) GO TO 58
819 CALL REOSTP(RES)
820 IPIBRESH(I, EQ, RES) GO TO 58
821 IPIBRESH(I, EQ, 0) REST(I)=1.0
822 PREDV=(REST(I)-RES)*100.0/REST(I)
823 IFCORR(I, EQ, 1, 0) REST(I)=0.0
824 IFCORR(I, EQ, 1, 0) REST(I)=0.0
825 IFCORR(I, EQ, 0) RESTV=-PREDV
826 IFCORR(I, EQ, 0) RESTV=0.0
827 SALTER(I)=1
828 REST(I)=RES+REST(I)
829 GO TO 60
830 SALTER(I)=0
831 CONTINUE
832 C
833 C THOSE CONCRETE AND REINFORCEMENT ELEMENTS THAT HAVE UNDERGONE
834 C STIFFNESS CHANGES NOW HAVE THEIR RESPECTIVE TOTAL STIFFNESS

```

```

771 C CONTRIBUTIONS ADJUSTED. THIS PROCESS IS DONE BLOCK BY BLOCK.
772 C
773 C TWO STIFFNESS BLOCKS IN THE PREVIOUS LOAD INCREMENT ARE READ INTO
774 C REIN=0 THAT APPROPRIATE STIFFNESS CHANGES CAN BE MADE
775 C
776 C STIFFNESS TERMS ARE READ INTO SECOND BLOCK.
777 K=1
778 KI=LEN
779 DO 90 I=1, NUBRCK
780 CALL READ(AR(K), LEN, 0, LEUH, PDUB1, S305)
781 K=K+LEN/4
782 IPIBRESH(MURRNC-1)) LEN=(MS3-K+1)*4
783 CONTINUE
784 LEN=K1
785 IPIBRESH(ME, J) GO TO 110
786 IPIBRESH(ME, J) GO TO 110
787 IPIBRESH(ME, J) GO TO 110
788 IPIBRESH(ME, J) GO TO 110
789 IPIBRESH(ME, J) GO TO 110
790 IPIBRESH(ME, J) GO TO 110
791 IPIBRESH(ME, J) GO TO 110
792 IPIBRESH(ME, J) GO TO 110
793 IPIBRESH(ME, J) GO TO 110
794 IPIBRESH(ME, J) GO TO 110
795 IPIBRESH(ME, J) GO TO 110
796 IPIBRESH(ME, J) GO TO 110
797 IPIBRESH(ME, J) GO TO 110
798 IPIBRESH(ME, J) GO TO 110
799 IPIBRESH(ME, J) GO TO 110
800 IPIBRESH(ME, J) GO TO 110
801 IPIBRESH(ME, J) GO TO 110
802 IPIBRESH(ME, J) GO TO 110
803 IPIBRESH(ME, J) GO TO 110
804 IPIBRESH(ME, J) GO TO 110
805 IPIBRESH(ME, J) GO TO 110
806 IPIBRESH(ME, J) GO TO 110
807 IPIBRESH(ME, J) GO TO 110
808 IPIBRESH(ME, J) GO TO 110
809 IPIBRESH(ME, J) GO TO 110
810 IPIBRESH(ME, J) GO TO 110
811 IPIBRESH(ME, J) GO TO 110
812 IPIBRESH(ME, J) GO TO 110
813 IPIBRESH(ME, J) GO TO 110
814 IPIBRESH(ME, J) GO TO 110
815 IPIBRESH(ME, J) GO TO 110
816 IPIBRESH(ME, J) GO TO 110
817 IPIBRESH(ME, J) GO TO 110
818 IPIBRESH(ME, J) GO TO 110
819 IPIBRESH(ME, J) GO TO 110
820 IPIBRESH(ME, J) GO TO 110
821 IPIBRESH(ME, J) GO TO 110
822 IPIBRESH(ME, J) GO TO 110
823 IPIBRESH(ME, J) GO TO 110
824 IPIBRESH(ME, J) GO TO 110
825 IPIBRESH(ME, J) GO TO 110
826 IPIBRESH(ME, J) GO TO 110
827 IPIBRESH(ME, J) GO TO 110
828 IPIBRESH(ME, J) GO TO 110
829 IPIBRESH(ME, J) GO TO 110
830 IPIBRESH(ME, J) GO TO 110

```



```

831 CALL STRES(DSH)
832 DO 146 L=1,J
833 DO 146 M=1,K
834 DO 146 N=1,L
835 SSTR(BEL,H,L)-DSH(H,L)-SSTR(BEL,H,L)
836 SSTR(BEL,H,L)-DSH(H,L)
837 CALL ELSTP(BELOD)
838 PARTITIONING OF ELEMENT STIFFNESS DIFFERENCE INTO COMPONENT SUB-
839 BLOCKS, AND ADDITION OF SUB-BLOCKS INTO TOTAL STIFFNESS MATRIX.
840 CALL ADDSUB(BS1,BS2,BS3,TS,AL,AR)
841 GO TO 130
842 CONTINUE
843 CONTINUE
844 ADDITION OF STIFFNESS DIFFERENCES OF SINGLE REINFORCING AND
845 PRESSURE BARS AND BOND SLIP LINKAGES TO TSUBARD,HBARD*2)
846 DO 150 I=1,NBRO
847 IF(BALTER(I).EQ.0) GO TO 150
848 HB=I
849 DO 145 J=1,2
850 IF((MODS(I,J).LT.HBTH).OR.(MODS(I,J).GT.HBTH)) GO TO 145
851 DO 140 K=1,2
852 IF((MODS(I,K).EQ.HKOLD)) GO TO 150
853 CONTINUE
854 STIP=BSSTDP(I)
855 CALL STADD(BS1, BS3,TS,AL,AR,STIP)
856 GO TO 150
857 CONTINUE
858 CONTINUE
859 THE ADJUSTED STIFFNESS BLOCK IS THEN MODIFIED AND WRITTEN BACK ON
860 REPLYARY DISC FILE -FILE1
861 CALL MODIF(BS1,BS2,BS3,TS,AL,AR)
862 IFO(2)-LFOINT(HBL,1)
863 CALL POINT(PDB1,INPO,2)
864 J=1
865 JI=JN
866 DO 160 I=1,NBROBC
867 CALL WRITE(AL(J),LBN,ROD,LNUM,PDB1,6325)
868 J=J/LBN/4
869 IF(L.EQ.(NBROBC-1)) LBN=(BS3-J+1)
870 CONTINUE
871 LBN=J1
872 GO TO 100
873 DO 302 I=1,NBRO
874 CALTER(I)=0
875 CONTINUE
876 DO 304 I=1,NBRO
877 HALTER(I)=0
878 CONTINUE
879 RETURN
880 WRITE (6,310)
881 FORMAT('..... ERROR IN SYSTEM SUBROUTINE READ IN SUBROUTINE
882 LINE KUTIA .....')
883 STOP
884 WRITE (6,330)
885 FORMAT('..... ERROR IN SYSTEM SUBROUTINE WRITE CALLED IN SUBROUT
886 LINE KUTIA .....')
887 STOP
888 END
889 SUBROUTINE DOVEL(HY)
890 C.....

```

```

891 C THIS SUBROUTINE CHECKS THAT THE DOVEL STIFFNESS MECHANISM FOR A
892 CRACKED ELEMENT HAS NOT FAILED.
893 C.....
894 C
895 CONOH/BLOCK/REQS,HBARD,HBL,HBRC,ICOHBT
896 CONOH/BLOCK/REL,REL,RELCHK,RLD,IBCEL(185),IBELSE(185),
897 IMPDL(185),WIDTBC(185),CARGLE(185),CALTR(185),
898 ZIBELT(215),ELTBC(215),MORBL(215,4),RDEP(215),OPRMO(215)
899 CONOH/BLOCK/COMOD,REMOD,REMOD,SIFMOD,SRSROD,PC,PI,
900 IPACO,TPR,FOP,PMAS,DP,ESLIP,ECULT,REGLT,SPULX,HSBLT,PI,P2,P3,P4,
901 ZPU,REMO,REPR,CONDV,DETCO,DETPO,FRIDEV,SLFDT,IDFV,ATCSP,BELAX
902 CONOH/BLOCK/SICOH(185,3),BCOH(185,3),SICGS(185,4),SRS(185,4),
903 IYSCOH(185,3),SICOM(185,3),ZSCCC(185,3),SICGS(185,4),SRS(185,4),
904 ZTECC(185),TSTC(185),XSSES(185,4),TSHS(185,4),SICRZO(190),
905 ZREZO(190),ZSRO(190),ZREZO(190)
906 CONOH/BLOCK/BIRESH(185,4),EDOVEL(185),FCRACK(185),BTAGG(185),
907 ZREZO(190),BYCRO(190)
908 IRECR=0
909 DIRECTION F(J)
910 ZETA-CANGLE(BEL)*3.141593/180.0
911 C-COS(ZETA)
912 S-SIN(ZETA)
913 IF(ICOUNT.EQ.1) GO TO 10
914 DO 5 J=1,3
915 Z(J)-TECOM(BEL,J)
916 CONTINUE
917 GO TO 20
918 DO 15 J=1,3
919 E(J)-TECOM(BEL,J)*PCOH(BEL,J)
920 CONTINUE
921 C
922 CBBHA IS THE SHEAR STRAIN AT THE CENTROID PARALLEL TO THE CRACK.
923 CBBHA=2.0*CS*(Z(1)-Z(2))/(C*E2-S*E2)*E(J)
924 DELTA=BT*GABHA
925 IF(DELTA.LT.DP.AND.DELTA.GT.-DP) RETURN
926 EDVEL(BEL)=1
927 WRITE (6,25) BEL,DELTA
928 FORMAT('..... DOVEL STIFFNESS MECHANISM FOR CRACKED ELEMENT',15,
929 ' HAS FAILED: SHEAR DISPLACEMENT ACROSS CRACK =',E11.4)
930 RETURN
931 END

```

END OF FILE

SLIST FILE51

```

1 SUBROUTINE NORN(ANGLE,II,INTELE)
2 C.....
3 C.....
4 C.....
5 C.....
6 C.....
7 C.....
8 C.....
9 C.....
10 C.....
11 C.....
12 C.....
13 C.....
14 C.....
15 C.....
16 C.....
17 C.....
18 C.....
19 C.....
20 C.....
21 C.....
22 C.....
23 C.....
24 C.....
25 C.....
26 C.....
27 C.....
28 C.....
29 C.....
30 C.....
31 C.....
32 C.....
33 C.....
34 C.....
35 C.....
36 C.....
37 C.....
38 C.....
39 C.....
40 C.....
41 C.....
42 C.....
43 C.....
44 C.....
45 C.....
46 C.....
47 C.....
48 C.....
49 C.....
50 C.....
51 C.....
52 C.....
53 C.....
54 C.....
55 C.....
56 C.....
57 C.....
58 C.....

```

```

59 C.....
60 C.....
61 C.....
62 C.....
63 C.....
64 C.....
65 C.....
66 C.....
67 C.....
68 C.....
69 C.....
70 C.....
71 C.....
72 C.....
73 C.....
74 C.....
75 C.....
76 C.....
77 C.....
78 C.....
79 C.....
80 C.....
81 C.....
82 C.....
83 C.....
84 C.....
85 C.....
86 C.....
87 C.....
88 C.....
89 C.....
90 C.....
91 C.....
92 C.....
93 C.....
94 C.....
95 C.....
96 C.....
97 C.....
98 C.....
99 C.....
100 C.....
101 C.....
102 C.....
103 C.....
104 C.....
105 C.....
106 C.....
107 C.....
108 C.....
109 C.....
110 C.....
111 C.....
112 C.....
113 C.....
114 C.....
115 C.....
116 C.....
117 C.....
118 C.....

```

SUBROUTINE NORN(ANGLE,II,INTELE)  
 THIS SUBROUTINE CALCULATES THE STRAIN IN THE UNIAXIAL DIRECTION  
 OF A STEEL REIN BAR AT AN ANGLE (HEL,I) TO THE HORIZONTAL  
 CONHOH/BLOCK1/NEONS,NBAND,NBLK,NUNING,ICOUNT  
 CONHOH/BLOCK2/HEL,NELT,NELCK,NELD,INDCEL(185),IBELSI(185),  
 1INDOVL(185),NIDTRC(185),CANGLE(185),CALTER(185),  
 2INELTY(215),NIDTRN(215),MODEPL(215,4),NDEFP(215),DPHROD(215),  
 CONHOH/BLC1/2/SIGCON(185,3),ZCON(185,3),SIGHS(185,4),EHS(185,4),  
 1TSGCON(185,3),TECON(185,3),TSGCC(185,3),TSGCT(185),TSGAGC(185),  
 2TECC(185),TECT(185),TSGHS(185,4),TEHS(185,4),SIGRPO(190),  
 3TEPO(190),TSGRO(190),TEARO(190)  
 DIRECTION ANGLE(185,4)  
 INTERGR4 CALTER  
 IF(ICOUNT.EQ.2) GO TO 5  
 E1=ECOH(HEL,1)  
 E2=ECOH(HEL,2)  
 E3=ECOH(HEL,3)  
 GO TO 10  
 5 E1=TECOH(HEL,1)  
 E2=TECOH(HEL,2)  
 E3=TECOH(HEL,3)  
 10 THETA=ANGLE(HEL,II)\*2\*PI\*(SIN(THETA))\*\*2+E2\*SIN(THETA)\*\*2+E3\*SIN(THETA)\*\*2  
 1E1A=E1  
 1E2A=E2  
 1E3A=E3  
 RETURN  
 END  
 SUBROUTINE PRINC  
 THIS SUBROUTINE CALCULATES THE TOTAL PRINCIPAL TENSILE AND  
 COMPRESSIVE STRESSES (TSGCC(HEL),TECC(HEL),TECT(HEL)) THAT CORRESPOND TO THEIR  
 RESPECTIVE PRINCIPAL STRESSES  
 CONHOH/BLOCK1/NEONS,NBAND,NBLK,NUNING,ICOUNT  
 CONHOH/BLOCK2/HEL,NELT,NELCK,NELD,INDCEL(185),IBELSI(185),  
 1INDOVL(185),NIDTRC(185),CANGLE(185),CALTER(185),  
 2INELTY(215),NIDTRN(215),MODEPL(215,4),NDEFP(215),DPHROD(215),  
 CONHOH/BLC1/2/SIGCON(185,3),ZCON(185,3),SIGHS(185,4),EHS(185,4),  
 1TSGCON(185,3),TECON(185,3),TSGCC(185,3),TSGCT(185),TSGAGC(185),  
 2TECC(185),TECT(185),TSGHS(185,4),TEHS(185,4),SIGRPO(190),  
 3TEPO(190),TSGRO(190),TEARO(190)  
 CONHOH/BLC1/3/STRES(185,4),NDOVEL(185),MCPACK(185),NYAGG(185),  
 1NYEPO(190),NYCREPO(190)  
 INTERGR4 CALTER  
 IF(ICOUNT.EQ.2) GO TO 5  
 E1=ECOH(HEL,1)+TECOH(HEL,1)  
 E2=ECOH(HEL,2)+TECOH(HEL,2)  
 E3=ECOH(HEL,3)+TECOH(HEL,3)/2.0  
 GO TO 10  
 5 E1=TECOH(HEL,1)  
 E2=TECOH(HEL,2)  
 E3=TECOH(HEL,3)/2.0  
 10 IF(BCRACK(HEL).EQ.0) GO TO 20  
 ONCE A CONCRETE ELEMENT HAS CRACKED, PRINCIPAL STRAIN DIRECTIONS  
 ARE NOT PERMITTED TO CHANGE

```

119 TSOC(185)=-S1*S+2*S2*C+2*S3*2.0*S+C
120 RETURN
121
122
123
124
125
126
127
128
129
130
131
132
133
134
135
136
137
138
139
140
141
142
143
144
145
146
147
148
149
150
151
152
153
154
155
156
157
158
159
160
161
162
163
164
165
166
167
168
169
170
171
172
173
174
175
176
177
178
179
180
181
182
183
184
185
186
187
188
189
190
191
192
193
194
195
196
197
198
199
200
201
202
203
204
205
206
207
208
209
210
211
212
213
214
215
216
217
218
219
220
221
222
223
224
225
226
227
228
229
230
231
232
233
234
235
236
237
238
239
240
241
242
243
244
245
246
247
248
249
250
251
252
253
254
255
256
257
258
259
260
261
262
263
264
265
266
267
268
269
270
271
272
273
274
275
276
277
278
279
280
281
282
283
284
285
286
287
288
289
290
291
292
293
294
295
296
297
298
299
300
301
302
303
304
305
306
307
308
309
310
311
312
313
314
315
316
317
318
319
320
321
322
323
324
325
326
327
328
329
330
331
332
333
334
335
336
337
338
339
340
341
342
343
344
345
346
347
348
349
350
351
352
353
354
355
356
357
358
359
360
361
362
363
364
365
366
367
368
369
370
371
372
373
374
375
376
377
378
379
380
381
382
383
384
385
386
387
388
389
390
391
392
393
394
395
396
397
398
399
400
401
402
403
404
405
406
407
408
409
410
411
412
413
414
415
416
417
418
419
420
421
422
423
424
425
426
427
428
429
430
431
432
433
434
435
436
437
438
439
440
441
442
443
444
445
446
447
448
449
450
451
452
453
454
455
456
457
458
459
460
461
462
463
464
465
466
467
468
469
470
471
472
473
474
475
476
477
478
479
480
481
482
483
484
485
486
487
488
489
490
491
492
493
494
495
496
497
498
499
500
501
502
503
504
505
506
507
508
509
510
511
512
513
514
515
516
517
518
519
520
521
522
523
524
525
526
527
528
529
530
531
532
533
534
535
536
537
538
539
540
541
542
543
544
545
546
547
548
549
550
551
552
553
554
555
556
557
558
559
560
561
562
563
564
565
566
567
568
569
570
571
572
573
574
575
576
577
578
579
580
581
582
583
584
585
586
587
588
589
590
591
592
593
594
595
596
597
598
599
600
601
602
603
604
605
606
607
608
609
610
611
612
613
614
615
616
617
618
619
620
621
622
623
624
625
626
627
628
629
630
631
632
633
634
635
636
637
638
639
640
641
642
643
644
645
646
647
648
649
650
651
652
653
654
655
656
657
658
659
660
661
662
663
664
665
666
667
668
669
670
671
672
673
674
675
676
677
678
679
680
681
682
683
684
685
686
687
688
689
690
691
692
693
694
695
696
697
698
699
700
701
702
703
704
705
706
707
708
709
710
711
712
713
714
715
716
717
718
719
720
721
722
723
724
725
726
727
728
729
730
731
732
733
734
735
736
737
738
739
740
741
742
743
744
745
746
747
748
749
750
751
752
753
754
755
756
757
758
759
760
761
762
763
764
765
766
767
768
769
770
771
772
773
774
775
776
777
778
779
780
781
782
783
784
785
786
787
788
789
790
791
792
793
794
795
796
797
798
799
800
801
802
803
804
805
806
807
808
809
810
811
812
813
814
815
816
817
818
819
820
821
822
823
824
825
826
827
828
829
830
831
832
833
834
835
836
837
838
839
840
841
842
843
844
845
846
847
848
849
850
851
852
853
854
855
856
857
858
859
860
861
862
863
864
865
866
867
868
869
870
871
872
873
874
875
876
877
878
879
880
881
882
883
884
885
886
887
888
889
890
891
892
893
894
895
896
897
898
899
900
901
902
903
904
905
906
907
908
909
910
911
912
913
914
915
916
917
918
919
920
921
922
923
924
925
926
927
928
929
930
931
932
933
934
935
936
937
938
939
940
941
942
943
944
945
946
947
948
949
950
951
952
953
954
955
956
957
958
959
960
961
962
963
964
965
966
967
968
969
970
971
972
973
974
975
976
977
978
979
980
981
982
983
984
985
986
987
988
989
990
991
992
993
994
995
996
997
998
999
1000

```

```

239 GO TO 10
240 B=(I*(MODHEL(BEL,2)))-I*(MODHEL(BEL,1)))/2.0
241 C=0.0
242 ELSE
243 DO 25 J=1,4
244 XI=MODHEL(I,J)
245 JJ=1
246 WHILE=1
247 CALL LOCATE(I,J,EROW,ECOL)
248 R(I,J)=3.0
249 IF (ICORR(I)-EQ.1) GO TO 15
250 R(I,J)=3.0
251 R(I,J)=3.0
252 IF (ICORR(I)-EQ.2) R(I,J)=3.0
253 IF (ICORR(I)-EQ.0) R(I,J)=3.0
254 GO TO 25
255 IF (ICORR(I)-EQ.2)
256 TRANSPORTION OF DISPLACEMENTS OF CORNER NODE OF AN INCLINED
257 ELEMENT FROM GLOBAL TO LOCAL FOR
258 C=(I*(MODHEL(BEL,2)))-I*(MODHEL(BEL,1)))/(2.0*B)
259 S=(I*(MODHEL(BEL,2)))-I*(MODHEL(BEL,1)))/(2.0*B)
260 NOTE THAT THE TRANSPORSED TRANSFORMATION MATRIX LT(5,5) IS BELOW
261 DO 17 K=1,5
262 LT(K,1)=0.0
263 CONTINUE
264 LT(1,1)=1.0
265 LT(2,2)=C
266 LT(3,3)=S
267 LT(4,4)=C
268 LT(5,5)=S
269 DO 18 K=1,5
270 DLOCAL(K)=D1(EROW+K-1)
271 LOCAL(K)=0.0
272 CONTINUE
273 DO 19 L=1,5
274 DGLOBAL(L)=DLOCAL(L)+LT(K,L)*DGLOBAL(K)
275 CONTINUE
276 B((J-1)*3+2)=DLOCAL(2)
277 B((J-1)*3+3)=DLOCAL(5)
278 GO TO 25
279 B((J-1)*3+2)=D1(EROW+2)
280 B((J-1)*3+3)=D1(EROW+3)
281 GO TO 25
282 R(I,J)=3.0
283 R(I,J)=3.0
284 R(I,J)=3.0
285 R(I,J)=3.0
286 R(I,J)=3.0
287 R(I,J)=3.0
288 R(I,J)=3.0
289 R(I,J)=3.0
290 R(I,J)=3.0
291 R(I,J)=3.0
292 R(I,J)=3.0
293 R(I,J)=3.0
294 R(I,J)=3.0
295 R(I,J)=3.0
296 R(I,J)=3.0
297 R(I,J)=3.0
298 R(I,J)=3.0

```

```

299 CONTINUE
300 DO 27 J=1, BELTOP
301 XI=MODHEL(I,J)
302 JJ=1
303 WHILE=1
304 R(I,J)=3.0
305 R(I,J)=3.0
306 R(I,J)=3.0
307 R(I,J)=3.0
308 R(I,J)=3.0
309 R(I,J)=3.0
310 R(I,J)=3.0
311 R(I,J)=3.0
312 R(I,J)=3.0
313 R(I,J)=3.0
314 R(I,J)=3.0
315 R(I,J)=3.0
316 R(I,J)=3.0
317 R(I,J)=3.0
318 R(I,J)=3.0
319 R(I,J)=3.0
320 R(I,J)=3.0
321 R(I,J)=3.0
322 R(I,J)=3.0
323 R(I,J)=3.0
324 R(I,J)=3.0
325 R(I,J)=3.0
326 R(I,J)=3.0
327 R(I,J)=3.0
328 R(I,J)=3.0
329 R(I,J)=3.0
330 R(I,J)=3.0
331 R(I,J)=3.0
332 R(I,J)=3.0
333 R(I,J)=3.0
334 R(I,J)=3.0
335 R(I,J)=3.0
336 R(I,J)=3.0
337 R(I,J)=3.0
338 R(I,J)=3.0
339 R(I,J)=3.0
340 R(I,J)=3.0
341 R(I,J)=3.0
342 R(I,J)=3.0
343 R(I,J)=3.0
344 R(I,J)=3.0
345 R(I,J)=3.0
346 R(I,J)=3.0
347 R(I,J)=3.0
348 R(I,J)=3.0
349 R(I,J)=3.0
350 R(I,J)=3.0
351 R(I,J)=3.0
352 R(I,J)=3.0
353 R(I,J)=3.0
354 R(I,J)=3.0
355 R(I,J)=3.0
356 R(I,J)=3.0
357 R(I,J)=3.0
358 R(I,J)=3.0

```

```

26 CONTINUE
27 DO 28 K=1,3
28 R(K)=3.0
29 R(K)=3.0
30 CALL CCALC(A,B,AA)
31 R(K)=0.0
32 E(J)=E(J)+AA*(K,J)*R(K)
33 R(K)=0.0
34 CONTINUE
35 R(K)=3.0
36 R(K)=3.0
37 R(K)=3.0
38 R(K)=3.0
39 R(K)=3.0
40 R(K)=3.0
41 R(K)=3.0
42 R(K)=3.0
43 R(K)=3.0
44 R(K)=3.0
45 R(K)=3.0
46 R(K)=3.0
47 R(K)=3.0
48 R(K)=3.0
49 R(K)=3.0
50 R(K)=3.0
51 R(K)=3.0
52 R(K)=3.0
53 R(K)=3.0
54 R(K)=3.0
55 R(K)=3.0
56 R(K)=3.0
57 R(K)=3.0
58 R(K)=3.0

```

```

C POPULATION OF CRACKED CONCRETE CONSTITUTIVE MATRIX FOR STRESS
C CALCULATION-SHEAR STRENGTH ACROSS CRACK IS NOT INCLUDED
37 TETRAE=CRACK(BEL)*3.1415926/180.0
38 C=COS(THETA)
39 S=SIN(THETA)
40 DC(1,1)=S**2
41 DC(2,1)=C*S
42 DC(3,1)=S**2
43 DC(1,2)=C*S
44 DC(2,2)=C**2
45 DC(3,2)=S**2
46 DC(1,3)=S**2
47 DC(2,3)=C*S
48 DC(3,3)=S**2
49 DO 38 K=1,3
50 DO 38 J=1,3
51 DCRACK(BEL) IS THE CONCRETE STIFFNESS IN THE DIRECTION

```

```

359 C      PARALLEL TO THE CRACK.
360 DC(J,K)=DC(J,K)-DCRACK(BEL)
361 CONTINUE
362 GO TO 41
363 C
364 ELEMENT CRACKED IN TWO DIRECTIONS REMAINS UNSTRESSED
365 DO 40 J=1,3
366 DO 40 K=1,3
367 DC(J,K)=0.0
368 CONTINUE
369 DO 42 J=1,3
370 DO 42 K=1,3
371 SIGMA(I)=SIGMA(I)+DC(K,J)*R(J)
372 IF(ICOEFF.EQ.2) GO TO 43
373 SIGCOM(BEL,K)=SIGMA(K)
374 GO TO 44
375 TSCOM(BEL,K)=SIGMA(K)
376 IF(DCRACK(BEL).NE.0) GO TO 44
377 TSCOM(BEL,K)=SIGMA(K)+TSCRHR(BEL,K)
378 CONTINUE
379 C***** CALCULATION OF AGGREGATE INTERLOCK STRESS
380 IF(DCRACK(BEL).NE.1) GO TO 55
381 IF(ICOEFF.EQ.1) GO TO 55
382 DO 46 J=1,3
383 DO 46 K=1,3
384 R(J)=R(J)+TSCOM(BEL,J)
385 CONTINUE
386 TSCGG(BEL)=(R(1)+R(2))+2.0*SC*(C*2-SC*2)*R(3)*DAGC(BEL)
387 C***** CALCULATION OF PRINCIPAL CONCRETE STRESSES AND CORRESPONDING
388 STRESS
389 CALL PRINCC
390 CALL PRINCC
391 IF(KRHRH(BEL).EQ.0) GO TO 60
392 C***** CALCULATION OF STEEL WESH COMPONENT STRESSES AND STRAINS. WHEN
393 WESH HAS YIELDED, STRESS LEVEL REMAINS AT YIELD STRESS.
394 DO 56 J=1,NDIRS
395 IF(WMESH(BEL,J).EQ.0) GO TO 56
396 II=J
397 CALL KORR(ANGLE,II,ISTEEL)
398 SH=SMESH(BEL,J)
399 IF(WRHRH(BEL,J).EQ.1) GO TO 58
400 SIGSTL=STEEL*SH
401 IF(ICOEFF.EQ.2) GO TO 58
402 SIGSHR(J)=SIGSTL
403 HRH(BEL,J)=ESTEEL
404 GO TO 56
405 TSCS(BEL,J)=SIGSTL
406 TRAS(BEL,J)=ESTEEL
407 CONTINUE
408 C***** CALCULATION OF CONVENTIONAL AND PRESTRESS REINFORCEMENT AND BOND
409 STRESSES
410 IF(WRHRH(BEL).NE.0) GO TO 64
411 IF(WRHRM.EQ.1-OR.WRHR.GE.1) GO TO 65
412 DO 64 I=1,NRMO
413 IF(LBRTY(I).NE.0) GO TO 64
414 TSGRO(I)=TSGRFR(I)
415 TSGRO(I)=TSGRFR(I)
416 TSGRO(I)=SIGR+STRESI
417 CONTINUE
418 DO 110 I=1,NRMO
419
420
421
422
423
424
425
426
427
428
429
430
431
432
433
434
435
436
437
438
439
440
441
442
443
444
445
446
447
448
449
450
451
452
453
454
455
456
457
458
459
460
461
462
463
464
465
466
467
468
469
470
471
472
473
474
475
476
477
478
479
480
481
482
483
484
485
486
487
488
489
490
491
492
493
494
495
496
497
498
499
500
501
502
503
504
505
506
507
508
509
510
511
512
513
514
515
516
517
518
519
520
521
522
523
524
525
526
527
528
529
530
531
532
533
534
535
536
537
538
539
540
541
542
543
544
545
546
547
548
549
550
551
552
553
554
555
556
557
558
559
560
561
562
563
564
565
566
567
568
569
570
571
572
573
574
575
576
577
578
579
580
581
582
583
584
585
586
587
588
589
590
591
592
593
594
595
596
597
598
599
600
601
602
603
604
605
606
607
608
609
610
611
612
613
614
615
616
617
618
619
620
621
622
623
624
625
626
627
628
629
630
631
632
633
634
635
636
637
638
639
640
641
642
643
644
645
646
647
648
649
650
651
652
653
654
655
656
657
658
659
660
661
662
663
664
665
666
667
668
669
670
671
672
673
674
675
676
677
678
679
680
681
682
683
684
685
686
687
688
689
690
691
692
693
694
695
696
697
698
699
700
701
702
703
704
705
706
707
708
709
710
711
712
713
714
715
716
717
718
719
720
721
722
723
724
725
726
727
728
729
730
731
732
733
734
735
736
737
738
739
740
741
742
743
744
745
746
747
748
749
750
751
752
753
754
755
756
757
758
759
760
761
762
763
764
765
766
767
768
769
770
771
772
773
774
775
776
777
778
779
780
781
782
783
784
785
786
787
788
789
790
791
792
793
794
795
796
797
798
799
800
801
802
803
804
805
806
807
808
809
810
811
812
813
814
815
816
817
818
819
820
821
822
823
824
825
826
827
828
829
830
831
832
833
834
835
836
837
838
839
840
841
842
843
844
845
846
847
848
849
850
851
852
853
854
855
856
857
858
859
860
861
862
863
864
865
866
867
868
869
870
871
872
873
874
875
876
877
878
879
880
881
882
883
884
885
886
887
888
889
890
891
892
893
894
895
896
897
898
899
900
901
902
903
904
905
906
907
908
909
910
911
912
913
914
915
916
917
918
919
920
921
922
923
924
925
926
927
928
929
930
931
932
933
934
935
936
937
938
939
940
941
942
943
944
945
946
947
948
949
950
951
952
953
954
955
956
957
958
959
960
961
962
963
964
965
966
967
968
969
970
971
972
973
974
975
976
977
978
979
980
981
982
983
984
985
986
987
988
989
990
991
992
993
994
995
996
997
998
999

```

```

479 110 CONTINUE
480 RETURN
481 END
482 SUBROUTINE SHSTP(I)
483 C.....
484 C THIS SUBROUTINE CALCULATES THE STIFFNESS OF A PARTICULAR LAYER
485 C OF A STEEL SHEET FOR EITHER THE INCREMENTAL OR TOTAL LOAD CASES
486 C.....
487 C
488 COHON/BLOCK1/NEONS, HEAD, BELT, MURINC, ICOUNT
489 COHON/BLOCK2/NEI, BELT, BELCH, BELD, INDCEL (185), IHELST (185),
490 IINDOVL (185), MIDTNC (185), CAUGLE (185), CALTER (185),
491 ZIBELT (215), ELTNC (215), MDOVEL (215, 4), MDREF (215), DPHMO (215)
492 COHON/BLOCK3/NEISH, IMESH (185), IASZAS (185), MDIENS, PERSTL (185, 4),
493 IANGLE (185, 4), SHSTP (185, 3, 3), SHESH (185, 1)
494 COHON/BLOCK4/COMOD, ROMOD, PRMOD, SLPMOD, SESHOD, FC, FT,
495 IFRAG, FR, FRP, FRMS, DT, BELT, ECOLT, ROKLT, RPKLT, ERSOLE, P1, P2, P3, P4,
496 ZBO, ZBRO, ZBRC, CONDEY, DEYCON, DEYREG, PREDEF, SLEDEF, IDY, AVCS, RELAI
497 COHON/BLOCK12/SIGCON (185, 3), PCOM (185, 3), SIGMS (185, 4), EMS (185, 4),
498 IISCON (185, 3), TISCON (185, 3), TISGCC (185), TISGCT (185), TISGAGC (185),
499 ZTECC (185), TECT (185), TSGMS (185, 4), TMS (185, 4), SIGNEO (190),
500 JEREO (190), TSGRO (190), TEREO (190)
501 COHON/BLOCK13/NEVESH (185, 4), MDOVEL (185), MCRACK (185), MYAGG (185),
502 MYREO (190), MYCRO (190)
503 IFRGER=4 CALTER
504 IF (MYRESH (NEL, I), EQ, 1) GO TO *0
505 IF (ICOUNT, EQ, 2) GO TO 10
506 A (STRESS-TSGMS (NEL, I)+SIGMS (NEL, I)
507 STRAIN-TSMS (NEL, I)+EMS (NEL, I)
508 IF (STRAIN, GT, ZELAND, STRAIN, LT, EN) GO TO 5
509 IF (STRAIN, LE, ZERSOLE, OR, STRAIN, GE, ERSOLE) GO TO 25
510 SHESH (NEL, I)=30000.0
511 RETURN
512
513 5 SHESH (NEL, I)=SHSHOD
514 RETURN
515 10 A (STRESS-TSGMS (NEL, I)
516 STRAIN-TSMS (NEL, I)
517 IF (STRAIN, LT, ZERSOLE, OR, STRAIN, GT, ERSOLE) GO TO 25
518 IF (STRAIN, GE, ZELAND, STRAIN, LE, E2) GO TO 5
519 STRESS=53800.0+430000.0*STRAIN
520 PRCTG=(A (STRESS-STRESS)*100.0)/STRESS
521 IF (PRCTG, GE, PREDEF) GO TO 20
522 SHESH (NEL, I)=STRESS/STRAIN
523 RETURN
524 C RELAXATION IS EMPLOYED TO INCREASE RATE OF CONVERGENCE
525 A (STRAIN-RELAX
526 STRESS=53800.0+430000.0*STRAIN
527 SHESH (NEL, I)=STRESS/ASTRN
528 RETURN
529 25 MYRESH (NEL, I)=1
530 TSMS (NEL, I)=PMS
531 IF (STRAIN, LT, 0.0) TSMS (NEL, I)--PMS
532 SH=0.0
533 WRITE (6, 30) I, NEL
534 FORMAT (' ***** STEEL SHEET LAYER NUMBER', I, ' IN ELEMENT NUMBER ', I
535 15, ' HAS FAILED ***** ')
536 RETURN
537 SH=0.0
538 RETURN
539
540 SUBROUTINE PREST
541 C.....
542 C THIS SUBROUTINE INITIALIZES ALL VARIABLES, VECTORS AND ARRAYS
543 C WHOSE INCORPORATION INTO THE PROGRAM LOGIC NECESSITATES SUCH
544 C PRESTTING
545 C.....
546 C
547 COHON/BLOCK1/NEONS, HEAD, BELT, MURINC, ICOUNT
548 COHON/BLOCK2/NEI, BELT, BELCH, BELD, INDCEL (185), IHELST (185),
549 IINDOVL (185), MIDTNC (185), CAUGLE (185), CALTER (185),
550 ZIBELT (215), ELTNC (215), MDOVEL (215, 4), MDREF (215), DPHMO (215)
551 COHON/BLOCK3/NEISH, IMESH (185), IASZAS (185), MDIENS, PERSTL (185, 4),
552 IANGLE (185, 4), SHSTP (185, 3, 3), SHESH (185, 1)
553 COHON/BLOCK4/NE, NEPO, MDES (190, 2), TNRDM (190), TWRTY (190),
554 IHALTER (190), HARA (190), CARA (190), B (190), B (190), TSGPR (190), TSPRE (190)
555 COHON/BLOCK11/RTOT (750), PROTOT (750), DTOT (750), *2 (2, 750), *2 (2, 750)
556 COHON/BLOCK12/SIGCON (185, 3), PCOM (185, 3), SIGMS (185, 4), EMS (185, 4),
557 IISCON (185, 3), TISCON (185, 3), TISGCC (185), TISGCT (185), TISGAGC (185),
558 ZTECC (185), TECT (185), TSGMS (185, 4), TMS (185, 4), SIGNEO (190),
559 JEREO (190), TSGRO (190), TEREO (190)
560 COHON/BLOCK13/NEVESH (185, 4), MDOVEL (185), MCRACK (185), MYAGG (185),
561 MYREO (190), MYCRO (190)
562 IFRGER=4 CALTER, HALTER
563 IF (MYRESH (NEL, I), EQ, 1) GO TO *0
564 IF (ICOUNT, EQ, 2) GO TO 10
565 A (STRESS-TSGMS (NEL, I)+SIGMS (NEL, I)
566 STRAIN-TSMS (NEL, I)+EMS (NEL, I)
567 IF (STRAIN, GT, ZELAND, STRAIN, LT, EN) GO TO 5
568 IF (STRAIN, LE, ZERSOLE, OR, STRAIN, GE, ERSOLE) GO TO 25
569 SHESH (NEL, I)=30000.0
570 RETURN
571
572 5 SHESH (NEL, I)=SHSHOD
573 RETURN
574 10 A (STRESS-TSGMS (NEL, I)
575 STRAIN-TSMS (NEL, I)
576 IF (STRAIN, LT, ZERSOLE, OR, STRAIN, GT, ERSOLE) GO TO 25
577 IF (STRAIN, GE, ZELAND, STRAIN, LE, E2) GO TO 5
578 STRESS=53800.0+430000.0*STRAIN
579 PRCTG=(A (STRESS-STRESS)*100.0)/STRESS
580 IF (PRCTG, GE, PREDEF) GO TO 20
581 SHESH (NEL, I)=STRESS/STRAIN
582 RETURN
583 C RELAXATION IS EMPLOYED TO INCREASE RATE OF CONVERGENCE
584 A (STRAIN-RELAX
585 STRESS=53800.0+430000.0*STRAIN
586 SHESH (NEL, I)=STRESS/ASTRN
587 RETURN
588 25 MYRESH (NEL, I)=1
589 TSMS (NEL, I)=PMS
590 IF (STRAIN, LT, 0.0) TSMS (NEL, I)--PMS
591 SH=0.0
592 WRITE (6, 30) I, NEL
593 FORMAT (' ***** STEEL SHEET LAYER NUMBER', I, ' IN ELEMENT NUMBER ', I
594 15, ' HAS FAILED ***** ')
595 RETURN
596 SH=0.0
597 RETURN
598
599 SUBROUTINE PREST
600 C.....
601 C THIS SUBROUTINE INITIALIZES ALL VARIABLES, VECTORS AND ARRAYS
602 C WHOSE INCORPORATION INTO THE PROGRAM LOGIC NECESSITATES SUCH
603 C PRESTTING
604 C.....
605 C
606 COHON/BLOCK1/NEONS, HEAD, BELT, MURINC, ICOUNT
607 COHON/BLOCK2/NEI, BELT, BELCH, BELD, INDCEL (185), IHELST (185),
608 IINDOVL (185), MIDTNC (185), CAUGLE (185), CALTER (185),
609 ZIBELT (215), ELTNC (215), MDOVEL (215, 4), MDREF (215), DPHMO (215)
610 COHON/BLOCK3/NEISH, IMESH (185), IASZAS (185), MDIENS, PERSTL (185, 4),
611 IANGLE (185, 4), SHSTP (185, 3, 3), SHESH (185, 1)
612 COHON/BLOCK4/NE, NEPO, MDES (190, 2), TNRDM (190), TWRTY (190),
613 IHALTER (190), HARA (190), CARA (190), B (190), B (190), TSGPR (190), TSPRE (190)
614 COHON/BLOCK11/RTOT (750), PROTOT (750), DTOT (750), *2 (2, 750), *2 (2, 750)
615 COHON/BLOCK12/SIGCON (185, 3), PCOM (185, 3), SIGMS (185, 4), EMS (185, 4),
616 IISCON (185, 3), TISCON (185, 3), TISGCC (185), TISGCT (185), TISGAGC (185),
617 ZTECC (185), TECT (185), TSGMS (185, 4), TMS (185, 4), SIGNEO (190),
618 JEREO (190), TSGRO (190), TEREO (190)
619 COHON/BLOCK13/NEVESH (185, 4), MDOVEL (185), MCRACK (185), MYAGG (185),
620 MYREO (190), MYCRO (190)
621 IFRGER=4 CALTER, HALTER
622 IF (MYRESH (NEL, I), EQ, 1) GO TO *0
623 IF (ICOUNT, EQ, 2) GO TO 10
624 A (STRESS-TSGMS (NEL, I)+SIGMS (NEL, I)
625 STRAIN-TSMS (NEL, I)+EMS (NEL, I)
626 IF (STRAIN, GT, ZELAND, STRAIN, LT, EN) GO TO 5
627 IF (STRAIN, LE, ZERSOLE, OR, STRAIN, GE, ERSOLE) GO TO 25
628 SHESH (NEL, I)=30000.0
629 RETURN
630
631 5 SHESH (NEL, I)=SHSHOD
632 RETURN
633 10 A (STRESS-TSGMS (NEL, I)
634 STRAIN-TSMS (NEL, I)
635 IF (STRAIN, LT, ZERSOLE, OR, STRAIN, GT, ERSOLE) GO TO 25
636 IF (STRAIN, GE, ZELAND, STRAIN, LE, E2) GO TO 5
637 STRESS=53800.0+430000.0*STRAIN
638 PRCTG=(A (STRESS-STRESS)*100.0)/STRESS
639 IF (PRCTG, GE, PREDEF) GO TO 20
640 SHESH (NEL, I)=STRESS/STRAIN
641 RETURN
642 C RELAXATION IS EMPLOYED TO INCREASE RATE OF CONVERGENCE
643 A (STRAIN-RELAX
644 STRESS=53800.0+430000.0*STRAIN
645 SHESH (NEL, I)=STRESS/ASTRN
646 RETURN
647 25 MYRESH (NEL, I)=1
648 TSMS (NEL, I)=PMS
649 IF (STRAIN, LT, 0.0) TSMS (NEL, I)--PMS
650 SH=0.0
651 WRITE (6, 30) I, NEL
652 FORMAT (' ***** STEEL SHEET LAYER NUMBER', I, ' IN ELEMENT NUMBER ', I
653 15, ' HAS FAILED ***** ')
654 RETURN
655 SH=0.0
656 RETURN
657
658 SUBROUTINE PREST
659 C.....
660 C THIS SUBROUTINE INITIALIZES ALL VARIABLES, VECTORS AND ARRAYS
661 C WHOSE INCORPORATION INTO THE PROGRAM LOGIC NECESSITATES SUCH
662 C PRESTTING
663 C.....
664 C
665 COHON/BLOCK1/NEONS, HEAD, BELT, MURINC, ICOUNT
666 COHON/BLOCK2/NEI, BELT, BELCH, BELD, INDCEL (185), IHELST (185),
667 IINDOVL (185), MIDTNC (185), CAUGLE (185), CALTER (185),
668 ZIBELT (215), ELTNC (215), MDOVEL (215, 4), MDREF (215), DPHMO (215)
669 COHON/BLOCK3/NEISH, IMESH (185), IASZAS (185), MDIENS, PERSTL (185, 4),
670 IANGLE (185, 4), SHSTP (185, 3, 3), SHESH (185, 1)
671 COHON/BLOCK4/NE, NEPO, MDES (190, 2), TNRDM (190), TWRTY (190),
672 IHALTER (190), HARA (190), CARA (190), B (190), B (190), TSGPR (190), TSPRE (190)
673 COHON/BLOCK11/RTOT (750), PROTOT (750), DTOT (750), *2 (2, 750), *2 (2, 750)
674 COHON/BLOCK12/SIGCON (185, 3), PCOM (185, 3), SIGMS (185, 4), EMS (185, 4),
675 IISCON (185, 3), TISCON (185, 3), TISGCC (185), TISGCT (185), TISGAGC (185),
676 ZTECC (185), TECT (185), TSGMS (185, 4), TMS (185, 4), SIGNEO (190),
677 JEREO (190), TSGRO (190), TEREO (190)
678 COHON/BLOCK13/NEVESH (185, 4), MDOVEL (185), MCRACK (185), MYAGG (185),
679 MYREO (190), MYCRO (190)
680 IFRGER=4 CALTER, HALTER
681 IF (MYRESH (NEL, I), EQ, 1) GO TO *0
682 IF (ICOUNT, EQ, 2) GO TO 10
683 A (STRESS-TSGMS (NEL, I)+SIGMS (NEL, I)
684 STRAIN-TSMS (NEL, I)+EMS (NEL, I)
685 IF (STRAIN, GT, ZELAND, STRAIN, LT, EN) GO TO 5
686 IF (STRAIN, LE, ZERSOLE, OR, STRAIN, GE, ERSOLE) GO TO 25
687 SHESH (NEL, I)=30000.0
688 RETURN
689
690 5 SHESH (NEL, I)=SHSHOD
691 RETURN
692 10 A (STRESS-TSGMS (NEL, I)
693 STRAIN-TSMS (NEL, I)
694 IF (STRAIN, LT, ZERSOLE, OR, STRAIN, GT, ERSOLE) GO TO 25
695 IF (STRAIN, GE, ZELAND, STRAIN, LE, E2) GO TO 5
696 STRESS=53800.0+430000.0*STRAIN
697 PRCTG=(A (STRESS-STRESS)*100.0)/STRESS
698 IF (PRCTG, GE, PREDEF) GO TO 20
699 SHESH (NEL, I)=STRESS/STRAIN
700 RETURN
701 C RELAXATION IS EMPLOYED TO INCREASE RATE OF CONVERGENCE
702 A (STRAIN-RELAX
703 STRESS=53800.0+430000.0*STRAIN
704 SHESH (NEL, I)=STRESS/ASTRN
705 RETURN
706 25 MYRESH (NEL, I)=1
707 TSMS (NEL, I)=PMS
708 IF (STRAIN, LT, 0.0) TSMS (NEL, I)--PMS
709 SH=0.0
710 WRITE (6, 30) I, NEL
711 FORMAT (' ***** STEEL SHEET LAYER NUMBER', I, ' IN ELEMENT NUMBER ', I
712 15, ' HAS FAILED ***** ')
713 RETURN
714 SH=0.0
715 RETURN
716
717 SUBROUTINE PREST
718 C.....
719 C THIS SUBROUTINE INITIALIZES ALL VARIABLES, VECTORS AND ARRAYS
720 C WHOSE INCORPORATION INTO THE PROGRAM LOGIC NECESSITATES SUCH
721 C PRESTTING
722 C.....
723 C
724 COHON/BLOCK1/NEONS, HEAD, BELT, MURINC, ICOUNT
725 COHON/BLOCK2/NEI, BELT, BELCH, BELD, INDCEL (185), IHELST (185),
726 IINDOVL (185), MIDTNC (185), CAUGLE (185), CALTER (185),
727 ZIBELT (215), ELTNC (215), MDOVEL (215, 4), MDREF (215), DPHMO (215)
728 COHON/BLOCK3/NEISH, IMESH (185), IASZAS (185), MDIENS, PERSTL (185, 4),
729 IANGLE (185, 4), SHSTP (185, 3, 3), SHESH (185, 1)
730 COHON/BLOCK4/NE, NEPO, MDES (190, 2), TNRDM (190), TWRTY (190),
731 IHALTER (190), HARA (190), CARA (190), B (190), B (190), TSGPR (190), TSPRE (190)
732 COHON/BLOCK11/RTOT (750), PROTOT (750), DTOT (750), *2 (2, 750), *2 (2, 750)
733 COHON/BLOCK12/SIGCON (185, 3), PCOM (185, 3), SIGMS (185, 4), EMS (185, 4),
734 IISCON (185, 3), TISCON (185, 3), TISGCC (185), TISGCT (185), TISGAGC (185),
735 ZTECC (185), TECT (185), TSGMS (185, 4), TMS (185, 4), SIGNEO (190),
736 JEREO (190), TSGRO (190), TEREO (190)
737 COHON/BLOCK13/NEVESH (185, 4), MDOVEL (185), MCRACK (185), MYAGG (185),
738 MYREO (190), MYCRO (190)
739 IFRGER=4 CALTER, HALTER
740 IF (MYRESH (NEL, I), EQ, 1) GO TO *0
741 IF (ICOUNT, EQ, 2) GO TO 10
742 A (STRESS-TSGMS (NEL, I)+SIGMS (NEL, I)
743 STRAIN-TSMS (NEL, I)+EMS (NEL, I)
744 IF (STRAIN, GT, ZELAND, STRAIN, LT, EN) GO TO 5
745 IF (STRAIN, LE, ZERSOLE, OR, STRAIN, GE, ERSOLE) GO TO 25
746 SHESH (NEL, I)=30000.0
747 RETURN
748
749 5 SHESH (NEL, I)=SHSHOD
750 RETURN
751 10 A (STRESS-TSGMS (NEL, I)
752 STRAIN-TSMS (NEL, I)
753 IF (STRAIN, LT, ZERSOLE, OR, STRAIN, GT, ERSOLE) GO TO 25
754 IF (STRAIN, GE, ZELAND, STRAIN, LE, E2) GO TO 5
755 STRESS=53800.0+430000.0*STRAIN
756 PRCTG=(A (STRESS-STRESS)*100.0)/STRESS
757 IF (PRCTG, GE, PREDEF) GO TO 20
758 SHESH (NEL, I)=STRESS/STRAIN
759 RETURN
760 C RELAXATION IS EMPLOYED TO INCREASE RATE OF CONVERGENCE
761 A (STRAIN-RELAX
762 STRESS=53800.0+430000.0*STRAIN
763 SHESH (NEL, I)=STRESS/ASTRN
764 RETURN
765 25 MYRESH (NEL, I)=1
766 TSMS (NEL, I)=PMS
767 IF (STRAIN, LT, 0.0) TSMS (NEL, I)--PMS
768 SH=0.0
769 WRITE (6, 30) I, NEL
770 FORMAT (' ***** STEEL SHEET LAYER NUMBER', I, ' IN ELEMENT NUMBER ', I
771 15, ' HAS FAILED ***** ')
772 RETURN
773 SH=0.0
774 RETURN
775
776 SUBROUTINE PREST
777 C.....
778 C THIS SUBROUTINE INITIALIZES ALL VARIABLES, VECTORS AND ARRAYS
779 C WHOSE INCORPORATION INTO THE PROGRAM LOGIC NECESSITATES SUCH
780 C PRESTTING
781 C.....
782 C
783 COHON/BLOCK1/NEONS, HEAD, BELT, MURINC, ICOUNT
784 COHON/BLOCK2/NEI, BELT, BELCH, BELD, INDCEL (185), IHELST (185),
785 IINDOVL (185), MIDTNC (185), CAUGLE (185), CALTER (185),
786 ZIBELT (215), ELTNC (215), MDOVEL (215, 4), MDREF (215), DPHMO (215)
787 COHON/BLOCK3/NEISH, IMESH (185), IASZAS (185), MDIENS, PERSTL (185, 4),
788 IANGLE (185, 4), SHSTP (185, 3, 3), SHESH (185, 1)
789 COHON/BLOCK4/NE, NEPO, MDES (190, 2), TNRDM (190), TWRTY (190),
790 IHALTER (190), HARA (190), CARA (190), B (190), B (190), TSGPR (190), TSPRE (190)
791 COHON/BLOCK11/RTOT (750), PROTOT (750), DTOT (750), *2 (2, 750), *2 (2, 750)
792 COHON/BLOCK12/SIGCON (185, 3), PCOM (185, 3), SIGMS (185, 4), EMS (185, 4),
793 IISCON (185, 3), TISCON (185, 3), TISGCC (185), TISGCT (185), TISGAGC (185),
794 ZTECC (185), TECT (185), TSGMS (185, 4), TMS (185, 4), SIGNEO (190),
795 JEREO (190), TSGRO (190), TEREO (190)
796 COHON/BLOCK13/NEVESH (185, 4), MDOVEL (185), MCRACK (185), MYAGG (185),
797 MYREO (190), MYCRO (190)
798 IFRGER=4 CALTER, HALTER
799 IF (MYRESH (NEL, I), EQ, 1) GO TO *0
800 IF (ICOUNT, EQ, 2) GO TO 10
801 A (STRESS-TSGMS (NEL, I)+SIGMS (NEL, I)
802 STRAIN-TSMS (NEL, I)+EMS (NEL, I)
803 IF (STRAIN, GT, ZELAND, STRAIN, LT, EN) GO TO 5
804 IF (STRAIN, LE, ZERSOLE, OR, STRAIN, GE, ERSOLE) GO TO 25
805 SHESH (NEL, I)=30000.0
806 RETURN
807
808 5 SHESH (NEL, I)=SHSHOD
809 RETURN
810 10 A (STRESS-TSGMS (NEL, I)
811 STRAIN-TSMS (NEL, I)
812 IF (STRAIN, LT, ZERSOLE, OR, STRAIN, GT, ERSOLE) GO TO 25
813 IF (STRAIN, GE, ZELAND, STRAIN, LE, E2) GO TO 5
814 STRESS=53800.0+430000.0*STRAIN
815 PRCTG=(A (STRESS-STRESS)*100.0)/STRESS
816 IF (PRCTG, GE, PREDEF) GO TO 20
817 SHESH (NEL, I)=STRESS/STRAIN
818 RETURN
819 C RELAXATION IS EMPLOYED TO INCREASE RATE OF CONVERGENCE
820 A (STRAIN-RELAX
821 STRESS=53800.0+430000.0*STRAIN
822 SHESH (NEL, I)=STRESS/ASTRN
823 RETURN
824 25 MYRESH (NEL, I)=1
825 TSMS (NEL, I)=PMS
826 IF (STRAIN, LT, 0.0) TSMS (NEL, I)--PMS
827 SH=0.0
828 WRITE (6, 30) I, NEL
829 FORMAT (' ***** STEEL SHEET LAYER NUMBER', I, ' IN ELEMENT NUMBER ', I
830 15, ' HAS FAILED ***** ')
831 RETURN
832 SH=0.0
833 RETURN
834
835 SUBROUTINE PREST
836 C.....
837 C THIS SUBROUTINE INITIALIZES ALL VARIABLES, VECTORS AND ARRAYS
838 C WHOSE INCORPORATION INTO THE PROGRAM LOGIC NECESSITATES SUCH
839 C PRESTTING
840 C.....
841 C
842 COHON/BLOCK1/NEONS, HEAD, BELT, MURINC, ICOUNT
843 COHON/BLOCK2/NEI, BELT, BELCH, BELD, INDCEL (185), IHELST (185),
844 IINDOVL (185), MIDTNC (185), CAUGLE (185), CALTER (185),
845 ZIBELT (215), ELTNC (215), MDOVEL (215, 4), MDREF (215), DPHMO (215)
846 COHON/BLOCK3/NEISH, IMESH (185), IASZAS (185), MDIENS, PERSTL (185, 4),
847 IANGLE (185, 4), SHSTP (185, 3, 3), SHESH (185, 1)
848 COHON/BLOCK4/NE, NEPO, MDES (190, 2), TNRDM (190), TWRTY (190),
849 IHALTER (190), HARA (190), CARA (190), B (190), B (190), TSGPR (190), TSPRE (190)
850 COHON/BLOCK11/RTOT (750), PROTOT (750), DTOT (750), *2 (2, 750), *2 (2, 750)
851 COHON/BLOCK12/SIGCON (185, 3), PCOM (185, 3), SIGMS (185, 4), EMS (185, 4),
852 IISCON (185, 3), TISCON (185, 3), TISGCC (185), TISGCT (185), TISGAGC (185),
853 ZTECC (185), TECT (185), TSGMS (185, 4), TMS (185, 4), SIGNEO (190),
854 JEREO (190), TSGRO (190), TEREO (190)
855 COHON/BLOCK13/NEVESH (185, 4), MDOVEL (185), MCRACK (185), MYAGG (185),
856 MYREO (190), MYCRO (190)
857 IFRGER=4 CALTER, HALTER
858 IF (MYRESH (NEL, I), EQ, 1) GO TO *0
859 IF (ICOUNT, EQ, 2) GO TO 10
860 A (STRESS-TSGMS (NEL, I)+SIGMS (NEL, I)
861 STRAIN-TSMS (NEL, I)+EMS (NEL, I)
862 IF (STRAIN, GT, ZELAND, STRAIN, LT, EN) GO TO 5
863 IF (STRAIN, LE, ZERSOLE, OR, STRAIN, GE, ERSOLE) GO TO 25
864 SHESH (NEL, I)=30000.0
865 RETURN
866
867 5 SHESH (NEL, I)=SHSHOD
868 RETURN
869 10 A (STRESS-TSGMS (NEL, I)
870 STRAIN-TSMS (NEL, I)
871 IF (STRAIN, LT, ZERSOLE, OR, STRAIN, GT, ERSOLE) GO TO 25
872 IF (STRAIN, GE, ZELAND, STRAIN, LE, E2) GO TO 5
873 STRESS=53800.0+430000.0*STRAIN
874 PRCTG=(A (STRESS-STRESS)*100.0)/STRESS
875 IF (PRCTG, GE, PREDEF) GO TO 20
876 SHESH (NEL, I)=STRESS/STRAIN
877 RETURN
878 C RELAXATION IS EMPLOYED TO INCREASE RATE OF CONVERGENCE
879 A (STRAIN-RELAX
880 STRESS=53800.0+430000.0*STRAIN
881 SHESH (NEL, I)=STRESS/ASTRN
882 RETURN
883 25 MYRESH (NEL, I)=1
884 TSMS (NEL, I)=PMS
885 IF (STRAIN, LT, 0.0) TSMS (NEL, I)--PMS
886 SH=0.0
887 WRITE (6, 30) I, NEL
888 FORMAT (' ***** STEEL SHEET LAYER NUMBER', I, ' IN ELEMENT NUMBER ', I
889 15, ' HAS FAILED ***** ')
890 RETURN
891 SH=0.0
892 RETURN
893
894 SUBROUTINE PREST
895 C.....
896 C THIS SUBROUTINE INITIALIZES ALL VARIABLES, VECTORS AND ARRAYS
897 C WHOSE INCORPORATION INTO THE PROGRAM LOGIC NECESSITATES SUCH
898 C PRESTTING
899 C.....
900 C
901 COHON/BLOCK1/NEONS, HEAD, BELT, MURINC, ICOUNT
902 COHON/BLOCK2/NEI, BELT, BELCH, BELD, INDCEL (185), IHELST (185),
903 IINDOVL (185), MIDTNC (185), CAUGLE (185), CALTER (185),
904 ZIBELT (215), ELTNC (215), MDOVEL (215, 4), MDREF (215), DPHMO (215)
905 COHON/BLOCK3/NEISH, IMESH (185), IASZAS (185), MDIENS, PERSTL (185, 4),
906 IANGLE (185, 4), SHSTP (185, 3, 3), SHESH (185, 1)
907 COHON/BLOCK4/NE, NEPO, MDES (190, 2), TNRDM (190), TWRTY (190),
908 IHALTER (190), HARA (190), CARA (190), B (190), B (190), TSGPR (190), TSPRE (190)
909 COHON/BLOCK11/RTOT (750), PROTOT (750), DTOT (750), *2 (2, 750), *2 (2, 750)
910 COHON/BLOCK12/SIGCON (185, 3), PCOM (185, 3), SIGMS (185, 4), EMS (185, 4),
911 IISCON (185, 3), TISCON (185, 3), TISGCC (185), TISGCT (185), TISGAGC (185),
912 ZTECC (185), TECT (185), TSGMS (185, 4), TMS (185, 4), SIGNEO (190),
913 JEREO (190), TSGRO (190), TEREO (190)
914 COHON/BLOCK13/NEVESH (185, 4), MDOVEL (185), MCRACK (185), MYAGG (185),
915 MYREO (190), MYCRO (190)
916 IFRGER=4 CALTER, HALTER
917 IF (MYRESH (NEL, I), EQ, 1) GO TO *0
918 IF (ICOUNT, EQ, 2) GO TO 10
919 A (STRESS-TSGMS (NEL, I)+SIGMS (NEL, I)
920 STRAIN-TSMS (NEL, I)+EMS (NEL, I)
921 IF (STRAIN, GT, ZELAND, STRAIN, LT, EN) GO TO 5
922 IF (STRAIN, LE, ZERSOLE, OR, STRAIN, GE, ERSOLE) GO TO 25
923 SHESH (NEL, I)=30000.0
924 RETURN
925
926 5 SHESH (NEL, I)=SHSHOD
927 RETURN
928 10 A (STRESS-TSGMS (NEL, I)
929 STRAIN-TSMS (NEL, I)
930 IF (STRAIN, LT, ZERSOLE, OR, STRAIN, GT, ERSOLE) GO TO 25
931 IF (STRAIN, GE, ZELAND, STRAIN, LE, E2) GO TO 5
932 STRESS=53800.0+430000.0*STRAIN
933 PRCTG=(A (STRESS-STRESS)*100.0)/STRESS
934 IF (PRCTG, GE, PREDEF) GO TO 20
935 SHESH (NEL, I)=STRESS/STRAIN
936 RETURN
937 C RELAXATION IS EMPLOYED TO INCREASE RATE OF CONVERGENCE
938 A (STRAIN-RELAX
939 STRESS=53800.0+430000.0*STRAIN
940 SHESH (NEL, I)=STRESS/ASTRN
941 RETURN
942 25 MYRESH (NEL, I)=1
943 TSMS (NEL, I)=PMS
944 IF (STRAIN, LT, 0.0) TSMS (NEL, I)--PMS
945 SH=0.0
946 WRITE (6, 30) I, NEL
947 FORMAT (' ***** STEEL SHEET LAYER NUMBER', I, ' IN ELEMENT NUMBER ', I
948 15, ' HAS FAILED ***** ')
949 RETURN
950 SH=0.0
951 RETURN
952
953 SUBROUTINE PREST
954 C.....
955 C THIS SUBROUTINE INITIALIZES ALL VARIABLES, VECTORS AND ARRAYS
956 C WHOSE INCORPORATION INTO THE PROGRAM LOGIC NECESSITATES SUCH
957 C PRESTTING
958 C.....
959 C
960 COHON/BLOCK1/NEONS, HEAD, BELT, MURINC, ICOUNT
961 COHON/BLOCK2/NEI, BELT, BELCH, BELD, INDCEL (185), IHELST (185),
962 IINDOVL (185), MIDTNC (185), CAUGLE (185), CALTER (185),
963 ZIBELT (215), ELTNC (215), MDOVEL (215, 4), MDREF (215), DPHMO (215)
964 COHON/BLOCK3/NEISH, IMESH (185), IASZAS (185), MDIENS, PERSTL (185, 4),
965 IANGLE (185, 4), SHSTP (185, 3, 3), SHESH (185, 1)
966 COHON/BLOCK4/NE, NEPO, MDES (190, 2), TNRDM (190), TWRTY (190),
967 IHALTER (190), HARA (190), CARA (190), B (190), B (190), TSGPR (190), TSPRE (190)
968 COHON/BLOCK11/RTOT (750), PROTOT (750), DTOT (750), *2 (2, 750), *2 (2, 750)
969 COHON/BLOCK12/SIGCON (185, 3), PCOM (185, 3), SIGMS (185, 4), EMS (185, 4),
970 IISCON (185, 3), TISCON (185, 3), TISGCC (185), TISGCT (185), TISGAGC (185),
971 ZTECC (185), TECT (185), TSGMS (185, 4), TMS (185, 4), SIGNEO (190),
972 JEREO (190), TSGRO (190), TEREO (190)
973 COHON/BLOCK13/NEVESH (185, 4), MDOVEL (185), MCRACK (185), MYAGG (185),
974 MYREO (190), MYCRO (190)
975 IFRGER=4 CALTER, HALTER
976 IF (MYRESH (NEL, I), EQ, 1) GO TO *0
977 IF (ICOUNT, EQ, 2) GO TO 10
978 A (STRESS-TSGMS (NEL, I)+SIGMS (NEL, I)
979 STRAIN-TSMS (NEL, I)+EMS (NEL, I)
980 IF (STRAIN, GT, ZELAND, STRAIN, LT, EN) GO TO 5
981 IF (STRAIN, LE, ZERSOLE, OR, STRAIN, GE, ERSOLE) GO TO 25
982 SHESH (NEL, I)=30000.0
983 RETURN
984
985 5 SHESH (NEL, I)=SHSHOD
986 RETURN
987 10 A (STRESS-TSGMS (NEL, I)
988 STRAIN-TSMS (NEL, I)
989 IF (STRAIN, LT, ZERSOLE, OR, STRAIN, GT, ERSOLE) GO TO 25
990 IF (STRAIN, GE, ZELAND, STRAIN, LE, E2) GO TO 5
991 STRESS=53800.0+430000.0*STRAIN
992 PRCTG=(A (STRESS-STRESS)*100.0)/STRESS
993 IF (PRCTG, GE, PREDEF) GO TO 20
994 SHESH (NEL, I)=STRESS/STRAIN
995 RETURN
996 C RELAXATION IS EMPLOYED TO INCREASE RATE OF CONVERGENCE
997 A (STRAIN-RELAX
998 STRESS=53800.0+430000.0*STRAIN
999 SHESH (NEL, I)=STRESS/ASTRN
1000 RETURN
1001 25 MYRESH (NEL, I)=1
1002 TSMS (NEL, I)=PMS
1003 IF (STRAIN, LT, 0.0) TSMS (NEL, I)--PMS
1004 SH=0.0
1005 WRITE (6, 30) I, NEL
1006 FORMAT (' ***** STEEL SHEET LAYER NUMBER', I, ' IN ELEMENT NUMBER ', I
1007 15, ' HAS FAILED ***** ')
1008 RETURN
1009 SH=0.0
1010 RETURN

```

```

599 2INELTY(215), ELTWH(215), MODELL(215), MDRP(215), DPHMOD(215)
600 COMMON/BLOCK1/HR, HRO, MODRS(190,2), CARA(190), INRTY(190),
601 VALYER(190), BARRA(190), CARA(190), BSTR(190), TSGPRE(190), TEPRE(190)
602 COMMON/BLOCK2/CONMOD, RMOD, PREMOD, PREMOD, SLMOD, SLMOD, FC, FT,
603 TPAE, PFR, PUP, PUS, DP, KSLIP, KULT, RESULT, RESULT, P1, P2, P3, P4,
604 2RU, TERRO, REPR, CONDEV, DEVCON, DEVRKO, PRDEV, SLDREV, IDEM, ATGSP, PLAI
605 COMMON/BLOCK3/ICOM(185, 3), ECOM(185, 3), SIGM(185, 4), EAS(185, 4),
606 TSGCOM(185, 3), TFCOM(185, 3), TSGCC(185), TSGCT(185), TSGAG(185),
607 ZIGCC(185), ZIGCT(185), TSGHS(185, 4), TENS(185, 4), SIGPRE(190),
608 3REZO(190), TSGRO(190), TERRO(190)
609 INTERGR4 CALTER, HALTER
610 CHECK ON CRUSHING FAILURE OF CONCRETE
611 DO 50 I=1, NLT
612 HEL=I
613 IF(TSGCC(I)-GE.0.0) GO TO 50
614 IF(TSGCT(I)-LT.0.0) GO TO 10
615 IF(TSGCC(I)-LE.PC) GO TO 100
616 GO TO 50
617 ALPHA=TSGCT(I)/TSGCC(I)
618 IF(ALPHA-GE.2) GO TO 20
619 PFAIL=(1.0-ALPHA)*PC
620 GO TO 30
621 PFAIL=1.2*PC
622 30 IF(TSGCC(BEL).LE.PFAIL) GO TO 100
623 50 CONTINUE
624 C
625 CHECK ON FAILURE OF PRESTRESS STRANDS
626 DO 90 I=1, NRO
627 IF(HRNY(I)-HR.0) GO TO 90
628 IF(TERRO(I)-GE.PULT) GO TO 110
629 CONTINUE
630 RETURN
631 100 WRITE(6,105) I, TSGCC(I), TSGCT(I)
632 WRITE(7,105) I, TSGCC(I), TSGCT(I)
633 105 FORMAT('.....', //, '... BEAN FAILURE .....', //)
634 CRUSHING OF CONCRTE', //, ELEMENT NUMBER', I5, ' HAS FAILED BY
635 3' PRINCIPAL TENSILE STRESS =', E13.5)
636 STOP
637 110 WRITE(6,115) I, TERRO(I)
638 WRITE(7,115) I, TERRO(I)
639 115 FORMAT('.....', //, '... BEAN FAILURE .....', //)
640 1' PRESTRESS REINFORCEMENT NUMBER', I5
641 2, ' HAS FAILED IN TENSION', //, TENSILE STRAIN IN CABLE AT FAILURE =
642 2', E13.5)
643 STOP
644 END
645 SUBROUTINE DEFIL(LO)
646 C.....
647 C THIS SUBROUTINE CHECKS THE (STRESS, STRAIN) CONDITION OF ALL
648 MATERIALS TO DETECT IF ANY DEVIATION FROM THE RESPECTIVE
649 MATERIAL BEHAVIOUR HAS OCCURRED. ALSO, THE AGGREGATE INTERLOCK
650 LEAKAGE FOR CHECKED ELEMENTS IS CHECKED FOR FAILURE.
651 C.....
652 C
653 COMMON/BLOCK1/HR05, BRAND, BELK, BULCHK, BELD, INDCEL(185), IMBELSI(185),
654 1INDOIL(185), HINDHC(185), CANGLE(185), CALTER(185),
655 2INELTY(215), ELTWH(215), MODELL(215, 4), MDRP(215), DPHMOD(215)
656 COMMON/BLOCK2/HR, HRO, MODRS(185, 4), TENS(185, 4), HDIENS, PERSTL(185, 4),
657 1ANGLE(185, 4), SHSTP(185, 3), TRESH(185, 1)
658

```

```

599 COMMON/BLOCK1/HR, HRO, MODRS(190,2), CARA(190), INRTY(190),
600 VALYER(190), BARRA(190), CARA(190), BSTR(190), TSGPRE(190), TEPRE(190)
601 COMMON/BLOCK2/CONMOD, RMOD, PREMOD, PREMOD, SLMOD, SLMOD, FC, FT,
602 TPAE, PFR, PUP, PUS, DP, KSLIP, KULT, RESULT, RESULT, P1, P2, P3, P4,
603 2RU, TERRO, REPR, CONDEV, DEVCON, DEVRKO, PRDEV, SLDREV, IDEM, ATGSP, PLAI
604 COMMON/BLOCK3/ICOM(185, 3), ECOM(185, 3), SIGM(185, 4), EAS(185, 4),
605 TSGCOM(185, 3), TFCOM(185, 3), TSGCC(185), TSGCT(185), TSGAG(185),
606 ZIGCC(185), ZIGCT(185), TSGHS(185, 4), TENS(185, 4), SIGPRE(190),
607 3REZO(190), TSGRO(190), TERRO(190)
608 1DCBC(185, 3), DCRACK(185), DAGG(185)
609 COMMON/BLOCK11/HRSHR(185, 4), HDOWEL(185), HCRACK(185), H1AGG(185),
610 1RYFO(190), WYREZO(190)
611 COMMON/BLOCK14/IDELM, ICOM3, ICOMPR, IMPSR, IREO, ILOAD, TLOAD, ISTIP,
612 1HAKIT, WYTCOM, WYTFPO, WYTPRE
613 ID=0
614 C IF ANY SIGNIFICANT DEVIATION OF CURS, LD YS INCREMNTED.
615 FIRSTLY, CONCRETE BEHAVIOUR IN PRINCIPAL DIRECTIONS IS CHECKED
616 DO 20 I=1, NLT
617 IF(CRACK(I)-Z0.-1) GO TO 20
618 IF(CRACK(I)-LT.-1.0R, MCRACK(I)-GT.1) GO TO 12
619 BEL=I
620 CALL PRNCS
621 CALL PRNCE
622 STRESS=TSGCC(BEL)
623 STRO=TSGCT(BEL)
624 STRAIN=TSGC(BEL)
625 IF(STRESS-GE.-1000.0-OR-STRAIN-GE.0.0) GO TO 12
626 IF THE PRINCIPAL COMPRESSIVE STRESS IS LESS THAN 1000 PSI,
627 DEVIATION WILL BE SMALL IN ALL OF THE CALCULATIONS BELOW. SIGA
628 IS THE CORRECT VALUE OF STRESS THAT CORRESPONDS TO THE
629 MATERIAL ELEMENT STRAIN.
630 P5=PC/ACULT
631 ALPHA=STRO/STRESS
632 IF(STRESS-GE.0.0-AND-STRO-GE.0.0) P=P2
633 IF(STRESS-LT.0.0-AND-STRO-LT.0.0) P=P1
634 IF(MCRACK(BEL).NE.0) GO TO 5
635 SIGA=STRAIN*COMMOD/((1.0-P*ALPHA)*(1.0*(COMMOD/(1.0-P*ALPHA)*ES
636 1)-2.0)*STRAIN/ZCULT+(STRAIN/ZCULT)**2))
637 GO TO 10
638 5 SIGA=STRAIN*COMMOD/(1.0*(COMMOD/ES-2.0)*STRAIN/ZCULT+
639 1(STRAIN/ZCULT)**2)
640 CDEVI=CONDEV*2.0
641 IF(STRESS-LT.-1000.0) GO TO 11
642 IF(PFCTG-GE.-CONDEV-AND-PFCTG-LE.CDEVI) GO TO 12
643 IF(PFCTG-LE.-CONDEV-AND-PFCTG-LE.CDEVI) GO TO 12
644 WRITE(6,100) I, STRESS, STRO, STRAIN, ALPHA, SIGA, PFCTG
645 WRITE(7,100) I, STRESS, STRO, STRAIN, ALPHA, SIGA, PFCTG
646 FORHA1/' CONCRETE DEVIATION CHECK FOR ELEMENT NO.', I3/
647 1' STRESS =', E14.5, ' STRO =', E14.5, ' STRAIN =', E14.5/
648 2' ALPHA =', E14.5, ' SIGA =', E14.5, ' PFCTG =', E14.5/
649 1' TEGOM(BEL, 3) =', E12, ' TSGCOM(BEL, 3) =', E14.5/
650 120 WRITE(6,120) I, COMHT, TSGCOM(BEL, 3), J=1, 3), TSGCOM(BEL, J), J=1, 3)
651 FORHA1(' I, COMHT =', E12, ' TSGCOM(BEL, 3) =', E14.5/
652 1D-ID=WTCON
653 WRITE(6,105)
654 WRITE(7,105)

```

```

719 C
720 C
721 C
722 C
723 C
724 C
725 C
726 C
727 C
728 C
729 C
730 C
731 C
732 C
733 C
734 C
735 C
736 C
737 C
738 C
739 C
740 C
741 C
742 C
743 C
744 C
745 C
746 C
747 C
748 C
749 C
750 C
751 C
752 C
753 C
754 C
755 C
756 C
757 C
758 C
759 C
760 C
761 C
762 C
763 C
764 C
765 C
766 C
767 C
768 C
769 C
770 C
771 C
772 C
773 C
774 C
775 C
776 C
777 C
778 C

105 'FORMAT', ***** ELEMENT HAS DEVIATED *****
C
C
C
12 DO 17 J=1,NRETS
  IF (VRESH(1,J),EQ.1) GO TO 17
  IF (ICOUNT.EQ.2) GO TO 13
  STRESS=TSCHS(1,J)*SIGS(1,J)
  STRAIN=TRHS(1,J)*EPS(1,J)
  GO TO 14
13 STRESS=TSCHS(1,J)
  STRAIN=TRHS(1,J)
14 IF (STRAIN.LT..00185) GO TO 17
  STRESS=53600.0*STRAIN+430000.0
  PERCTG=(ASTRESS-STRESS)*100.0/STRESS
  IF (PERCTG.LT.PRDDEV) GO TO 17
  WRITE (6,160) J,NEL,ASTRESS,STRAIN,STRESS,PERCTG
  WRITE (7,160) J,NEL,ASTRESS,STRAIN,STRESS,PERCTG
  FORMAT('/// ***** SHEAR STRESS, STRAIN, STRESS, PERCTG
160 '/// ***** ELEMENT NUMBER', I4,
  STRAIN=',E14.5', STRESS=',E14.5', PERCTG=',E14.5',
  /)
17 CONTINUE
C
C
C
130 AGGREGATE INTERLOCK LINKAGE FAILURE CHECK
  IF (CRACK(NEL),NE.1) GO TO 20
  IF (TSAGG(NEL)-GT.PAGG-AND.TSGAGG(NEL).LT.-PAGG) GO TO 20
  NYAG(NEL)=1
  WRITE (6,130) NEL,TSAGG(NEL)
  FORMAT('/// ***** AGGREGATE INTERLOCK LINKAGE FOR ELEMENT NO.',I3,
  ' HAS FAILED *****',//, ' SHEAR STRESS ACROSS CRACK =',E14.5)
  TSAGG(NEL)=0.0
  DAGG(NEL)=100.0
  GO TO 20
20 CONTINUE
C
C
C
20 REINFORCEMENT ELEMENTS' BEHAVIOUR IS EXAMINED TO DETECT ANY
  SIGNIFICANT DEVIATION. EITHER CONVENTIONAL REINFORCEMENT
  OR BOND LINKAGE DEVIATION WILL INITIATE A FURTHER ITERATION
  DO 35 I=1,NREDO
  IF (BYREO(I),EQ.1) GO TO 35
  IF (ICOUNT.EQ.2) GO TO 24
  STRESS=SIGREO(I)*TSGREO(I)
  STRAIN=EREO(I)+TEREO(I)
  GO TO 25
24 STRESS=TSGREO(I)
  STRAIN=TEREO(I)
  IF (INITY(I)) 26,27,28
  CHECK TO DETECT CONVENTIONAL REINFORCEMENT ELEMENT THAT HAS
  JUST YIELDED
  IF (STRAIN.LT.EZERO.OR.NYCREO(I).EQ.1) GO TO 35
  NYCREO(I)=1
  ID-ID*NYREO
  WRITE (6,140) I,STRESS, STRAIN
  WRITE (7,140) I,STRESS, STRAIN
  FORMAT('/// CONVENTIONAL REINFORCEMENT ELEMENT NUMBER',I3,
  ' HAS JUST YIELDED',//, ' STRESS=',E14.5, ' STRAIN=',E14.5)
  GO TO 35
27 DEVIATION CHECK FOR PRESTRESS STRAND
  IF (STRAIN.GT.EZERO) NYCREO(I)=1
  IF (STRAIN.LT.EZERO) GO TO 35
  SIGA=255360.0+470000.0*STRAIN
  DEV=PREDEV
  THE STRESS-STRAIN STATE OF ANY PRESTRESS STRAND THAT HAS ALREADY
  YIELDED IS PRINTED OUT
  IF (NYCREO(I),NE.1) GO TO 29
  WRITE (6,150) I,STRESS,STRAIN
  WRITE (7,150) I,STRESS,STRAIN
  FORMAT('/// ***** PRESTRESS ELEMENT NUMBER',I3, ' IS YIELDING *****
150 '/// STRESS=',E14.5, ' STRAIN=',E14.5)
  GO TO 29
28 DO-STRAIN
  SIGA=(1950000.0*DD-2.35E+09*DD**2+1.39E+12*DD**3-.33E+15*DD**4)*
  /SOFT(YC/50000.0)
  DEV=SLPDEV
  IF (STRESS.LT.0.0) SIGA=-SIGA
  PERCTG=(STRESS-SIGA)*100.0/SIGA
  IF (PERCTG.GT.-DEV-AND.PERCTG.LT.DEV) GO TO 35
  IF (INITY(I),EQ.1) GO TO 32
  WRITE (6,110) I,STRESS,STRAIN,SIGA,PERCTG
  WRITE (7,110) I,STRESS,STRAIN,SIGA,PERCTG
  FORMAT('/// PRESTRESS ELEMENT NUMBER',I3,
  ' HAS DEVIATED SIGNIFICANTLY',//, ' STRESS=',E14.5,
  ' STRAIN=',E14.5, ' SIGA=',E14.5, ' PERCTG =',E14.5)
  ID-ID*NYTPE
  GO TO 35
32 IF (STRAIN.LT..0001) GO TO 35
  WRITE (6,33) I,PERCTG,DEV
  FORMAT('/// BOND SLIP REINFORCEMENT NO.',I3, ' HAS DEVIATED SIGNIFICA
  INTLY',//, ' PERCENTAGE DEVIATION =',E15.5)
  2. WHILE ALLOWABLE DEVIATION PERCENTAGE =',E15.5/)
35 CONTINUE
  RETURN
  END
  END OF FILE

```



```

1 LIST FILE52(1,1721)
2 SUBROUTINE TOTSTP(NS1,NS2,NS3,TS,AL,AB)
3 C*****
4 C THIS SUBROUTINE ASSEMBLES THE TOTAL STIFFNESS MATRIX BLOCK BY
5 C BLOCK (EACH BLOCK BEING A BAND WIDTH SQUARE). AS EACH BLOCK IS
6 C COMPLETELY FILLED, IT IS WRITTEN OUT ON DISC STORAGE
7 C*****
8 C*****
9 C*****
10 C*****
11 C*****
12 C*****
13 C*****
14 C*****
15 C*****
16 C*****
17 C*****
18 C*****
19 C*****
20 C*****
21 C*****
22 C*****
23 C*****
24 C*****
25 C*****
26 C*****
27 C*****
28 C*****
29 C*****
30 C*****
31 C*****
32 C*****
33 C*****
34 C*****
35 C*****
36 C*****
37 C*****
38 C*****
39 C*****
40 C*****
41 C*****
42 C*****
43 C*****
44 C*****
45 C*****
46 C*****
47 C*****
48 C*****
49 C*****
50 C*****
51 C*****
52 C*****
53 C*****
54 C*****
55 C*****
56 C*****
57 C*****
58 C*****
59 C*****
60 C*****
61 C*****
62 C*****
63 C*****
64 C*****
65 C*****
66 C*****
67 C*****
68 C*****
69 C*****
70 C*****
71 C*****
72 C*****
73 C*****
74 C*****
75 C*****
76 C*****
77 C*****
78 C*****
79 C*****
80 C*****
81 C*****
82 C*****
83 C*****
84 C*****
85 C*****
86 C*****
87 C*****
88 C*****
89 C*****
90 C*****
91 C*****
92 C*****
93 C*****
94 C*****
95 C*****
96 C*****
97 C*****
98 C*****
99 C*****
100 C*****
101 C*****
102 C*****
103 C*****
104 C*****
105 C*****
106 C*****
107 C*****
108 C*****
109 C*****
110 C*****
111 C*****
112 C*****
113 C*****
114 C*****
115 C*****
116 C*****
117 C*****
118 C*****
119 C*****
120 C*****
121 C*****
122 C*****
123 C*****
124 C*****
125 C*****
126 C*****
127 C*****
128 C*****
129 C*****
130 C*****
131 C*****
132 C*****
133 C*****
134 C*****
135 C*****
136 C*****
137 C*****
138 C*****
139 C*****
140 C*****
141 C*****
142 C*****
143 C*****
144 C*****
145 C*****
146 C*****
147 C*****
148 C*****
149 C*****
150 C*****
151 C*****
152 C*****
153 C*****
154 C*****
155 C*****
156 C*****
157 C*****
158 C*****
159 C*****
160 C*****
161 C*****
162 C*****
163 C*****
164 C*****
165 C*****
166 C*****
167 C*****
168 C*****
169 C*****
170 C*****
171 C*****
172 C*****
173 C*****
174 C*****
175 C*****
176 C*****
177 C*****
178 C*****
179 C*****
180 C*****
181 C*****
182 C*****
183 C*****
184 C*****
185 C*****
186 C*****
187 C*****
188 C*****
189 C*****
190 C*****
191 C*****
192 C*****
193 C*****
194 C*****
195 C*****
196 C*****
197 C*****
198 C*****
199 C*****
200 C*****
201 C*****
202 C*****
203 C*****
204 C*****
205 C*****
206 C*****
207 C*****
208 C*****
209 C*****
210 C*****
211 C*****
212 C*****
213 C*****
214 C*****
215 C*****
216 C*****
217 C*****
218 C*****
219 C*****
220 C*****
221 C*****
222 C*****
223 C*****
224 C*****
225 C*****
226 C*****
227 C*****
228 C*****
229 C*****
230 C*****
231 C*****
232 C*****
233 C*****
234 C*****
235 C*****
236 C*****
237 C*****
238 C*****
239 C*****
240 C*****
241 C*****
242 C*****
243 C*****
244 C*****
245 C*****
246 C*****
247 C*****
248 C*****
249 C*****
250 C*****
251 C*****
252 C*****
253 C*****
254 C*****
255 C*****
256 C*****
257 C*****
258 C*****
259 C*****
260 C*****
261 C*****
262 C*****
263 C*****
264 C*****
265 C*****
266 C*****
267 C*****
268 C*****
269 C*****
270 C*****
271 C*****
272 C*****
273 C*****
274 C*****
275 C*****
276 C*****
277 C*****
278 C*****
279 C*****
280 C*****
281 C*****
282 C*****
283 C*****
284 C*****
285 C*****
286 C*****
287 C*****
288 C*****
289 C*****
290 C*****
291 C*****
292 C*****
293 C*****
294 C*****
295 C*****
296 C*****
297 C*****
298 C*****
299 C*****
300 C*****
301 C*****
302 C*****
303 C*****
304 C*****
305 C*****
306 C*****
307 C*****
308 C*****
309 C*****
310 C*****
311 C*****
312 C*****
313 C*****
314 C*****
315 C*****
316 C*****
317 C*****
318 C*****
319 C*****
320 C*****
321 C*****
322 C*****
323 C*****
324 C*****
325 C*****
326 C*****
327 C*****
328 C*****
329 C*****
330 C*****
331 C*****
332 C*****
333 C*****
334 C*****
335 C*****
336 C*****
337 C*****
338 C*****
339 C*****
340 C*****
341 C*****
342 C*****
343 C*****
344 C*****
345 C*****
346 C*****
347 C*****
348 C*****
349 C*****
350 C*****
351 C*****
352 C*****
353 C*****
354 C*****
355 C*****
356 C*****
357 C*****
358 C*****
359 C*****
360 C*****
361 C*****
362 C*****
363 C*****
364 C*****
365 C*****
366 C*****
367 C*****
368 C*****
369 C*****
370 C*****
371 C*****
372 C*****
373 C*****
374 C*****
375 C*****
376 C*****
377 C*****
378 C*****
379 C*****
380 C*****
381 C*****
382 C*****
383 C*****
384 C*****
385 C*****
386 C*****
387 C*****
388 C*****
389 C*****
390 C*****
391 C*****
392 C*****
393 C*****
394 C*****
395 C*****
396 C*****
397 C*****
398 C*****
399 C*****
400 C*****
401 C*****
402 C*****
403 C*****
404 C*****
405 C*****
406 C*****
407 C*****
408 C*****
409 C*****
410 C*****
411 C*****
412 C*****
413 C*****
414 C*****
415 C*****
416 C*****
417 C*****
418 C*****
419 C*****
420 C*****
421 C*****
422 C*****
423 C*****
424 C*****
425 C*****
426 C*****
427 C*****
428 C*****
429 C*****
430 C*****
431 C*****
432 C*****
433 C*****
434 C*****
435 C*****
436 C*****
437 C*****
438 C*****
439 C*****
440 C*****
441 C*****
442 C*****
443 C*****
444 C*****
445 C*****
446 C*****
447 C*****
448 C*****
449 C*****
450 C*****
451 C*****
452 C*****
453 C*****
454 C*****
455 C*****
456 C*****
457 C*****
458 C*****
459 C*****
460 C*****
461 C*****
462 C*****
463 C*****
464 C*****
465 C*****
466 C*****
467 C*****
468 C*****
469 C*****
470 C*****
471 C*****
472 C*****
473 C*****
474 C*****
475 C*****
476 C*****
477 C*****
478 C*****
479 C*****
480 C*****
481 C*****
482 C*****
483 C*****
484 C*****
485 C*****
486 C*****
487 C*****
488 C*****
489 C*****
490 C*****
491 C*****
492 C*****
493 C*****
494 C*****
495 C*****
496 C*****
497 C*****
498 C*****
499 C*****
500 C*****
501 C*****
502 C*****
503 C*****
504 C*****
505 C*****
506 C*****
507 C*****
508 C*****
509 C*****
510 C*****
511 C*****
512 C*****
513 C*****
514 C*****
515 C*****
516 C*****
517 C*****
518 C*****
519 C*****
520 C*****
521 C*****
522 C*****
523 C*****
524 C*****
525 C*****
526 C*****
527 C*****
528 C*****
529 C*****
530 C*****
531 C*****
532 C*****
533 C*****
534 C*****
535 C*****
536 C*****
537 C*****
538 C*****
539 C*****
540 C*****
541 C*****
542 C*****
543 C*****
544 C*****
545 C*****
546 C*****
547 C*****
548 C*****
549 C*****
550 C*****
551 C*****
552 C*****
553 C*****
554 C*****
555 C*****
556 C*****
557 C*****
558 C*****
559 C*****
560 C*****
561 C*****
562 C*****
563 C*****
564 C*****
565 C*****
566 C*****
567 C*****
568 C*****
569 C*****
570 C*****
571 C*****
572 C*****
573 C*****
574 C*****
575 C*****
576 C*****
577 C*****
578 C*****
579 C*****
580 C*****
581 C*****
582 C*****
583 C*****
584 C*****
585 C*****
586 C*****
587 C*****
588 C*****
589 C*****
590 C*****
591 C*****
592 C*****
593 C*****
594 C*****
595 C*****
596 C*****
597 C*****
598 C*****
599 C*****
600 C*****
601 C*****
602 C*****
603 C*****
604 C*****
605 C*****
606 C*****
607 C*****
608 C*****
609 C*****
610 C*****
611 C*****
612 C*****
613 C*****
614 C*****
615 C*****
616 C*****
617 C*****
618 C*****
619 C*****
620 C*****
621 C*****
622 C*****
623 C*****
624 C*****
625 C*****
626 C*****
627 C*****
628 C*****
629 C*****
630 C*****
631 C*****
632 C*****
633 C*****
634 C*****
635 C*****
636 C*****
637 C*****
638 C*****
639 C*****
640 C*****
641 C*****
642 C*****
643 C*****
644 C*****
645 C*****
646 C*****
647 C*****
648 C*****
649 C*****
650 C*****
651 C*****
652 C*****
653 C*****
654 C*****
655 C*****
656 C*****
657 C*****
658 C*****
659 C*****
660 C*****
661 C*****
662 C*****
663 C*****
664 C*****
665 C*****
666 C*****
667 C*****
668 C*****
669 C*****
670 C*****
671 C*****
672 C*****
673 C*****
674 C*****
675 C*****
676 C*****
677 C*****
678 C*****
679 C*****
680 C*****
681 C*****
682 C*****
683 C*****
684 C*****
685 C*****
686 C*****
687 C*****
688 C*****
689 C*****
690 C*****
691 C*****
692 C*****
693 C*****
694 C*****
695 C*****
696 C*****
697 C*****
698 C*****
699 C*****
700 C*****
701 C*****
702 C*****
703 C*****
704 C*****
705 C*****
706 C*****
707 C*****
708 C*****
709 C*****
710 C*****
711 C*****
712 C*****
713 C*****
714 C*****
715 C*****
716 C*****
717 C*****
718 C*****
719 C*****
720 C*****
721 C*****
722 C*****
723 C*****
724 C*****
725 C*****
726 C*****
727 C*****
728 C*****
729 C*****
730 C*****
731 C*****
732 C*****
733 C*****
734 C*****
735 C*****
736 C*****
737 C*****
738 C*****
739 C*****
740 C*****
741 C*****
742 C*****
743 C*****
744 C*****
745 C*****
746 C*****
747 C*****
748 C*****
749 C*****
750 C*****
751 C*****
752 C*****
753 C*****
754 C*****
755 C*****
756 C*****
757 C*****
758 C*****
759 C*****
760 C*****
761 C*****
762 C*****
763 C*****
764 C*****
765 C*****
766 C*****
767 C*****
768 C*****
769 C*****
770 C*****
771 C*****
772 C*****
773 C*****
774 C*****
775 C*****
776 C*****
777 C*****
778 C*****
779 C*****
780 C*****
781 C*****
782 C*****
783 C*****
784 C*****
785 C*****
786 C*****
787 C*****
788 C*****
789 C*****
790 C*****
791 C*****
792 C*****
793 C*****
794 C*****
795 C*****
796 C*****
797 C*****
798 C*****
799 C*****
800 C*****
801 C*****
802 C*****
803 C*****
804 C*****
805 C*****
806 C*****
807 C*****
808 C*****
809 C*****
810 C*****
811 C*****
812 C*****
813 C*****
814 C*****
815 C*****
816 C*****
817 C*****
818 C*****
819 C*****
820 C*****
821 C*****
822 C*****
823 C*****
824 C*****
825 C*****
826 C*****
827 C*****
828 C*****
829 C*****
830 C*****
831 C*****
832 C*****
833 C*****
834 C*****
835 C*****
836 C*****
837 C*****
838 C*****
839 C*****
840 C*****
841 C*****
842 C*****
843 C*****
844 C*****
845 C*****
846 C*****
847 C*****
848 C*****
849 C*****
850 C*****
851 C*****
852 C*****
853 C*****
854 C*****
855 C*****
856 C*****
857 C*****
858 C*****
859 C*****
860 C*****
861 C*****
862 C*****
863 C*****
864 C*****
865 C*****
866 C*****
867 C*****
868 C*****
869 C*****
870 C*****
871 C*****
872 C*****
873 C*****
874 C*****
875 C*****
876 C*****
877 C*****
878 C*****
879 C*****
880 C*****
881 C*****
882 C*****
883 C*****
884 C*****
885 C*****
886 C*****
887 C*****
888 C*****
889 C*****
890 C*****
891 C*****
892 C*****
893 C*****
894 C*****
895 C*****
896 C*****
897 C*****
898 C*****
899 C*****
900 C*****
901 C*****
902 C*****
903 C*****
904 C*****
905 C*****
906 C*****
907 C*****
908 C*****
909 C*****
910 C*****
911 C*****
912 C*****
913 C*****
914 C*****
915 C*****
916 C*****
917 C*****
918 C*****
919 C*****
920 C*****
921 C*****
922 C*****
923 C*****
924 C*****
925 C*****
926 C*****
927 C*****
928 C*****
929 C*****
930 C*****
931 C*****
932 C*****
933 C*****
934 C*****
935 C*****
936 C*****
937 C*****
938 C*****
939 C*****
940 C*****
941 C*****
942 C*****
943 C*****
944 C*****
945 C*****
946 C*****
947 C*****
948 C*****
949 C*****
950 C*****
951 C*****
952 C*****
953 C*****
954 C*****
955 C*****
956 C*****
957 C*****
958 C*****
959 C*****
960 C*****
961 C*****
962 C*****
963 C*****
964 C*****
965 C*****
966 C*****
967 C*****
968 C*****
969 C*****
970 C*****
971 C*****
972 C*****
973 C*****
974 C*****
975 C*****
976 C*****
977 C*****
978 C*****
979 C*****
980 C*****
981 C*****
982 C*****
983 C*****
984 C*****
985 C*****
986 C*****
987 C*****
988 C*****
989 C*****
990 C*****
991 C*****
992 C*****
993 C*****
994 C*****
995 C*****
996 C*****
997 C*****
998 C*****
999 C*****
1000 C*****

```

```

DO 8 J=1,3
DC (I,J)=DC (I,J)+CONMOD/(1.0-P1)**2)
DO 8 K=1,NELT
DCORC(K,I,J)=DC (I,J)
CONTINUE
DO 9 I=1,NELT
DAGG(I)=DC (I,3)
CONTINUE
NELE=0
NELEND=0
NELESH=0
IF (NELE.GT.NURBLK) GO TO 300
CALCULATION OF THE LOWEST AND HIGHEST MODE NUMBERS (HMAX AND HMIN)
WHOSE STIFFNESSES ARE TO BE ADDED INTO THE TOTAL STIFFNESS
BLOCK NUMBER NBLK. ALSO, THE HIGHEST MODE NUMBER (HMAXOLD) OF
THE PREVIOUS BLOCK IS CALCULATED TO BE USED IN CHECKING WHICH
ELEMENTS HAVE ALREADY BEEN ADDED INTO PREVIOUS BLOCKS.
HAXEN=NBLK+NBAND
IF (HAXEN.GT.NEQNS) HAXEN=NEQNS
HMINQ=(NBLK-1)*NBAND+1
HAXOLD=(NBLK-1)*NBAND
IF (NBLK.EQ.1) HAXOLD=0
NEQ=HAXEN
CALL MODLOC (NEQ,NE)
HMAX=NE
NEQ=HMINQ
CALL MODLOC (NEQ,NE)
HMIN=NE
NEQ=HAXOLD
CALL MODLOC (NEQ,NE)
HAXOLD=NE
IF (ISTIP.EQ.0) GO TO 12
WRITE (6,605) NBLK,HMIN,HMAX,HAXOLD
605 FORMAT (//,' *** NBLK=',I2,' ****',/, ' HMIN=',I3, ' HMAX=',I3
1, ' HAXOLD(PREVIOUS HMAX)',I3)
C SEARCH FOR CONCRETE ELEMENTS CONTRIBUTING TO STIFFNESS OF BLOCK
UNDER CONSIDERATION
NELEOT=NELE+NELE
DO 150 I=1,NELEOT
NELE=I
DO 100 J=1,4
IF (HODEL(I,J).LT.HMIN).OR.(HODEL(I,J).GT.HMAX)) GO TO 100
IF (HODEL(I,K).LE.HAXOLD) GO TO 150
CONTINUE
CHECK TO DETECT A DIAPHRAGM ELEMENT
IF (NELETY(NELE).GE.3) GO TO 60
BEFORE CONCRETE ELEMENT STIFFNESS IS ADDED IN, THE PRESENCE OF ANY
STEEL REINFORCING BARS IS VERIFIED
IF (HRESH(NELE).EQ.0) GO TO 30
BY ADDING CONCRETE AND STEEL BARS STIFFNESSES, STIFFNESS OF
REINFORCED CONCRETE ELEMENT IS ACHIEVED IN ONE FORMULATION
CALL STP5(US8,NELESH)
DO 20 L=1,3
DO 20 K=1,3
DIK(L)=DC (K,L)+DSH(K,L)
SSSTP(NELE,K,L)=DSH(K,L)

```

```

179 CONTINUE
180 GO TO 40
181 DO 35 L=1,3
182 DO 35 K=1,3
183 D(K,L)=DC(K,L)
184 CONTINUE
185 CALL ELSTP(BEOLD)
186 IF(LSTIP.EQ.0) GO TO 50
187 WRITE(6,610) I
188 FORMAT(/' ELEMENTARY STIFFNESS MATRIX D(3,3) FOR ELEMENT NUMBER',I
189 13, ' IS AS FOLLOWS')
190 DO 620 K=1,3
191 WRITE(6,615) D(K,L),L=1,3)
192 FORMAT(3X16.5)
193 CONTINUE
194 PARITIONING OF ELEMENT STIFFNESS INTO BLOCKS, AND ADDITION OF
195 BLOCKS INTO TS(EBAND,EBAND*2)
196 CALL ADDR( NS1, NS2, NS3, TS, AL, AB)
197 C
198 INCLUSION OF DIAPHRAGM STIFFNESS
199 IF( (INELTY(NEI).GT.4) GO TO 70
200 CALL DIAPHR( TS, NS1, NS2)
201 GO TO 150
202 C
203 INCLUSION OF WARPING RESTRAINT WHERE APPLICABLE
204 CALL WARP( TS, NS1, NS2)
205 GO TO 150
206 CONTINUE
207 C
208 ADDITION OF STIFFNESSES OF SINGLE REINFORCING AND PRESSURE BARS
209 AND BOND SLIP LINKAGES TO TS(EBAND,EBAND*2)
210 DO 250 I=1, NREO
211 RE=I
212 DO 225 J=1,2
213 IF( (NODES(I,J).LT.NREI) OR. (NODES(I,J).GT.NREAI)) GO TO 225
214 DO 210 K=1,2
215 IF( (NODES(I,K).LE.NR1OLD) GO TO 250
216 CONTINUE
217 IF( (LSTIP.EQ.0) GO TO 212
218 WRITE(6,625) I, NREI
219 FORMAT(/' REINFORCEMENT ELEMENT NUMBER', I3, ' HAS BEEN ADDED INTO B
220 LOCK NO. ', I2)
221 IF( (LSTIP.EQ.0) 214, 216, 218
222 STIP=REOHD
223 GO TO 220
224 STIP=PRHOD
225 GO TO 220
226 STIP=SLPHOD
227 IF( (LSTIP.EQ.0) GO TO 255
228 CALL STPADD( NS1, NS2, NS3, TS, AL, AR, STIP)
229 GO TO 250
230 CONTINUE
231 C
232 STIFFNESS BLOCK IS WRITTEN ON TEMPORARY DISC FILE -FILE1
233 CALL WRT( PDB1, IINFO, I510)
234 IF( (LSTIP.EQ.0) GO TO 255
235 FORMAT(/' WHITE POINTER FOR BLOCK NUMBER', I3, ' =', I8)
236 LPOINT( IBBAR, I) = IINFO(2)
237 CALL MODIFY( NS1, NS2, NS3, TS, AL, AB)
238 J=1
239
240
241
242
243
244
245
246
247
248
249
250
251
252
253
254
255
256
257
258
259
260
261
262
263
264
265
266
267
268
269
270
271
272
273
274
275
276
277
278
279
280
281
282
283
284
285
286
287
288
289
290
291
292
293
294
295
296
297
298
299
300
301
302
303
304
305
306
307
308
309
310
311
312
313
314
315
316
317
318
319
320
321
322
323
324
325
326
327
328
329
330
331
332
333
334
335
336
337
338
339
340
341
342
343
344
345
346
347
348
349
350
351
352
353
354
355
356
357
358
359
360
361
362
363
364
365
366
367
368
369
370
371
372
373
374
375
376
377
378
379
380
381
382
383
384
385
386
387
388
389
390
391
392
393
394
395
396
397
398
399
400
401
402
403
404
405
406
407
408
409
410
411
412
413
414
415
416
417
418
419
420
421
422
423
424
425
426
427
428
429
430
431
432
433
434
435
436
437
438
439
440
441
442
443
444
445
446
447
448
449
450
451
452
453
454
455
456
457
458
459
460
461
462
463
464
465
466
467
468
469
470
471
472
473
474
475
476
477
478
479
480
481
482
483
484
485
486
487
488
489
490
491
492
493
494
495
496
497
498
499
500
501
502
503
504
505
506
507
508
509
510
511
512
513
514
515
516
517
518
519
520
521
522
523
524
525
526
527
528
529
530
531
532
533
534
535
536
537
538
539
540
541
542
543
544
545
546
547
548
549
550
551
552
553
554
555
556
557
558
559
560
561
562
563
564
565
566
567
568
569
570
571
572
573
574
575
576
577
578
579
580
581
582
583
584
585
586
587
588
589
590
591
592
593
594
595
596
597
598
599
600
601
602
603
604
605
606
607
608
609
610
611
612
613
614
615
616
617
618
619
620
621
622
623
624
625
626
627
628
629
630
631
632
633
634
635
636
637
638
639
640
641
642
643
644
645
646
647
648
649
650
651
652
653
654
655
656
657
658
659
660
661
662
663
664
665
666
667
668
669
670
671
672
673
674
675
676
677
678
679
680
681
682
683
684
685
686
687
688
689
690
691
692
693
694
695
696
697
698
699
700
701
702
703
704
705
706
707
708
709
710
711
712
713
714
715
716
717
718
719
720
721
722
723
724
725
726
727
728
729
730
731
732
733
734
735
736
737
738
739
740
741
742
743
744
745
746
747
748
749
750
751
752
753
754
755
756
757
758
759
760
761
762
763
764
765
766
767
768
769
770
771
772
773
774
775
776
777
778
779
780
781
782
783
784
785
786
787
788
789
790
791
792
793
794
795
796
797
798
799
800
801
802
803
804
805
806
807
808
809
810
811
812
813
814
815
816
817
818
819
820
821
822
823
824
825
826
827
828
829
830
831
832
833
834
835
836
837
838
839
840
841
842
843
844
845
846
847
848
849
850
851
852
853
854
855
856
857
858
859
860
861
862
863
864
865
866
867
868
869
870
871
872
873
874
875
876
877
878
879
880
881
882
883
884
885
886
887
888
889
890
891
892
893
894
895
896
897
898
899
900
901
902
903
904
905
906
907
908
909
910
911
912
913
914
915
916
917
918
919
920
921
922
923
924
925
926
927
928
929
930
931
932
933
934
935
936
937
938
939
940
941
942
943
944
945
946
947
948
949
950
951
952
953
954
955
956
957
958
959
960
961
962
963
964
965
966
967
968
969
970
971
972
973
974
975
976
977
978
979
980
981
982
983
984
985
986
987
988
989
990
991
992
993
994
995
996
997
998
999

```

```

239 IF (INRESH (HEL, I) .EQ. 0) GO TO 50
240 TRIA=ANGLE (HEL, I)*3.141593/180.0
241 C=COS (TRIA)
242 S=SIN (TRIA)
243 DD (1, 1)=C**4
244 DD (2, 1)=C**2*S**2
245 DD (3, 1)=C**3*S
246 DD (1, 2)=DD (2, 1)
247 DD (2, 2)=S**4
248 DD (3, 2)=C**3*S
249 DD (1, 3)=DD (1, 1)
250 DD (2, 3)=DD (1, 2)
251 DD (3, 3)=DD (2, 1)
252 CALL SHSTP (I)
253
254 IF (INRESH (HEL, I) .EQ. 1) GO TO 50
255 DO 30 K=1, 3
256 DSH (J, K)=DSH (J, K)+DD (J, K)*PERSTL (HEL, I)*SHESH (HEL, I)/100.0
257
258 30 CONTINUE
259
260 IF (ISTIP .EQ. 0) RETURN
261 WRITE (6, 638)
262
263 638 FORMAT (/// '==== OUTPUT FROM STPSP =====')
264
265 640 FORMAT (' THE ELEMENTARY STEEL WESH STIFFNESS MATRIX DSH (3, 3) FOR
266 ELEMENT NUMBER ', I3, ' IS AS BELOW /')
267
268 645 WRITE (6, 645) (DSH (I, J), J=1, 3)
269
270 650 CONTINUE
271 RETURN
272
273 C*****
274 C SUBROUTINE ELSTP (BELOLD)
275 C THIS SUBROUTINE CALCULATES THE MCLDOD FINITE ELEMENT STIFFNESS
276 C OF A RECTANGULAR ELEMENT WHOSE ELEMENTARY STIFFNESS MATRICES
277 C D(3, 3)
278 C*****
279 COMMON /BLOCK1/ NROFS, NBAR, NBL, NURINC, ICONF
280 COMMON /BLOCK2/ BEL, BELT, BELCH, BELD, IBCDL (185), IRESE (185),
281 IREOL (185), ITRIC (185), CARGL (185), CALTR (185),
282 IRELT (215), IRETR (215), IODER (215, 4), IODER (215), OPHROD (215)
283 COMMON /BLOCK3/ NLSH, IRESH (185), IRESH (185), NDIRS, PERSTL (185, 4),
284 IANGL (185, 4), SHSTP (185, 3), SHESH (185, 1)
285 COMMON /BLOCK4/ NRODS, ICONF (220), I (220), I (220), Z (220)
286 COMMON /BLOCK5/ ISTEP (12, 42), BS (3, 3), B1 (3, 42, 9), B2 (3, 42, 9), D (3, 3),
287 IBCORC (185, 3), DCBACK (185), DAGG (185)
288 COMMON /BLOCK11/ IYRESH (185, 4), IDOVEL (185), NCRACK (185), NYAGG (185),
289 IYRO (190), IYCRHO (190)
290 COMMON /BLOCK14/ IYRFLX, ICONF1, ICONF2, IRESH, IREG, ILOAD, ITLOAD, ISTEP,
291 IYTRG, NTCOH, NTRBO, NTRPE
292 IYTRG=0
293 DIMENSION N13 (4, 3), STP2 (12, 12), CC1 (3, 42), CC2 (3, 12)
294 DATA W/, .5555556, .8888889, .5555556, .0, .77459667/
295
296 IYTRG=0
297 IF (NURINC .EQ. 0) GO TO 3
298 IF (BELOLD .EQ. 0) GO TO 2
299 IF (INRESH (NBY, NB, INRESH (BELOLD))) GO TO 2

```

```

299 IF (INRESH (HEL, EQ, INRESH (BELOLD)) .AND. (INRESH (HEL) .EQ. INRESH (
300 BELOLD))) GO TO 100
301 CALCULATION OF ELEMENT DIMENSIONS
302
303 2 IYTRG=1
304
305 BELD IS THE ELEMENT NUMBER OF THE LAST ELEMENT WHOSE STIFFNESS
306 WAS CALCULATED
307 A=(I*(MODEL (HEL, 3))-I*(MODEL (HEL, 2)))/2.0
308 IF (MODEL (HEL, 2))=4, 6
309 B=(SQRT ((I*(MODEL (HEL, 2))-I*(MODEL (HEL, 1)))**2+(I*(MODEL (HEL, 2))-I
310 (MODEL (HEL, 1)))**2))/2.0
311 GO TO 10
312 B=(I*(MODEL (HEL, 2))-I*(MODEL (HEL, 1)))/2.0
313 GO TO 10
314
315 8 B=(I*(MODEL (HEL, 2))-I*(MODEL (HEL, 1)))/2.0
316 ELEMENT STIFFNESS FORMULATION USING GAUSS-LEGENDRE INTEGRATION
317 IF (A.NE.0.0 .AND. B.NE.0.0) GO TO 12
318 WRITE (6, 200) A, B, HEL
319
320 200 FORMAT (/// '==== WESHING =====')
321
322 12 A=, B13.4, AND B=, B13.4, FOR ELEMENT NO., I(///)
323 DO 15 I=1, 12
324 DO 15 J=1, 12
325 STP1 (I, J)=0.0
326 STP2 (I, J)=0.0
327
328 15 CONTINUE
329 IF (ISTIP .EQ. 0) GO TO 18
330 WRITE (6, 653)
331
332 653 FORMAT (/// '==== OUTPUT FROM ELSTP =====')
333
334 655 WRITE (6, 655) HEL, A, B
335
336 655 FORMAT (' FOR ELEMENT', I3, ' A=', F6.1, ' AND B=', F6.1)
337
338 DO 40 N=1, 3
339 DO 40 M=1, 3
340 IZ=GM(A)*A
341 IY=GM(B)*B
342 L=(I-1)*3+M
343 CALL SCALC (A, B, IZ, IY, L)
344 DO 20 J=1, 12
345 DO 20 I=1, 3
346 CC1 (I, J)=0.0
347 CC2 (I, J)=0.0
348 CONTINUE
349 DO 30 J=1, 12
350 DO 30 I=1, 3
351 CC1 (I, J)=CC1 (I, J)+D (I, K)*B1 (K, J, L)
352 CC2 (I, J)=CC2 (I, J)+D (I, K)*B2 (K, J, L)
353 CONTINUE
354 DO 32 J=1, 12
355 DO 32 I=1, 12
356 DO 35 K=1, 3
357 DO 35 L=1, 3
358 STP1 (I, J)=STP1 (I, J)+ELTRH (HEL) *A*B*B1 (I, L)*CC1 (I, J)*B1 (L) *B1 (L)
359 STP2 (I, J)=STP2 (I, J)+ELTRH (HEL) *A*B*B2 (I, L)*CC2 (I, J)*B1 (L) *B1 (L)
360 CONTINUE
361
362 35 CONTINUE
363 40 CONTINUE
364
365 ELEMENT STIFFNESS MATRICES FOR TYPE 1 AND TYPE 2 ELEMENTS HAVE
366 BEEN CALCULATED
367 IF (INRESH (HEL) .EQ. 1) GO TO 110
368 DO 105 J=1, 12
369 DO 105 I=1, 12

```

```

359 ESTP(I,J)-STP2(I,J)
360 CONTINUE
361 GO TO 150
362 DO 115 J=1,12
363 DO 115 I=1,12
364 ESTP(I,J)=STP1(I,J)
365
366
367
368
369
370
371
372
373
374
375
376
377
378
379
380
381
382
383
384
385
386
387
388
389
390
391
392
393
394
395
396
397
398
399
400
401
402
403
404
405
406
407
408
409
410
411
412
413
414
415
416
417
418

```

```

105 ESTP(I,J)-STP2(I,J)
106 CONTINUE
107 GO TO 150
108 DO 115 J=1,12
109 DO 115 I=1,12
110 ESTP(I,J)=STP1(I,J)
111
112
113
114
115
116
117
118
119
120
121
122
123
124
125
126
127
128
129
130
131
132
133
134
135
136
137
138
139
140
141
142
143
144
145
146
147
148
149
150
151
152
153
154
155
156
157
158
159
160
161
162
163
164
165
166
167
168
169
170
171
172
173
174
175
176
177
178
179
180
181
182
183
184
185
186
187
188
189
190
191
192
193
194
195
196
197
198
199
200
201
202
203
204
205
206
207
208
209
210
211
212
213
214
215
216
217
218
219
220
221
222
223
224
225
226
227
228
229
230
231
232
233
234
235
236
237
238
239
240
241
242
243
244
245
246
247
248
249
250
251
252
253
254
255
256
257
258
259
260
261
262
263
264
265
266
267
268
269
270
271
272
273
274
275
276
277
278
279
280
281
282
283
284
285
286
287
288
289
290
291
292
293
294
295
296
297
298
299
300
301
302
303
304
305
306
307
308
309
310
311
312
313
314
315
316
317
318
319
320
321
322
323
324
325
326
327
328
329
330
331
332
333
334
335
336
337
338
339
340
341
342
343
344
345
346
347
348
349
350
351
352
353
354
355
356
357
358
359
360
361
362
363
364
365
366
367
368
369
370
371
372
373
374
375
376
377
378
379
380
381
382
383
384
385
386
387
388
389
390
391
392
393
394
395
396
397
398
399
400
401
402
403
404
405
406
407
408
409
410
411
412
413
414
415
416
417
418

```

```

15
20
25
30
35
40
45
50
55
60
65
70
75
80
85
90
95
100
105
110
115
120
125
130
135
140
145
150
155
160
165
170
175
180
185
190
195
200
205
210
215
220
225
230
235
240
245
250
255
260
265
270
275
280
285
290
295
300
305
310
315
320
325
330
335
340
345
350
355
360
365
370
375
380
385
390
395
400
405
410
415
420
425
430
435
440
445
450
455
460
465
470
475
480
485
490
495
500
505
510
515
520
525
530
535
540
545
550
555
560
565
570
575
580
585
590
595
600
605
610
615
620
625
630
635
640
645
650
655
660
665
670
675
680
685
690
695
700
705
710
715
720
725
730
735
740
745
750
755
760
765
770
775
780
785
790
795
800
805
810
815
820
825
830
835
840
845
850
855
860
865
870
875
880
885
890
895
900
905
910
915
920
925
930
935
940
945
950
955
960
965
970
975
980
985
990
995

```

```

IF (IBOVL-GR-MCOL) GO TO 15
TS(J(I-1),I)-TS(J(I),I+1,I)-STP
RETURN
TS(I(I-1),J)-TS(I(I),J+1,I)-STP
RETURN
C
ALGTH=SQRT((Y(JJ)-Y(I))**2+(Z(JJ)-Z(I))**2)
STP=AREA(MR)*STP/ALGTH
S=Y(I)-Y(I+1)/ALGTH
J(I)=MROW+1
K(I)=MROW+1
K(I)=MROW+1
DO 80 I=1,2
I1=NODES(MR,I)
IF (ICHOOR(I1).EQ.0) GO TO 60
TS(I,J(I))-TS(I,J(I+1))+STP*E*2
TS(I,J(I+1))-TS(I,J(I))+STP*E*2
TS(I,J(I))-TS(I,J(I+1))+STP*E*5
IF (J(I)-I1.K(I)) GO TO 80
TS(I,J(I)-K(I)+1,K(I))-TS(I,J(I)-K(I)+2,K(I))-STP*5
GO TO 80
TS(I,J(I))-TS(I,J(I+1))+STP
IF (J(I)-I1.K(I)) GO TO 80
TS(I,J(I)-K(I)+1,K(I))-TS(I,J(I)-K(I)+1,K(I))-C*STP
TS(I,J(I)-K(I)+1,K(I)+1)-TS(I,J(I)-K(I)+1,K(I)+1)-S*STP
RETURN
C
ADDING IN BOND SLIP STIFFNESSES
STP=STP+C*AREA(MR)
TS(I,MROW)-TS(I,MROW)+STP
TS(I,MROW)-TS(I,MROW)+STP
IF (I1.LT.JJ) GO TO 110
TS(MROW-MCOL+1,MCOL)-TS(MROW-MCOL+1,MROW)-STP
RETURN
TS(MCOL-MROW+1,MROW)-TS(MCOL-MROW+1,MROW)-STP
RETURN
END
SUBROUTINE BKADD(I1,JJ,MS1,MS2,MS3,TS,AL,AR)
C
THIS SUBROUTINE ADDS THE REINFORCED CONCRETE ELEMENT STIFFNESS
SUB-BLOCKS BS(3,3) INTO THE TOTAL STIFFNESS MATRIX IN CORE.
C
CONOR/BLOCK2/RELT,BELT,BELCKR,BELD,IBDCCL(165),IBELSL(165),
IBDORL(165),IBDTRC(165),CANGLE(165),CALTR(165),
ZIBELTY(215),ELTFC(215),MODEL(215),MDEFP(215),DPRHOD(215)
CONOR/BLOCK5/IBODES,ICMODE(220),I(220),Y(220),Z(220)
CONOR/BLOCK10/ESTP(12,12),BS(3,3),B1(3,12,9),B2(3,12,9),B(3,3),
IDCGR(165,3,3),DCRACK(165),DAGG(165)
CONOR/BLOCK13/IBRHS(165,4),BDORL(165),MCRACK(165),BTAGG(165),
IBTRFO(190),BYCRO(190)
CONOR/BLOCK14/IDEPFL,ICOM3,ICOPPR,IAESE,IBEO,ILOAD,ITLOAD,ISTIP,
IBAKIT,BWCON,BTBEQ,WTBE
DIMENSION BR(5),BC(5),BS(5),BS2(5,5),BS2(5,5),BS3(5,5)
DIMENSION TS(MS1,MS2),AL(MS3),AR(MS3)
REAL*4 LT(5,5)

```

```

479 INTEGER CALTR
480 CALL LOCATE(I1,JJ,ROW,NCOL)
481 NR(I)=EROW
482 NC(I)=NCOL
483 I1=J
484 J1=J
485
486 C THE STIFFNESS BLOCK BS(I,J) HAS TO BE CONVERTED FROM A LOCAL
487 STIFFNESS MATRIX TO A GLOBAL STIFFNESS MATRIX IF THE ELEMENT
488 IS INCLUDED AND EITHER II OR JJ NODES ARE CORNER NODES
489 IF(INODEL(NEL),GE.0) GO TO 100
490 IF(ICMODE(II),NE.1.AND.ICMODE(JJ),NE.1) GO TO 100
491 DO 10 J=1,5
492 DO 10 I=1,5
493 LT(I,J)=0.0
494 BS(I,J)=0.0
495 BS2(I,J)=0.0
496 BS3(I,J)=0.0
497 CONTINUE
498
499 C DEFINITION OF TRANSFORMATION MATRIX LT(5,5)
500 B=SQRT((Y(NODEL(NEL,2))-Y(NODEL(NEL,1)))**2+(X(NODEL(NEL,2))-X
501 (NODEL(NEL,1)))**2)
502 S=(X(NODEL(NEL,2))-X(NODEL(NEL,1)))/B
503 LT(1,1)=1.0
504 LT(2,2)=C
505 LT(3,2)=-S
506 LT(2,3)=S
507 LT(3,3)=C
508 LT(4,4)=C
509 LT(5,4)=S
510 LT(5,5)=S
511
512 C TRANSFORMATION OF BS(I,J) TO GLOBAL FORM
513 IF(ICMODE(JJ),EQ.1) GO TO 15
514 DO 12 J=1,3
515 DO 12 I=1,3
516 BS1(I,J)=BS(I,J)
517 CONTINUE
518
519 MC(2)=NCOL+1
520 MC(3)=NCOL+2
521 IF(ICMODE(JJ),EQ.2) MC(3)=NCOL+3
522 GO TO 22
523 BS1(I,1)=BS(I,1)
524 BS1(I,2)=BS(I,2)
525 BS1(I,3)=BS(I,3)
526
527 CONTINUE
528
529 DO 18 J=1,5
530 MC(J)=NCOL+J-1
531 CONTINUE
532 DO 19 J=1,5
533 DO 19 I=1,5
534 BS2(I,J)=BS2(I,J)+BS1(I,I)*LT(I,I)
535 CONTINUE
536 DO 20 J=1,5
537 DO 20 I=1,5
538 BS1(I,J)=BS2(I,J)

```

```

539
540
541
542
543
544
545
546
547
548
549
550
551
552
553
554
555
556
557
558
559
560
561
562
563
564
565
566
567
568
569
570
571
572
573
574
575
576
577
578
579
580
581
582
583
584
585
586
587
588
589
590
591
592
593
594
595
596
597
598

```

```

BS2(I,J)=0.0
CONTINUE
IF(ICMODE(II),NE.1) GO TO 40
DO 25 J=1,5
BS2(1,J)=BS1(1,J)
BS2(2,J)=BS1(2,J)
BS2(5,J)=BS1(3,J)
CONTINUE
11=11+2
DO 30 I=1,5
NR(I)=EROW+I-1
CONTINUE
DO 35 J=1,5
DO 35 I=1,5
DO 35 K=1,5
BS3(I,J)=BS3(I,J)+LT(K,I)*BS2(K,J)
CONTINUE
GO TO 140
DO 45 J=1,5
45 I=1,5
BS3(I,J)=BS3(I,J)
CONTINUE
NR(2)=EROW+1
NR(3)=EROW+2
IF(ICMODE(II),EQ.2) NR(3)=EROW+3
GO TO 140
C CALCULATION OF ROW AND COLUMN LOCATIONS OF UNALTERED BLOCK BS(3,3)
100 DO 105 J=1,3
DO 105 I=1,3
BS3(I,J)=BS(I,J)
CONTINUE
105 IF(ICMODE(II),EQ.1) GO TO 110
NR(2)=EROW+1
NR(3)=EROW+2
IF(ICMODE(II),EQ.2) NR(3)=EROW+3
GO TO 120
IF(LNDCOL(NEL),EQ.0) GO TO 115
NR(2)=EROW+1
NR(3)=EROW+4
GO TO 120
115 NR(2)=EROW+2
NR(3)=EROW+3
IF(ICMODE(JJ),EQ.1) GO TO 130
MC(2)=NCOL+1
MC(3)=NCOL+2
IF(ICMODE(JJ),EQ.2) MC(3)=NCOL+3
GO TO 140
IF(LNDCOL(NEL),EQ.0) GO TO 135
MC(2)=NCOL+1
MC(3)=NCOL+4
GO TO 140
135 MC(2)=NCOL+2
MC(3)=NCOL+3
C ADDITION OF BS(5,5) MATRIX TO TOTAL STIFFNESS MATRIX IF CORE
140 DO 160 J=1,J1
DO 160 I=1,I1
ZM=NR(I)-NC(J)+1
IF(NR,LT.1) GO TO 160
TS(NR,NC(J))=TS(NR,NC(J))+BS3(I,J)
CONTINUE
160

```

```

599 IF (HEL.GT.3) RETURN
600 IF (ISYIP.EQ.0) RETURN
601 WRITE (6,456)
602
603 SUBROUTINE HORIZ
604 .....
605 THIS SUBROUTINE ADJUSTS THE SIGNS OF BLOCK B5(3,3) IF ITS
606 ELEMENT IS HORIZONTAL. THIS IS TO CONVERT THE LOCAL STIFFNESS
607 BLOCK INTO A GLOBAL STIFFNESS BLOCK
608 .....
609 COMMON/BLCK10/ESTP(12,12),BS(3,3),B1(3,12,9),B2(3,12,9),D(3,3),
610 DCORC(185,3,3),DCRACK(185),DAGG(185)
611 DO 5 I=1,2
612 BS(1,3)=-BS(1,3)
613 BS(3,1)=-BS(3,1)
614 CONTINUE
615 RETURN
616 END
617
618 SUBROUTINE BCALC(A,B,I,I,L)
619 .....
620 THIS SUBROUTINE CALCULATES THE 'B' MATRICES FOR ELEMENT TYPES 1&2
621 AT INTEGRATION POINT NUMBER L
622 .....
623 COMMON/BLCK10/ESTP(12,12),BS(3,3),B1(3,12,9),B2(3,12,9),D(3,3),
624 DCORC(185,3,3),DCRACK(185),DAGG(185)
625 DO 5 I=1,2
626 B1(I,J,L)=0.0
627 B2(I,J,L)=0.0
628 CONTINUE
629
630 B1(1,1,L)=-1.0/(8.0*A)-I*E2/(8.0*A*B*E2)+Y/(4.0*A*B)
631 B1(3,1,L)=Y/(4.0*B*E2)-.25/B-I*Y/(4.0*A*B*E2)+X/(4.0*A*B)
632 B1(2,2,L)=-.375/B*X/(4.0*A*B)+I*E2/(8.0*A*B*E2)
633 B1(3,2,L)=Y/(4.0*A*B)-.25/A-X/(4.0*A*B*E2)+X*Y/(4.0*A*B*E2*B)
634 B1(2,3,L)=-A/(4.0*B)+I*E2/(4.0*A*B)
635 B1(3,3,L)=-X/(4.0*B)+I*Y/(4.0*A*B)
636 B1(1,4,L)=-3.0/(8.0*A)+I*E2/(8.0*A*B*E2)-Y/(4.0*A*B)
637 B1(3,4,L)=-Y/(4.0*B*E2)+.25/B*Y/(4.0*A*B*E2)-I/(4.0*A*B)
638 B1(2,5,L)=-.125/B-X/(4.0*A*B)+I*E2/(8.0*A*B*E2)
639 B1(3,5,L)=-Y/(4.0*A*B)-.25/A*Y/(4.0*A*B*E2)+I*Y/(4.0*A*B*E2*B)
640 B1(1,6,L)=-B/(4.0*A)+I*E2/(4.0*A*B)
641 B1(3,6,L)=-Y/(4.0*B*E2)+.25/B*Y/(4.0*A*B*E2)+Y/(4.0*A*B)
642 B1(1,7,L)=.0/(8.0*A)+I*E2/(8.0*A*B*E2)+Y/(4.0*A*B)
643 B1(2,7,L)=-.375/B*X/(4.0*A*B)+I*E2/(8.0*A*B*E2)
644 B1(3,7,L)=-Y/(4.0*A*B)-.25/A-X/(4.0*A*B*E2)+X*Y/(4.0*A*B*E2*B)
645 B1(2,8,L)=-A/(4.0*B)+I*E2/(4.0*A*B)
646 B1(3,8,L)=-X/(4.0*B)+I*Y/(4.0*A*B)
647 B1(1,9,L)=-3.0/(8.0*A)+I*E2/(8.0*A*B*E2)-Y/(4.0*A*B)
648 B1(3,9,L)=-Y/(4.0*B*E2)+.25/B*Y/(4.0*A*B*E2)-I/(4.0*A*B)
649 B1(2,10,L)=-.125/B-X/(4.0*A*B)+I*E2/(8.0*A*B*E2)
650 B1(3,10,L)=-Y/(4.0*A*B)-.25/A-X/(4.0*A*B*E2)+X*Y/(4.0*A*B*E2*B)
651 B1(2,11,L)=-A/(4.0*B)+I*E2/(4.0*A*B)
652 B1(3,11,L)=-X/(4.0*B)+I*Y/(4.0*A*B)
653 B1(1,12,L)=-B/(4.0*A)+I*E2/(4.0*A*B)
654 B1(3,12,L)=-Y/(4.0*B*E2)+.25/B*Y/(4.0*A*B*E2)+Y/(4.0*A*B)
655 ***** FORMATION OF B2(3,12,9) *****
656 B2(1,1,L)=-.375/A*Y/(4.0*A*B*E2)+Y/(4.0*A*B)
657 B2(3,1,L)=-.25/B*Y/(4.0*A*B*E2)+Y/(4.0*A*B)
658 B2(2,2,L)=-.375/B*X/(4.0*A*B*E2)+X/(4.0*A*B)
659 B2(3,2,L)=-.25/A*Y/(4.0*A*B*E2)+X*Y/(4.0*A*B*E2*B)

```

```

659
660
661
662
663
664
665
666
667
668
669
670
671
672
673
674
675
676
677
678
679
680
681
682
683
684
685
686
687
688
689
690
691
692
693
694
695
696
697
698
699
700
701
702
703
704
705
706
707
708
709
710
711
712
713
714
715
716
717
718
719
720
721
722
723
724
725
726
727
728
729
730
731
732
733
734
735
736
737
738
739
740
741
742
743
744
745
746
747
748
749
750
751
752
753
754
755
756
757
758
759
760
761
762
763
764
765
766
767
768
769
770
771
772
773
774
775
776
777
778
779
780
781
782
783
784
785
786
787
788
789
790
791
792
793
794
795
796
797
798
799
800
801
802
803
804
805
806
807
808
809
810
811
812
813
814
815
816
817
818
819
820
821
822
823
824
825
826
827
828
829
830
831
832
833
834
835
836
837
838
839
840
841
842
843
844
845
846
847
848
849
850
851
852
853
854
855
856
857
858
859
860
861
862
863
864
865
866
867
868
869
870
871
872
873
874
875
876
877
878
879
880
881
882
883
884
885
886
887
888
889
890
891
892
893
894
895
896
897
898
899
900
901
902
903
904
905
906
907
908
909
910
911
912
913
914
915
916
917
918
919
920
921
922
923
924
925
926
927
928
929
930
931
932
933
934
935
936
937
938
939
940
941
942
943
944
945
946
947
948
949
950
951
952
953
954
955
956
957
958
959
960
961
962
963
964
965
966
967
968
969
970
971
972
973
974
975
976
977
978
979
980
981
982
983
984
985
986
987
988
989
990
991
992
993
994
995
996
997
998
999

```

```

IF (HEL.GT.3) RETURN
IF (ISYIP.EQ.0) RETURN
WRITE (6,456)
.....
THIS SUBROUTINE ADJUSTS THE SIGNS OF BLOCK B5(3,3) IF ITS
ELEMENT IS HORIZONTAL. THIS IS TO CONVERT THE LOCAL STIFFNESS
BLOCK INTO A GLOBAL STIFFNESS BLOCK
.....
COMMON/BLCK10/ESTP(12,12),BS(3,3),B1(3,12,9),B2(3,12,9),D(3,3),
DCORC(185,3,3),DCRACK(185),DAGG(185)
DO 5 I=1,2
BS(1,3)=-BS(1,3)
BS(3,1)=-BS(3,1)
CONTINUE
RETURN
END
SUBROUTINE BCALC(A,B,I,I,L)
.....
THIS SUBROUTINE CALCULATES THE 'B' MATRICES FOR ELEMENT TYPES 1&2
AT INTEGRATION POINT NUMBER L
.....
COMMON/BLCK10/ESTP(12,12),BS(3,3),B1(3,12,9),B2(3,12,9),D(3,3),
DCORC(185,3,3),DCRACK(185),DAGG(185)
DO 5 I=1,2
B1(I,J,L)=0.0
B2(I,J,L)=0.0
CONTINUE
B1(1,1,L)=-1.0/(8.0*A)-I*E2/(8.0*A*B*E2)+Y/(4.0*A*B)
B1(3,1,L)=Y/(4.0*B*E2)-.25/B-I*Y/(4.0*A*B*E2)+X/(4.0*A*B)
B1(2,2,L)=-.375/B*X/(4.0*A*B)+I*E2/(8.0*A*B*E2)
B1(3,2,L)=Y/(4.0*A*B)-.25/A-X/(4.0*A*B*E2)+X*Y/(4.0*A*B*E2*B)
B1(2,3,L)=-A/(4.0*B)+I*E2/(4.0*A*B)
B1(3,3,L)=-X/(4.0*B)+I*Y/(4.0*A*B)
B1(1,4,L)=-3.0/(8.0*A)+I*E2/(8.0*A*B*E2)-Y/(4.0*A*B)
B1(3,4,L)=-Y/(4.0*B*E2)+.25/B*Y/(4.0*A*B*E2)-I/(4.0*A*B)
B1(2,5,L)=-.125/B-X/(4.0*A*B)+I*E2/(8.0*A*B*E2)
B1(3,5,L)=-Y/(4.0*A*B)-.25/A*Y/(4.0*A*B*E2)+I*Y/(4.0*A*B*E2*B)
B1(1,6,L)=-B/(4.0*A)+I*E2/(4.0*A*B)
B1(3,6,L)=-Y/(4.0*B*E2)+.25/B*Y/(4.0*A*B*E2)+Y/(4.0*A*B)
B1(1,7,L)=.0/(8.0*A)+I*E2/(8.0*A*B*E2)+Y/(4.0*A*B)
B1(2,7,L)=-.375/B*X/(4.0*A*B)+I*E2/(8.0*A*B*E2)
B1(3,7,L)=-Y/(4.0*A*B)-.25/A-X/(4.0*A*B*E2)+X*Y/(4.0*A*B*E2*B)
B1(2,8,L)=-A/(4.0*B)+I*E2/(4.0*A*B)
B1(3,8,L)=-X/(4.0*B)+I*Y/(4.0*A*B)
B1(1,9,L)=-3.0/(8.0*A)+I*E2/(8.0*A*B*E2)-Y/(4.0*A*B)
B1(3,9,L)=-Y/(4.0*B*E2)+.25/B*Y/(4.0*A*B*E2)-I/(4.0*A*B)
B1(2,10,L)=-.125/B-X/(4.0*A*B)+I*E2/(8.0*A*B*E2)
B1(3,10,L)=-Y/(4.0*A*B)-.25/A-X/(4.0*A*B*E2)+X*Y/(4.0*A*B*E2*B)
B1(2,11,L)=-A/(4.0*B)+I*E2/(4.0*A*B)
B1(3,11,L)=-X/(4.0*B)+I*Y/(4.0*A*B)
B1(1,12,L)=-B/(4.0*A)+I*E2/(4.0*A*B)
B1(3,12,L)=-Y/(4.0*B*E2)+.25/B*Y/(4.0*A*B*E2)+Y/(4.0*A*B)
***** FORMATION OF B2(3,12,9) *****
B2(1,1,L)=-.375/A*Y/(4.0*A*B*E2)+Y/(4.0*A*B)
B2(3,1,L)=-.25/B*Y/(4.0*A*B*E2)+Y/(4.0*A*B)
B2(2,2,L)=-.375/B*X/(4.0*A*B*E2)+X/(4.0*A*B)
B2(3,2,L)=-.25/A*Y/(4.0*A*B*E2)+X*Y/(4.0*A*B*E2*B)

```

```

719 B2(1,3,1)=B/(4.0A)-Y002/(4.0A*B)
720 B2(3,1)=Y/(2.0B)-XY/(2.0A*B)
721 B2(1,4,1)=-.125/A*Y002/(8.0A*B*B2)-Y/(4.0A*B)
722 B2(4,1)=Y/(4.0B*B2)+.25/B*XY/(4.0A*B*B2)-X/(4.0A*B)
723 B2(5,1)=-.375/B*X/(4.0A*B)-XY/(8.0A*B*B2)
724 B2(3,5,1)=-Y/(4.0A*B)-.25/A*X/(4.0A*B*B2)-XY/(4.0A*B*B2)
725 B2(4,5,1)=X/(4.0B)-XY/(2.0A*B)
726 B2(5,5,1)=-Y/(2.0A)-XY/(2.0A*B)
727 B2(1,7,1)=-.375/A*Y002/(8.0A*B*B2)+Y/(4.0A*B)
728 B2(7,1)=-.125/B*X/(4.0A*B)+XY/(8.0A*B*B2)
729 B2(8,1)=-.125/B*X/(4.0A*B)+XY/(8.0A*B*B2)
730 B2(9,1)=-.125/B*X/(4.0A*B)+XY/(8.0A*B*B2)+X/(4.0A*B)
731 B2(10,1)=-Y/(2.0B)-XY/(2.0A*B)
732 B2(3,10,1)=-.125/A*Y002/(8.0A*B*B2)-Y/(4.0A*B)
733 B2(4,10,1)=-.375/B*X/(4.0A*B)-XY/(8.0A*B*B2)
734 B2(5,10,1)=-Y/(4.0A*B)+XY/(8.0A*B*B2)
735 B2(3,11,1)=-.375/B*X/(4.0A*B)+XY/(8.0A*B*B2)
736 B2(4,11,1)=-Y/(4.0A*B)+XY/(8.0A*B*B2)
737 B2(12,1)=A/(4.0B)-XY/(4.0A*B)
738 B2(13,1)=X/(2.0A)-XY/(2.0A*B)
739 END
740
741 SUBROUTINE MODLOC (REQ,NI)
742 .....
743 C THIS SUBROUTINE CALCULATES THE NODE NUMBER NI THAT CONTAINS THE
744 C REQ TH. EQUATION
745 C .....
746 C
747 IF (REQ.GT.0) GO TO 2
748 NI=0
749 RETURN
750
751 I=1
752 IF (ICHOR(I)) 4,5,6
753 NI=NI+1
754 IF (NI=1) 4,5,6
755 NI=NI+1
756 IF (NI=2) 4,5,6
757 NI=NI+1
758 IF (ICOR(I)) 1,2
759 IF (ICCC) 7,8,9
760 NI=NI+1
761 IF (NI=3) 4,5,6
762 NI=NI+1
763 IF (NI=4) 4,5,6
764 NI=NI+1
765 IF (NI=5) 4,5,6
766 NI=NI+1
767 IF (NI=6) 4,5,6
768 NI=NI+1
769 NI=NI+1
770 NI=NI+1
771 NI=NI+1
772 NI=NI+1
773 NI=NI+1
774 NI=NI+1
775 NI=NI+1
776 NI=NI+1
777 NI=NI+1
778 NI=NI+1

```

```

CONOM/BLOCKS/NEHS,INRESH(185),INRESH(185),EDIRS,PERSTL(185,4),
TABLR(185,4),SSTF(185,3,3),SRESH(185,1)
CONOM/BLOCKS/RR,RRRO,RRROD(190,2),IRDR(190),IRNT(190),
HEALTH(190),AREA(190),CARPA(190),RSTP(190),ISGRRE(190),TEPRE(190)
CONOM/BLOCKS/IMODES,ICMODE(220),I(220),I(220),I(220)
CONOM/BLOCKS/COMBOD,COMBOD,PRBOD,PRBOD,SLPMOD,SMSMOD,PC,PI,
IFACE,FR,FRF,FRS,DT,RELIF,ICULT,IRULT,IRULT,IRULT,PI,P2,P3,PA,
ZPU,RRPO,RRPOF,CONDIV,DTYCOB,DTYVRO,PRKEY,SLPPOF,IDET,AVCSF,RELAI
CONOM/BLOCKS/ALTY,ALTY,ALTY(6),LOADS(6),MODER(40,6),
IKORR(40,6),VALBR(40,6)
CONOM/BLOCKS/ROISPL,ROISPL(30),KORPD(30),VALBRD(30),D1(750)
CONOM/BLOCKS/POIPT(20,2),POB1,POB2,ROBEC,
URBLE,ISOLV,LEN
CONOM/BLOCKS/SICOH(185,3),MCOH(185,3),SIGHS(185,4),RES(185,4),
ITSOCOH(185,3),MCOH(185,3),ISGCC(185),ISGCC(185),ISGACC(185),
ZTRCC(185),IBCT(185),TSOBS(185,4),TEHS(185,4),SICRNO(190),
JERO(190),ISGRNO(190),TERRO(190)
CONOM/BLOCKS/INRESH(185,4),EDORBL(185),EDORBL(185),BTACC(185),
BTERO(190),BTICRNO(190)
CONOM/BLOCKS/IDEPH,ICON3,ICOPR,INRESH,IREO,ILOAD,ITLOAD,ISTIF,
IRAIT,IRVCOH,IRVRO,IRVPRR
CONOM/BLOCKS/BLTPOF,BLTPOF(40),BLB(40),SIGHT1,SIGHT2,SIGR1,
SISIGR2,SIGR3,SIGR4,RT1,RT2,RT3,RT4,RT5,RT6,RT7,RT8,RT9,RT10,
CONOM/BLOCKS/PELT,PELT(10),PELSE,PSH(10),PRMO,PR(10),
IPDOT,PD(10)
DIMENSION IS(185)
INRESH(4,1)=1
IPR,IPROT,IPOT
INRESH(4,2)=1
INRESH(4,3)=1
C ***** READ STATEMENTS
800 READ (5,90) REQNS,REAND,LEN
801 WRITE ELEMENT DATA
802 READ (5,90) BELT,BELCHK
803 DO 5 I=1,BELT
804 READ (5,70) EDORBL(I),INRESH(I),IBLT(I),ELTRN(I),
805 1(MODBL(I,3),J=1,4),EDORBL(I),INRESH(I),INRESH(I),EDORBL(I)
806 CONTINUE
807 CONCRETE BRIDGE STRESSES DATA
808 READ (5,70) BELTPOF,SIGR1,SIGR2,SIGR3,SIGR4,SIGR5,SIGR6,SIGR7,
809 INRESH,RT7,RT8,RT9,RT10,RT11,RT12
810 DO 8 I=1,4
811 I=I-1)+10+1
812 IF (I.GT.BELTPOF) GO TO 8
813 I2=I+10
814 IF (I2.GT.BELTPOF) I2=BELTPOF
815 READ (5,70) (BLTR(J),J=I1,I2)
816 READ (5,70) (BLBR(J),J=I1,I2)
817 CONTINUE
818 ELEMENT STEEL RESH DATA
819 READ (5,90) BELSH
820 IF (BELSH.EQ.0) GO TO 12
821 DO 10 I=1,BELSH
822 READ (5,90) RS(I)
823 I=RS(I)
824 I=RS(I)
825 READ (5,60) (PERSTL(I,1),ABGR(I,1),J), J=1,
826 (ADDRESS)
827 CONTINUE
828 DIAPHRAGM INPUT DATA

```

```

839 READ (5,80) HELD
840 IF (HELD.EQ.0) GO TO 14
841 X1=HELT+1
842 X2=HELT+HELD
843 DO 13 J=1,I,12
844 READ (5,80) I,ELTNS(I),ELTNS(I),ELTNS(I),ELTNS(I),ELTNS(I),ELTNS(I),
845 I,MODEL(I,J),J=1,4),IMODL(I),I,RESHS(I),RESHS(I),RESHS(I),
846 CONTINUE
847 PRINT*RESHS DATA
848 READ (5,90) NRO
849 IF (NRO.EQ.0) GO TO 26
850 DO 15 I=1,NRO
851 READ (5,90) MODES(I,1),MODES(I,2),INERTY(I)
852 CONTINUE
853 DO 25 I=1,NRO
854 IF (INERTY(I) .GT. 22.224)
855 READ (5,90) I,RESHS(I),RAREA(I)
856 GO TO 25
857 READ (5,90) I,RESHS(I),RESHS(I),RESHS(I),RESHS(I),RESHS(I),
858 GO TO 25
859 READ (5,90) RAREA(I)
860 CONTINUE
861 MODAL DATA
862 READ (5,90) NRODES
863 DO 30 J=1,NRODES
864 READ (5,90) I,RESHS(I),I(I),I(I),I(I)
865 CONTINUE
866 STRENGTH PARAMETERS
867 READ (5,90) CONMOD,REMOD,PREMOD,SLP,MOD,SHS,MOD
868 READ (5,90) FC,FT,FAGG,FUP,FUP,FURS
869 READ (5,90) ERO,REPR,ECULT,ECULT,ECULT,ECULT,ECULT,ECULT,DF
870 READ (5,90) P1,P2,P3,PU
871 READ (5,80) CONDEV,DEVCON,DEVNO,PREDEV,SLPDEV,IDEV,AVCSP,RELAX
872 LOADING DATA
873 READ (5,90) BLDY
874 DO 40 I=1,BLDY
875 READ (5,90) I,RESHS(I),I,RESHS(I),I,RESHS(I),I,RESHS(I)
876 EL=LOADS(I)
877 DO 35 J=1,EL
878 READ (5,90) MODER(J,I),MODER(J,I),VALUER(J,I)
879 CONTINUE
880 EXPOSED BOUNDARY CONDITIONS
881 READ (5,90) HDISPL
882 DO 45 I=1,HDISPL
883 READ (5,90) I,RESHS(I),I,RESHS(I),I,RESHS(I),I,RESHS(I)
884 CONTINUE
885 SCREEN PRINTOUT CONTROL DATA
886 READ (5,70) PHELT
887 READ (5,70) I,RESHS(I),I=1,PHELT
888 READ (5,70) PHELSH
889 READ (5,70) I,RESHS(I),I=1,PHELSH
890 READ (5,70) PHEFOT
891 READ (5,70) I,RESHS(I),I=1,PHEFOT
892 READ (5,70) PHEFOT
893 READ (5,70) I,RESHS(I),I=1,PHEFOT
894 PRINT*CONTROL INFORMATION
895 READ (5,80) I,RESHS(I),I,RESHS(I),I,RESHS(I),I,RESHS(I)
896 C***** WRITE STATEMENTS
897
898

```

```

899 IF (INERTY.EQ.0) RETURN
900 WRITE (6,100) NRODES, BRAND,LEM,HELT,HELCH
901 WRITE (6,105)
902 DO 112 J=1,HELT
903 WRITE (6,110) I,IMODL(I),I,RESHS(I),I,RESHS(I),I,RESHS(I),
904 I,MODEL(I,J),J=1,4),IMODL(I),I,RESHS(I),I,RESHS(I),I,RESHS(I)
905 CONTINUE
906 WRITE (6,115) HELTOP,SIGIT1,SIGIT2,SIGIB1,SIGIB2,SIGIS1,
907 SIGIS2,EXT1,EXT2,EXT3,EXT4,EXT5,EXT6,EXT7,EXT8,EXT9,EXT10,EXT11,EXT12
908 DO 118 I=1,4
909 IF (I-1)*10+1
910 IF (I-1)*10+1
911 I2=I*10
912 IF (I2.GT.HELTOP) I2=HELTOP
913 WRITE (6,116) I1,I2,(HELT(I),I,RESHS(I),I,RESHS(I),I,RESHS(I),
914 I,MODEL(I,J),J=1,4),I,RESHS(I),I,RESHS(I),I,RESHS(I),I,RESHS(I)
915 CONTINUE
916 WRITE (6,120) HELSH
917 IF (HELSH.NE.0) GO TO 135
918 WRITE (6,125)
919 DO 133 J=1,HELSH
920 I1=HS(I)
921 DO 133 J=1,HELSH
922 WRITE (6,130) HS(I),HELSH,J,PERSTL(I,J),ANGLE(I,J)
923 CONTINUE
924 IF (HELD.EQ.0) GO TO 151
925 WRITE (6,140) HZLD
926 WRITE (6,145)
927 I1=HELT+1
928 I2=HELT+HELD
929 DO 149 I=1,I2
930 WRITE (6,148) I,HELT(I),ELTNS(I),ELTNS(I),MODEL(I,J),J=1,4),NDRZF(I),
931 CONMOD(I)
932 CONTINUE
933 WRITE (6,150) NRO
934 WRITE (6,152)
935 DO 170 I=1,NRO
936 IF (INERTY(I).GT.0) GO TO 160
937 IF (INERTY(I).EQ.0) GO TO 156
938 WRITE (6,155) I,MODES(I,1),MODES(I,2),INERTY(I),INERTY(I),RAREA(I)
939 GO TO 170
940 WRITE (6,155) I,MODES(I,1),MODES(I,2),INERTY(I),INERTY(I),RAREA(I),
941 I,MODEL(I),I,RESHS(I)
942 GO TO 170
943 WRITE (6,158) I,MODES(I,1),MODES(I,2),INERTY(I),RAREA(I)
944 CONTINUE
945 WRITE (6,175) NRODES
946 DO 190 I=1,NRODES
947 WRITE (6,185) I,ICORDE(I),I(I),I(I),I(I),I(I),I(I),I(I),I(I),I(I),I(I),I(I)
948 CONTINUE
949 WRITE (6,195)
950 WRITE (6,200) CONMOD,REMOD,PREMOD,SLP,MOD,SHS,MOD
951 WRITE (6,205) FC,FT,FAGG,FUP,FUP,FURS
952 WRITE (6,210) ERO,REPR,ECULT,ECULT,ECULT,ECULT,ECULT,ECULT,DF
953 WRITE (6,215) P1,P2,P3,PU
954 WRITE (6,218) CONDEV,DEVCON,DEVNO,PREDEV,SLPDEV,IDEV,AVCSP,RELAX
955 WRITE (6,219) BLDY,DEVCON,DEVNO,PREDEV,SLPDEV,IDEV,AVCSP,RELAX
956 WRITE (6,220) BLDY
957 DO 250 I=1,HELD
958

```







```

1199 IF(I.EQ.(NURREC-1)) LFM=(MSJ-J+1)*4
1200 CONTINUE
1201 LFM=J1
1202 DO 27 I=1,NBAND
1203 I1=(NBLEK-I)*NBAND*I
1204 DO 27 J=1,2
1205 IF(I1.LE.NREQS) GO TO 26
1206 RE(I,J)=0.0
1207 GO TO 27
1208 SB(I,J)=R2(J,I)
1209 CONTINUE
1210 IF(NBLEK.LT.1) GO TO 10
1211 IF(NBLEK.EQ.1) OR (SOLVE.GT.1) GO TO 34
1212 CALL TIME(1,0,ITIME)
1213 WRITE (6,210) ITIME
1214 GO TO 34
1215 DO 30 I=1,MSJ
1216 AR(I)=0.0
1217 CONTINUE
1218 DO 32 I=1,NBAND
1219 DO 32 K=1,2
1220 RE(I,K)=0.0
1221 CONTINUE
1222 C COMPLETE REDUCTION OF FIRST BLOCK IN CORE
1223 DO 70 I=1,NBAND
1224 IF(NBLEK.LT.NBLEK) GO TO 36
1225 RE(I,NBLEK-1)*NBAND*I
1226 IF(SO.GT.NREQS) GO TO 75
1227 IF(ITS(I,J).LE.0.0) GO TO 240
1228 DO 38 J=1,2
1229 RE(I,J)=R2(J,I)/TS(I,I)
1230 CONTINUE
1231 DO 60 J=2,NBAND
1232 IF(ITS(J,I)) 40,60,40
1233 C-TS(I,J)/TS(I,I)
1234 K=I-J-1
1235 L=0
1236 DO 50 M=J,NBAND
1237 L=L+1
1238 TS(L,K)=TS(L,K)-CTS(M,I)
1239 DO 55 M=1,2
1240 RE(M,K)=RE(M,K)-TS(J,I)*RE(M,I)
1241 CONTINUE
1242 TS(M,J)=C
1243 CONTINUE
1244 DO 90 I=1,NURREC
1245 CALL TIME(1,0,ITIME)
1246 WRITE (6,215) ITIME
1247 REMOVED BLOCK IS WRITTEN OUT ON DISC
1248 CALL NOTE(PDB2,INFO,6260)
1249 LEVYIT(NBLEK,2)=LEPO(2)
1250 J=1
1251 J1=NB
1252 DO 150 J1=1,2
1253 I1=NBLEK-1
1254 CALL WRITE(AL(J),LEB,0,LEUB,FOUR2,6270)
1255 J=J+LEH/4
1256 IF(I.EQ.(NURREC-1)) LFM=(MSJ-J+1)*4
1257 CONTINUE
1258 LFM=J1

```

```

1259 DO 90 I=1,NBAND
1260 I1=(NBLEK-I)*NBAND*I
1261 DO 90 J=1,2
1262 RE(I,J)=R2(J,I)
1263 CONTINUE
1264 IF(NBLEK.EQ.NBLEK) GO TO 100
1265 IF(NBLEK.EQ.1) OR (SOLVE.GT.1) GO TO 10
1266 CALL TIME(1,0,ITIME)
1267 WRITE (6,220) ITIME
1268 GO TO 10
1269 C FINAL STEP IS EQUATION SOLUTION INVOLVING BACKSUBSTITUTION OF
1270 REMOVED EQUATIONS AND LOAD ARRAY
1271 DO 95 I=1,NBAND
1272 RE(I,J)=0.0
1273 CONTINUE
1274 IF(NBLEK.EQ.1)
1275 IF(SOLVE.GT.1) GO TO 110
1276 CALL TIME(1,0,ITIME)
1277 WRITE (6,225) ITIME
1278 INFO(1)=LPOINT(NBLEK,2)
1279 CALL POINT(PDB2,INFO,1,6280)
1280 J=1
1281 J1=LEH
1282 DO 120 I=1,NURREC
1283 CALL READ(AL(J),LEB,0,LEUB,FOUR2,6290)
1284 J=J+LEH/4
1285 IF(I.EQ.(NURREC-1)) LFM=(MSJ-J+1)*4
1286 CONTINUE
1287 LFM=J1
1288 DO 130 I=1,NBAND
1289 I1=(NBLEK-I)*NBAND*I
1290 DO 130 J=1,2
1291 IF(I1.LE.NREQS) GO TO 125
1292 RE(I,J)=0.0
1293 GO TO 130
1294 RL(J,I)=R2(J,I)
1295 CONTINUE
1296 DO 150 I=1,NBAND
1297 J=NBAND*I-1
1298 JB=(NBLEK-1)*NBAND*I
1299 L=J+K-1
1300 DO 140 J1=1,2
1301 RE(J1,J)=RE(J1,J)-TS(K,J)*RE(J1,I)
1302 RE=RE+J
1303 DO 150 J1=1,2
1304 RE(J1,K)=RE(J1,J)
1305 IF(JD.GT.NREQS) GO TO 150
1306 DZ(J1,J)=RE(J1,J)
1307 CONTINUE
1308 NBLEK=NBLEK-1
1309 BACK SUBSTITUTION COMPLETED
1310 IF(SOLVE.GT.1) RETURN
1311 CALL TIME(1,0,ITIME)
1312 COSTY=COSTY+10
1313 WRITE (6,230) ITIME,COSTY
1314 C FORMAT STATEMENTS
1315

```

```

1374 SSION FAYL RIBBON-CA PRINT-TH
1375 JOB-TYPE-BATCH, PRIO-NORMAL, CLASS-INTERNAL/TEACHING, RESEARCH
1376 **LAST SIGNOR WAS: 42:47:46
1377 USER "TAYL" SIGNED ON AT 14:13:37 ON THU JUN 30/77
1378 SLIST FILE52(1319,1721)
1379 200 FORMAT(//, '***** OUTPUT FROM SUBROUTINE SOLVE *****', //, ' CPU TI
1380 ME AT INITIAL STAGE IN SUBROUTINE SOLVE ', I8,
1381 21 PROGRAM COST ', F7.2)
1382 188 N ' ', I8)
1383 210 FORMAT( CPU TIME AT COMPLETION OF BLOCK MANIPULATION OF BLOCK NUB
1384 188 N ' ', I8)
1385 215 FORMAT( CPU TIME AT COMPLETION OF GAUSSIAN ELIMINATION OF BLOCK N
1386 188 N ' ', I8)
1387 220 FORMAT( CPU TIME AFTER REDUCED EQUATIONS OF BLOCK NUMBER 1 HAVE B
1388 188 N ' ', I8)
1389 225 FORMAT( CPU TIME AT BEGINNING OF BACKSUBSTITUTION PROCESS ', I8)
1390 230 FORMAT( CPU TIME AT END OF SOLUTION PROCESS ', I8,
1391 1 PROGRAM COST ', F7.2)
1392 RETURN
1393 240 WRITE (6,265) I, TS(1,I), NBLK
1394 245 FORMAT(//, '*** DIAGONAL TERM TS(', I3, ', 1)', ' ', I4, 5,
1395 1' IN BLOCK NO. ', I3, ' ***'//)
1396 STOP
1397 250 WRITE (6,262)
1398 252 FORMAT(//, '*** ERROR IN FIRST READ SYSTEM SUBROUTINE IN SOLVE,
1399 1 AS BEAT STIFFNESS BLOCK IS READ INTO CORE ***')
1400 STOP
1401 260 WRITE (6,262)
1402 262 FORMAT(//, '*** ERROR IN FIRST SYSTEM SUBROUTINE IN SOLVE')
1403 STOP
1404 270 WRITE (6,272)
1405 272 FORMAT(//, '*** ERROR IN WRITE SYSTEM SUBROUTINE IN SOLVE AS REDU
1406 1 CED BLOCK OF EQUATIONS IS WRITTEN OUT ONTO DISC')
1407 STOP
1408 280 WRITE (6,282)
1409 282 FORMAT(//, '*** ERROR IN SECOND SYSTEM SUBROUTINE IN SOLVE')
1410 STOP
1411 290 WRITE (6,292)
1412 292 FORMAT(//, '*** ERROR IN SECOND READ SYSTEM SUBROUTINE IN SOLVE AS BL
1413 1 CK OF REDUCED EQUATIONS IS READ INTO CORE, PRECEDING BACKSUBSTITU
1414 2TION')
1415 STOP
1416 300 SUBROUTINE MODIFY (N51, N52, N53, IS, AL, AR)
1417 C*****
1418 C THIS SUBROUTINE MODIFIES A GIVEN STIFFNESS BLOCK, WHERE APPLICABLE
1419 C FOR SPECIFIED BOUNDARY CONDITIONS
1420 C*****
1421 C
1422 COMMON/BLOCK1/IBND, NBLK, NUBINC, ICONF1, ICONF2, ICONF3, ICONF4, ICONF5,
1423 ICONF6, ICONF7, ICONF8, ICONF9, ICONF10, ICONF11, ICONF12, ICONF13, ICONF14,
1424 ICONF15, ICONF16, ICONF17, ICONF18, ICONF19, ICONF20, ICONF21, ICONF22, ICONF23,
1425 ICONF24, ICONF25, ICONF26, ICONF27, ICONF28, ICONF29, ICONF30, ICONF31, ICONF32,
1426 ICONF33, ICONF34, ICONF35, ICONF36, ICONF37, ICONF38, ICONF39, ICONF40, ICONF41,
1427 ICONF42, ICONF43, ICONF44, ICONF45, ICONF46, ICONF47, ICONF48, ICONF49, ICONF50,
1428 ICONF51, ICONF52, ICONF53, ICONF54, ICONF55, ICONF56, ICONF57, ICONF58, ICONF59,
1429 ICONF60, ICONF61, ICONF62, ICONF63, ICONF64, ICONF65, ICONF66, ICONF67, ICONF68,
1430 ICONF69, ICONF70, ICONF71, ICONF72, ICONF73, ICONF74, ICONF75, ICONF76, ICONF77,
1431 ICONF78, ICONF79, ICONF80, ICONF81, ICONF82, ICONF83, ICONF84, ICONF85, ICONF86,
1432 ICONF87, ICONF88, ICONF89, ICONF90, ICONF91, ICONF92, ICONF93, ICONF94, ICONF95,
1433 ICONF96, ICONF97, ICONF98, ICONF99, ICONF100, ICONF101, ICONF102, ICONF103,
1434 ICONF104, ICONF105, ICONF106, ICONF107, ICONF108, ICONF109, ICONF110, ICONF111,
1435 ICONF112, ICONF113, ICONF114, ICONF115, ICONF116, ICONF117, ICONF118, ICONF119,
1436 ICONF120, ICONF121, ICONF122, ICONF123, ICONF124, ICONF125, ICONF126, ICONF127,
1437 ICONF128, ICONF129, ICONF130, ICONF131, ICONF132, ICONF133, ICONF134, ICONF135,
1438 ICONF136, ICONF137, ICONF138, ICONF139, ICONF140, ICONF141, ICONF142, ICONF143,
1439 ICONF144, ICONF145, ICONF146, ICONF147, ICONF148, ICONF149, ICONF150, ICONF151,
1440 ICONF152, ICONF153, ICONF154, ICONF155, ICONF156, ICONF157, ICONF158, ICONF159,
1441 ICONF160, ICONF161, ICONF162, ICONF163, ICONF164, ICONF165, ICONF166, ICONF167,
1442 ICONF168, ICONF169, ICONF170, ICONF171, ICONF172, ICONF173, ICONF174, ICONF175,
1443 ICONF176, ICONF177, ICONF178, ICONF179, ICONF180, ICONF181, ICONF182, ICONF183,
1444 ICONF184, ICONF185, ICONF186, ICONF187, ICONF188, ICONF189, ICONF190, ICONF191,
1445 ICONF192, ICONF193, ICONF194, ICONF195, ICONF196, ICONF197, ICONF198, ICONF199,
1446 ICONF200, ICONF201, ICONF202, ICONF203, ICONF204, ICONF205, ICONF206, ICONF207,
1447 ICONF208, ICONF209, ICONF210, ICONF211, ICONF212, ICONF213, ICONF214, ICONF215,
1448 ICONF216, ICONF217, ICONF218, ICONF219, ICONF220, ICONF221, ICONF222, ICONF223,
1449 ICONF224, ICONF225, ICONF226, ICONF227, ICONF228, ICONF229, ICONF230, ICONF231,
1450 ICONF232, ICONF233, ICONF234, ICONF235, ICONF236, ICONF237, ICONF238, ICONF239,
1451 ICONF240, ICONF241, ICONF242, ICONF243, ICONF244, ICONF245, ICONF246, ICONF247,
1452 ICONF248, ICONF249, ICONF250, ICONF251, ICONF252, ICONF253, ICONF254, ICONF255,
1453 ICONF256, ICONF257, ICONF258, ICONF259, ICONF260, ICONF261, ICONF262, ICONF263,
1454 ICONF264, ICONF265, ICONF266, ICONF267, ICONF268, ICONF269, ICONF270, ICONF271,
1455 ICONF272, ICONF273, ICONF274, ICONF275, ICONF276, ICONF277, ICONF278, ICONF279,
1456 ICONF280, ICONF281, ICONF282, ICONF283, ICONF284, ICONF285, ICONF286, ICONF287,
1457 ICONF288, ICONF289, ICONF290, ICONF291, ICONF292, ICONF293, ICONF294, ICONF295,
1458 ICONF296, ICONF297, ICONF298, ICONF299, ICONF300, ICONF301, ICONF302, ICONF303,
1459 ICONF304, ICONF305, ICONF306, ICONF307, ICONF308, ICONF309, ICONF310, ICONF311,
1460 ICONF312, ICONF313, ICONF314, ICONF315, ICONF316, ICONF317, ICONF318, ICONF319,
1461 ICONF320, ICONF321, ICONF322, ICONF323, ICONF324, ICONF325, ICONF326, ICONF327,
1462 ICONF328, ICONF329, ICONF330, ICONF331, ICONF332, ICONF333, ICONF334, ICONF335,
1463 ICONF336, ICONF337, ICONF338, ICONF339, ICONF340, ICONF341, ICONF342, ICONF343,
1464 ICONF344, ICONF345, ICONF346, ICONF347, ICONF348, ICONF349, ICONF350, ICONF351,
1465 ICONF352, ICONF353, ICONF354, ICONF355, ICONF356, ICONF357, ICONF358, ICONF359,
1466 ICONF360, ICONF361, ICONF362, ICONF363, ICONF364, ICONF365, ICONF366, ICONF367,
1467 ICONF368, ICONF369, ICONF370, ICONF371, ICONF372, ICONF373, ICONF374, ICONF375,
1468 ICONF376, ICONF377, ICONF378, ICONF379, ICONF380, ICONF381, ICONF382, ICONF383,
1469 ICONF384, ICONF385, ICONF386, ICONF387, ICONF388, ICONF389, ICONF390, ICONF391,
1470 ICONF392, ICONF393, ICONF394, ICONF395, ICONF396, ICONF397, ICONF398, ICONF399,
1471 ICONF400, ICONF401, ICONF402, ICONF403, ICONF404, ICONF405, ICONF406, ICONF407,
1472 ICONF408, ICONF409, ICONF410, ICONF411, ICONF412, ICONF413, ICONF414, ICONF415,
1473 ICONF416, ICONF417, ICONF418, ICONF419, ICONF420, ICONF421, ICONF422, ICONF423,
1474 ICONF424, ICONF425, ICONF426, ICONF427, ICONF428, ICONF429, ICONF430, ICONF431,
1475 ICONF432, ICONF433, ICONF434, ICONF435, ICONF436, ICONF437, ICONF438, ICONF439,
1476 ICONF440, ICONF441, ICONF442, ICONF443, ICONF444, ICONF445, ICONF446, ICONF447,
1477 ICONF448, ICONF449, ICONF450, ICONF451, ICONF452, ICONF453, ICONF454, ICONF455,
1478 ICONF456, ICONF457, ICONF458, ICONF459, ICONF460, ICONF461, ICONF462, ICONF463,
1479 ICONF464, ICONF465, ICONF466, ICONF467, ICONF468, ICONF469, ICONF470, ICONF471,
1480 ICONF472, ICONF473, ICONF474, ICONF475, ICONF476, ICONF477, ICONF478, ICONF479,
1481 ICONF480, ICONF481, ICONF482, ICONF483, ICONF484, ICONF485, ICONF486, ICONF487,
1482 ICONF488, ICONF489, ICONF490, ICONF491, ICONF492, ICONF493, ICONF494, ICONF495,
1483 ICONF496, ICONF497, ICONF498, ICONF499, ICONF500, ICONF501, ICONF502, ICONF503,
1484 ICONF504, ICONF505, ICONF506, ICONF507, ICONF508, ICONF509, ICONF510, ICONF511,
1485 ICONF512, ICONF513, ICONF514, ICONF515, ICONF516, ICONF517, ICONF518, ICONF519,
1486 ICONF520, ICONF521, ICONF522, ICONF523, ICONF524, ICONF525, ICONF526, ICONF527,
1487 ICONF528, ICONF529, ICONF530, ICONF531, ICONF532, ICONF533, ICONF534, ICONF535,
1488 ICONF536, ICONF537, ICONF538, ICONF539, ICONF540, ICONF541, ICONF542, ICONF543,
1489 ICONF544, ICONF545, ICONF546, ICONF547, ICONF548, ICONF549, ICONF550, ICONF551,
1490 ICONF552, ICONF553, ICONF554, ICONF555, ICONF556, ICONF557, ICONF558, ICONF559,
1491 ICONF560, ICONF561, ICONF562, ICONF563, ICONF564, ICONF565, ICONF566, ICONF567,
1492 ICONF568, ICONF569, ICONF570, ICONF571, ICONF572, ICONF573, ICONF574, ICONF575,
1493 ICONF576, ICONF577, ICONF578, ICONF579, ICONF580, ICONF581, ICONF582, ICONF583,
1494 ICONF584, ICONF585, ICONF586, ICONF587, ICONF588, ICONF589, ICONF590, ICONF591,
1495 ICONF592, ICONF593, ICONF594, ICONF595, ICONF596, ICONF597, ICONF598, ICONF599,
1496 ICONF600, ICONF601, ICONF602, ICONF603, ICONF604, ICONF605, ICONF606, ICONF607,
1497 ICONF608, ICONF609, ICONF610, ICONF611, ICONF612, ICONF613, ICONF614, ICONF615,
1498 ICONF616, ICONF617, ICONF618, ICONF619, ICONF620, ICONF621, ICONF622, ICONF623,
1499 ICONF624, ICONF625, ICONF626, ICONF627, ICONF628, ICONF629, ICONF630, ICONF631,
1500 ICONF632, ICONF633, ICONF634, ICONF635, ICONF636, ICONF637, ICONF638, ICONF639,
1501 ICONF640, ICONF641, ICONF642, ICONF643, ICONF644, ICONF645, ICONF646, ICONF647,
1502 ICONF648, ICONF649, ICONF650, ICONF651, ICONF652, ICONF653, ICONF654, ICONF655,
1503 ICONF656, ICONF657, ICONF658, ICONF659, ICONF660, ICONF661, ICONF662, ICONF663,
1504 ICONF664, ICONF665, ICONF666, ICONF667, ICONF668, ICONF669, ICONF670, ICONF671,
1505 ICONF672, ICONF673, ICONF674, ICONF675, ICONF676, ICONF677, ICONF678, ICONF679,
1506 ICONF680, ICONF681, ICONF682, ICONF683, ICONF684, ICONF685, ICONF686, ICONF687,
1507 ICONF688, ICONF689, ICONF690, ICONF691, ICONF692, ICONF693, ICONF694, ICONF695,
1508 ICONF696, ICONF697, ICONF698, ICONF699, ICONF700, ICONF701, ICONF702, ICONF703,
1509 ICONF704, ICONF705, ICONF706, ICONF707, ICONF708, ICONF709, ICONF710, ICONF711,
1510 ICONF712, ICONF713, ICONF714, ICONF715, ICONF716, ICONF717, ICONF718, ICONF719,
1511 ICONF720, ICONF721, ICONF722, ICONF723, ICONF724, ICONF725, ICONF726, ICONF727,
1512 ICONF728, ICONF729, ICONF730, ICONF731, ICONF732, ICONF733, ICONF734, ICONF735,
1513 ICONF736, ICONF737, ICONF738, ICONF739, ICONF740, ICONF741, ICONF742, ICONF743,
1514 ICONF744, ICONF745, ICONF746, ICONF747, ICONF748, ICONF749, ICONF750, ICONF751,
1515 ICONF752, ICONF753, ICONF754, ICONF755, ICONF756, ICONF757, ICONF758, ICONF759,
1516 ICONF760, ICONF761, ICONF762, ICONF763, ICONF764, ICONF765, ICONF766, ICONF767,
1517 ICONF768, ICONF769, ICONF770, ICONF771, ICONF772, ICONF773, ICONF774, ICONF775,
1518 ICONF776, ICONF777, ICONF778, ICONF779, ICONF780, ICONF781, ICONF782, ICONF783,
1519 ICONF784, ICONF785, ICONF786, ICONF787, ICONF788, ICONF789, ICONF790, ICONF791,
1520 ICONF792, ICONF793, ICONF794, ICONF795, ICONF796, ICONF797, ICONF798, ICONF799,
1521 ICONF800, ICONF801, ICONF802, ICONF803, ICONF804, ICONF805, ICONF806, ICONF807,
1522 ICONF808, ICONF809, ICONF810, ICONF811, ICONF812, ICONF813, ICONF814, ICONF815,
1523 ICONF816, ICONF817, ICONF818, ICONF819, ICONF820, ICONF821, ICONF822, ICONF823,
1524 ICONF824, ICONF825, ICONF826, ICONF827, ICONF828, ICONF829, ICONF830, ICONF831,
1525 ICONF832, ICONF833, ICONF834, ICONF835, ICONF836, ICONF837, ICONF838, ICONF839,
1526 ICONF840, ICONF841, ICONF842, ICONF843, ICONF844, ICONF845, ICONF846, ICONF847,
1527 ICONF848, ICONF849, ICONF850, ICONF851, ICONF852, ICONF853, ICONF854, ICONF855,
1528 ICONF856, ICONF857, ICONF858, ICONF859, ICONF860, ICONF861, ICONF862, ICONF863,
1529 ICONF864, ICONF865, ICONF866, ICONF867, ICONF868, ICONF869, ICONF870, ICONF871,
1530 ICONF872, ICONF873, ICONF874, ICONF875, ICONF876, ICONF877, ICONF878, ICONF879,
1531 ICONF880, ICONF881, ICONF882, ICONF883, ICONF884, ICONF885, ICONF886, ICONF887,
1532 ICONF888, ICONF889, ICONF890, ICONF891, ICONF892, ICONF893, ICONF894, ICONF895,
1533 ICONF896, ICONF897, ICONF898, ICONF899, ICONF900, ICONF901, ICONF902, ICONF903,
1534 ICONF904, ICONF905, ICONF906, ICONF907, ICONF908, ICONF909, ICONF910, ICONF911,
1535 ICONF912, ICONF913, ICONF914, ICONF915, ICONF916, ICONF917, ICONF918, ICONF919,
1536 ICONF920, ICONF921, ICONF922, ICONF923, ICONF924, ICONF925, ICONF926, ICONF927,
1537 ICONF928, ICONF929, ICONF930, ICONF931, ICONF932, ICONF933, ICONF934, ICONF935,
1538 ICONF936, ICONF937, ICONF938, ICONF939, ICONF940, ICONF941, ICONF942, ICONF943,
1539 ICONF944, ICONF945, ICONF946, ICONF947, ICONF948, ICONF949, ICONF950, ICONF951,
1540 ICONF952, ICONF953, ICONF954, ICONF955, ICONF956, ICONF957, ICONF958, ICONF959,
1541 ICONF960, ICONF961, ICONF962, ICONF963, ICONF964, ICONF965, ICONF966, ICONF967,
1542 ICONF968, ICONF969, ICONF970, ICONF971, ICONF972, ICONF973, ICONF974, ICONF975,
1543 ICONF976, ICONF977, ICONF978, ICONF979, ICONF980, ICONF981, ICONF982, ICONF983,
1544 ICONF984, ICONF985, ICONF986, ICONF987, ICONF988, ICONF989, ICONF990, ICONF991,
1545 ICONF992, ICONF993, ICONF994, ICONF995, ICONF996, ICONF997, ICONF998, ICONF999,
1546 ICONF1000, ICONF1001, ICONF1002, ICONF1003, ICONF1004, ICONF1005, ICONF1006, ICONF1007,
1547 ICONF1008, ICONF1009, ICONF1010, ICONF1011, ICONF1012, ICONF1013, ICONF1014, ICONF1015,
1548 ICONF1016, ICONF1017, ICONF1018, ICONF1019, ICONF1020, ICONF1021, ICONF1022, ICONF1023,
1549 ICONF1024, ICONF1025, ICONF1026, ICONF1027, ICONF1028, ICONF1029, ICONF1030, ICONF1031,
1550 ICONF1032, ICONF1033, ICONF1034, ICONF1035, ICONF1036, ICONF1037, ICONF1038, ICONF1039,
1551 ICONF1040, ICONF1041, ICONF1042, ICONF1043, ICONF1044, ICONF1045, ICONF1046, ICONF1047,
1552 ICONF1048, ICONF1049, ICONF1050, ICONF1051, ICONF1052, ICONF1053, ICONF1054, ICONF1055,
1553 ICONF1056, ICONF1057, ICONF1058, ICONF1059, ICONF1060, ICONF1061, ICONF1062, ICONF1063,
1554 ICONF1064, ICONF1065, ICONF1066, ICONF1067, ICONF1068, ICONF1069, ICONF1070, ICONF1071,
1555 ICONF1072, ICONF1073, ICONF1074, ICONF1075, ICONF1076, ICONF1077, ICONF1078, ICONF1079,
1556 ICONF1080, ICONF1081, ICONF1082, ICONF1083, ICONF1084, ICONF1085, ICONF1086, ICONF1087,
1557 ICONF1088, ICONF1089, ICONF1090, ICONF1091, ICONF1092, ICONF1093, ICONF1094, ICONF1095,
1558 ICONF1096, ICONF1097, ICONF1098, ICONF1099, ICONF1100, ICONF1101, ICONF1102, ICONF1103,
1559 ICONF1104, ICONF1105, ICONF1106, ICONF1107, ICONF1108, ICONF1109, ICONF1110, ICONF1111,
1560 ICONF1112, ICONF1113, ICONF1114, ICONF1115, ICONF1116, ICONF1117, ICONF1118, ICONF1119,
1561 ICONF1120, ICONF1121, ICONF1122, ICONF1123, ICONF1124, ICONF1125, ICONF1126, ICONF1127,
1562 ICONF1128, ICONF1129, ICONF1130, ICONF1131, ICONF1132, ICONF1133, ICONF1134, ICONF1135,
1563 ICONF1136, ICONF1137, ICONF1138, ICONF1139, ICONF1140, ICONF1141, ICONF1142, ICONF1143,
1564 ICONF1144, ICONF1145, ICONF1146, ICONF1147, ICONF1148, ICONF1149, ICONF1150, ICONF1151,
1565 ICONF1152, ICONF1153, ICONF1154, ICONF1155, ICONF1156, ICONF1157, ICONF1158, ICONF1159,
1566 ICONF1160, ICONF1161, ICONF1162, ICONF1163, ICONF1164, ICONF1165, ICONF1166, ICONF1167,
1567 ICONF1168, ICONF1169, ICONF1170, ICONF1171, ICONF1172, ICONF1173, ICONF1174, ICONF1175,
1568 ICONF1176, ICONF1177, ICONF1178, ICONF1179, ICONF1180, ICONF1181, ICONF1182, ICONF1183,
1569 ICONF1184, ICONF1185, ICONF1186, ICONF1187, ICONF1188, ICONF1189, ICONF1190, ICONF1191,
1570 ICONF1192, ICONF1193, ICONF1194, ICONF1195, ICONF1196, ICONF1197, ICONF1198, ICONF1199,
1571 ICONF1200, ICONF1201, ICONF1202, ICONF1203, ICONF1204, ICONF1205, ICONF1206, ICONF1207,
1572 ICONF1208, ICONF1209, ICONF1210, ICONF1211, ICONF1212, ICONF1213, ICONF1214, ICONF1215,
1573 ICONF1216, ICONF1217, ICONF1218, ICONF1219, ICONF1220, ICONF1221, ICONF1222, ICONF1223,
1574 ICONF1224, ICONF1225, ICONF1226, ICONF1227, ICONF1228, ICONF1229, ICONF1230, ICONF1231,
1575 ICONF1232, ICONF1233, ICONF1234, ICONF1235, ICONF1236, ICONF1237, ICONF1238, ICONF1239,
1576 ICONF1240, ICONF1241, ICONF1242, ICONF1243, ICONF1244, ICONF1245, ICONF1246, ICONF1247,
1577 ICONF1248, ICONF1249, ICONF1250, ICONF1251, ICONF1252, ICONF1253, ICONF1254, ICONF1255,
1578 ICONF1256, ICONF1257, ICONF1258, ICONF1259, ICONF1260, ICONF1261, ICONF1262, ICONF1263,
1579 ICONF1264, ICONF1265, ICONF1266, ICONF1267, ICONF1268, ICONF1269, ICONF1270, ICONF1271,
1580 ICONF1272, ICONF1273, ICONF1274, ICONF1275, ICONF1276, ICONF1277, ICONF1278, ICONF1279,
1581 ICONF1280, ICONF1281, ICONF1282, ICONF1283, ICONF1284, ICONF1285, ICONF1286, ICONF1287,
1582 ICONF1288, ICONF1289, ICONF1290, ICONF1291, ICONF1292, ICONF1293, ICONF1294, ICONF1295,
1583 ICONF1296, ICONF1297, ICONF1298, ICONF1299, ICONF1300, ICONF1301, ICONF1302, ICONF1303,
1584 ICONF1304, ICONF1305, ICONF1306, ICONF1307, ICONF1308, ICONF1309, ICONF1310, ICONF1311,
1585 ICONF1312, ICONF1313, ICONF1314, ICONF1315, ICONF1316, ICONF1317, ICONF1318, ICONF1319,
1586 ICONF1320, ICONF1321, ICONF1322, ICONF1323, ICONF1324, ICONF1325, ICONF1326, ICONF1327,
1587 ICONF1328, ICONF1329, ICONF1330, ICONF1331, ICONF1332, ICONF1333, ICONF1334, ICONF1335,
1588 ICONF1336, ICONF1337, ICONF1338, ICONF1339, ICONF1340, ICONF1341, ICONF1342, ICONF1343,
1589 ICONF1344, ICONF1345, ICONF1346, ICONF1347, ICONF1348, ICONF1349, ICONF1350, ICONF1351,
1590 ICONF1352, ICONF1353, ICONF1354, ICONF1355, ICONF1356, ICONF1357, ICONF1358, ICONF1359,
1591 ICONF1360, ICONF1361, ICONF1362, ICONF1363, ICONF1364, ICONF1365, ICONF1366, ICONF1367,
1592 ICONF1368, ICONF1369, ICONF1370, ICONF1371, ICONF1372, ICONF1373, ICONF1374, ICONF1375,
1593 ICONF1376, ICONF1377, ICONF1378, ICONF1379, ICONF1380, ICONF1381, ICONF1382, ICONF1383,
1594 ICONF1384, ICONF1385, ICONF1386, ICONF1387, ICONF1388, ICONF1389, ICONF1390, ICONF1391,
1595 ICONF1392, ICONF1393, ICONF1394, ICONF1395, ICONF1396, ICONF1397, ICONF1398, ICONF1399,
1596 ICONF1400, ICONF1401, ICONF1402, ICONF1403, ICONF1404, ICONF1405, ICONF1406, ICONF1407,
1597 ICONF1408, ICONF1409, ICONF1410, ICONF1411, ICONF1412, ICONF1413, ICONF1414, ICONF1415,
1598 ICONF1416, ICONF1417, ICONF1418, ICONF1419, ICONF1420, ICONF1421, ICONF1422, ICONF1423,
1599 ICONF1424, ICONF1425, ICONF1426, ICONF1427, ICONF1428, ICONF1429, ICONF1430, ICONF1431,
1600 ICONF1432, ICONF1433, ICONF1434, ICONF1435, ICONF1436, ICONF1437, ICONF1438, ICONF1439,
1601 ICONF1440, ICONF1441, ICONF1442, ICONF1443, ICONF1444, ICONF1445, ICONF1446, ICONF1447,
1602 ICONF1448, ICONF1449, ICONF1450, ICONF1451, ICONF1452, ICONF1453, ICONF1454, ICONF1455,
1603 ICONF1456, ICONF1457, ICONF1458, ICONF1459, ICONF1460, ICONF1461, ICONF1462, ICONF1463,
1604 ICONF1464, ICONF1465, ICONF1466, ICONF1467, ICONF1468, ICONF1469, ICONF1470, ICONF1471,
1605 ICONF1472, ICONF1473, ICONF1474, ICONF1475, ICONF1476, ICONF1477, ICONF1478, ICONF1479,
1606 ICONF1480, ICONF1481, ICONF1482, ICONF1483, ICONF1484, ICONF1485, ICONF1486, ICONF1487,
1607 ICONF1488, ICONF1489, ICONF1490, ICONF1491, ICONF1492, ICONF1493, ICONF1494, ICONF1495,
1608 ICONF1496, ICONF1497, ICONF1498, ICONF1499, ICONF1500, ICONF1501, ICONF1502, ICONF1503,
1609 ICONF1504, ICONF1505, ICONF1506, ICONF1507, ICONF1508, ICONF1509, ICONF1510, ICONF1511,
1610 ICONF1512, ICONF1513, ICONF1514, ICONF1515, ICONF1516, ICONF1517, ICONF1518, ICONF1519,
1611 ICONF1520, ICONF1521, ICONF1522, ICONF1523, ICONF1524, ICONF1525, ICONF1526, ICONF1527,
1612 ICONF1528, ICONF1529, ICONF1530, ICONF1531, ICONF1532, ICONF1533, ICONF1534, ICONF1535,
1613 ICONF1536, ICONF1537, ICONF1538, ICONF1539, ICONF1540, ICONF1541, ICONF1542, ICONF1543,
1614 ICONF1544, ICONF1545, ICONF1546, ICONF1547, ICONF1548, ICONF1549, ICONF1550, ICONF1551,
1615 ICONF1552, ICONF1553, ICONF1554, ICONF1555, ICONF1556, ICONF1557, ICONF1558, ICONF1559,
1616 ICONF1560, ICONF1561, ICONF1562, ICONF1563, ICONF1564, ICONF1565, ICONF1566, ICONF1567,
1617 ICONF1568, ICONF1569, ICONF1570, ICONF1571, ICONF1572, ICONF1573, ICONF1574, ICONF1575,
1618 ICONF1576, ICONF1577, ICONF1578, ICONF1579, ICONF1580, ICONF1581, ICONF1582, ICONF1583,
1619 ICONF1584, ICONF1585, ICONF1586, ICONF1587, ICONF1588, ICONF1589, ICONF1590, ICONF1591,
1620 ICONF1592, ICONF1593, ICONF1594, ICONF1595, ICONF1596, ICONF1597, ICONF1598, ICONF1599,
1621 ICONF1600, ICONF1601, ICONF1602, ICONF1603, ICONF1604, ICONF1605, ICONF1606, ICONF1607,
1622 ICONF1608, ICONF1609, ICONF1610, ICONF1611, ICONF1612, ICONF1613, ICONF1614, ICONF1615,
1623 ICONF1616, ICONF1617, ICONF1618, ICONF1619, ICONF1620, ICONF1621, ICONF1622, ICONF1623,
1624 ICONF1624, ICONF1625, ICONF1626, ICONF1627, ICONF1628, ICONF1629, ICONF1630, ICONF1631,
1625 ICONF1632, ICONF1633, ICONF1634, ICONF1635, ICONF1636, ICONF1637, ICONF1638, ICONF1639,
1626 ICONF1640, I
```

```

1434 C MODAL DISPLACEMENT PRINTOUT
1435 IP (IDRPLM.EQ.0) GO TO 25
1436 WRITE (6,115)
1437 WRITE (7,115)
1438 J=1
1439 DO 20 I=1,NRODES
1440 NDT=0
1441 DO 5 K=1,PDOT
1442 IP (DOT(K).NE.1) GO TO 5
1443 NDT=1
1444 GO TO 6
1445 CONTINUE
1446 8 IP (ICHOE(I)) 10,12,16
1447 WRITE (6,120) I,DTOT(J)
1448 IP (NDT.EQ.1) WRITE (7,120) I,DTOT(J)
1449 J=J+1
1450 GO TO 20
1451 J1=J+2
1452 NODENO=1
1453 CALL ELLOC (NODENO,NL)
1454 IP (NDCZ(NL).EQ.0) GO TO 14
1455 WRITE (6,125) I, (DTOT(K),K=J,J1)
1456 IP (NDT.EQ.1) WRITE (7,125) I, (DTOT(K),K=J,J1)
1457 J=J+3
1458 GO TO 20
1459 WRITE (6,127) I, (DTOT(K),K=J,J1)
1460 IP (NDT.EQ.1) WRITE (7,127) I, (DTOT(K),K=J,J1)
1461 J=J+3
1462 GO TO 20
1463 ICC=ICNODE(1)-2
1464 IP (ICCC) 19,18,17
1465 J1=J+1
1466 WRITE (6,128) I, (DPOF(K),K=J,J1)
1467 IP (NDT.EQ.1) WRITE (7,128) I, (DPOF(K),K=J,J1)
1468 J=J+2
1469 GO TO 20
1470 J1=J+3
1471 WRITE (6,129) I, (DTOT(K),K=J,J1)
1472 IP (NDT.EQ.1) WRITE (7,129) I, (DTOT(K),K=J,J1)
1473 J=J+4
1474 GO TO 20
1475 J1=J+4
1476 WRITE (6,130) I, (DPOF(K),K=J,J1)
1477 IP (NDT.EQ.1) WRITE (7,130) I, (DPOF(K),K=J,J1)
1478 J=J+5
1479 CONTINUE
1480 C CENTROIDAL CONCRETE STRESSES PRINTOUT FOR EACH ELEMENT
1481 IP (ICOR3.EQ.0) GO TO 35
1482 WRITE (6,135)
1483 WRITE (7,135)
1484 DO 30 I=1,NELT
1485 WRITE (6,140) I, (TSGCR(I,K),K=1,3), TSGAGG(I)
1486 DO 28 J=1,PELX
1487 IP (I.NE.PHEL(J)) GO TO 28
1488 WRITE (7,140) I, (TSGCR(I,K),K=1,3), TSGAGG(I)
1489 GO TO 30
1490 CONTINUE
1491 28 C
1492 30 CENTROIDAL PRINCIPAL COMPRESSIVE AND TENSILE STRESSES AND
1493 STRAINS ARE PRINTED OUT FOR EACH ELEMENT

```

```

1494 35 MODAL DISPLACEMENT PRINTOUT
1495 IP (IDRPLM.EQ.0) GO TO 50
1496 WRITE (6,145)
1497 DO 45 I=1,NELT
1498 IF (ICRACK(I).EQ.1) GO TO 40
1499 WRITE (6,150) I, TSGCC(I), TCC(I), TSGCT(I), TCT(I)
1500 GO TO 45
1501 WRITE (6,155) I, TSGCC(I), TCC(I), TSGCT(I), TCT(I)
1502 CONTINUE OF STEEL BESH STRESSES
1503 I, (LHESH.EQ.0) GO TO 60
1504 WRITE (7,160)
1505 CONTINUE
1506 DO 55 I=1,PELX
1507 IF (LHESH(I).EQ.0) GO TO 55
1508 DO 51 J=1,EDIMS
1509 WRITE (6,165) I, J, TSGHS(I, J), TSHS(I, J)
1510 CONTINUE
1511 DO 53 J=1,PELMS
1512 IF (I.NE.PSH(J)) GO TO 53
1513 DO 52 K=1,EDIMS
1514 WRITE (7,165) I, K, TSGHS(I, K), TSHS(I, K)
1515 CONTINUE
1516 GO TO 55
1517 CONTINUE
1518 CONTINUE
1519 REINFORCEMENT ELEMENT STRESS PRINTOUT
1520 IP (IREQ.EQ.0) GO TO 75
1521 WRITE (6,168)
1522 DO 70 I=1,NREQ
1523 IER=0
1524 DO 61 J=1,PERZO
1525 IF (I.NE.PHR(J)) GO TO 61
1526 IER=1
1527 GO TO 62
1528 CONTINUE
1529 IF (IER(I)) 63,64,66
1530 WRITE (6,170) I, TSGRO(I), TERO(I)
1531 IP (IREQ.EQ.0) GO TO 70
1532 WRITE (7,170) I, TSGRO(I), TERO(I)
1533 GO TO 70
1534 WRITE (6,175) I, TSGRO(I), TERO(I)
1535 IF (IER.EQ.0) GO TO 70
1536 WRITE (7,175) I, TSGRO(I), TERO(I)
1537 GO TO 70
1538 WRITE (6,180) I, TSGRO(I), TERO(I)
1539 IF (IER.EQ.0) GO TO 70
1540 WRITE (7,180) I, TSGRO(I), TERO(I)
1541 CONTINUE
1542 LOAD INCREMENT PRINTOUT
1543 CALL LOAD (MAXINC)
1544 WRITE (6,185)
1545 DO 80 I=1,NRODS
1546 IF (R2(I,1).GT.-1.0E-03.AND.R2(I,1).LT.1.0E-03) GO TO 80
1547 PEQ=I
1548 CALL MODLOC (REQ,NH)
1549 II=NH
1550 JJ=1
1551 BELK=1
1552
1553

```

```

1554 CALL LOCATE(IJ,JJ,NROW,NCOL)
1555 HB-I-NROW+1
1556 WRITE (6,190) HB,HR,R2(1,I)
1557 CONTINUE
1558 C
1559 TOTAL LOAD PRINTOUT
1560 IF (ILOAD.EQ.0) RETURN
1561 WRITE (6,195)
1562 DO 90 I=1,NEQMS
1563 IP(TOT(I),OF-1,0E-03,AND,RTOT(I),LT,1,0E-03) GO TO 90
1564 BEQ-I
1565 CALL MODLOC (REQ,HB)
1566 JJ=NN
1567 II=NN
1568 HBLK=1
1569 CALL LOCATE(IJ,JJ,NROW,NCOL)
1570 HB-I-NROW+1
1571 HR=I-NROW+1
1572 RTOT(I)
1573 CONTINUE
1574 C
1575 TOTAL REINFORCEMENT RESTRAINT VECTOR PRINTOUT
1576 WRITE (6,210)
1577 DO 95 I=1,REQMS
1578 IP(ROTOT(I),RQ,0,0) GO TO 95
1579 BEQ-I
1580 CALL MODLOC (REQ,HB)
1581 JJ=1
1582 HBLK=1
1583 CALL LOCATE(IJ,JJ,NROW,NCOL)
1584 HB-I-NROW+1
1585 WRITE (6,220) HB,HR,ROTOT(I)
1586 WRITE (7,220) HB,HR,ROTOT(I)
1587 CONTINUE
1588 RETURN
1589 C**** FORAY STATEMENTS
1590 FORAY(1) = 0
1591 DO 100 I=1,15
1592 TOUT(I) = 0
1593 C
1594 100 FORAY(I) = 0
1595 C
1596 105 FORAY(1) = THE NUMBER OF CONCRETE ELEMENTS THAT CRACKED IN THIS LOAD
1597 1 INCREMENT = 1,15
1598 2TOUT(I) = 0
1599 C
1600 115 FORAY(1) = THE MODAL DISPLACEMENTS ARE AS FOLLOWS:
1601 1' MODE
1602 2' THETA1
1603 3' THETA2
1604 4' THETA3
1605 5' THETA4
1606 6' THETA5
1607 7' THETA6
1608 8' THETA7
1609 9' THETA8
1610 10' THETA9
1611 11' THETA10
1612 12' THETA11
1613 13' THETA12
1614 14' THETA13
1615 15' THETA14
1616 16' THETA15
1617 17' THETA16
1618 18' THETA17
1619 19' THETA18
1620 20' THETA19
1621 21' THETA20
1622 22' THETA21
1623 23' THETA22
1624 24' THETA23
1625 25' THETA24
1626 26' THETA25
1627 27' THETA26
1628 28' THETA27
1629 29' THETA28
1630 30' THETA29
1631 31' THETA30
1632 32' THETA31
1633 33' THETA32
1634 34' THETA33
1635 35' THETA34
1636 36' THETA35
1637 37' THETA36
1638 38' THETA37
1639 39' THETA38
1640 40' THETA39
1641 41' THETA40
1642 42' THETA41
1643 43' THETA42
1644 44' THETA43
1645 45' THETA44
1646 46' THETA45
1647 47' THETA46
1648 48' THETA47
1649 49' THETA48
1650 50' THETA49
1651 51' THETA50
1652 52' THETA51
1653 53' THETA52
1654 54' THETA53
1655 55' THETA54
1656 56' THETA55
1657 57' THETA56
1658 58' THETA57
1659 59' THETA58
1660 60' THETA59
1661 61' THETA60
1662 62' THETA61
1663 63' THETA62
1664 64' THETA63
1665 65' THETA64
1666 66' THETA65
1667 67' THETA66
1668 68' THETA67
1669 69' THETA68
1670 70' THETA69
1671 71' THETA70
1672 72' THETA71
1673 73' THETA72
1674 74' THETA73
1675 75' THETA74
1676 76' THETA75
1677 77' THETA76
1678 78' THETA77
1679 79' THETA78
1680 80' THETA79
1681 81' THETA80
1682 82' THETA81
1683 83' THETA82
1684 84' THETA83
1685 85' THETA84
1686 86' THETA85
1687 87' THETA86
1688 88' THETA87
1689 89' THETA88
1690 90' THETA89
1691 91' THETA90
1692 92' THETA91
1693 93' THETA92
1694 94' THETA93
1695 95' THETA94
1696 96' THETA95
1697 97' THETA96
1698 98' THETA97
1699 99' THETA98
1700 100' THETA99
1701 101' THETA100
1702 102' THETA101
1703 103' THETA102
1704 104' THETA103
1705 105' THETA104
1706 106' THETA105
1707 107' THETA106
1708 108' THETA107
1709 109' THETA108
1710 110' THETA109
1711 111' THETA110
1712 112' THETA111
1713 113' THETA112
1714 114' THETA113
1715 115' THETA114
1716 116' THETA115
1717 117' THETA116
1718 118' THETA117
1719 119' THETA118
1720 120' THETA119
1721 121' THETA120
1722 122' THETA121
1723 123' THETA122
1724 124' THETA123
1725 125' THETA124
1726 126' THETA125
1727 127' THETA126
1728 128' THETA127
1729 129' THETA128
1730 130' THETA129
1731 131' THETA130
1732 132' THETA131
1733 133' THETA132
1734 134' THETA133
1735 135' THETA134
1736 136' THETA135
1737 137' THETA136
1738 138' THETA137
1739 139' THETA138
1740 140' THETA139
1741 141' THETA140
1742 142' THETA141
1743 143' THETA142
1744 144' THETA143
1745 145' THETA144
1746 146' THETA145
1747 147' THETA146
1748 148' THETA147
1749 149' THETA148
1750 150' THETA149
1751 151' THETA150
1752 152' THETA151
1753 153' THETA152
1754 154' THETA153
1755 155' THETA154
1756 156' THETA155
1757 157' THETA156
1758 158' THETA157
1759 159' THETA158
1760 160' THETA159
1761 161' THETA160
1762 162' THETA161
1763 163' THETA162
1764 164' THETA163
1765 165' THETA164
1766 166' THETA165
1767 167' THETA166
1768 168' THETA167
1769 169' THETA168
1770 170' THETA169
1771 171' THETA170
1772 172' THETA171
1773 173' THETA172
1774 174' THETA173
1775 175' THETA174
1776 176' THETA175
1777 177' THETA176
1778 178' THETA177
1779 179' THETA178
1780 180' THETA179
1781 181' THETA180
1782 182' THETA181
1783 183' THETA182
1784 184' THETA183
1785 185' THETA184
1786 186' THETA185
1787 187' THETA186
1788 188' THETA187
1789 189' THETA188
1790 190' THETA189
1791 191' THETA190
1792 192' THETA191
1793 193' THETA192
1794 194' THETA193
1795 195' THETA194
1796 196' THETA195
1797 197' THETA196
1798 198' THETA197
1799 199' THETA198
1800 200' THETA199
1801 201' THETA200
1802 202' THETA201
1803 203' THETA202
1804 204' THETA203
1805 205' THETA204
1806 206' THETA205
1807 207' THETA206
1808 208' THETA207
1809 209' THETA208
1810 210' THETA209
1811 211' THETA210
1812 212' THETA211
1813 213' THETA212
1814 214' THETA213
1815 215' THETA214
1816 216' THETA215
1817 217' THETA216
1818 218' THETA217
1819 219' THETA218
1820 220' THETA219
1821 221' THETA220
1822 222' THETA221
1823 223' THETA222
1824 224' THETA223
1825 225' THETA224
1826 226' THETA225
1827 227' THETA226
1828 228' THETA227
1829 229' THETA228
1830 230' THETA229
1831 231' THETA230
1832 232' THETA231
1833 233' THETA232
1834 234' THETA233
1835 235' THETA234
1836 236' THETA235
1837 237' THETA236
1838 238' THETA237
1839 239' THETA238
1840 240' THETA239
1841 241' THETA240
1842 242' THETA241
1843 243' THETA242
1844 244' THETA243
1845 245' THETA244
1846 246' THETA245
1847 247' THETA246
1848 248' THETA247
1849 249' THETA248
1850 250' THETA249
1851 251' THETA250
1852 252' THETA251
1853 253' THETA252
1854 254' THETA253
1855 255' THETA254
1856 256' THETA255
1857 257' THETA256
1858 258' THETA257
1859 259' THETA258
1860 260' THETA259
1861 261' THETA260
1862 262' THETA261
1863 263' THETA262
1864 264' THETA263
1865 265' THETA264
1866 266' THETA265
1867 267' THETA266
1868 268' THETA267
1869 269' THETA268
1870 270' THETA269
1871 271' THETA270
1872 272' THETA271
1873 273' THETA272
1874 274' THETA273
1875 275' THETA274
1876 276' THETA275
1877 277' THETA276
1878 278' THETA277
1879 279' THETA278
1880 280' THETA279
1881 281' THETA280
1882 282' THETA281
1883 283' THETA282
1884 284' THETA283
1885 285' THETA284
1886 286' THETA285
1887 287' THETA286
1888 288' THETA287
1889 289' THETA288
1890 290' THETA289
1891 291' THETA290
1892 292' THETA291
1893 293' THETA292
1894 294' THETA293
1895 295' THETA294
1896 296' THETA295
1897 297' THETA296
1898 298' THETA297
1899 299' THETA298
1900 300' THETA299
1901 301' THETA300
1902 302' THETA301
1903 303' THETA302
1904 304' THETA303
1905 305' THETA304
1906 306' THETA305
1907 307' THETA306
1908 308' THETA307
1909 309' THETA308
1910 310' THETA309
1911 311' THETA310
1912 312' THETA311
1913 313' THETA312
1914 314' THETA313
1915 315' THETA314
1916 316' THETA315
1917 317' THETA316
1918 318' THETA317
1919 319' THETA318
1920 320' THETA319
1921 321' THETA320
1922 322' THETA321
1923 323' THETA322
1924 324' THETA323
1925 325' THETA324
1926 326' THETA325
1927 327' THETA326
1928 328' THETA327
1929 329' THETA328
1930 330' THETA329
1931 331' THETA330
1932 332' THETA331
1933 333' THETA332
1934 334' THETA333
1935 335' THETA334
1936 336' THETA335
1937 337' THETA336
1938 338' THETA337
1939 339' THETA338
1940 340' THETA339
1941 341' THETA340
1942 342' THETA341
1943 343' THETA342
1944 344' THETA343
1945 345' THETA344
1946 346' THETA345
1947 347' THETA346
1948 348' THETA347
1949 349' THETA348
1950 350' THETA349
1951 351' THETA350
1952 352' THETA351
1953 353' THETA352
1954 354' THETA353
1955 355' THETA354
1956 356' THETA355
1957 357' THETA356
1958 358' THETA357
1959 359' THETA358
1960 360' THETA359
1961 361' THETA360
1962 362' THETA361
1963 363' THETA362
1964 364' THETA363
1965 365' THETA364
1966 366' THETA365
1967 367' THETA366
1968 368' THETA367
1969 369' THETA368
1970 370' THETA369
1971 371' THETA370
1972 372' THETA371
1973 373' THETA372
1974 374' THETA373
1975 375' THETA374
1976 376' THETA375
1977 377' THETA376
1978 378' THETA377
1979 379' THETA378
1980 380' THETA379
1981 381' THETA380
1982 382' THETA381
1983 383' THETA382
1984 384' THETA383
1985 385' THETA384
1986 386' THETA385
1987 387' THETA386
1988 388' THETA387
1989 389' THETA388
1990 390' THETA389
1991 391' THETA390
1992 392' THETA391
1993 393' THETA392
1994 394' THETA393
1995 395' THETA394
1996 396' THETA395
1997 397' THETA396
1998 398' THETA397
1999 399' THETA398
2000 400' THETA399
2001 401' THETA400
2002 402' THETA401
2003 403' THETA402
2004 404' THETA403
2005 405' THETA404
2006 406' THETA405
2007 407' THETA406
2008 408' THETA407
2009 409' THETA408
2010 410' THETA409
2011 411' THETA410
2012 412' THETA411
2013 413' THETA412
2014 414' THETA413
2015 415' THETA414
2016 416' THETA415
2017 417' THETA416
2018 418' THETA417
2019 419' THETA418
2020 420' THETA419
2021 421' THETA420
2022 422' THETA421
2023 423' THETA422
2024 424' THETA423
2025 425' THETA424
2026 426' THETA425
2027 427' THETA426
2028 428' THETA427
2029 429' THETA428
2030 430' THETA429
2031 431' THETA430
2032 432' THETA431
2033 433' THETA432
2034 434' THETA433
2035 435' THETA434
2036 436' THETA435
2037 437' THETA436
2038 438' THETA437
2039 439' THETA438
2040 440' THETA439
2041 441' THETA440
2042 442' THETA441
2043 443' THETA442
2044 444' THETA443
2045 445' THETA444
2046 446' THETA445
2047 447' THETA446
2048 448' THETA447
2049 449' THETA448
2050 450' THETA449
2051 451' THETA450
2052 452' THETA451
2053 453' THETA452
2054 454' THETA453
2055 455' THETA454
2056 456' THETA455
2057 457' THETA456
2058 458' THETA457
2059 459' THETA458
2060 460' THETA459
2061 461' THETA460
2062 462' THETA461
2063 463' THETA462
2064 464' THETA463
2065 465' THETA464
2066 466' THETA465
2067 467' THETA466
2068 468' THETA467
2069 469' THETA468
2070 470' THETA469
2071 471' THETA470
2072 472' THETA471
2073 473' THETA472
2074 474' THETA473
2075 475' THETA474
2076 476' THETA475
2077 477' THETA476
2078 478' THETA477
2079 479' THETA478
2080 480' THETA479
2081 481' THETA480
2082 482' THETA481
2083 483' THETA482
2084 484' THETA483
2085 485' THETA484
2086 486' THETA485
2087 487' THETA486
2088 488' THETA487
2089 489' THETA488
2090 490' THETA489
2091 491' THETA490
2092 492' THETA491
2093 493' THETA492
2094 494' THETA493
2095 495' THETA494
2096 496' THETA495
2097 497' THETA496
2098 498' THETA497
2099 499' THETA498
2100 500' THETA499
2101 501' THETA500
2102 502' THETA501
2103 503' THETA502
2104 504' THETA503
2105 505' THETA504
2106 506' THETA505
2107 507' THETA506
2108 508' THETA507
2109 509' THETA508
2110 510' THETA509
2111 511' THETA510
2112 512' THETA511
2113 513' THETA512
2114 514' THETA513
2115 515' THETA514
2116 516' THETA515
2117 517' THETA516
2118 518' THETA517
2119 519' THETA518
2120 520' THETA519
2121 521' THETA520
2122 522' THETA521
2123 523' THETA522
2124 524' THETA523
2125 525' THETA524
2126 526' THETA525
2127 527' THETA526
2128 528' THETA527
2129 529' THETA528
2130 530' THETA529
2131 531' THETA530
2132 532' THETA531
2133 533' THETA532
2134 534' THETA533
2135 535' THETA534
2136 536' THETA535
2137 537' THETA536
2138 538' THETA537
2139 539' THETA538
2140 540' THETA539
2141 541' THETA540
2142 542' THETA541
2143 543' THETA542
2144 544' THETA543
2145 545' THETA544
2146 546' THETA545
2147 547' THETA546
2148 548' THETA547
2149 549' THETA548
2150 550' THETA549
2151 551' THETA550
2152 552' THETA551
2153 553' THETA552
2154 554' THETA553
2155 555' THETA554
2156 556' THETA555
2157 557' THETA556
2158 558' THETA557
2159 559' THETA558
2160 560' THETA559
2161 561' THETA560
2162 562' THETA561
2163 563' THETA562
2164 564' THETA563
2165 565' THETA564
2166 566' THETA565
2167 567' THETA566
2168 568' THETA567
2169 569' THETA568
2170 570' THETA569
2171 571' THETA570
2172 572' THETA571
2173 573' THETA572
2174 574' THETA573
2175 575' THETA574
2176 576' THETA575
2177 577' THETA576
2178 578' THETA577
2179 579' THETA578
2180 580' THETA579
2181 581' THETA580
2182 582' THETA581
2183 583' THETA582
2184 584' THETA583
2185 585' THETA584
2186 586' THETA585
2187 587' THETA586
2188 588' THETA587
2189 589' THETA588
2190 590' THETA589
2191 591' THETA590
2192 592' THETA591
2193 593' THETA592
2194 594' THETA593
2195 595' THETA594
2196 596' THETA595
2197 597' THETA596
2198 598' THETA597
2199 599' THETA598
2200 600' THETA599
2201 601' THETA600
2202 602' THETA601
2203 603' THETA602
2204 604' THETA603
2205 605' THETA604
2206 606' THETA605
2207 607' THETA606
2208 608' THETA607
2209 609' THETA608
2210 610' THETA609
2211 611' THETA610
2212 612' THETA611
2213 613' THETA612
2214 614' THETA613
2215 615' THETA614
2216 616' THETA615
2217 617' THETA616
2218 618' THETA617
2219 619' THETA618
2220 620' THETA619
2221 621' THETA620
2222 622' THETA621
2223 623' THETA622
2224 624' THETA623
2225 625' THETA624
2226 626' THETA625
2227 627' THETA626
2228 628' THETA627
2229 629' THETA628
2230 630' THETA629
2231 631' THETA630
2232 632' THETA631
2233 633' THETA632
2234 634' THETA633
2235 635' THETA634
2236 636' THETA635
2237 637' THETA636
2238 638' THETA637
2239 639' THETA638
2240 640' THETA639
2241 641' THETA640
2242 642' THETA641
2243 643' THETA642
2244 644' THETA643
2245 645' THETA644
2246 646' THETA645
2247 647' THETA646
2248 648' THETA647
2249 649' THETA648
2250 650' THETA649
2251 651' THETA650
2252 652' THETA651
2253 653' THETA652
2254 654' THETA653
2255 655' THETA654
2256 656' THETA655
2257 657' THETA656
2258 658' THETA657
2259 659' THETA658
2260 660' THETA659
2261 661' THETA660
2262 662' THETA661
2263 663' THETA662
2264 664' THETA663
2265 665' THETA664
2266 666' THETA665
2267 667' THETA666
2268 668' THETA667
2269 669' THETA668
2270 670' THETA669
2271 671' THETA670
2272 672' THETA671
2273 673' THETA672
2274 674' THETA673
2275 675' THETA674
2276 676' THETA675
2277 677' THETA676
2278 678' THETA677
2279 679' THETA678
2280 680' THETA679
2281 681' THETA680
2282 682' THETA681
2283 683' THETA682
2284 684' THETA683
2285 685' THETA684
2286 686' THETA685
2287 687' THETA686
2288 688' THETA687
2289 689' THETA688
2290 690' THETA689
2291 691' THETA690
2292 692' THETA691
2293 693' THETA692
2294 694' THETA693
2295 695' THETA694
2296 696' THETA695
2297 697' THETA696
2298 698' THETA697
2299 699' THETA698
2300 700' THETA699
2301 701' THETA700
2302 702' THETA701
2303 703' THETA702
2304 704' THETA703
2305 705' THETA704
2306 706' THETA705
2307 707' THETA706
2308 708' THETA707
2309 709' THETA708
2310 710' THETA709
2311 711' THETA710
2312 712' THETA711
2313 713' THETA712
2314 714' THETA713
2315 715' THETA714
2316 716' THETA715
2317 717' THETA716
2318 718' THETA717
2319 719' THETA718
2320 720' THETA719
2321 721' THETA720
2322 722' THETA721
2323 723' THETA722
2324 724' THETA723
2325 725' THETA724
2326 726' THETA725
2327 727' THETA726
2328 728' THETA727
2329 729' THETA728
2330 730' THETA729
2331 731' THETA730
2332 732' THETA731
2333 733' THETA732
2334 734' THETA733
2335 735' THETA734
2336 736' THETA735
2337 737' THETA736
2338 738' THETA737
2339 739' THETA738
2340 740' THETA739
2341 741' THETA740
2342 742' THETA741
2343 743' THETA742
2344 744' THETA743
2345 745' THETA744
2346 746' THETA745
2347 747' THETA746
2348 748' THETA747
2349 749' THETA748
2350 750' THETA749
2351 751' THETA750
2352 752' THETA751
2353 753' THETA752
2354 754' THETA753
2355 755' THETA754
2356 756' THETA755
2357 757' THETA756
2358 758' THETA757
2359 759' THETA758
2360 760' THETA759
2361 761' THETA760
2362 762' THETA761
2363 763' THETA762
2364 764' THETA763
2365 765' THETA764
2366 766' THETA765
2367 767' THETA766
2368 768' THETA767
2369 769' THETA768
2370 770' THETA769
2371 771' THETA770
2372 772' THETA771
2373 773' THETA772
2374 774' THETA773
2375 775' THETA774
2376 776' THETA775
2377 777' THETA776
2378 778' THETA777
2379 779' THETA778
2380 780' THETA779
2381 781' THETA780
2382 782' THETA781
2383 783' THETA782
2384 784' THETA783
2385 785' THETA784
2386 786' THETA785
2387 787' THETA786
2388 788' THETA787
2389 789' THETA788
2390 790' THETA789
2391 791' THETA790
2392 792' THETA791
2393 793' THETA792
2394 794'
```

```

1960 R2(I,J)=0.0
1961 CONTINUE
1962 IF (NUMINC.GT.1) GO TO 4
1963 HAINC=0
1964 CALCULATION OF TOTAL NUMBER OF LOAD INCREMENTS.
1965 DO 3 I=1,NLOADY
1966 HAINC=HAINC+NUMICRT(I)
1967 CONTINUE
1968 C DETERMINATION OF LOAD INCREMENT TYPE
1969 I=0
1970 IC=0
1971 I=I+1
1972 IC=IC+NUMICRT(I)
1973 IF (HAINC.GT.IC) GO TO 5
1974 C FORMATION OF FULL LOAD INCREMENT VECTOR TO BE STORED IN FIRST
1975 C COLUMN OF R2(2,NFOMS)
1976 NL=NFOMS(I)
1977 DO 8 J=1,NL
1978 XI=MODER(J,I)
1979 JJ=1
1980 NBLK=1
1981 CALL LOCATZ(II,JJ,NROW,NCOL)
1982 K=MODER(J,I)-1
1983 R2(1,K)=VALUER(J,I)
1984 CONTINUE
1985 C FORMATION OF HALF LOAD INCREMENT OF NEXT LOAD ITERATION AND
1986 C STORAGE IN SECOND COLUMN OF R2(2,NFOMS)
1987 IF (HAINC.EQ.1) GO TO 11
1988 IF (HAINC.LT.HAINC) GO TO 10
1989 C FOLLOWING HALF LOAD INCREMENT IS SET TO ZERO IF CURRENT LOAD
1990 C INCREMENT IS THE LAST INCREMENT.
1991 DO 9 J=1,NFOMS
1992 R2(2,J)=0.0
1993 CONTINUE
1994 RETURN
1995 10 IF ((NUMINC+1).GT.IC) GO TO 15
1996 11 DO 12 J=1,NFOMS
1997 R2(2,J)=-.5*R2(1,J)
1998 CONTINUE
1999 RETURN
2000 J=I+1
2001 NL=NFOMS(J)
2002 DO 18 K=1,NL
2003 XI=MODER(K,J)
2004 JJ=1
2005 NBLK=1
2006 CALL LOCATZ(II,JJ,NROW,NCOL)
2007 L=MODER(K,J)-1
2008 R2(2,L)=VALUER(K,J)*.5
2009 CONTINUE
2010 RETURN
2011 END

```

APPENDIX E  
SUBROUTINE LOGIC NOTES



## APPENDIX E

### SUBROUTINE LOGIC NOTES

The purpose of this appendix is to clarify any subroutine logic development that might not be sufficiently illustrated by the numerous comment cards inserted throughout the program. The comment card heading in each subroutine states the routine's principal function. Those routines warranting comment are listed in alphabetical order.

#### Subroutine DOWEL

To detect the failure of a dowel mechanism across a concrete crack, the dowel displacement of the adjacent crack surfaces at the concrete element's centroid is calculated and compared to the critical dowel displacement value DF.

#### Subroutine FORCE

When a bi-linear stress-strain curve is assumed for the conventional reinforcement, considerable difficulty is experienced in modelling the reinforcement's behaviour beyond yielding. Inevitably, an excessive number of modified Newton-Rapson iterations is required to produce convergence, especially when the second linear segment of the stress-strain curve is almost perfectly plastic. To eliminate this particular cause of time consuming and costly iteration, a yielding conventional reinforcement bar is modelled in the total stress condition as a bar of zero stiffness with externally applied nodal forces at each bar node representing the influence of the bar of the remainder

of the structure. In the incremental stress condition, the bar's stiffness corresponds to the slope of the strain-hardening portion of the stress-strain curve. For the range of strain-hardening usually encountered, this approach simulates reinforcement yielding accurately.

#### Subroutine HORIZ

Before the stiffness terms of a horizontal rectangular element are added into the in-core total stiffness matrix, the component (3x3) element stiffness blocks must be transformed as the local element axes, as shown in Figure A-1, do not correspond to the global axis orientation. The sign of four stiffness terms is changed as a result of the transformation process.

#### Subroutine NDCONC

The formulations used in this subroutine are given in detail in Sections 3.4.2.1 and 3.4.2.6. In deriving the stiffness of a cracked concrete element, the constitutive matrix is formulated for axes in the crack and orthogonal to crack directions. Consequently, transformation of the constitutive matrix must be undertaken.

#### Subroutine SHRMOD

The shear rigidity of a cracked concrete element in a direction parallel to the crack direction is the sum of the aggregate interlock and dowel stiffnesses. The empirical derivations of the two contributing stiffnesses are given in Sections 3.4.2.4 and 3.4.2.5. In formulation of the dowel stiffness, the magnitude is not permitted to exceed twenty percent of the aggregate interlock value.

Subroutine WARP

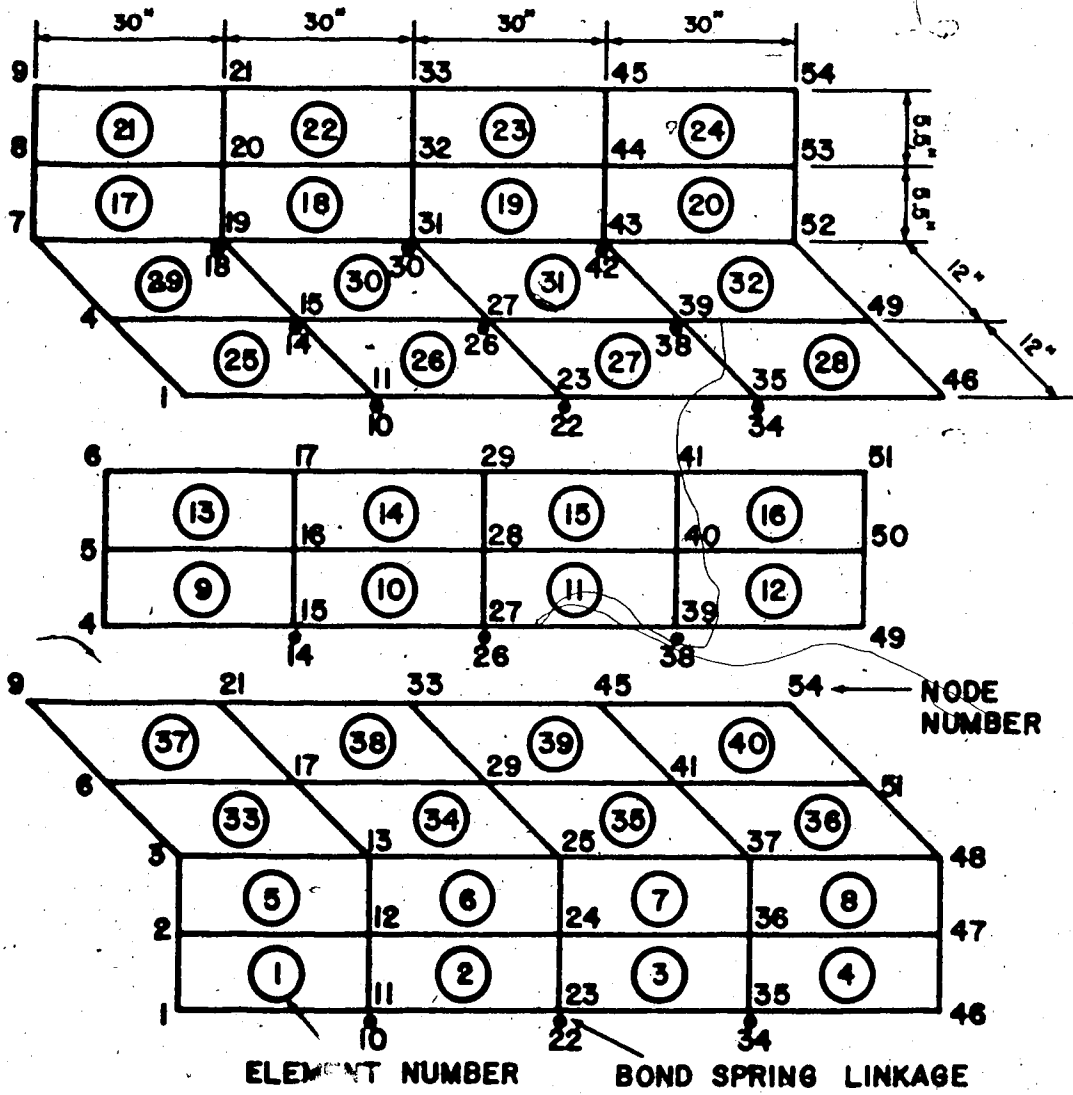
The warping resistance of "thick" diaphragms is greatly overestimated by classical thin plate theory, as detailed in Section 3.4.2.8. However, the warping stiffness formulation used in this subroutine is the classical form given in 3.4.2.7, with real behaviour reflected by the insertion of an equivalent diaphragm thickness.

**APPENDIX F**  
**INPUT DATA FILE EXAMPLE**

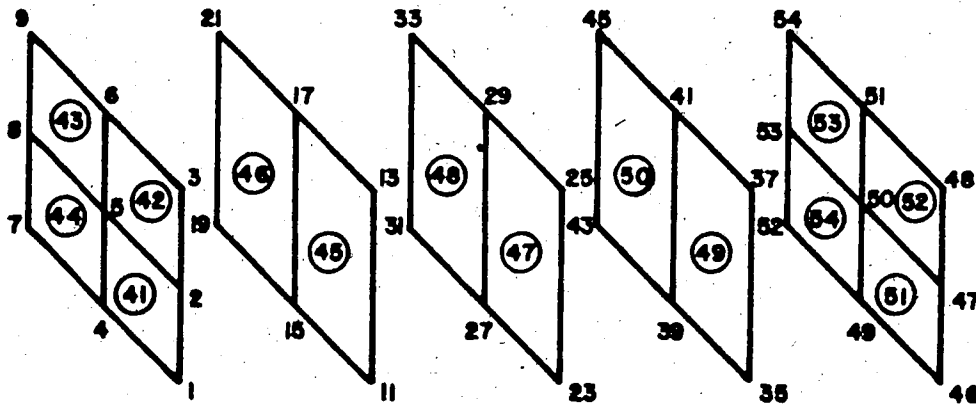








(a) Exploded view of concrete web and flange elements



(b) Diaphragm elements

FIG. F-1 BEAM MESH FOR INPUT DATA FILE EXAMPLE



**APPENDIX G**

**OUTPUT EXAMPLE**





10	1	1	2.5000	90.0
11	1	1	2.5000	90.0
12	1	1	2.5000	90.0
13	1	1	2.5000	90.0
14	1	1	2.5000	90.0
15	1	1	2.5000	90.0
16	1	1	2.5000	90.0
17	1	1	2.5000	90.0
18	1	1	2.5000	90.0
19	1	1	2.5000	90.0
20	1	1	2.5000	90.0
21	1	1	2.5000	90.0
22	1	1	2.5000	90.0
23	1	1	2.5000	90.0
24	1	1	2.5000	90.0
25	1	1	2.5000	90.0
26	1	1	2.5000	90.0
27	1	1	2.5000	90.0
28	1	1	2.5000	90.0
29	1	1	2.5000	90.0
30	1	1	2.5000	90.0
31	1	1	2.5000	90.0
32	1	1	2.5000	90.0
33	1	1	2.5000	90.0
34	1	1	2.5000	90.0
35	1	1	2.5000	90.0
36	1	1	2.5000	90.0
37	1	1	2.5000	90.0
38	1	1	2.5000	90.0
39	1	1	2.5000	90.0
40	1	1	2.5000	90.0

DIAPHRAGM INPUT DATA IS AS BELOW

TOTAL NUMBER OF DIAPHRAGM ELEMENTS IN COMPLETE BEAR = 16

DATA FOR ACTUAL AND PSEUDO DIAPHRAGMS IS AS BELOW

ELEMENT NO.	TYPE	THICKNESS	ELEMENT NO.	REFERENCE	SHEAR MODULUS
41	3	25.50	4	1	0.3000E+07
42	3	25.50	5	2	0.3000E+07
43	3	25.50	6	3	0.3000E+07
44	3	25.50	7	4	0.3000E+07
45	3	25.50	8	5	0.3000E+07
46	3	25.50	9	6	0.3000E+07
47	3	25.50	10	7	0.3000E+07
48	3	25.50	11	8	0.3000E+07
49	4	1.00	12	47	0.3000E+07
50	4	1.00	13	48	0.3000E+07
51	4	1.00	14	49	0.3000E+07
52	4	1.00	15	50	0.3000E+07
53	4	1.00	16	51	0.3000E+07
54	4	1.00	17	52	0.3000E+07
55	5	8.50	23	25	0.5700E+06
56	5	8.50	24	29	0.5700E+06
			25	33	0.5700E+06
			26	37	0.5700E+06
			27	41	0.5700E+06
			28	45	0.5700E+06
			29	49	0.3000E+07
			30	53	0.3000E+07
			31	57	0.3000E+07
			32	61	0.3000E+07
			33	65	0.3000E+07
			34	69	0.3000E+07
			35	73	0.3000E+07
			36	77	0.3000E+07
			37	81	0.3000E+07
			38	85	0.3000E+07
			39	89	0.3000E+07
			40	93	0.3000E+07
			41	97	0.3000E+07
			42	101	0.3000E+07
			43	105	0.3000E+07
			44	109	0.3000E+07
			45	113	0.3000E+07
			46	117	0.3000E+07
			47	121	0.3000E+07
			48	125	0.3000E+07
			49	129	0.3000E+07
			50	133	0.3000E+07
			51	137	0.3000E+07
			52	141	0.3000E+07
			53	145	0.3000E+07
			54	149	0.3000E+07
			55	153	0.3000E+07
			56	157	0.3000E+07

NUMBER OF SINGLE REINFORCING BARS AND BOND SLIP LINKAGES = 45

ELEMENT NUMBER	FIRST NODE	SECOND NODE	REQ. TYPE	DIRECTION INDICATOR	AREA	INITIAL PRESTRESS	INITIAL PRESTRAIN
1	34	46	-1	-1	0.1100		
2	38	49	-1	-1	0.2200		
3	42	52	-1	-1	0.1100		
4	22	34	-1	-1	0.1100		
5	26	38	-1	-1	0.2200		
6	30	42	-1	-1	0.1100		
7	10	22	-1	-1	0.1100		
8	14	26	-1	-1	0.2200		
9	18	30	-1	-1	0.1100		
10	1	10	-1	-1	0.1100		
11	4	14	-1	-1	0.2200		
12	7	18	-1	-1	0.1100		
13	37	48	-1	-1	0.1100		
14	41	51	-1	-1	0.2200		
15	45	54	-1	-1	0.1100		
16	25	37	-1	-1	0.1100		
17	29	41	-1	-1	0.2200		
18	33	45	-1	-1	0.1100		
19	13	25	-1	-1	0.1100		
20	17	29	-1	-1	0.2200		
21	21	33	-1	-1	0.1100		
22	3	13	-1	-1	0.1100		
23	6	17	-1	-1	0.2200		
24	9	21	-1	-1	0.1100		
25	34	46	0	-1	0.0990	0.16667E+06	0.66670E-02
26	38	49	0	-1	0.1980	0.16667E+06	0.66670E-02
27	42	52	0	-1	0.0990	0.16667E+06	0.66670E-02
28	22	34	0	-1	0.0990	0.16667E+06	0.66670E-02
29	26	38	0	-1	0.1980	0.16667E+06	0.66670E-02
30	30	42	0	-1	0.0990	0.16667E+06	0.66670E-02
31	10	22	0	-1	0.0990	0.16667E+06	0.66670E-02
32	14	26	0	-1	0.1980	0.16667E+06	0.66670E-02
33	18	30	0	-1	0.0990	0.16667E+06	0.66670E-02
34	1	10	0	-1	0.0990	0.16667E+06	0.66670E-02
35	4	14	0	-1	0.1980	0.16667E+06	0.66670E-02
36	7	18	0	-1	0.0990	0.16667E+06	0.66670E-02
37	34	35	1	-1	0.0990	0.16667E+06	0.66670E-02
38	38	39	1	-1	125.4000		
39	42	43	1	-1	215.4000		
40	22	23	1	-1	125.4000		
41	26	27	1	-1	125.4000		
42	30	31	1	-1	215.4000		
43	10	11	1	-1	125.4000		
44	14	15	1	-1	215.4000		
45	18	19	1	-1	125.4000		

NUMBER OF FINITE ELEMENT NODES = 54

NODE NUMBER	NODE TYPE	COORDINATE X	COORDINATE Y	COORDINATE Z
1	1	0.0	0.0	0.0
24	0	0.0	0.0	24.00

2	0.0	5.50	24.00
3	0.0	11.00	24.00
4	0.0	0.0	12.00
5	0.0	0.0	12.00
6	0.0	11.00	12.00
7	0.0	0.0	0.0
8	0.0	5.50	0.0
9	0.0	11.00	0.0
10	30.00	0.0	24.00
11	30.00	0.0	24.00
12	30.00	5.50	24.00
13	30.00	11.00	24.00
14	30.00	0.0	12.00
15	30.00	0.0	12.00
16	30.00	5.50	12.00
17	30.00	11.00	12.00
18	30.00	0.0	0.0
19	30.00	0.0	0.0
20	30.00	5.50	0.0
21	30.00	11.00	0.0
22	60.00	0.0	0.0
23	60.00	0.0	24.00
24	60.00	5.50	24.00
25	60.00	11.00	24.00
26	60.00	0.0	12.00
27	60.00	0.0	12.00
28	60.00	5.50	12.00
29	60.00	11.00	12.00
30	60.00	0.0	0.0
31	60.00	0.0	0.0
32	60.00	5.50	0.0
33	60.00	11.00	0.0
34	90.00	0.0	24.00
35	90.00	0.0	24.00
36	90.00	5.50	24.00
37	90.00	11.00	24.00
38	90.00	0.0	12.00
39	90.00	0.0	12.00
40	90.00	5.50	12.00
41	90.00	11.00	12.00
42	90.00	0.0	0.0
43	90.00	0.0	0.0
44	90.00	5.50	0.0
45	90.00	11.00	0.0
46	120.00	0.0	24.00
47	120.00	5.50	24.00
48	120.00	11.00	24.00
49	120.00	0.0	12.00
50	120.00	5.50	12.00
51	120.00	11.00	12.00
52	120.00	0.0	0.0
53	120.00	5.50	0.0
54	120.00	11.00	0.0

THE STRENGTH AND DEVIATION PARAMETERS ARE AS BELOW  
 INITIAL YOUNG'S MODULUS FOR CONCRETE = 0.3000E+07  
 INITIAL YOUNG'S MODULUS FOR CONVENTIONAL REINFORCEMENT = 0.29500E+08

INITIAL YOUNG'S MODULUS FOR PRESTRESSING STEEL = 0.26500E+08  
 INITIAL BOND SLIP LINKAGE STIFFNESS = 0.19500E+07 LBS/CU. INCH  
 INITIAL STEEL MESH MODULUS = 0.29500E+08  
 COMPRESSIVE CONCRETE STRENGTH = -0.50000E+04 LBS./SQ. INCH  
 TENSILE CONCRETE STRENGTH = 0.40000E+03 LBS./SQ. INCH  
 ULTIMATE AGGREGATE INTERLOCK STRENGTH = -0.50000E+04 LBS./SQ. IN.  
 ULTIMATE TENSILE STRENGTH OF CONVENTIONAL REINFORCEMENT = 0.75700E+05 LBS./SQ. INCH  
 ULTIMATE TENSILE STRENGTH OF PRESTRESSING STEEL = 0.27700E+06 LBS./SQ. INCH  
 ULTIMATE TENSILE STRENGTH OF STEEL MESH BARS = 0.75700E+05 LBS./SQ. INCH

YIELD STRAIN FOR CONVENTIONAL REINFORCEMENT = 0.16500E-02  
 YIELD STRAIN FOR PRESTRESS REINFORCEMENT = 0.98500E-02  
 MAXIMUM CONCRETE COMPRESSIVE STRAIN = -0.003000  
 MAXIMUM CONVENTIONAL REINFORCEMENT TENSILE STRAIN = 0.045000  
 MAXIMUM PRESTRESSING STEEL TENSILE STRAIN = 0.045000  
 MAXIMUM STEEL MESH BAR TENSILE STRAIN = 0.045000  
 MAXIMUM BOND LINKAGE SLIP = 0.001200 INCHES  
 DOWEL FAILURE DISPLACEMENT = 0.000500 INCHES

POISSON RATIO FOR CONCRETE IN BIAXIAL COMPRESSION = .20000  
 POISSON RATIO FOR CONCRETE IN BIAXIAL TENSION = .18000  
 POISSON RATIO FOR CONCRETE IN TENSION-COMPRESSION = .19000  
 BIAXIAL POISSON RATIO FOR CONCRETE = .20000  
 MAXIMUM ALLOWABLE PERCENTAGE DEVIATION OF CONCRETE = 8.000  
 MAXIMUM ALLOWABLE PERCENTAGE DEVIATION OF MAIN DIAGONAL  
 TERMS OF CONCRETE CONSTITUTIVE MATRIX = 0.00100  
 MAXIMUM ALLOWABLE PERCENTAGE DEVIATION OF REINFORCEMENT STIFFNESS  
 BEFORE CHANGE MUST BE MADE = 0.00100  
 MAXIMUM ALLOWABLE PERCENTAGE DEVIATION OF PRESTRESS BARS = 20.000  
 MAXIMUM ALLOWABLE PERCENTAGE DEVIATION FOR BOND SLIP LINKAGE = 50.000  
 CRITICAL NUMBER OF MATERIAL DEVIATIONS TO INVOKE ITERATIVE METHOD = 8  
 AVERAGE CRACK SPACING = 4.000 INCHES  
 RELAXATION FACTOR = 1.200

MAXIMUM NUMBER OF ITERATIONS BEFORE EXECUTION IS TERMINATED = 15  
 CONCRETE DEVIATION WEIGHTING = 1  
 CONVENTIONAL REINFORCEMENT DEVIATION WEIGHTING = 3  
 PRESTRESS STRAND DEVIATION WEIGHTING = 4

LOADING INFORMATION FOLLOWS

LOAD TYPE NUMBER	NO. OF INCREMENTS	NO. OF MODAL LOADS
1	1	6
1	1	0.164650E+05
4	1	0.329300E+05
7	1	0.164650E+05
46	1	-0.164650E+05
49	1	-0.329300E+05
52	1	-0.164650E+05
LOAD TYPE NUMBER	NO. OF INCREMENTS	NO. OF MODAL LOADS
2	10	3
24	2	LOAD MAGNITUDE
26	2	-0.500000E+04
32	2	-0.500000E+04

NUMBER OF DIFFERENT LOADING TYPES TO BE SUPERIMPOSED ON MODEL = 2

IMPOSED BOUNDARY CONDITIONS ARE AS BELOW

NUMBER OF IMPOSED BOUNDARY CONDITIONS = 6

MODE OF APPLICATION OF IMPOSED BOUNDARY CONDITIONS	DIRECTION OF APPLICATION	IMPOSED VALUE
1		0.0
2		0.0
3		0.0
3		0.0
3		0.0
2		0.0

SCREEN PRINTOUT DATA IS AS BELOW

THE ELEMENT NUMBERS OF THE 4 CONCRETE ELEMENTS WHOSE (STRESS,STRAIN) STATE WILL BE DISPLAYED, ARE BELOW  
26 27 34 35

THE 2 STEEL MESH ELEMENT NUMBERS WHOSE (STRESS,STRAIN) STATES WILL BE DISPLAYED, ARE BELOW  
2 6

THE 10 REINFORCEMENT ELEMENTS WHOSE (STRESS,STRAIN) STATES WILL BE DISPLAYED, ARE BELOW  
1 2 3 13 14 15 25 26 27 37

THE 1 NODES WHOSE DISPLACEMENTS WILL BE DISPLAYED ARE BELOW  
28

PRINTOUT FORMAT CONTROL VARIABLES ARE AS BELOW

DEFLECTIONS CONTROL VARIABLE = 1  
 CENTROIDAL CONCRETE STRESSES CONTROL VARIABLE = 1  
 PRINCIPAL CONCRETE STRESSES CONTROL VARIABLE = 1  
 STEEL MESH STRESSES CONTROL VARIABLE = 1  
 REINFORCEMENT ELEMENT STRESSES CONTROL VARIABLE = 1  
 LOAD INCREMENT CONTROL VARIABLE = 1  
 TOTAL LOAD CONTROL VARIABLE = 1  
 STIFFNESS ASSEMBLAGE CONTROL VARIABLE = 0

\*\*\* END OF INPUT ECHO CHECK \*\*\*

AFTER DATA IS READ IN, CPU TIME = 1616 PROGRAMME COST = 0.66

BYTES = 15376 LEN = 15376 NUMBER = 1



STRUCTURE STIFFNESS MATRIX HAS BEEN FULLY ASSEMBLED AND WRITTEN ON -FILE-

AFTER TOTAL STIFFNESS MATRIX HAS BEEN ASSEMBLED AND CERTAIN MATRICES RESET TO ZERO,  
 CPU TIME = 3470 PROGRAMME COST = 1.17

\*\*\*\*\*  
 \* LOAD INCREMENT NUMBER 1 \*  
 \*\*\*\*\*

\*\*\*\*\* OUTPUT FROM SUBROUTINE SOLVE \*\*\*\*\*

CPU TIME AT INITIAL STAGE IN SUBROUTINE SOLVE = 3479 PROGRAM COST = 1.18  
 CPU TIME AT COMPLETION OF BLOCK MANIPULATION OF BLOCK NUMBER 1 = 3504  
 CPU TIME AT COMPLETION OF GAUSSIAN ELIMINATION OF BLOCK NUMBER 1 = 3981  
 CPU TIME AFTER REDUCED EQUATIONS OF BLOCK NUMBER 1 HAVE BEEN WRITTEN OUT ON DISC = 4004  
 CPU TIME AT BEGINNING OF BACKSUBSTITUTION PROCESS = 5263  
 CPU TIME AT END OF SOLUTION PROCESS = 5477 PROGRAM COST = 1.73

BEFORE ROUTINE STRESS IS CALLED IN FIRST LOAD INCREMENT,  
 CPU TIME = 5480 PROGRAMME COST = 1.74

AFTER ROUTINE STRESS HAS BEEN CALLED AND BEFORE ROUTINE KUTTA IS CALLED IN THE FIRST LOAD INCREMENT,  
 CPU TIME = 5536 PROGRAMME COST = 1.75

AFTER ROUTINE KUTTA HAS BEEN CALLED IN FIRST LOAD INCREMENT,  
 CPU TIME = 7227 PROGRAMME COST = 2.22

BEFORE BEAM IS CHECKED FOR FURTHER CRACKING,  
 CPU TIME = 9209 PROGRAMME COST = 2.78

\*\*\*\*\*  
 \* LOAD INCREMENT NUMBER 1 STRESS-DEFORMATION PRINTOUT \*  
 \*\*\*\*\*

THE NUMBER OF CONCRETE ELEMENTS THAT CRACKED IN THIS LOAD INCREMENT = 0

THE MODAL DISPLACEMENTS ARE AS FOLLOWS

MODE	X	Y	Z	THETA	THETA
1	0.99936E-02	0.36988E-04	0.52861E-04	0.34184E-03	0.18010E-02
2	-0.39375E-03	0.43202E-04	0.65843E-05	-0.76227E-04	0.17471E-02
3	-0.9448E-02	0.46680E-04	-0.24967E-04	-0.60900E-07	0.18175E-02
4	0.10573E-01	-0.69880E-06	-0.28306E-05	0.0	0.18023E-02
5	0.0	0.0	0.0	0.28372E-05	0.17733E-02
6	-0.96088E-02	0.35095E-05	-0.58372E-04	-0.34193E-03	0.18213E-02
7	0.9945E-02	0.49371E-04	-0.58537E-04	0.0	0.18014E-02
8	-0.39427E-03	0.55577E-04	-0.65797E-05	0.76335E-04	0.17474E-02
9	-0.9895E-02	0.59086E-04	0.30637E-04	0.0	0.18177E-02
10	0.10539E-02	0.0	0.0	0.24908E-05	0.81834E-02
11	0.10534E-02	0.40308E-01	0.54888E-03	0.0	0.87636E-03
12	-0.36414E-02	0.40456E-01	0.0	0.0	0.0

13	-0.85336E-02	0.40489E-01	-0.47548E-04	0.22171E-05	0.89192E-03
14	0.12249E-02	0.40244E-01	-0.13830E-05	0.26399E-08	0.82518E-03
15	0.12241E-02	0.40411E-01	0.15497E-05	0.39597E-08	0.87417E-03
16	-0.35383E-02	0.40430E-01	-0.55124E-03	-0.26189E-05	0.91443E-03
17	-0.85261E-02	0.40500E-01	0.50210E-04	-0.20950E-05	0.81827E-03
18	0.10336E-02	0.53396E-01	0.57705E-03	-0.79025E-09	0.87652E-03
19	0.10531E-02	0.53529E-01	-0.55690E-04	0.43934E-07	0.89201E-03
20	-0.36413E-02	0.53327E-01	0.0	0.12085E-07	-0.14912E-06
21	-0.85335E-02	0.53569E-01	0.0	0.12085E-07	-0.13679E-07
22	-0.73006E-02	0.53363E-01	0.0	-0.19418E-09	-0.10656E-06
23	-0.73007E-02	0.53363E-01	-0.57727E-03	0.58092E-07	-0.24671E-06
24	-0.73005E-02	0.53590E-01	0.55906E-04	-0.63056E-07	-0.99830E-07
25	-0.73004E-02	0.40314E-01	0.54813E-03	-0.24564E-05	-0.24052E-06
26	-0.73018E-02	0.40462E-01	-0.48373E-04	-0.21764E-05	-0.25796E-06
27	-0.73018E-02	0.40492E-01	-0.16613E-05	0.12005E-07	-0.70402E-07
28	-0.73009E-02	0.40430E-01	0.10850E-05	0.14522E-07	-0.27254E-06
29	-0.73007E-02	0.40324E-01	-0.55108E-03	0.25770E-05	-0.81783E-03
30	-0.73013E-02	0.40472E-01	0.50150E-04	0.21081E-05	-0.87535E-03
31	-0.73014E-02	0.40502E-01	0.52772E-04	-0.34225E-03	-0.89168E-03
32	-0.73008E-02	0.38219E-04	0.58753E-05	0.76380E-04	-0.18020E-02
33	-0.73004E-02	0.44403E-04	-0.26217E-04	0.59516E-07	-0.17476E-02
34	-0.15452E-01	-0.71870E-06	-0.30635E-05	0.31025E-07	-0.18183E-02
35	-0.15451E-01	0.35534E-05	0.16418E-05	-0.34238E-03	-0.17735E-02
36	-0.10958E-01	0.48498E-04	-0.58892E-04	0.34238E-03	-0.18218E-02
37	-0.60674E-02	0.54678E-04	-0.72968E-05	-0.76436E-04	-0.17477E-02
38	-0.15824E-01	0.58163E-04	0.29493E-04	0.76436E-04	-0.18185E-02
39	-0.15824E-01	0.40246E-01	-0.16613E-05	0.12005E-07	-0.82461E-03
40	-0.11070E-01	0.40412E-01	0.10850E-05	0.14522E-07	-0.87361E-03
41	-0.60742E-02	0.40430E-01	0.10850E-05	0.14522E-07	-0.91486E-03
42	-0.15652E-01	0.40324E-01	-0.55108E-03	0.25770E-05	-0.81783E-03
43	-0.15651E-01	0.40472E-01	0.50150E-04	0.21081E-05	-0.87535E-03
44	-0.10959E-01	0.40502E-01	0.52772E-04	-0.34225E-03	-0.89168E-03
45	-0.60682E-02	0.38219E-04	0.58753E-05	0.76380E-04	-0.18020E-02
46	-0.24593E-01	0.44403E-04	-0.26217E-04	0.59516E-07	-0.17476E-02
47	-0.74202E-01	-0.71870E-06	-0.30635E-05	0.31025E-07	-0.18183E-02
48	-0.46988E-02	0.35534E-05	0.16418E-05	-0.34238E-03	-0.17735E-02
49	-0.25167E-01	0.48498E-04	-0.58892E-04	0.34238E-03	-0.18218E-02
50	-0.44586E-01	0.54678E-04	-0.72968E-05	-0.76436E-04	-0.17477E-02
51	-0.49823E-02	0.58163E-04	0.29493E-04	0.76436E-04	-0.18185E-02
52	-0.24598E-01	0.40246E-01	-0.16613E-05	0.12005E-07	-0.82461E-03
53	-0.44203E-01	0.40412E-01	0.10850E-05	0.14522E-07	-0.87361E-03
54	-0.46985E-02	0.58163E-04	0.29493E-04	0.76436E-04	-0.18185E-02

CENTROIDAL CONCRETE STRESSES (SGCON(SEL,3)) AND AGGREGATE INTERLOCK STRESS (SGAGG(SEL)) ARE AS BELOW

ELEMENT NO.      SIGMA      SIGMA(Y)      SIGMA(X)      SIGMA(Y)      SIGMA(X)

1	-0.59586E+03	-0.27457E+02	-0.32231E+02	0.0	0.0
2	-0.61559E+03	-0.21985E+02	0.12743E+02	0.0	0.0
3	-0.61537E+03	-0.22100E+02	-0.12694E+02	0.0	0.0
4	-0.59579E+03	-0.27369E+02	0.33153E+02	0.0	0.0
5	-0.94145E+02	-0.13564E+02	0.49406E+02	0.0	0.0
6	-0.12288E+03	-0.47805E+01	-0.86846E+01	0.0	0.0
7	-0.12280E+03	-0.45861E+01	0.87228E+01	0.0	0.0
8	-0.93808E+02	-0.14799E+02	-0.49397E+02	0.0	0.0
9	-0.63013E+03	-0.30825E+02	-0.62066E+02	0.0	0.0
10	-0.63075E+03	-0.23391E+02	0.56014E+01	0.0	0.0
11	-0.63058E+03	-0.23441E+02	-0.55446E+01	0.0	0.0
12	-0.62885E+03	-0.30892E+02	0.62752E+02	0.0	0.0
13	-0.12118E+03	-0.14744E+02	0.24860E+02	0.0	0.0
14	-0.12201E+03	-0.12946E+01	-0.20764E+02	0.0	0.0

ELEMENT NO.	PRINCIPAL COMPRESSIVE AND TENSILE STRESSES AND STRAINS FOR EACH ELEMENT CENTROID ARE AS BELOW		ELEMENT CRACKED ?
	PRINCIPAL COMPRESSIVE STRESS	PRINCIPAL TENSILE STRESS	
15	-0.12896E+03	0.20965E+02	0.0
16	-0.11978E+03	-0.25182E+02	0.0
17	-0.59588E+03	-0.33272E+02	0.0
18	-0.61563E+03	0.12572E+02	0.0
19	-0.61534E+03	-0.12574E+02	0.0
20	-0.59577E+03	0.33188E+02	0.0
21	-0.59428E+02	0.49351E+02	0.0
22	-0.12292E+03	-0.88374E+01	0.0
23	-0.12287E+03	0.86439E+01	0.0
24	-0.93772E+02	-0.49367E+02	0.0
25	-0.60165E+03	-0.28938E+02	0.0
26	-0.66161E+03	-0.82854E+01	0.0
27	-0.66131E+03	0.84904E+01	0.0
28	-0.60740E+03	0.28780E+02	0.0
29	-0.60769E+03	-0.29048E+02	0.0
30	-0.66161E+03	0.84423E+01	0.0
31	-0.66127E+03	-0.85779E+01	0.0
32	-0.60744E+03	-0.28845E+02	0.0
33	0.20897E+03	0.16055E+02	0.0
34	0.22374E+03	-0.59046E+00	0.0
35	0.22382E+03	0.55573E+00	0.0
36	0.20967E+03	0.15859E+02	0.0
37	0.20901E+03	0.15983E+02	0.0
38	0.22373E+03	0.46257E+00	0.0
39	0.22378E+03	-0.43837E+00	0.0
40	0.20970E+03	-0.15776E+02	0.0
1	-0.59780E+03	-0.25521E+02	0.31346E-04
2	-0.61566E+03	-0.21711E+02	0.33620E-04
3	-0.61564E+03	-0.21828E+02	0.33767E-04
4	-0.59765E+03	-0.25442E+02	0.31363E-04
5	-0.11761E+03	0.98972E+01	0.10747E-04
6	-0.12352E+03	-0.41450E+01	0.68528E-05
7	-0.12344E+03	-0.39460E+01	0.59140E-05
8	-0.11755E+03	0.89475E+01	0.10428E-04
9	-0.63649E+03	-0.24464E+02	0.34278E-04
10	-0.63080E+03	-0.23340E+02	0.34273E-04
11	-0.63063E+03	-0.23390E+02	0.34245E-04
12	-0.63537E+03	-0.24378E+02	0.34232E-04
13	-0.12861E+03	-0.93080E+01	0.53361E-05
14	-0.13234E+03	0.28807E+00	0.64774E-05
15	-0.13236E+03	0.43718E+00	0.85283E-05
16	-0.12552E+03	-0.22556E+01	0.52829E-05
17	-0.59782E+03	-0.25469E+02	0.31365E-04
18	-0.61590E+03	-0.21748E+02	0.33610E-04
19	-0.61561E+03	-0.21634E+02	0.33763E-04
20	-0.59770E+03	-0.25388E+02	0.31367E-04
21	-0.11787E+03	0.98555E+01	0.31389E-04
22	-0.12357E+03	-0.40791E+01	0.10417E-04
23	-0.12353E+03	-0.40653E+01	0.68785E-05
24	-0.11751E+03	0.88773E+01	0.68796E-05
25	-0.60915E+03	-0.48654E+02	0.10401E-04
26	-0.66172E+03	-0.48654E+02	0.37690E-04
27	-0.66143E+03	-0.37693E+02	0.44833E-04
28	-0.60889E+03	-0.48654E+02	0.44830E-04
		0.37635E-04	0.37635E-04



29	-0.60919E+03	-0.19097E-03	-0.48619E+02	0.37704E-04
30	-0.66173E+03	-0.21807E-03	-0.37747E+02	0.4864E-04
31	-0.66139E+03	-0.21669E-03	-0.37690E+02	0.48660E-04
32	-0.60893E+03	-0.19887E-03	-0.48140E+02	0.37646E-04
33	0.11467E+02	-0.2832E-05	0.21027E+03	0.69115E-04
34	0.56231E+01	-0.5505E-05	0.22375E+03	0.73912E-04
35	0.55872E+01	-0.55671E-05	0.22382E+03	0.73939E-04
36	0.11526E+02	-0.28592E-05	0.21094E+03	0.69333E-04
37	0.11451E+02	-0.28460E-05	0.21030E+03	0.69125E-04
38	0.55295E+01	-0.55805E-05	0.22373E+03	0.73910E-04
39	0.54977E+01	-0.55943E-05	0.22378E+03	0.73930E-04
40	0.11513E+02	-0.28627E-05	0.21095E+03	0.69337E-04

STEEL WESH STRESSES ARE AS BELOW.  
 REINFORCEMENT  
 NO. DIRECTION

1	1	STRESS=	0.90204E+03	STRAIN=	0.30578E-04
2	1	STRESS=	0.99498E+03	STRAIN=	0.33712E-04
3	1	STRESS=	0.99294E+03	STRAIN=	0.33652E-04
4	1	STRESS=	0.90265E+03	STRAIN=	0.30598E-04
6	1	STRESS=	0.19467E+03	STRAIN=	0.65991E-05
7	1	STRESS=	0.19643E+03	STRAIN=	0.66583E-05
8	1	STRESS=	0.3037E+02	STRAIN=	0.10292E-05
9	1	STRESS=	0.93677E+03	STRAIN=	0.31755E-04
10	1	STRESS=	0.10105E+04	STRAIN=	0.34252E-04
11	1	STRESS=	0.10096E+04	STRAIN=	0.34225E-04
12	1	STRESS=	0.93360E+03	STRAIN=	0.31647E-04
13	1	STRESS=	0.93460E+03	STRAIN=	0.31682E-05
14	1	STRESS=	0.21116E+03	STRAIN=	0.71581E-05
15	1	STRESS=	0.21193E+03	STRAIN=	0.71840E-05
16	1	STRESS=	0.86280E+02	STRAIN=	0.29925E-05
17	1	STRESS=	0.90253E+03	STRAIN=	0.30594E-04
18	1	STRESS=	0.99429E+03	STRAIN=	0.33702E-04
19	1	STRESS=	0.99288E+03	STRAIN=	0.33657E-04
20	1	STRESS=	0.90322E+03	STRAIN=	0.30617E-04
21	1	STRESS=	0.31507E+02	STRAIN=	0.10680E-05
22	1	STRESS=	0.19518E+03	STRAIN=	0.66161E-05
23	1	STRESS=	0.19520E+03	STRAIN=	0.66168E-05
24	1	STRESS=	0.29704E+02	STRAIN=	0.10062E-05
25	1	STRESS=	0.10954E+04	STRAIN=	0.37137E-04
26	1	STRESS=	0.13213E+04	STRAIN=	0.44791E-04
27	1	STRESS=	0.13212E+04	STRAIN=	0.44787E-04
28	1	STRESS=	0.10939E+04	STRAIN=	0.37082E-04
29	1	STRESS=	0.10957E+04	STRAIN=	0.37141E-04
30	1	STRESS=	0.13222E+04	STRAIN=	0.44821E-04
31	1	STRESS=	0.13221E+04	STRAIN=	0.44816E-04
32	1	STRESS=	0.10942E+04	STRAIN=	0.37091E-04
33	1	STRESS=	-0.67279E+02	STRAIN=	-0.22807E-05
34	1	STRESS=	-0.16372E+03	STRAIN=	-0.55498E-05
35	1	STRESS=	-0.16421E+03	STRAIN=	-0.55665E-05
36	1	STRESS=	-0.68235E+02	STRAIN=	-0.23151E-05
37	1	STRESS=	-0.67631E+02	STRAIN=	-0.22926E-05
38	1	STRESS=	-0.16461E+03	STRAIN=	-0.55800E-05
39	1	STRESS=	-0.16502E+03	STRAIN=	-0.55939E-05
40	1	STRESS=	-0.66601E+02	STRAIN=	-0.23255E-05

REINFORCEMENT ELEMENT STRESSES AND STRAINS ARE AS BELOW;

REINFORCEMENT NUMBER	REINFORCEMENT TYPE	STRESS	STRAIN
1	CONVENTIONAL	-0.87923E+04	-0.29804E-03
2	CONVENTIONAL	-0.91870E+04	-0.3112E-03
3	CONVENTIONAL	-0.87933E+04	-0.29808E-03
4	CONVENTIONAL	-0.82117E+04	-0.27836E-03
5	CONVENTIONAL	-0.83607E+04	-0.28809E-03
6	CONVENTIONAL	-0.82111E+04	-0.27834E-03
7	CONVENTIONAL	-0.82153E+04	-0.27848E-03
8	CONVENTIONAL	-0.83845E+04	-0.28422E-03
9	CONVENTIONAL	-0.82156E+04	-0.27850E-03
10	CONVENTIONAL	-0.87909E+04	-0.29800E-03
11	CONVENTIONAL	-0.94277E+04	-0.31162E-03
12	CONVENTIONAL	-0.87919E+04	-0.29803E-03
13	CONVENTIONAL	0.13458E+04	0.45620E-04
14	CONVENTIONAL	0.10738E+04	0.36398E-04
15	CONVENTIONAL	0.13468E+04	0.45655E-04
16	CONVENTIONAL	0.12125E+04	0.4102E-04
17	CONVENTIONAL	0.12061E+04	0.40883E-04
18	CONVENTIONAL	0.12117E+04	0.41074E-04
19	CONVENTIONAL	0.12127E+04	0.41107E-04
20	CONVENTIONAL	0.12049E+04	0.40846E-04
21	CONVENTIONAL	0.12126E+04	0.41104E-04
22	CONVENTIONAL	0.13385E+04	0.45373E-04
23	CONVENTIONAL	0.10647E+04	0.36092E-04
24	CONVENTIONAL	0.13396E+04	0.45412E-04
25	PRESTRESSED	0.15877E+06	0.63556E-02
26	PRESTRESSED	0.15841E+06	0.63556E-02
27	PRESTRESSED	0.15872E+06	0.63889E-02
28	PRESTRESSED	0.15929E+06	0.63886E-02
29	PRESTRESSED	0.15914E+06	0.63829E-02
30	PRESTRESSED	0.15929E+06	0.63887E-02
31	PRESTRESSED	0.15929E+06	0.63885E-02
32	PRESTRESSED	0.15913E+06	0.63828E-02
33	PRESTRESSED	0.15929E+06	0.63885E-02
34	PRESTRESSED	0.15877E+06	0.63690E-02
35	PRESTRESSED	0.15841E+06	0.63554E-02
36	PRESTRESSED	0.15872E+06	0.63690E-02
37	BONDED	0.78424E+00	0.40233E-06
38	BONDED	0.13647E+01	0.70035E-06
39	BONDED	0.81326E+00	0.41723E-06
40	BONDED	0.10170E+00	0.52154E-07
41	BONDED	0.11623E+00	0.59605E-07
42	BONDED	0.14528E+00	0.74506E-07
43	BONDED	0.90346E+00	0.46357E-06
44	BONDED	0.14797E+01	0.75949E-06
45	BONDED	0.90436E+00	0.46403E-06

THE LOAD INCREMENT VECTOR IS AS BELOW:

INCR( 1,1 ) = 0.16465E+05
INCR( 4,1 ) = 0.32930E+05
INCR( 7,1 ) = 0.16465E+05
INCR( 46,1 ) = -0.16465E+05
INCR( 49,1 ) = -0.32930E+05
INCR( 52,1 ) = -0.16465E+05

THE TOTAL LOAD VECTOR IS AS BELOW:

TOTAL( 1,1 ) = 0.16465E+05
----------------------------

RTOTAL( 4 , 1 ) = 0.32930E+05  
RTOTAL( 7 , 1 ) = 0.16465E+05  
RTOTAL( 46 , 1 ) = -0.16465E+05  
RTOTAL( 49 , 1 ) = -0.32930E+05  
RTOTAL( 52 , 1 ) = -0.16465E+05

TOTAL REINFORCEMENT FORCE RESTRAINT VECTOR:

\*\*\*\*\*  
\* LOAD INCREMENT NUMBER 2 \*  
\*\*\*\*\*

BEFORE BEAM IS CHECKED FOR FURTHER CRACKING,  
CPU TIME = 12806 PROGRAMME COST = 3.90

\*\*\*\*\*  
\* LOAD INCREMENT NUMBER 5 \*  
\*\*\*\*\*

BEFORE BEAM IS CHECKED FOR FURTHER CRACKING,  
CPU TIME = 42853 PROGRAMME COST = 12.66

\*\*\*\*\* CONCRETE ELEMENT NUMBER 14 HAS JUST CRACKED \*\*\*\*\*

\*\*\*\*\* CONCRETE ELEMENT NUMBER 15 HAS JUST CRACKED \*\*\*\*\*

CONVENTIONAL REINFORCEMENT ELEMENT NUMBER 4 HAS JUST YIELDED  
STRESS= 0.63238E+05 STRAIN= 0.21437E-02

CONVENTIONAL REINFORCEMENT ELEMENT NUMBER 5 HAS JUST YIELDED  
STRESS= 0.62074E+05 STRAIN= 0.21042E-02

CONVENTIONAL REINFORCEMENT ELEMENT NUMBER 6 HAS JUST YIELDED  
STRESS= 0.63228E+05 STRAIN= 0.21433E-02

CONVENTIONAL REINFORCEMENT ELEMENT NUMBER 7 HAS JUST YIELDED  
STRESS= 0.63315E+05 STRAIN= 0.21463E-02

CONVENTIONAL REINFORCEMENT ELEMENT NUMBER 8 HAS JUST YIELDED  
STRESS= 0.62213E+05 STRAIN= 0.21089E-02

CONVENTIONAL REINFORCEMENT ELEMENT NUMBER 9 HAS JUST YIELDED  
STRESS= 0.63362E+05 STRAIN= 0.21479E-02

BEFORE STIFFNESS ADJUSTMENTS HAVE BEEN MADE,  
CPU TIME = 42875 PROGRAMME COST = 12.67

\*\*\*\* ITERATION CYCLE NO. 1 \*\*\*\*

AFTER STIFFNESS ADJUSTMENTS HAVE BEEN MADE,  
CPU TIME = 44577 PROGRAMME COST = 13.15

BEFORE BEAM IS CHECKED FOR FURTHER CRACKING,  
CPU TIME = 46540 PROGRAMME COST = 13.70

\*\*\*\*\* CONCRETE ELEMENT NUMBER 6 HAS JUST CRACKED \*\*\*\*\*  
 \*\*\*\*\* CONCRETE ELEMENT NUMBER 7 HAS JUST CRACKED \*\*\*\*\*  
 \*\*\*\*\* CONCRETE ELEMENT NUMBER 22 HAS JUST CRACKED \*\*\*\*\*  
 \*\*\*\*\* CONCRETE ELEMENT NUMBER 23 HAS JUST CRACKED \*\*\*\*\*

BEFORE STIFFNESS ADJUSTMENTS HAVE BEEN MADE,  
 CPU TIME = 46560 PROGRAMME COST = 13.71

\*\*\*\* ITERATION CYCLE NO. 2 \*\*\*\*

AFTER STIFFNESS ADJUSTMENTS HAVE BEEN MADE,  
 CPU TIME = 48263 PROGRAMME COST = 14.19  
 BEFORE BEAM IS CHECKED FOR FURTHER CRACKING,  
 CPU TIME = 50238 PROGRAMME COST = 14.74

\*\*\*\* PRESTRESS ELEMENT NUMBER 28 IS YIELDING \*\*\*\*  
 STRESS= 0.25533E+06 STRAIN= 0.10013E-01

\*\*\*\* PRESTRESS ELEMENT NUMBER 29 IS YIELDING \*\*\*\*  
 STRESS= 0.25440E+06 STRAIN= 0.99778E-02

\*\*\*\* PRESTRESS ELEMENT NUMBER 30 IS YIELDING \*\*\*\*  
 STRESS= 0.25527E+06 STRAIN= 0.10010E-01

\*\*\*\* PRESTRESS ELEMENT NUMBER 31 IS YIELDING \*\*\*\*  
 STRESS= 0.25608E+06 STRAIN= 0.10041E-01

\*\*\*\* PRESTRESS ELEMENT NUMBER 32 IS YIELDING \*\*\*\*  
 STRESS= 0.25545E+06 STRAIN= 0.10017E-01

\*\*\*\* PRESTRESS ELEMENT NUMBER 33 IS YIELDING \*\*\*\*  
 STRESS= 0.25615E+06 STRAIN= 0.10044E-01

\*\*\*\*\*  
 \* LOAD INCREMENT NUMBER 5 STRESS-DEFORMATION PRINTOUT \*  
 \*\*\*\*\*

THE NUMBER OF CONCRETE ELEMENTS THAT CRACKED IN THIS LOAD INCREMENT = 6

THE NODAL DISPLACEMENTS ARE AS FOLLOWS  
 NODE I Y Z THETA Y THETA Z

THETA Z



1	-0.63200E-01	-0.13257E-03	-0.74226E-04	-0.14483E-03	-0.12472E-04
2	-0.11541E-03	-0.13452E-05	-0.45251E-05	-0.45251E-05	-0.12167E-01
3	-0.66030E-01	-0.10204E-03	0.61611E-04	0.10686E-03	-0.12073E-01
4	-0.61701E-01	-0.49890E-04	0.95676E-04	-0.18705E-05	-0.12527E-01
5	-0.0	-0.0	-0.0	-0.0	-0.12031E-01
6	-0.66156E-01	-0.30815E-04	-0.95559E-04	-0.18245E-05	-0.12065E-01
7	-0.63153E-01	-0.54993E-03	0.26530E-03	0.14086E-03	-0.12472E-01
8	-0.71909E-04	-0.55176E-03	0.45325E-05	-0.10973E-03	-0.12165E-01
9	0.66081E-01	-0.51761E-03	-0.25252E-03	-0.10973E-03	-0.12069E-01
10	-0.61958E-01	-0.62022E-01	0.17057E-03	0.29135E-05	-0.10934E-01
11	-0.21901E-02	-0.37213E+00	-0.37213E+00	0.29135E-05	-0.12801E-01
12	-0.62713E-01	-0.37058E+00	0.84525E-03	-0.2658E-04	-0.12574E-01
13	0.61021E-01	-0.37058E+00	0.84525E-03	-0.2658E-04	-0.12574E-01
14	-0.61096E-01	-0.37201E+00	0.15311E-03	-0.23944E-05	-0.10651E-01
15	-0.32863E-02	-0.37101E+00	-0.33174E-04	-0.16105E-05	-0.12755E-01
16	0.60858E-01	-0.36916E+00	-0.33174E-04	-0.16105E-05	-0.12193E-01
17	-0.61905E-01	-0.3715E+00	0.12135E-03	-0.51241E-05	-0.10934E-01
18	-0.61969E-01	-0.37249E+00	0.12135E-03	-0.51241E-05	-0.10934E-01
19	-0.27371E-02	-0.37110E+00	-0.91114E-03	0.38030E-04	-0.12575E-01
20	0.62768E-01	-0.37110E+00	-0.91114E-03	0.38030E-04	-0.12575E-01
21	0.39262E-01	-0.5614E+00	-0.37679E-03	-0.18159E-04	0.24726E-04
22	0.39092E-01	-0.5614E+00	-0.37679E-03	-0.18159E-04	0.24726E-04
23	0.39092E-01	-0.5614E+00	-0.37679E-03	-0.18159E-04	0.24726E-04
24	0.39092E-01	-0.5614E+00	-0.37679E-03	-0.18159E-04	0.24726E-04
25	0.39480E-01	-0.5614E+00	0.12548E-02	0.11662E-05	0.30923E-04
26	0.39480E-01	-0.5614E+00	0.12548E-02	0.11662E-05	0.30923E-04
27	0.39480E-01	-0.5614E+00	0.12548E-02	0.11662E-05	0.30923E-04
28	0.39480E-01	-0.5614E+00	0.12548E-02	0.11662E-05	0.30923E-04
29	0.39480E-01	-0.5614E+00	0.12548E-02	0.11662E-05	0.30923E-04
30	0.39396E-01	-0.56708E+00	-0.0	0.94361E-05	0.38290E-04
31	0.39396E-01	-0.56708E+00	-0.0	0.94361E-05	0.38290E-04
32	0.39166E-01	-0.5693E+00	-0.0	0.37551E-06	0.46463E-04
33	0.38922E-01	-0.56636E+00	-0.0	0.37551E-06	0.46463E-04
34	0.13964E+00	-0.37281E-03	0.37281E-03	0.70815E-05	0.42645E-04
35	0.13970E+00	-0.37281E-03	0.37281E-03	0.70815E-05	0.42645E-04
36	0.80540E-01	-0.37174E+00	-0.10686E-03	-0.78285E-05	0.10926E-01
37	0.15082E-01	-0.37034E+00	0.90720E-03	0.38285E-04	0.12779E-01
38	0.13881E+00	-0.37120E+00	-0.13651E-03	-0.21731E-05	0.10627E-01
39	0.13881E+00	-0.37120E+00	-0.13651E-03	-0.21731E-05	0.10627E-01
40	0.16982E-01	-0.36835E+00	0.19305E-04	-0.98916E-06	0.12738E-01
41	0.16982E-01	-0.36835E+00	0.19305E-04	-0.98916E-06	0.12738E-01
42	0.13970E+00	-0.37203E+00	-0.16029E-03	0.47699E-05	0.12194E-01
43	0.13970E+00	-0.37203E+00	-0.16029E-03	0.47699E-05	0.12194E-01
44	0.80554E-01	-0.37139E+00	-0.86858E-03	-0.41526E-04	0.16930E-01
45	0.15112E-01	-0.36999E+00	-0.25640E-03	-0.41526E-04	0.12561E-01
46	0.14074E+00	-0.51634E-03	-0.51634E-03	0.14073E-03	0.12439E-01
47	0.77759E-01	-0.51771E-03	-0.40758E-04	0.14073E-03	0.12180E-01
48	0.11750E-01	-0.48285E-03	0.22895E-03	-0.10278E-05	0.12038E-01
49	0.13421E+00	-0.47847E-04	-0.88500E-04	-0.12291E-05	0.12483E-01
50	0.77353E-01	-0.0	-0.63707E-05	-0.12291E-05	0.11992E-01
51	0.11561E-01	-0.31813E-04	0.75732E-05	-0.22012E-05	0.12023E-01
52	0.14078E+00	-0.15781E-03	0.79493E-04	-0.14300E-03	0.12436E-01
53	0.77798E-01	-0.15923E-03	-0.19804E-05	-0.14300E-03	0.12139E-01
54	0.11796E-01	-0.12427E-03	-0.77438E-04	0.98766E-04	0.12035E-01

CENTROIDAL CONCRETE STRESSES TSCOM(NEL,3)- AND AGGREGATE INTERLOCK STRESS TSCAGG(NEL) ARE AS BELOW  
 ELEMENT NO.      SIGNAL      SIGNAL (Z)      SIGNAL (XZ)  
 1      -0.83323E+03  
 2      0.25875E+02      0.25971E+02      0.81976E+02

3	0.26013E+02	0.26144E+03	-0.82468E+02	-0.28369E+02
4	-0.82825E+03	-0.31859E+03	0.51368E+03	0.55641E+01
5	-0.45256E+03	-0.17054E+03	-0.51802E+03	0.0
6	-0.17184E+03	-0.45642E+03	-0.28046E+03	0.65053E+02
7	-0.17053E+03	-0.44783E+03	0.27635E+03	-0.63619E+02
8	-0.45589E+03	-0.16757E+03	0.51568E+03	0.0
9	-0.95736E+03	0.22074E+03	-0.63467E+03	-0.27388E+02
10	0.42347E+02	0.27071E+03	-0.10735E+03	-0.42328E+02
11	0.42539E+02	-0.41610E+03	0.62853E+03	0.31951E+02
12	-0.94940E+03	-0.22312E+03	-0.62595E+03	0.0
13	-0.55775E+03	-0.44094E+03	-0.32348E+03	0.12557E+03
14	-0.23728E+03	-0.43644E+03	0.32098E+03	-0.12979E+03
15	-0.23566E+03	-0.21747E+03	0.63661E+03	0.0
16	-0.59052E+03	-0.31940E+03	-0.51552E+03	-0.36327E+01
17	-0.82209E+03	0.25833E+03	-0.81267E+02	0.24643E+02
18	0.25566E+02	0.25909E+03	-0.81668E+02	-0.23910E+02
19	0.25743E+02	-0.31846E+03	0.51371E+03	0.55614E+01
20	-0.82866E+03	0.16632E+03	-0.51882E+03	0.0
21	-0.45069E+03	0.44842E+03	-0.27467E+03	0.56154E+02
22	-0.16825E+03	-0.45003E+03	0.27752E+03	0.0
23	-0.17117E+03	-0.16810E+03	0.51320E+03	-0.64209E+02
24	-0.45534E+03	0.22543E+02	-0.12131E+03	0.0
25	0.34960E+03	0.21790E+02	0.22138E+01	0.25966E+02
26	0.17829E+00	0.28477E+02	-0.21253E+01	-0.27596E+02
27	0.17052E+00	0.27846E+02	0.12159E+03	0.0
28	0.29746E+03	0.21849E+02	0.12049E+03	0.0
29	0.86969E+03	0.26491E+02	-0.21167E+01	-0.26700E+02
30	0.16913E+00	-0.26650E+02	0.21512E+01	0.26822E+02
31	0.17364E+00	0.23263E+02	-0.12264E+03	0.0
32	0.28877E+03	0.13771E+02	0.11016E+03	0.0
33	-0.34473E+03	-0.12720E+03	0.10440E+03	0.0
34	-0.21296E+04	-0.12709E+03	-0.10384E+03	0.0
35	-0.21350E+04	0.15503E+02	-0.11005E+03	0.0
36	-0.35049E+03	0.13957E+02	-0.10362E+03	0.0
37	-0.34479E+03	-0.12727E+03	0.10533E+03	0.0
38	-0.21324E+04	-0.12701E+03	0.10455E+03	0.0
39	-0.21333E+04	0.15448E+02	0.0	0.0
40	-0.34955E+03	0.0	0.0	0.0

PRINCIPAL COMPRESSIVE AND TENSILE STRESSES AND STRAINS FOR EACH ELEMENT CENTROID ARE AS BELOW  
ELEMENT NO. PRINCIPAL COMPRESSIVE STRESS PRINCIPAL TENSILE STRESS PRINCIPAL TENSILE STRAIN ELEMENT CRACKED ?

1	-0.11532E+04	-0.38072E-03	0.0	0.10692E-02	YES
2	0.28558E+03	0.91387E-04	0.0	0.25158E-02	YES
3	0.28746E+03	0.91984E-04	0.0	0.24919E-02	YES
4	-0.11468E+04	-0.37863E-03	0.0	0.10588E-02	YES
5	-0.84841E+03	-0.29187E-03	0.22532E+03	0.12844E-03	NO
6	-0.62826E+03	-0.20746E-03	0.0	0.50329E-03	YES
7	-0.61836E+03	-0.20419E-03	0.0	0.49263E-03	YES
8	-0.84514E+03	-0.29058E-03	0.22168E+03	0.12742E-03	NO
9	-0.13781E+04	-0.45568E-03	0.0	0.12549E-02	YES
10	0.31289E+03	0.10042E-03	0.0	0.25274E-02	YES
11	0.31345E+03	0.10030E-03	0.0	0.24942E-02	YES
12	-0.13655E+04	-0.45148E-03	0.0	0.12260E-02	YES
13	-0.10384E+04	-0.35602E-03	0.0	0.15159E-03	NO
14	-0.67822E+03	-0.22392E-03	0.25749E+03	0.58763E-03	YES
15	-0.67269E+03	-0.22210E-03	0.0	0.57131E-03	YES
16	-0.10674E+04	-0.36562E-03	0.25937E+03	0.15405E-03	NO

17	-0.11515E+04	-0.38016E-03	0.0	0.10676E-02	YES
18	0.28389E+03	0.90846E-04	0.0	0.25155E-02	YES
19	0.28463E+03	0.91147E-04	0.0	0.24912E-02	YES
20	-0.11471E+04	-0.37872E-03	0.0	0.10583E-02	NO
21	-0.84646E+03	-0.29147E-03	0.0	0.13009E-03	YES
22	-0.61666E+03	-0.20363E-03	0.0	0.49951E-03	YES
23	-0.62120E+03	-0.20513E-03	0.0	0.49290E-03	NO
24	-0.84467E+03	-0.29040E-03	0.0	0.12722E-03	NO
25	-0.21856E+02	-0.18609E-04	0.35400E+03	0.12043E-03	YES
26	0.27668E+02	0.85337E-05	0.0	0.33400E-02	YES
27	0.26848E+02	0.85273E-05	0.0	0.33045E-02	YES
28	-0.24272E+02	-0.18484E-04	0.38659E+03	0.11496E-03	NO
29	-0.21904E+02	-0.18560E-04	0.35364E+03	0.12029E-03	NO
30	0.26661E+02	0.85314E-05	0.0	0.33402E-02	YES
31	0.26824E+02	0.85337E-05	0.0	0.33043E-02	YES
32	-0.24714E+02	-0.18669E-04	0.33676E+03	0.11507E-03	NO
33	-0.37588E+03	-0.12855E-03	0.44911E+02	0.44632E-04	NO
34	-0.21351E+04	-0.17150E-03	-0.12174E+03	0.10840E-03	NO
35	-0.21404E+04	-0.17169E-03	-0.12168E+03	0.10878E-03	NO
36	-0.37790E+03	-0.12715E-03	0.42915E+02	0.44151E-04	NO
37	-0.37586E+03	-0.12855E-03	0.45028E+02	0.44670E-04	NO
38	-0.21377E+04	-0.17157E-03	-0.12193E+03	0.10852E-03	NO
39	-0.21368E+04	-0.17137E-03	-0.12149E+03	0.10874E-03	NO
40	-0.37737E+03	-0.12699E-03	0.43274E+02	0.44231E-04	NO

STEEL MPSE STRESSES ARE AS BLOW.

ELEMENT NO. DIRECTION

1	1	STRESS=	0.19881E+05	STRAIN=	0.67393E-03
2	1	STRESS=	0.67444E+04	STRAIN=	0.22862E-03
3	1	STRESS=	0.66988E+04	STRAIN=	0.22707E-03
4	1	STRESS=	0.19755E+05	STRAIN=	0.66965E-03
6	1	STRESS=	-0.10695E+04	STRAIN=	-0.36255E-04
7	1	STRESS=	-0.10256E+04	STRAIN=	-0.34767E-04
8	1	STRESS=	-0.73981E+03	STRAIN=	-0.25078E-04
9	1	STRESS=	0.23607E+05	STRAIN=	0.80025E-03
10	1	STRESS=	0.73674E+04	STRAIN=	0.24974E-03
11	1	STRESS=	0.72109E+04	STRAIN=	0.24444E-03
12	1	STRESS=	0.23368E+05	STRAIN=	0.79215E-03
13	1	STRESS=	-0.10857E+04	STRAIN=	-0.36803E-04
14	1	STRESS=	-0.10333E+03	STRAIN=	-0.35027E-05
15	1	STRESS=	-0.22757E+03	STRAIN=	-0.77142E-05
16	1	STRESS=	-0.96871E+03	STRAIN=	-0.32838E-04
17	1	STRESS=	0.19844E+05	STRAIN=	0.67266E-03
18	1	STRESS=	0.66599E+04	STRAIN=	0.22576E-03
19	1	STRESS=	0.67133E+04	STRAIN=	0.22757E-03
20	1	STRESS=	0.19751E+05	STRAIN=	0.66953E-03
21	1	STRESS=	-0.73632E+03	STRAIN=	-0.24960E-04
22	1	STRESS=	-0.10434E+04	STRAIN=	-0.35369E-04
23	1	STRESS=	-0.10543E+04	STRAIN=	-0.35740E-04
24	1	STRESS=	-0.74597E+03	STRAIN=	-0.25287E-04
25	1	STRESS=	0.18816E+02	STRAIN=	0.63783E-06
26	1	STRESS=	-0.23766E+03	STRAIN=	-0.80563E-05
27	1	STRESS=	-0.31506E+03	STRAIN=	-0.10680E-04
28	1	STRESS=	0.59468E+02	STRAIN=	0.20157E-05
29	1	STRESS=	0.11470E+02	STRAIN=	0.38882E-06
30	1	STRESS=	-0.28047E+03	STRAIN=	-0.95074E-05
31	1	STRESS=	-0.27941E+03	STRAIN=	-0.94716E-05

REINFORCEMENT MEMBER	REINFORCEMENT TYPE	STRESS	STRAIN	REINFORCEMENT MEMBER	REINFORCEMENT TYPE	STRESS	STRAIN
32	1	0.64889E+02	0.21996E-05	1	CONVENTIONAL	0.10869E+04	0.36846E-04
33	1	0.96504E+03	0.32849E-04	2	CONVENTIONAL	0.39270E+03	0.43312E-04
34	1	0.31333E+04	0.40621E-03	3	CONVENTIONAL	0.80649E+04	0.36071E-04
35	1	0.31447E+04	0.10660E-03	4	CONVENTIONAL	0.52447E+05	0.33459E-02
36	1	0.99658E+03	0.33742E-04	5	CONVENTIONAL	0.52226E+05	0.33108E-02
37	1	0.97098E+03	0.32915E-04	6	CONVENTIONAL	0.52440E+05	0.33434E-02
38	1	0.31379E+04	0.10637E-03	7	CONVENTIONAL	0.52533E+05	0.33740E-02
39	1	0.31424E+04	0.10652E-03	8	CONVENTIONAL	0.52438E+05	0.33503E-02
40	1	0.99430E+03	0.33705E-04	9	CONVENTIONAL	0.52542E+05	0.33767E-02
				10	CONVENTIONAL	0.12207E+04	0.41381E-04
				11	CONVENTIONAL	0.66893E+03	0.22675E-04
				12	CONVENTIONAL	0.42266E+04	0.41581E-04
				13	CONVENTIONAL	0.32771E+04	-0.11109E-03
				14	CONVENTIONAL	-0.53308E+04	-0.18070E-03
				15	CONVENTIONAL	-0.32609E+04	-0.11054E-03
				16	CONVENTIONAL	-0.23460E+05	-0.79524E-03
				17	CONVENTIONAL	-0.21593E+05	-0.73197E-03
				18	CONVENTIONAL	-0.23413E+05	-0.79365E-03
				19	CONVENTIONAL	-0.23378E+05	-0.79246E-03
				20	CONVENTIONAL	-0.21547E+05	-0.73040E-03
				21	CONVENTIONAL	-0.23448E+05	-0.79486E-03
				22	CONVENTIONAL	-0.32689E+04	-0.11081E-03
				23	CONVENTIONAL	-0.52137E+04	-0.17674E-03
				24	CONVENTIONAL	-0.32584E+04	-0.11045E-03
				25	PRESTRESSED	0.16764E+06	0.67038E-02
				26	PRESTRESSED	0.16702E+06	0.66803E-02
				27	PRESTRESSED	0.16762E+06	0.67031E-02
				28	PRESTRESSED	0.25533E+06	0.10013E-01
				29	PRESTRESSED	0.25440E+06	0.99778E-02
				30	PRESTRESSED	0.25527E+06	0.10010E-01
				31	PRESTRESSED	0.25608E+06	0.10041E-01
				32	PRESTRESSED	0.25545E+06	0.10017E-01
				33	PRESTRESSED	0.25615E+06	0.10044E-01
				34	PRESTRESSED	0.16776E+06	0.67084E-02
				35	PRESTRESSED	0.16727E+06	0.66897E-02
				36	PRESTRESSED	0.16777E+06	0.67086E-02
				37	BONDED	0.11844E+03	0.65029E-04
				38	BONDED	0.13655E+03	0.75877E-04
				39	BONDED	0.11814E+03	0.64850E-04
				40	BONDED	0.68998E+00	0.35390E-06
				41	BONDED	0.10457E+01	0.53644E-06
				42	BONDED	0.87149E+00	0.44703E-06
				43	BONDED	0.11695E+03	0.64146E-04
				44	BONDED	0.13662E+03	0.75873E-04
				45	BONDED	0.11702E+03	0.64187E-04

REINFORCEMENT MEMBER STRESSES AND STRAINS ARE AS BELOW:

THE LOAD INCREMENT VECTOR IS AS BELOW:

RINC( 24 , 2 ) = -0.50000E+04  
RINC( 28 , 2 ) = -0.50000E+04  
RINC( 32 , 2 ) = -0.50000E+04

THE TOTAL LOAD VECTOR IS AS BELOW:

TOTAL( 1 , 1 ) = 0.16465E+05  
TOTAL( 4 , 1 ) = 0.32930E+05  
TOTAL( 7 , 1 ) = 0.16465E+05  
TOTAL( 24 , 2 ) = -0.20000E+05  
TOTAL( 28 , 2 ) = -0.20000E+05  
TOTAL( 32 , 2 ) = -0.20000E+05  
TOTAL( 46 , 1 ) = -0.16465E+05  
TOTAL( 49 , 1 ) = -0.32930E+05  
TOTAL( 52 , 1 ) = -0.16465E+05

TOTAL REINFORCEMENT FORCE RESTRAINT VECTOR:

RESTRAINT FORCE AT NODE 10 IN DIRECTION 1 = 0.60417E+04  
RESTRAINT FORCE AT NODE 14 IN DIRECTION 1 = 0.12081E+05  
RESTRAINT FORCE AT NODE 18 IN DIRECTION 1 = 0.60418E+04  
RESTRAINT FORCE AT NODE 22 IN DIRECTION 1 = -0.43750E+00  
RESTRAINT FORCE AT NODE 26 IN DIRECTION 1 = -0.17031E+01  
RESTRAINT FORCE AT NODE 30 IN DIRECTION 1 = -0.61328E+00  
RESTRAINT FORCE AT NODE 34 IN DIRECTION 1 = -0.60417E+04  
RESTRAINT FORCE AT NODE 38 IN DIRECTION 1 = -0.12080E+05  
RESTRAINT FORCE AT NODE 42 IN DIRECTION 1 = -0.60412E+04

\*\*\*\*\*  
\* LOAD INCREMENT NUMBER 6 \*  
\*\*\*\*\*

\*\*\* DIAGONAL TERM IS( 24 , 1 ) = -0.46834E+07 IN BLOCK NO. 4 \*\*\*

20:58:16 56.427 PC=0

APPENDIX H  
INPUT PREPARATION NOTES

## APPENDIX H

The purpose of this appendix is to assist the computer program user in the compilation of the input data file. Units of inches and pounds are used throughout, and if large numbers are to be read in, the E format should be used. The user should be especially conscious of the sign conventions listed in Appendix A. In referring to several input variables in the description below, the symbolic name may be used for the sake of brevity. The alphabetic listing of all symbolic names and their corresponding codes, where applicable, are given in Appendix B. Complete freedom in input data entry is provided through the use of a semi-freefield format, where commas are used to separate adjacent entries, as illustrated in the sample input listing in Appendix F. A sufficient number of columns have been allocated for the entry on all variables of realistic size, but reference to the format statements in subroutine READIN listed in Appendix D will clarify the maximum number of assigned columns to accommodate the full digit length. Following the description of each input card or assemblage of associated cards, the significance and qualifications that pertain to the important variable entries will be commented upon.

The data cards must occur in the following order:

1. Echo Check Card

Order of Entries

1

Description

IWRITE

Comments: If IWRITE = 1, the input data will be printed out so that it can be quickly checked.

## 2. Number of Finite Elements Card

<u>Order of Entries</u>	<u>Description</u>
1	NELT
2	NELCHK

Comments: (a) If it is recognized that all concrete elements will not crack, the element numbering system should be chosen such that only the first NELCHK number of elements will be checked for cracking.

(b) NELT does not include the number of diaphragm elements.

## 3. Concrete Finite Elements Description Cards

One card for each concrete finite element in ascending order.

<u>Order of Entries</u>	<u>Description</u>
1	INDCEL (NEL)
2	INELSZ (NEL)
3	INELTY (NEL)
4	ELTHN (NEL)
5	First element node number
6	Second node number
7	Third node number
8	Fourth node number
9	INDOWL (NEL)
10	INMESH (NEL)
11	INSZMS (NEL)
12	WIDTHC (NEL)

Comments: (a) Concrete elements of the same dimensions, thickness, and percentage of reinforcement are assigned the same arbitrary integer number INELSZ (NEL).



(b) Only those web elements that adjoin a tension flange element will develop dowel shear resistance.

(c) Elements that have the same percentages of steel mesh reinforcement are assigned the same arbitrary integer number INSZMS (NEL).

(d) The effective dowel width of the beam is distributed proportionately between the web elements that adjoin the tension flange.

#### 4. Concrete Shrinkage Data Card

<u>Order of Entries</u>	<u>Description</u>
1	NELTOP
2	SIGXT1
3	SIGXT2
4	SIGXB1
5	SIGXB2
6	SIGXS1
7	SIGXS2
8	EXT1
9	EXT2
10	EXB1
11	EXB2
12	EXS1
13	EXS2

#### 5. Alternate Top and Bottom Flange Shrinkage Elements Cards

Alternate cards for top and bottom flange concrete elements that develop shrinkage stresses.

The first card will list ten top flange concrete elements, the second card ten bottom flange concrete elements. This sequence of cards is continued until all flange elements subjected to shrinkage stresses are listed. The last two cards will contain at least one entry, but will not exceed ten entries.

6. Number of Elements with Steel Mesh Card

The only entry on the card is NELSM.

Comments: It is imperative for the proper functioning of the program that all transverse shear or torsion reinforcement be represented by an equivalent steel mesh distributed throughout the element.

7. Number of Layers in Steel Mesh Card

The only entry is NDIRNS.

Comments: If NELSM = 0, omit this card and proceed to card 9.

8. Steel Mesh Description Cards

Two cards for each element containing a steel mesh. The element number is contained on the first card. The second card is as below:

<u>Order of Entries</u>	<u>Description</u>
1	Steel mesh percentages for all layers
2	Corresponding inclinations

Comments: A steel mesh layer is defined as a discrete system of parallel bars.

9. Number of Diaphragms Card

The only entry is NELD.

Comments: (a) NELD is the total sum of actual, equivalent, and warping diaphragm elements.

(b) If NELD = 0, proceed directly to card 11.

#### 10. Diaphragm Description Cards

One card for each diaphragm.

<u>Order of Entries</u>	<u>Description</u>
1	INELTY (NEL)
2	ELTHN (NEL)
3	First element node number
4	Second element node number
5	Third element node number
6	Fourth element node number
7	NDREF (NEL)
8	DPMOD (NEL)

Comments: Identical diaphragm elements have the same NDREF (NEL) integer value.

#### 11. Number of Reinforcement Elements Card

The only entry is NREO.

Comments: NREO is the sum of all prestress and conventional longitudinal reinforcement elements and bond linkages.

#### 12. Reinforcement Type Description Cards

One card for each reinforcement element.

<u>Order of Entries</u>	<u>Description</u>
1	First reinforcement node number
2	Second reinforcement node number
3	Reinforcement element type indicator

Comments: (a) The reinforcement node numbers must be numbered in the positive axis direction.

(b) The following individual reinforcement cards must be in the same order.

### 13. Conventional Longitudinal Reinforcement Card

This card is read if INRTY(NR) = -1.

<u>Order of Entries</u>	<u>Description</u>
1	INRDN (NR)
2	RAREA (NR)

### 14. Prestress Reinforcement Card

This card is read if INRTY (NR) = 0.

<u>Order of Entries</u>	<u>Description</u>
1	INRDN (NR)
2	RAREA (NR)
3	TSGPRE (NR)
4	<del>TAREA (NR)</del>

### 15. Bond Linkage Card

This card is read if INRTY (NR) = 1.

The only entry is CAREA (NR).

#### 16. Number of Finite Element Nodes Card

The only entry is NNODES.

Comments: Bond spring linkage elements adjoin adjacent concrete and reinforcement nodes. However, no bond spring linkages are provided at beam ends.

#### 17. Finite Element Node Description Cards

One card for each node.

<u>Order of Entries</u>	<u>Description</u>
1	ICNODE (I)
2	X (I)
3	Y (I)
4	Z (I)

Comments: (a) Nodes adjoining two non-planar elements must be designated as corner nodes: ie. they possess five degrees of freedom.

(b) Internal node numbers connecting web diaphragm elements are assigned ICNODE (I) = 2: ie. they have four degrees of freedom.

(c) Node adjoining co-planar elements are designated as interior nodes, with three degrees of freedom.

(d) The X, Y, and Z coordinates are global axis coordinates, the direction of the global axes being defined in Appendix A.

#### 18. Strength Moduli Card

<u>Order of Entries</u>	<u>Description</u>
1	CONMOD
2	RECOMOD

3	PREMOD
4	SLPMOD
5	SMSMOD

19. Ultimate Strength Card

<u>Order of Entries</u>	<u>Description</u>
1	FC
2	FT
3	FAGG
4	FUR
5	FUP
6	FUMS

20. Ultimate Strain Cards

<u>Order of Entries</u>	<u>Description</u>
1	EEREO
2	EEPRE
3	ECULT
4	ERULT
5	EPULT
6	EMSULT
7	ESLIP
8	DF

21. Poisson Ratios Card

<u>Order of Entries</u>	<u>Description</u>
1	P1
2	P2
3	P3
4	PU

22. Material Deviation Card

<u>Order of Entries</u>	<u>Description</u>
1	CONDEV
2	DEVCON
3	DEVREO
4	PREDEV
5	SLPDEV
6	LDEV
7	AVCSP
8	RELAX

Comments: (a) Entries 1 to 5 specify the maximum allowable deviation percentages in material behaviour that is permitted before corrective measures are taken. Only CONDEV and PREDEV of the five variables mentioned above have a direct influence on the decision to invoke the iterative process. Obviously, if the tolerances expressed by CONDEV and PREDEV are too demanding, the expensive iterative process will be undertaken frequently. Thus, a compromise has to be struck between the maximum allowable deviation that is acceptable and the cost incurred if that maximum level of deviation is to be enforced. Values used in this application of the computer model were CONDEV = 8% and

PREDEV = 10%. Severe tolerances expressed by DEVCON and DEVREO do not increase computing cost significantly, and it is recommended that these values be kept small.

(b) IDEV is the critical weighted iteration integer that determines whether the iterative procedure will be invoked. Each important aspect of structural deviation is given a weighting, as declared in the following card. If the sum total of the deviation counters exceeds IDEV, a cycle of the iterative process will be initiated.

(c) RELAX is the relaxation factor employed to improve the rate of convergence in the highly inelastic segments of reinforcement stress-strain curves during the iterative process. The variable will invariably exceed unity, but its optimum value is very much dependent upon the nature of the analysis.

### 23. Deviation Weighting Card

<u>Order of Entries</u>	<u>Description</u>
1	MAXIT
2	NWTCN
3	NWTREO
4	NWTPRE

Comments: If allowable behavioural deviation is exceeded in a concrete element, a conventional reinforcement or steel mesh element, or a prestress reinforcement element, the deviation integer counter is increased by the addition of NWTCN, NWTREO, or NWTPRE respectively. The deviation integer counter within the program is the variable ID. Thus, when ID exceeds IDEV after the application of a load increment, iteration is commenced until deviation is reduced to the extent that ID is less than or equal to IDEV.



24. Number of Load Types Card

The only entry on the card is NLDTY.

Comments: A load type is one where the relationship of the individual loads within successive load increments remains constant.

25. General Load Information Card

One card for each load type.

<u>Order of Entries</u>	<u>Description</u>
1	NINCRT (I)
2	NLOADS (I)

Comments: (a) For each load type, this card and the cards of item 26 are read in.

(b) The application of prestress forces comprises the first load increment in the study of prestressed concrete beam behaviour.

(c) Load increments can be heavy in the elastic and early post-cracking regions, but should become progressively lighter as behaviour becomes more inelastic. Small load increments are necessary close to failure if the ultimate load conditions are to be estimated within close bounds.

26. Individual Load Description Cards

One card for each nodal load.

<u>Order of Entries</u>	<u>Description</u>
1	NODER (I)
2	KODER (I)
3	VALUER (I)

27. Number of Boundary Conditions Card

The only entry on this card is NDISPL.

28. Individual Boundary Conditions Cards

One card for each boundary condition.

<u>Order of Entries</u>	<u>Description</u>
1	NODED (I)
2	KODED (I)
3	VALUED (I)

29. Number of Concrete Elements Display Card

The only entry on this card is PNELT (integre)

30. Concrete Elements Display Card

All the element numbers of those elements whose centroidal stresses will be displayed, are listed on this card. (integres)

31. Number of Steel Mesh Elements Display Card

The only entry on this card is PNELSM (integre).

32. Steel Mesh Elements Display Card

All steel mesh elements to be displayed have their element numbers listed on this card (integres).

33. Number of Reinforcement Elements Display Card

The only entry on this card is PNREO (integre).

34. Reinforcement Elements Display Card

Similar to card 30, but concerning reinforcement elements.

35. Number of Nodal Deflections Display Card

The only entry on this card is PDTOT.

36. Nodal Deflections Display Card

Similar to card 30, but with respect to nodal deflections.

37. Printout Control Card

All data entries are contained on one card.

<u>Order of Entries</u>	<u>Description</u>
1	IDEFLN
2	ICON3
3	ICONPR
4	IMESH
5	IREO
6	ILOAD
7	ITLOAD
8	ISTIF

The data file is now complete. If too few data cards have been included, the end of file card will be read, and execution will immediately cease. If too many cards have been inserted in the data file, the error will be apparent in the echo check printout of the data.

APPENDIX I

EXPERIMENTAL PROGRAM TEST RESULTS

APPENDIX I

EXPERIMENTAL PROGRAM TEST RESULTS

Note: Units of kips, inches, and degrees are used throughout.

1. Beam Dimensions and Reinforcement Details

Refer to Figures 4.3 and 4.4.

2. Loading Systems

Three different patterns of application of the torque and bending moment loads were employed in the testing of the seven beams, and are shown in Figure I-1.

3. Prestress Levels and Shrinkage Stresses

Refer to Table 4.3 for prestress levels.

Between transfer and testing, considerable concrete shrinkage occurred, stressing the longitudinal conventional steel in compression and surrounding concrete in tension. Only the concrete in the flanges is assumed to develop shrinkage stresses.

Shrinkage Stresses	Beam						
	R1	R2	R3	R4	R5	T1	T2
Tension in Top Flange Concrete	.115	.135	.125	.095	.12	.12	.075
Tension in Bottom Flange Concrete	.203	.23 <sup>o</sup>	.216	.117	.2	.25	.25
Compression in Top Reinforcement	13.5	15.75	14.6	11.1	14.	15.	9.
Compression in Bottom Reinforcement	24.0	27.0	25.5	19.9	25.	15.	15.

TABLE I-1 SHRINKAGE STRESSES

#### 4. Test Loading and Deformation Results

In the following tables, the rotation values are in degrees and were measured over a 30 inch central beam length. The deflection measurements are the pure bending vertical displacements of the central cross-section.

The torque and bending moments are those values at the central cross-section. The shear values are those close to the central cross-section.

#### 5. Reinforcement Stresses

Refer to Figures 5.6 to 5.12.

Load Increment No.	Loading					Deformations		
	System	T	P	Bending Moment	Torque	Shear	Central Defln.	Rotation
1		0.0		0.0	0.0		0.0	0.0
2		2.0		116	48		.024	.036
3		4.0		216	96		.048	.068
4		6.0		314	143		.073	.0575
5		8.0		414	192		.1045	.08
6		10.0		510	238		.139	.10
7		10.78		552	259		.182	.16
8		12.0		611	288		.24	.295
9		12.89		656	310		.24	.365
10		14.04		713	337		.4	.4776
11	A	14.96	0.0	759	359	0.0	.45	.585
12		16.06		813	385.4		.54	.667
13		17.0		859	408		.62	.768
14		17.97		908	431		.69	.881
15		19.0		959	456		.86	1.427
16		19.657		991	472		.97	1.306
17		21.1		1062	506			
18		21.65		1090	520			
19		21.05		1060	505			

Note: Linear transducers were removed after load increment No. 15.

TABLE I-2 BEAM R1 TEST RESULTS



Load Increment No.	Loading					Deformations		
	System	T	P	Bending Moment	Torque	Shear	Central Defln.	Rotation
1			0	0.0			0.0	
2			2	66.4			.0167	
3			4	136			.03	
4			6	206			.058	
5		0.0	8	276	0.0		.078	0.0
6			10	346			.097	
7			12	417			.117	
8			13	452			.128	
9			14	488			.14	
10		1.04		555	25		.163	.001
11		1.92		600	46		.18	.0032
12		3.1		657	74		.21	.009
13		4.03		703	97		.24	.017
14		5.07		755	122		.29	.043
15	A	6.0		797	142	0.0	.36	.104
16		7.0		850	168		.45	.2
17		7.9		896	190		.52	.26
18		9.0		949	216		.6	.33
19		10		998	240		.68	.39
20		10.9		1044	262		.77	.46
21		11.3		1064	271		.816	.52
22		12.		1097	287		.91	.61
23		12.19		1107	292		.97	.68
24		12.75		1135	306			
25		13.35		1165	321			
26		13.9		1192	334			
27		14.5		1222	348			
28		14.58		1226	350			
29		15.06		1249	361			
30		15.49	14.0	1271	372			

Note: Transducers were removed after load increment No. 23.

TABLE I-3 BEAM R2 TEST RESULTS

Load Increment No.	Loading						Deformations	
	System	T	P	Bending Moment	Torque	Shear	Central Defln.	Rotation
1			0.0	0.0		0.0	0.0	
2			2	72		1	.015	
3			2	72		1	.016	
4			4	145		2	.03	
5			6	218		3	.043	
6			8	291		4	.054	
7		0.0	10	364	0.0	5	.067	0.0
8			12	437		6	.078	
9			14	510		7	.09	
10			16	583		8	.102	
11			18	656		9	.115	
12			20	729		10	.13	
13			22	802		11	.15	
14		2.04		854	49		.177	0.0
15		4.1		906	99		.205	.007
16		5.8		947	138		.25	.02
17	C	8.0		1003	192		.325	.08
18		9.8		1049	236		.425	.16
19		11.86		1099	285		.52	.246
20		12.8		1123	307		.59	.32
21		13.9		1151	334		.64	.41
22		14.84		1174	356		.69	.4
23		15.8		1199	380		.77	.46
24		17		1229	409		.85	.54
25		17.3		1235	415		.89	.575
26		17.81		1248	428		.93	.6
27		18.2		1258	437		1.0	.72
28		19.2		1283	461			
29		19.6		1293	471			
30		20.14		1306	483			
31		20.76		1322	498			
32		21.3		1336	510			
33		21.65		1344	519			
34		22.2	22	1357	532	11		

Note: Linear transducers were removed after load increment No. 27.

TABLE I-4 BEAM R3 TEST RESULTS

Load Increment No.	Loading						Deformations	
	System	T	P	Bending Moment	Torque	Shear	Central Defln.	Rotation
1			0.0	0.0		0.0	0.0	
2			2	73		1	.01	
3			4	146		2	.023	
4			6	220		3	.036	
5		0.0	8	293	0.0	4	.05	0.0
6			10	366		5	.063	
7			12	440		6	.076	
8			14	513		7	.089	
9			16	587		8	.102	
10			18	660		9	.116	
11			20	733		10	.131	
12		4.04		831	97		.167	
13		6.1		883	147		.197	Similar
14	C	7.9		928	190		.244	to
15		9.84		976	236		.33	R3*
16		12.1		1032	290		.45	
17		13.95		1079	335		.55	
18			22	1152		11	.61	
19			24	1222		12	.6725	
20			26	1297		13	.78	
21			28	1366		14	.90	
22			30	1403		15	.99	
23			31	1443		15.5	1.09	
24			32	1484		16	1.28	
25			33	1511		16.5	1.51	
26			34	1554		17	1.665	
27			35	1591		17.5	2.02	
28		13.95	36	1624	335	18		

\* Rotation results for this short torsion loading interval are similar to those corresponding results for beam R3.

Note: Linear transducers were removed after load increment No. 27.

TABLE I-5 BEAM R4 TEST RESULTS

Load Increment No.	Loading					Deformations		
	System	T	P	Bending Moment	Torque	Shear	Central Defln.	Rotation
1		0.0		0.0	0.0		0.0	0.0
2		1.96		49	47		.02	.006
3		3.92		98	94		.043	.009
4		6.15		154	148		.068	.067
5		8		200	192		.085	.0125
6		9		250	240		.103	.0325
7		11		276	265		.113	.036
8		11.9		298	282		.122	.043
9		13		324	311		.131	.063
10		14.2		355	341		.173	.156
11		14.84		371	356		.196	.21
12		15.5		388	372		.217	.25
13		15.9		398	382		.233	.272
14		16.7		418	401		.253	.31
15		17.2		431	414		.273	.34
16	B	17.4	0.0	435	417	0.0	.294	.39
17		18		451	433		.307	.42
18		18.5		463	444		.327	.437
19		19		476	457		.354	.49
20		19.5		487	468		.383	.53
21		19.9		497	477		.4	.57
22		20.5		513	492		.426	.61
23		20.93		523	502		.44	.64
24		21.6		540	519		.47	.69
25		21.82		546	524		.486	.73
26		22.3		558	536		.504	.76
27		22.84		571	548		.53	.8
28		23.3		583	559		.55	.84
29		23.87		597	573		.583	.89
30		24.38		609	585		.617	.97
31		25		626	601		.65	1.06
32		2		640	615		.683	1.167

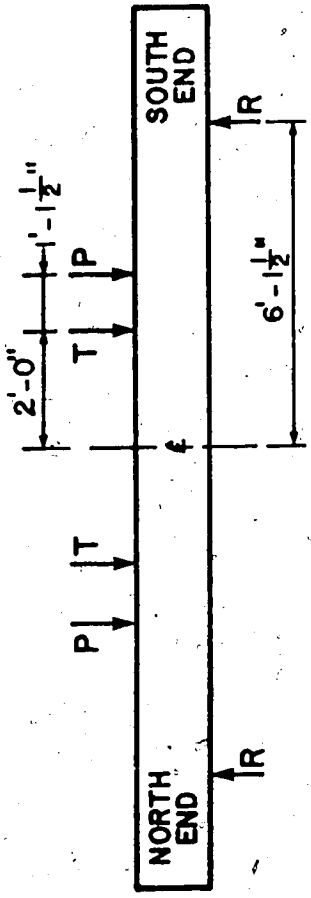
TABLE I-6 BEAM R5 TEST RESULTS

Beam	Load Increment No.	Loading					Deformations		
		System	T	P	Bending Moment	Torque	Shear	Central Defln.	Rotation
T1	1		0.0		0.0	0.0		0.0	0.0
	2		1.19		77	28.6		.0225	.018
	3		2.03		118	49		.04	.031
	4		2.95		164	71		.062	.032
	5		4.0		215	97		.085	.008
	6		5.08		269			.109	.02
	7	A	6.07	0.0	319	146		.14	.052
	8		6.75		352	10		.215	.067
	9		8.13		420	95		.316	.13
	10		10.0		511			.565	.38
	11		11.0		563	264		.68	.53
	12		11.3		577	271		.743	.63
	13		9.5		490	229			
T2	1			0.0	0.0			0.0	
	2			2	72			.029	
	3			4	145			.063	
	4		0.0	6	216	0.0		.1	0.0
	5			7	252			.12	
	6			8	289			.143	
	7			9	322			.166	
	8			10	361			.197	
	9			11	396			.24	
	10		.98		445	24		.32	-
	11	A	2		495	48	0.0	.38	-
	12		3		546	73		.49	.1
	13		4		594	96		.68	.035
	14		4.53		620	109		.74	.156
	15		5		647	121		.8	.225
	16		5.45		666	131		.86	.26
	17		6		690	142		.955	.286
	18		6.43		715	154		1.06	.4
	19		6.9		738	166		1.25	.528
	20		7.4		763	178		1.53	.79
	21		7.94		789	191			
	22		8.2		801	196.5			
	23		8.13	11	798	195			

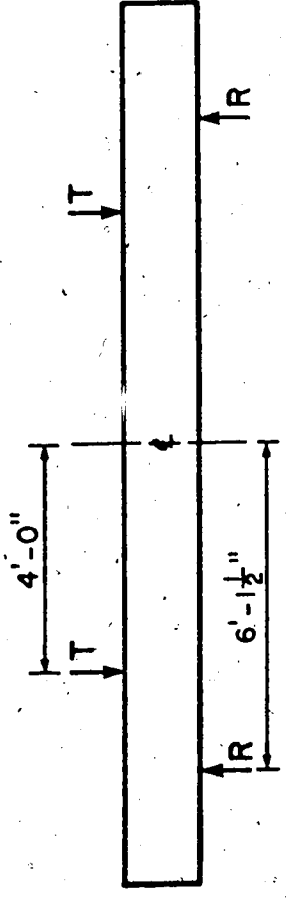
Notes: Linear transducers were removed after load increment 13 for T1, and increment 20 for beam T2

TABLE I-7 BEAMS T1 AND T2 TEST RESULTS

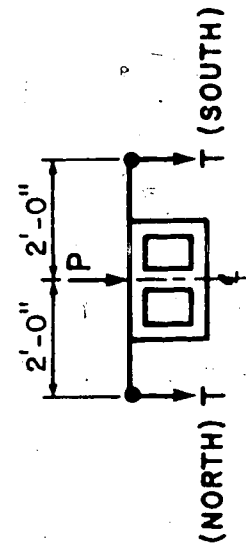
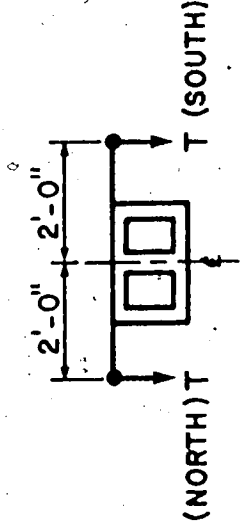
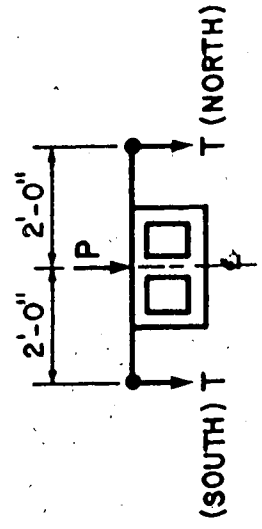
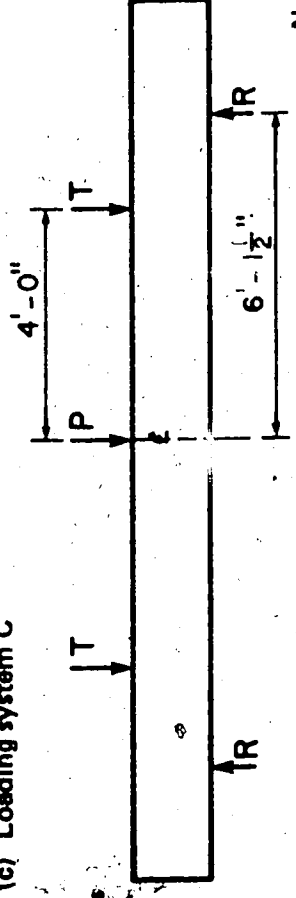
(a) Loading system A



(b) Loading system B



(c) Loading system C



- Notes : (1) Drawings not to scale  
 (2) Loading systems symmetrical about centreline  
 (3) T = torque load P = bending moment load

FIG. I-1 LOADING SYSTEMS